Thermoelectric transport in disordered mesoscopic systems

Raffaello Ferone

UNIVERSITÉ JOSEPH FOURIER
GRENOBLE 1

and

SCUOLA NORMALE SUPERIORE

PhD THESIS

RAFFAELLO FERONE

THERMOELECTRIC TRANSPORT IN DISORDERED MESOSCOPIC SYSTEMS

18 April 2006

Board of examiners:

Dr. Ines SAFI	Examiner
Prof. Maura SASSETTI	Examiner
Prof. Fabio BELTRAM	Examiner
Prof. Roberto RAIMONDI	Examiner
Dr. Stephan ROCHE	Examiner
Prof. Rosario FAZIO	Advisor
Prof. Frank HEKKING	Advisor

Contents

List of Figures

INTRODUCTION

In this PhD thesis we will discuss the transport properties of charge and heat in two different disordered mesoscopic systems. This first statement contains a lot of concepts, and some questions arise spontaneously: why should one be interested in the transport properties? What is a mesoscopic system and why could it be interesting to study disordered mesoscopic systems? What is the framework which these systems could be studied in?

Many other questions could arise, but for the moment we stop here, and we try to get an answer at least for some of them. The other ones will find their own answers in the remaining pages of this manuscript.

Since the dawning of theoretical and experimental exploration of the properties of condensed matter systems, particularly of metals, scientists supposed that the abilities of some systems to transfer charge and heat were profoundly bound to their deepest nature. For example, just three years after Thomson's discovery of the electron in 1897, an important result was achieved thanks to Drude's study on electrical conductivity, [Ashcroft87], confirming the strong connections existing between the transport properties and the nature of the systems: understanding the way metals transfer the charge and the heat means understanding how metals behave microscopically.

This is just a partial answer to the first question. Of course, the different theories that followed one another brought, little by little, other bricks to the comprehension of the problem, and then, of the microscopic nature of the condensed matter. Particularly, the birth of quantum mechanics completely changed the way to approach the problem, and it gave the opportunity to correct many previous assumptions that the

daily laboratory experience showed being false.

As we will see in the next chapter, until the seventies, most of the transport properties of a bulk metal could be explained by means of the Landau theory of Fermi liquids, [Abrikosov88]. It was originally conceived for ^{3}He, but it was then extended to several other fermionic systems. Its fundamental idea is that the electron gas in a bulk system can still be described as formed of independent particles under the assumption that the screening of interactions between two given electrons, due to the presence of the other electrons, is strong. The particles in terms of which the system is described are not real particles, but more complex quantities, generally called quasi-particles, preserving their fermionic character, and representing the low-energy long wavelength excitations of the interacting system. If the screening hypothesis is satisfied, then the theory foresees that the charge and the energy are transported by the same entities: the above-mentioned fermionic quasi-particles. The existence of such a relationship between charge and heat transport is expressed in a very general way by the Wiedemann-Franz (WF) law. It states that the ratio between thermal conductivity κ and the electrical one σ depends linearly on temperature T, with a proportionality constant which is more or less material independent. It can be expressed as

$$\frac{\kappa}{T\sigma} = \frac{\pi^2}{3e^2} = L_0 \ , \tag{1}$$

where e is the electron charge. Here, and in the rest of the the manuscript, we set $k_B = \hbar = 1$. The constant of proportionality L_0 is known as the Lorenz number and it is one of the signatures of Fermi liquid behaviour. It plays a very important role, since its value allows to understand whether or not the system is in a Fermi liquid state; then, it allows to have an idea about the possible dominating charge and heat transfer mechanism. In principle, if one could measure L_0 experimentally, one could have some information about the nature and the state of the system.

This kind of description is quite accurate for most of the so-called ohmic bulk conductors; that is for all bulk conductors for which Ohm's law holds. The latter reads

$$\mathbf{j} = \sigma \mathcal{E} \ . \tag{2}$$

Equation (4) is a *local* relation which connects the electrical field $\mathcal{E}$ which is present at time t at the position $\mathbf{r}$ to the current density $\mathbf{j}$ at the same time and at the same position. σ is the conductivity; it is constant and it is material dependent. We stress the two inherent features of Eq. (4): its local character and the need that the system is a bulk conductor. In the following, we will see that these two features are tightly bound: in abscence of the bulk system assumption, the local character of physical quantities concerning charge and heat transport will not always hold. This will lead us to think transport properties over from a different point of view with respect to the theories, as the aforementioned Landau theory, generally used to describe macroscopic metals.

During the eighties, the technological development, as imagined by Feynman even twenty years before, [Feynman59], allowed the fabrication of smaller and smaller samples. Such systems were characterised by physical dimensions making possible a description in terms of real one- or two-dimensional models. The new samples enabled for the first time to investigate the limits of validity of Eq. (4), and then a different interpretation of resistance at a microscopic level. For such samples, the assumption of bulk metal, necessary in order for Eq. (4) to hold, is no longer adequate. In the next chapter, we will see that Landau's hypothesis of well-screened particles is no longer valid under this condition. Consequently, a new kind of approach allowing a new and correct description should be followed. As mentioned above, abandoning the bulk system assumption will have deep consequences.

Following [Datta97], one could say that a conductor presents an ohmic behaviour if its linear dimensions are larger than three typical lengths: de Broglie wavelength $2\pi/k$, k being the electron wavevector, the elastic mean free path l_e, concerning electrons static-impurities scattering, and the coherence length L_ϕ, that is the length along which an electron can preserve the information concerning its quantum mechanical phase. All these lengths will be defined more precisely in the next sections. They can vary from one material to another, and can be influenced by external parameters, as for instance the temperature. See Tab. 2 for some typical electronic values in two

	(2DEG) GaAs/AlGaAs	CNT	Units
Fermi Wavelength $\lambda_F = 2\pi/k_F$	40	0.74	nm
Fermi velocity $v_F = k_F/m$	2.7	8.1	10^5m/s
Mean Free Path $l = v_F\tau$	$0.1 - 1$	~ 2	μm
Phase Coherence Length L_ϕ	~ 200	~ 200	nm

Table 1: Typical electronic properties for a 2DEG confined in GaAs/AlGaAs heterostructures and for single-wall carbon nanotubes, CNT.

different systems.

When the linear dimensions of the sample are not larger than the three above-mentioned lengths, a *non-local* spatial and time dependence of physical quantities arises. We will see that the physical quantities, as for instance the electrical conductivity, behave differently; they contain and can reveal more information about the nature of the sample. Particularly, we point out the role played by the coherence length L_ϕ which, if comparable to the linear dimensions of the sample, drastically changes the physical description. In the following chapter, we will better understand why. Here, we just observe, that at low temperatures, as $T \to 0$, all the scattering processes taking place in the sample, first among electrons and phonons, then among electrons, become elastic since the system goes into its ground state; then, a well defined phase correlation before and after collisions exists. The ability for an electron to preserve information about its phase, until a phase-breaking process occurs, confers to the physical quantities describing charge and heat transfer a non-local spatial and time dependence; on the contrary, the Landau theory just gives rise to a strictly local dependence.

Such a non-local behaviour is observed for the low-energy properties of physical systems having a typical size varying between some dozens of micrometers, (10^{-6}m), and some nanometers, (10^{-9}m). These systems, whose size is between the macroscopic scale and the atomic scale, and where the electron coherence length can largely exceed the size of the sample, are generally called mesoscopic systems; this word was coined

for the first time by Van Kampen in 1981, [Imry02]. We add that with respect to the macroscopic systems, the existance of the coherence length L_ϕ, comparable to the size of the samples, allows the observation of pure quantum mechanical interference effects.

In this thesis, we have studied two different mesoscopic systems: disordered quantum wires and granular metals. In the rest of the introduction, we shortly give a presentation of such systems and of our work. In both cases, some difficulties in describing them in terms of Landau approach will arise, as we will see. Consequently, a deviation from Fermi liquid behaviour can be expected.

Both for quantum wires and granular metals, the behaviour of electrical conductance was already known, while the thermal transport was not yet studied. The question which has driven our work is whether or not in such systems, under well defined conditions, the charge and heat transfer can be still described as in a Fermi liquid. This is the problem to which we have tried to give an answer for our two specific systems, by evaluating the thermal conductance, and then the validity of WF law.

We point out that our work follows the wake of the long list of papers trying, since many years, to investigate the behaviour of the Lorenz number, and then the dominating transfer mechanisms, for many different systems, [Castellani87, Kane96, Fazio98, Niven02, Beloborodov05, Biagini05, Ferone].

Quantum wires

In the first part of this thesis, we present the results about the thermal and electrical conductance in disordered quantum wires that is in one-dimensional (1D) conductors. Nowadays, it is possible to make samples with very strong confining potential along two directions. Such systems behave as electronic waveguides, since they present a strongly one-dimensional nature of conduction. Examples are the carbon nanotubes, [Tans97, Wildoer98, Odom98], or the AlGaAs/GaAs heterostructures, [Tarucha95, Levy05].

The study concerning 1D systems has been generally focused on electrical transport, [Tarucha95, Safi95, Safi97, Maslov95, Maslov95b, VanWees88, Wharam88]. For the thermal transport, experimentally, a measurement of thermal conductance requires a means of detecting the heat flow through the constriction. This was done for the first time in 1992, using quantum point contacts (QPC) as extremely accurate thermometers, [Molenkamp92, Appleyard98]. From a theoretical point of view, only in 1998 the expression for the thermal conductance for a one-dimensional system was theoretically studied, [Fazio98, Krive98].

For these low dimensional systems, Landau's assumptions are no longer valid since there will be always at least one direction in space along which the Coulomb interactions are not well screened. The need of a new approach arises.

This kind of systems is generally studied in the framework of the Luttinger liquids (LL) theory. The fundamental ideas will be given explicitly in the next chapters. Here, we content ourselves to claim that such a theory presents an exactly solvable model for one-dimensional conductors to take correctely into account Coulomb interactions. The eigenstates of such a system are no longer fermionic single quasi-particle excitations, but collective modes that have bosonic character: charge and spin density waves, which have linear spectra. In our work, we took into account the contribution due to charge density waves.

The charge density waves, also called plasmons, can be seen as the responsible modes for the heat transport, as the electrons are for charge transport. The scattering properties of plasmons are very different from electronic ones, and this yields drastic effects. Particularly, this makes one-dimensional wires extremely sensitive to the physical realization: an infinitely long wire will have different transport properties with respect to a finite-size one connected to measuring metallic electrodes. The latter are generally called reservoirs, and they play the role of source and drain.

The reservoirs play a fundamental role. The connections between the wire and the electrodes, practically, introduce inhomogeneities in the systems, and then, possible mechanisms of backscattering that strongly influence the transport. It is reasonable

imagining that such inhomogeneities have a typical spatial size $l_{\rm inh} \gg \lambda_F$, λ_F being the Fermi wavelength. If $l_{\rm inh}$ is the characteristic spatial scale of the disorder, then such a presence will not affect electron propagation, being the characteristic spatial scale of an electron of the order of λ_F. In other words, electrons, which can be seen as responsible of charge transfer, will not perceive such a disorder. This is not the case for the plasmons which can have a wavelength comparable to $l_{\rm inh}$; then, they could suffer backscattering and the thermal transport will be strongly affected, [Fazio98, Krive98].

For a clean quantum wire, that is a wire without impurities, connected to two reservoirs, in absence of backscattering for electrons, electrical conductance is not renormalised by interactions. It is given by the universal value $g_{\rm cw} = e^2/h$, [Safi95, Maslov95, Maslov95b, VanWees88, Wharam88]. On the contrary, the thermal one is strongly renormalized, and it causes a suppression of Lorenz number [Fazio98, Krive98]. The latter is always, for any temperature and any value of interaction strength in the wire, smaller than its non-interacting value L_0. The non-interacting value is attained only in the very low temperatures limit, $T \ll v/d$; v/d is the characteristic energy scale of the problem, v being the propagation velocity of plasmons in the wire, and d its length. If the temperature becomes much higher than v/d, the Lorenz number changes slowly.

Again, we stress that the results are completely different if the wire is infinitely long: the Lorenz number is always larger than L_0. Particularly, if the interactions inside the wire become very strong, it diverges as $T \to 0$, [Kane96].

This is for an ideally clean quantum wire. The presence of at least a weak desorder is, anyway, a general feature of the systems. For example, in [Levy05], see Fig. 3, the weak disorder is represented by the undulations on the side-walls of the wire of the order of 10-20 nm.

It is licit to wonder what is the role played by the disorder on electrical and thermal transport. Till now, the correction to electrical conductance is known, [Safi95, Safi97, Maslov95, Maslov95b]. We are evaluating the correction due to disorder for thermal transport; then, we will be able to evaluate the behaviour of the Lorenz number L.

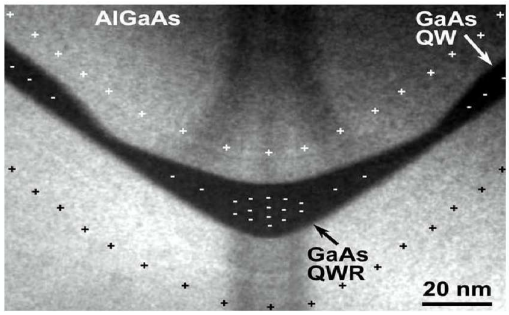

Figure 1: Image of a quantum wire region realised in a AlGaAs/GaAs heterostructure. Such a region presents a weak disorder due to the undulations on the side-walls of the wire of the order of 10-20 nm, [Levy05].

As we will see, the variation of Lorenz number depends on both the corrections to electrical and thermal conductances. So far, at our knowledge, few works exist which allow to determine the sign of the correction to Lorenz number, [Li02, Ferone]. In principle, it could be positive or negative, or the correction could even vanish. In this case, the presence of disorder would affect in the same way the charge and heat transport, as in a classical metal.

In our work, weak disorder has been modeled as a white noise (wn) potential, and the analytical expressions of the corrections will be presented in two different regimes: at low, $T \ll v/d$, and high, $T \gg v/d$, temperatures.

The evaluation of the corrections to electrical and thermal conductance is strongly different; it depends on the different nature of electrons, which are responsible of charge transport, and plasmons, responsible for the energy transfer. As a consequence, the contributions to charge and heat transport are not the same.

We reproduced the behaviour of the correction, due to disorder, to electrical conductance at low and high temperatures. Of course, the presence of weak disorder induces a negative correction, both at low and high temperatures.

For the thermal transport, at the moment, we recovered the expression of all different diagrams contributing to heat transfer. Their expressions demand an accurate analysis, and their analytical evaluation in presence of interactions has been not completed yet. We have verified that in absence of interactions, the Wiedemann-Franz

law is respected.

Granular metals

In the second part of this thesis, we have evaluated the corrections due to the superconducting fluctuations to the thermal conductivity in a granular metal.

Often, in discussing superconductivity, one assumes that the system will be in its ground state. It is, of course, the most probable possibility if $T \ll T_c$. As the temperature rises, close to T_c the presence of thermal energy of order $\sim T$, (we remember $k_B = \hbar = 1$), will allow the system to fluctuate in other states with a finite probability. Such phenomena, known under the name of superconducting fluctuations, induce the formation of Cooper pairs even in the normal phase in presence of a superconducting (BCS) interaction. Particularly, at $T \gtrsim T_c$, electrons can form Cooper pairs which have a finite lifetime, the Ginzburg-Landau (GL) time, inversely proportional to the distance from the critical temperature, $\tau_{GL} \sim 1/(T - T_c)$, [Tinkham96, Larkin04]. Under these conditions, particular phenomena appear since transport properties of the normal state mix with the ones which are characteristic of the superconducting state, giving rise to three different contributions to conductivity: the Aslamzov-Larkin (AL) contribution, also called paraconductivity, the Maki-Thompson (MT) contribution, and the density of state (DOS) contribution, [Larkin04]. They will be presented in more details in the following chapters; for the moment, we just want to give an idea of the physical phenomena they describe.

The AL term describes the contribution to charge and heat transport due to the presence, at temperature $T \gtrsim T_c$, of Cooper pairs. This contribution is generally positive since it takes into account the aptitude of Cooper pairs to propagate easily through the system. Electrons forming Cooper pairs will be no longer available for single particle transport; then, such a presence implies a variation of the one-particle density of state close to the Fermi level. This is exactly the contribution taken into

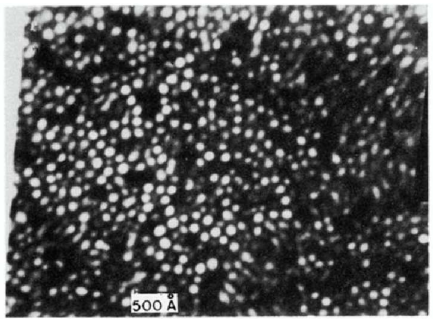

Figure 2: Image of a granular film composed of Al grains on amorphous Ge background. The typical size of the grains is ~ 120 Å, [Shapira83].

account by the DOS term. Finally, there is a purely quantum mechanical contribution, the MT contribution, which takes into account the coherent scattering of two electrons, forming a Cooper pair, on the same elastic impurity, [Larkin04].

For bulk systems and for thermal transport, it has been shown that the DOS and the MT contributions compensate exactly. The only surviving term is the AL contribution which is non-singular in the temperature, [Niven02]. Consequently, in bulk metals, no singular behaviour of the heat current is expected at the normal-superconductor phase transition.

A granular metal can be thought of as a d-dimensional array of metallic grains embedded in an insulating amorphous matrix, with impurities on the surface and inside each grain. In Fig. 4 an experimental realization is presented. The different grains communicate among them by means of single-electron tunneling, and we suppose that the dimensionless macroscopic tunnelling conductance g_T is much larger than one, which is equivalent to state that the system is a good metal. Of course, it is reasonable to imagine that the presence of tunneling strongly influences the transport properties. Indeed, depending on temperature regime, a different behaviour, with respect to the bulk case, emerges. As we will see, the different contributions present a tunneling-dependent behaviour; particularly, the AL and MT terms are of higher order in the tunneling amplitude than the DOS one. This will result into two distinct regions: in the first one, far from T_c, the tunneling among grains is not efficient and the granular structure prevails. A $1/\epsilon$ suppression is found, $\epsilon = (T - T_c)/T_c$ being the reduced temperature.

Close to critical temperature, the tunneling is effective: a saturation of the correction is found and the bulk general behaviour is recovered. In both regions, the sign of the correction is not univocally defined, but it depends on the barrier transparency and on the competition among the different contributions.

Outlook

The manuscript is organised as follows.

The following chapter is dedicated to the phenomenological foundations of transport theory: from classical to quantum transport. We will show the successes of the classical theory to describe most of the metals under ordinary conditions; then, its failure at low temperatures and for low dimensional systems. At the end of the chapter, we will consider the need of a new mesoscopic approach to give a correct description of non-local physical quantities. Step by step, we will analyse some important aspects; then, we will see how they should be modified to get a more faithful description. In this way, we will be able to build a coherent framework to study our own work.

The rest of the work is divided into two parts: the first one concerning the study of thermal transport in a disordered quantum wire, the second concerns the evaluation of thermal conductivity for a granular system.

For the quantum wires, first, we present the basic principle of Luttinger liquids theory. We give the necessary elements to understand the principal features of such 1D systems. Then, we introduce our system, and we motivate our work on the bases of experiences. We present the results for a clean quantum wire, then, we tackle the problem for a disordered one, presenting our results for the two regimes which can be studied analytically.

The same structure will be followed for the granular metals. In this case, we will give a very short reminder of BCS theory, and then we will motivate our work. Finally, we will present the known results and the ones we have found for the thermal

transport.

INTRODUCTION

Dans ce manuscrit de thèse nous étudions les propriétés de transport de la charge et de la chaleur dans deux différents systèmes mésoscopiques désordonnés. Cette première phrase contient plusieurs concepts, et beaucoup de questions se posent spontanément: pourquoi devrait-on être intéressé aux propriétés de transport? Qu'est-ce qu'un système mésoscopique et pour quoi devrait-il être intéressant d'étudier les systèmes mésoscopiques désordonnés? Dans quel contexte de tels systèmes pourraient-ils être étudiés?

D'autres questions pourraient se poser, mais pour l'instant nous nous arrêtons ici, et nous cherchons à donner des réponses au moins à quelques unes d'entre elles. Les autres trouverons une réponse dans la suite de ce manuscrit.

Depuis l'aube de l'exploration théorique et expérimentale des propriétés de la matière condensée, notamment des métaux, les scientifiques supposèrent que la capacité de quelques systèmes de transporter la charge et la chaleur était profondément liée à leur nature la plus intime. Par exemple, juste trois ans après la découverte de l'électron par Thomson en 1897, un résultat très important fut obtenu par Drude dans l'étude sur la conductivité électrique, [Ashcroft87], confirmant la relation très forte existante entre les propriétés de transport et la nature du système: comprendre la façon dont les métaux transfèrent la charge et la chaleur signifie comprendre comment ils se comportent au niveau microscopique.

Cette dernière est juste une réponse partielle à la première question. Naturellement, les différentes théories qui se sont suivies, ont apporté, petit à petit, d'autres briques à la compréhension du problème, et donc, de la nature microscopique de la

matière condensée. En particulier, la naissance de la mécanique quantique changea complètement la façon d'aborder le problème, et elle donna l'opportunité de corriger plusieurs hypothèses que l'expérience quotidienne dans les laboratoires avait montré être fausses.

Comme nous le verrons dans le prochain chapitre, jusqu'aux années soixante-dix, la plupart des propriétés de transport d'un métal massif pouvaient être expliquées grâce à la théorie de Landau des liquides de Fermi, [Abrikosov88]. Elle fut originairement conçue pour étudier l' ^{3}He, puis elle fut généralisée à plusieurs systèmes fermioniques. Son idée fondamentale est que le gaz électronique dans un système massif peut encore être décrit comme un ensemble de particules indépendantes, sous l'hypothèse que l'écrantage des interactions entre deux électrons donnés, dû à la présence des autres électrons, soit fort. Les particules en fonction desquelles le système est décrit ne sont pas des particules réelles, mais des entités plus complexes, généralement appelées quasi-particules, qui préservent leur caractère fermionique, et qui représentent les excitations à basse énergie et grande longueur d'onde du système en interaction. Si l'hypothèse d'écrantage est satisfaite, alors la théorie prévoit que la charge et la chaleur sont transportées par les mêmes entités: les susdites quasi-particules fermioniques. L'existence d'une telle relation entre le transport de la charge et de la chaleur est exprimée de façon générale par la loi de Wiedemann-Franz (WF). Elle affirme que le rapport entre la conductivité thermique κ et celle électrique σ dépend de façon linéaire de la température T, la constante de proportionnalité étant indépendante du métal. Cette loi peut être écrite de la façon suivante

$$\frac{\kappa}{T\sigma} = \frac{\pi^2}{3e^2} = L_0 \ , \tag{3}$$

où e est la charge de l'électron. Ici et dans le reste du manuscrit, nous utilisons des unités de mesure telles que $k_B = \hbar = 1$. La constante de proportionnalité L_0 est connue sous le nom de nombre de Lorenz et elle représente la signature du comportement de type Liquide de Fermi. Elle joue un rôle très important, car sa valeur permet de comprendre si le système se trouve ou non dans un état type liquide de Fermi; donc, elle permet d'avoir une idée sur le principal mécanisme de transport de la charge et

de la chaleur. En principe, si on pouvait mesurer L_0 expérimentalement, on pourrait avoir des informations sur la nature et l'état du système.

Ce type de description est valable pour la plupart des conducteurs dits ohmique et massifs; à savoir, tous les conducteurs massifs pour lesquels la loi de Ohm est valable. Cette dernière s'écrit

$$\mathbf{j} = \sigma\mathcal{E} \ . \tag{4}$$

L'équation (4) est une relation *locale* qui relie le champ électrique $\mathcal{E}$ présent au temps t à la position $\mathbf{r}$ à la densité de courant $\mathbf{j}$ au même instant et à la même position. σ est la conductivité électrique; elle est constante mais elle varie d'un métal à l'autre. Nous soulignons les deux caractéristiques inhérentes de l'Eq. (4): son caractère locale, et la nécessité que le système soit massif. Plus tard, nous verrons que ces deux caractéristiques sont profondément liées: en l'absence de l'hypothèse de système massif, le caractère local des grandeurs physiques concernant le transport de la charge et de la chaleur ne sera plus verifié. Cela nous conduira à réfléchir aux propriétés de transport d'un point de vue différent par rapport aux théories, telle que la susdite théorie de Landau, généralement utilisée pour décrire les métaux macroscopiques.

Pendant les années quatre-vingt, le développement technologique, ainsi que imaginé par Feynman même vingt ans auparavant, [Feynman59], permit la production d'échantillon de plus en plus petits. De tels systèmes étaient caractérisés par des dimensions physiques qui rendaient possible une description en termes de modèles à une ou deux dimensions. Les nouveaux échantillons permirent pour la première fois d'étudier les limites de validité de l'Eq. (4), et donc une interprétation différente au niveau microscopique. Pour des tels échantillons, l'hypothèse de métal massif, nécessaire afin que l'Eq. (4) soit valable, n'est plus adéquate. Dans le chapitre suivant, nous verrons que l'hypothèse de Landau sur des particules bien écrantés n'est plus valable dans ces conditions. De fait, une nouvelle approche permettant une description nouvelle et correcte devra être suivie. Comme nous l'avons mentionné, abandonner l'hypothèse de métal massif aura des conséquences profondes.

D'après [Datta97], on pourrait dire qu'un conducteur présente un comportement

	(2DEG) GaAs/AlGaAs	CNT	Unités
Longueur d'onde de Fermi $\lambda_F = 2\pi/k_F$	40	0.74	nm
Vitesse de Fermi $v_F = k_F/m$	2.7	8.1	10^5m/s
Libre parcours moyen $l = v_F\tau$	$0.1 - 1$	~ 2	μm
Longueur de cohérence de phase L_ϕ	~ 200	~ 200	nm

Table 2: Propriétés électroniques typiques pour un 2DEG confiné dans des hétérostructures GaAs/AlGaAs, et pour un nanotube de carbone à une seul parois, CNT.

ohmique si ses dimensions linéaires sont plus grands que trois longueurs typiques: la longueur d'onde de de Broglie $2\pi/k$, k étant le vecteur d'onde de l'électron, le libre parcours moyen élastique l_e, concernant la diffusion des électrons à cause de la présence d'impuretés statiques, et la longueur de cohérence L_ϕ, c'est à dire la longueur le long de laquelle un électron peut conserver l'information concernant la phase. Toutes ces longueurs seront definies plus précisément dans les paragraphes qui suivent. Elles peuvent varier d'un métal à un autre, et elles sont influencées par des paramètres externes, comme par exemple la température. Voir le Tableau 2 pour des valeurs typiques pour deux systèmes differents.

Quand les dimensions linéaires de l'échantillon ne sont pas plus grandes que les susdites longueurs, une dépendance spatiale et temporelle *non-locale* apparaît. Nous verrons que les grandeurs physiques, comme par exemple la conductivité électrique, se comportent différemment; elles contiennent et peuvent révéler plus d'informations sur la nature de l'échantillon. En particulier, nous soulignons le rôle joué par la longueur de cohérence L_ϕ qui, si comparable aux dimensions linéaires de l'échantillon, change drastiquement la description physique. Dans le chapitre suivant, nous comprendrons mieux la raison. Ici, nous observons qu'aux très basses températures, $T \to 0$, tous les processus de diffusion ayant lieu dans l'échantillon, d'abord entre les électrons et les phonons, puis parmi les électrons, deviennent élastiques car le système est dans son état fondamental; donc une corrélation de phase bien définie avant et après les colli-

sions existe. La capacité d'un électron de conserver l'information sur la phase, jusqu'à quand un processus de rupture de phase intervient, confére aux grandeurs physiques une dépendance spatiale et temporelle non-locale; en revanche, la théorie de Landau ne fait apparaître qu'une depandance strictement locale.

Un tel comportement non-local est observé pour les propriétés à basse-énergie des systèmes physiques ayants une taille typique qui varie entre quelques dizaines de micromètres (10^{-6}m), et quelques nanomètres, (10^{-9}m). Ces systèmes, dont la taille est entre l'échelle macroscopique et l'échelle atomique, et où la longueur de cohérence peut excéder la taille de l'échantillon, sont généralement appelés systèmes mésoscopiques; ce mot fut utilisé pour la première fois par Van Kampen en 1981, [Imry02]. Nous ajoutons que par rapport aux systèmes macroscopiques, l'existence de la longueur de cohérence L_ϕ, comparable à la taille de l'échantillon, permet l'observation d'effets d'interférence qui ont une origine purement quantique.

Dans cette thèse, nous avons étudié deux différents systèmes mésoscopiques: les fils quantiques désordonnés et les métaux granulaires. Dans le reste de l'introduction, nous présentons brièvement ces systèmes et notre travail. Dans les deux cas, quelques difficultés pour les décrire en termes de la théorie de Landau apparaîssent. Par conséquant, une déviation du comportement type liquide de Fermi peut être attendu.

Le comportement de la conductance électrique pour des systèmes tels que les fils quantiques et les métaux granulaires était déjà connu, alors que le transport thermique n'avait pas encore était étudié. La question qui a guidé notre travail est si dans de tels systèmes, sous des conditions bien définies, le transport de la charge et de la chaleur peut être encore ou non décrit comme dans un liquide de Fermi. Celui-ci est le problème auquel nous avons essayé de donner une réponse pour les deux systèmes en question, en évaluant la conductance thermique, et puis vérifiant la validité de la loi de WF.

Notre travail suit la vague de la longue liste de travaux qui cherchent, depuis plusieurs années à étudier le comportement du nombre de Lorenz, et donc de comprendre le mécanisme de transport dominant, dans plusieurs systèmes différents, [Castel-

lani87, Kane96, Fazio98, Niven02, Beloborodov05, Biagini05, Ferone].

Fils quantiques

Dans la première partie de cette thèse, nous présentons les résultats sur le transport de charge et de chaleur dans les fils quantiques désordonnés, c'est à dire dans les systèmes uni-dimensionnels. A nos jours, il est possible de fabriquer des échantillons caractérisés par un potentiel de confinement très fort le long de deux directions. De tels systèmes se comportent comme des guides d'ondes électroniques, car ils présentent une conduction à la nature fortement uni-dimensionnel. Des exemples sont donnés par les nanotubes de carbone, [Tans97, Wildoer98, Odom98], ou par les hétérostructures AlGaAs/GaAs, [Tarucha95, Levy05].

L'étude concernant les systèmes 1D a été généralement focalisée sur le transport électrique, [Tarucha95, Safi95, Safi97, Maslov95, Maslov95b, VanWees88, Wharam88]. En ce qui concerne le transport thermique, expérimentalement, une mesure de la conductance thermique demande un moyen pour détecter le flux de chaleur à travers le fil. Ceci fut fait pour la première fois en 1992, en utilisant des points quantiques (QPC) comme des thermomètres extrêmement sensibles, [Molenkamp92, Appleyard98]. D'un point de vue théorique, l'expression de la conductance thermique pour un système uni-dimensionnel ne fut obtenue qu'en 1998, [Fazio98, Krive98].

Pour de tels systèmes, les hypothèses de Landau ne sont plus valables car il y a toujours au moins une direction spatiale le long de laquelle les interactions coulombiennes ne sont plus écrantées. La nécessité d'une nouvelle approche apparaît.

De tels systèmes sont généralement étudiés dans le contexte de la théorie des liquides de Luttinger (LL). Les idées fondamentales seront données explicitement dans le chapitre suivant. Ici, nous disons juste que cette théorie présente un modèle exactement soluble pour les conducteurs uni-dimensionnels pour prendre correctement en compte les interactions coulombiennes. Les états propres d'un tel système ne sont

plus les excitations de simples quasi-particules fermioniques, mais des modes collectifs qui ont un caractère bosonique: les ondes de densité de spin et de charge, qui ont une relation de dispersion linéaire. Dans notre travail, nous avons pris en compte la contribution due aux ondes de densité de charge.

Les ondes de densité de charge, aussi appelés plasmons, peuvent être vus comme les modes responsables du transport de chaleur, de même que les électrons le sont pour le transport de la charge. Les propriétés de diffusion des plasmons sont très différentes de celle des électrons, et cela a des conséquences très fortes. En particulier, cela rend les fils uni-dimensionnels extrêmement sensible à la réalisation physique: un fil infiniment long aura des propriétés de transport différentes par rapport à un fil de taille finie connecté à deux électrodes métalliques de mesure. Ces derniers sont généralement appelés réservoirs, et jouent le rôle de la source et du drain.

Les réservoirs jouent un rôle fondamental. D'un point de vue strictement pratique, les connections entre le fil et les électrodes introduisent des inhomogénéités dans le système, et donc des possibles mécanismes de diffusion qui influencent fortement le transport. Il est raisonnable d'imaginer que des telles inhomogénéités ont une taille spatiale typique $l_{\rm inh} \gg \lambda_F$, λ_F étant la longueur d'onde de Fermi. Si $l_{\rm inh}$ est l'échelle spatiale typique du désordre, alors, une telle présence n'affectera pas la propagation des électrons, car l'échelle spatiale typique pour un électron est de l'ordre de λ_F. En d'autres termes, les électrons, qui peuvent être vus comme les responsables du transport de charge ne s'apercevront pas du désordre. Ceci n'est pas le cas des plasmons qui peuvent avoir, eux, une longueur d'onde comparable à $l_{\rm inh}$; alors, ils peuvent être diffusés, et le transport thermique sera fortement affecté, [Fazio98, Krive98].

Pour un fil propre, c'est à dire un fil sans impuretés, connecté à deux réservoirs, en absence de rétrodiffusion pour les électrons, la conductance électrique n'est pas renormalisée par les interactions; elle est donnée par la valeur universelle $g_{\rm cw} = e^2/h$, [Safi97, Maslov95, Maslov95b, VanWees88, Wharam88]. En revanche, la conductance thermique est fortement renormalisée, et cela engendre une suppression du nombre de Lorenz, [Fazio98, Krive98]. Ce dernier est toujours, pour n'importe quelle température

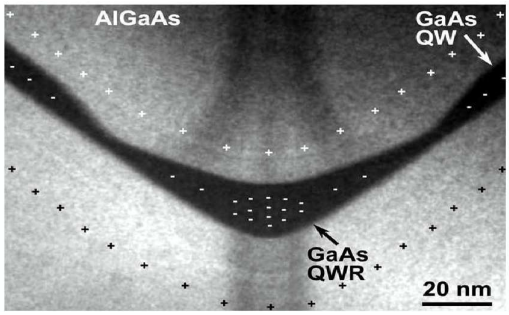

Figure 3: Image d'un fil quantique réalisé dans une hétérostructure AlGaAs/GaAs. Le fil présente un faible désordre représenté par les ondulations le long des parois de l'ordre de 10-20 nm, [Levy05].

et valeur des interactions dans le fil, plus petit que la valeur en absence d'interactions, L_0. Une telle valeur est atteinte seulement à la limite de très basses températures, $T \ll v/d$; v/d est l'échelle d'énergie caractéristique de notre système, v étant la vitesse de propagation des plasmons dans le fil, et d sa longueur. Si la température devient beaucoup plus grande que v/d, le nombre de Lorenz change lentement.

A nouveau, nous soulignons le fait que les résultats sont completement differents si le fil est infiniment long: le nombre de Lorenz est toujours plus grand que L_0. Particulièrement, si les interactions dans le fils deviennent très fortes, il diverge pour $T \to 0$, [Kane96].

Tout cela vaut pour un fil propre. La présence d'un faible désordre est, en tout cas, une caractéristique général du système. Par exemple, dans [Levy05], voir Fig. 3, le faible désordre est représenté par les ondulations le long des parois du fil, qui ont, elles, une longueur de l'ordre de 10-20 nm.

Il est naturel de se demander quelle est l'influence du désordre sur la conductivité électrique et thermique. Jusqu'ici, la correction à la conductivité électrique est connue, [Safi95, Safi97, Maslov95, Maslov95b]. Nous sommes en train d'évaluer la correction due au désordre au transport thermique; puis, nous serons capables d'évaluer le comportement du nombre de Lorenz L.

Comme nous le verrons, la variation du nombre de Lorenz dépend des corrections aux conductances électrique et thermique. A présent, à notre connaissance, très

peu de travaux existants qui permettent de determiner le signe de la correction au nombre de Lorenz, [Li02, Ferone]. En principe, elle pourrait être positive ou négative, ou elle pourrait même disparaître. Dans ce cas, la présence du désordre affecterait de la même façon le transport de la charge et de la chaleur, comme pour un métal classique.

Dans notre travail, le faible désordre a été modelisé par un potentiel du type bruit blanc (wn), et les expressions analytiques pour les corrections seront présentées dans deux régimes différents: basses, $T \ll v/d$, et hautes, $T \gg v/d$, températures.

L'évaluation des corrections aux conductances électrique et thermique est très différente; elle dépend de la nature différente des électrons, qui sont, eux, les responsable pour le transport de la charge, et les plasmons, responsable pour le transport d'énergie. Par conséquant, les contributions au transport de charge et de chaleur ne sont pas les mêmes.

Nous avons reproduit le comportement de la correction due au désordre à la conductance électrique à basses et à hautes températures. Naturellement, la présence du désordre induit une correction négative dans les deux cas.

En ce qui concerne le transport thermique, pour l'instant, nous avons reproduit l'expression de tout les différents diagrammes contribuant au transport. Leurs expressions demandent une analyse précise, et leurs évaluations en présence des interactions n'a pas encore été complétée. Nous avons verifié qu'en absence d'interactions, la loi de Wiedemann-Franz est respectée.

Métaux granulaires

Dans la deuxième partie de cette thèse, nous avons étudié les corrections dues aux fluctuations supraconductrices à la conductivité thermique dans un métal granulaire.

Souvent, en discutant de la supraconductivité, on suppose que le système est dans son état fondamental. C'est, naturellement, la possibilité la plus probable si

$T \ll T_c$. Dès que la température monte, près de T_c, la présence de l'énergie thermique de l'ordre de $\sim T$, (nous rappelons $k_B = \hbar = 1$), permettra au système de fluctuer dans d'autre états avec une probabilité finie. Ce phénomène, connu sous le nom de fluctuations supraconductrices, induit la formation de paires de Cooper même dans la phase normale en présence d'une interaction supraconductrice (BCS). En particulier, à une température $T \gtrsim T_c$, les électrons peuvent former des pairs de Cooper qui ont, eux, un temps de vie fini, le temps de Ginzburg-Landau (GL), qui est inversement proportionnel à la distance de la température critique, $\tau_{GL} \sim 1/(T-T_c)$, [Tinkham96, Larkin04]. Sous ces conditions, des phénomènes très particuliers peuvent apparaître car les propriétés de transport de la phase normale se mélangent avec celles caractéristiques de la phase supraconductrice, faisant apparaître trois différentes contributions à la conductivité: la contribution Aslamazov-Larkin (AL), aussi appelée paraconductivité, la contribution Maki-Thompson (MT), et la contribution dite densité d'états (DOS), [Larkin04]. Elles seront présentées en details dans les chapitres suivants; pour l'instant, nous ne voulons que donner une idée des phénomènes physiques qu'elles décrivent.

Le terme AL décrit la contribution au transport de la charge et de la chaleur due à la présence, à des températures $T \gtrsim T_c$, de paires de Cooper. Cette contribution est généralement positive car elle prend en compte l'aptitude des paires de Cooper à se propager facilement au travers du système. Les électrons qui forment des paires de Cooper ne seront plus disponibles pour le transport en tant que particules simples; donc, la présence des paires de Cooper implique une variation de la densité d'états à une particule près du niveau de Fermi. Il s'agit exactement de la contribution prise en compte par le terme DOS. Finalement, il y a une contribution purement quantique, la contribution MT, qui prend en considération la diffusion cohérente de deux électrons, qui forment un paire de Cooper, sur la même impureté élastique, [Larkin04].

Pour des systèmes massifs, il a été montré que les contributions DOS et MT se compensent exactement pour le transport thermique. Le seul terme qui survit est la contribution AL qui a un comportement non singulier en fonction de la température, [Niven02]. Par conséquant, dans les métaux massifs, aucun comportement singulier du

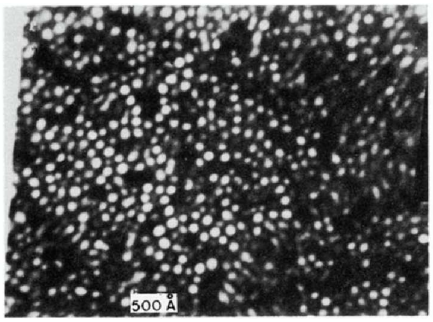

Figure 4: Image d'un film granulaire composé par des grains d'aluminium déposés sur un fond de Germanium amorphe. La taille typique des grains est de ~ 120 Å, [Shapira83].

courant thermique n'est attendu à la transition d'état normale-supraconducteur.

Un métal granulaire peut être imaginé comme un vecteur d-dimensionnel de grains métalliques renfermés dans une matrice d'isolant amorphe, avec des impuretés sur la surface et dans chaque grain. Sur la Fig. 4 une réalisation expérimentale est montrée. Les grains communiquent entre eux grâce au tunnelling à une particule, et nous supposons que la conductance tunnelling macroscopique sans dimension g_T est beaucoup plus grande que un, qui est equivalent à affirmer que le système est un bon métal. Naturellement, c'est raisonnable d'imaginer que la présence du tunnelling influence fortement les propriétés de transport. En effet, selon la température, un comportement différent, par rapport au cas massif, est observé. Comme nous le verrons, les différentes contributions présentent un comportement dépendant du tunnelling; en particulier, les termes AL et MT sont d'ordres supérieurs dans l'amplitude de tunnelling à celui de la contribution DOS. Cela donnera lieu à deux régions distinctes: dans la première, loin de T_c, le tunnelling entre les grains n'est pas efficace, et la structure granulaire prévaut. Une suppression du type $1/\epsilon$ est retrouvée, $\epsilon = (T - T_c)/T_c$ étant la température réduite. Près de la température critique, le tunnelling est efficace: une saturation de la correction est trouvée et le comportement massif est retrouvé. Dans les deux régimes, le signe de la correction n'est pas défini de façon univoque, mais dépend de la transparence de la barrière et de la compétition entre les différentes contributions.

Plan

Le manuscrit est organisé de la façon suivante.

Le prochain chapitre est dédié au principes phénoménologiques fondamentaux de la théorie du transport: du transport classique au transport quantique. Nous montrerons les succès de la théorie classique pour décrire la plupart des métaux dans des conditions ordinaires; puis, ses limites à basse température et pour des systèmes à dimension réduite. A la fin du chapitre, nous considérerons la nécessité d'une nouvelle approche pour donner une description fidèle et correcte des grandeurs physiques non-locales. De cette façon, nous allons bâtir un contexte cohérent où présenter notre propre travail.

Le reste du manuscrit est divisé en deux parties: la première concerne l'étude du transport thermique dans un fil quantique désordonné, la deuxième l'évaluation de la conductivité thermique pour un système granulaire.

Pour les fils quantiques, d'abord, nous présentons les principes de base de la théorie des liquides de Luttinger. Nous montrons les éléments nécessaires à la compréhension des propriétés pour un système uni-dimensionnel. Puis, nous présentons notre système, et motivons notre travail sur la base des expériences. Les résultats pour un fil propre sont présentés, puis le problème en présence d'impuretés est abordé.

La même structure sera suivie pour les métaux granulaires. Dans ce cas, nous allons donner un rappel de la théorie BCS, et puis les motivations pour notre travail. Finalement, nous présentons les résultats déjà connus, et ceux que nous avons trouvés concernant le transport thermique.

Chapter 1

FROM CLASSICAL THEORY TO QUANTUM EFFECTS

In this chapter, we want to discuss some fundamental aspects of the first formulated theories concerning the charge and heat transport in metals. Particularly, we will consider the ones who marked for different reasons this field. We will indicate a logical and historical development, presenting the most important achievements in the phenomenological and analytical understanding. Step by step, a coherent framework where presenting our own work will be built up.

After showing the classical foundations of the transport theory, we will see how deeply the quantum mechanics changed the way to approach such a problem in order to obtain a more faithful description. A new fundamental theory, taking partially into account the interactions among particles, was proposed by Landau. This theory, as already mentioned, is correct to describe bulk materials, where the transport properties can still be described by means of a semi-classical approach.

In the last section, we will discuss low-dimensional systems at low temperatures, where the quantum mechanical nature of particles can be no longer neglected.

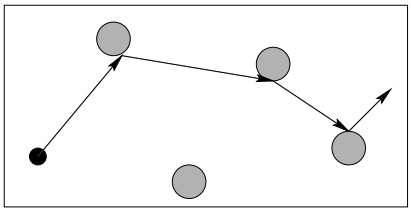

Figure 1.1: In accordance with Drude theory, collisions change drastically the velocity and the propagation direction of electrons. In absence of external fields, they propagate ballistically, and velocities before and after collisions have no correlations.

1.1 Independent particles and Drude conductivity

One of the first theories proposed to study the electrical conductivity in metals was the Drude model. In accordance with this theory, the metals are made up by heavy ions in well fixed positions, and an electron sea, to which each atom contributes with its valence electrons. The latter are not strongly bound to the nucleus, and they can propagate through the whole system.

To formulate his theory, Drude used the kinetic theory of gases, describing the above-mentioned electrons as identical hard spheres. As for a classical gas, he imagined that the interactions among electrons and among electrons and ions, between two subsequent collisions, were completely negligible. Under this assumption one speaks of *independent electron approximation* and *free electron approximation*, respectively. A consequence of the lack of any interaction is that the electron is supposed to move ballistically between two following shocks, see Fig. 1.1. The absence of interactions is one of the fundamental points of Drude theory; it will be also one of the first points to be changed when we shall consider the description of the analogous quantum mechanical system.

In accordance with the kinetic theory of gases, Drude considered collisions as sudden events able to change drastically the velocity and then the propagation direction of electrons, as shown in Fig. 1.1. Even if he guessed that the collisions were caused mostly by interactions with ions, he did not make any hypothesis about their nature. He just supposed that several diffusion mechanisms were present. Besides, in agreement

with the kinetic theory, he supposed that there were no correlations between velocities before and after shocks, [Ashcroft87]. The most important consequence of the lack of any correlations is that the state of the particle at time t does not depend on history. One speaks of *relaxation-time approximation*.

The latter is the second aspect that will be profoundly modified when we will consider the particle as a quantum mechanical object with its own quantum mechanical phase.

Drude was able to get not only qualitative, but also quantitative results. His most famous achievement is the evaluation of electrical conductivity. He found

$$\sigma = \frac{ne^2\tau}{m} \ , \tag{1.1}$$

where n is the density of charge carriers, e is the electron charge, and m is their mass. τ is the mean free time, and it plays an importante role to characterise the disorder in the system. The knowledge of conductivity allows an estimate of such a disorder as a function of τ. Generally, such a disorder is measured in terms of the so-called mobility, that is defined as $\mu = e\tau/m$. The higher is the mobility, the less disordered the system.

Notwithstanding the fact that Drude theory was not able to explain correctly the discrepancies between experimental and theoretical values of some physical quantities, as the specific heat and the thermopower, it was for long time accepted. Particularly for explaining, at least phenomenologically, the WF law; it states that the ratio between the thermal and electrical conductivity depends on temperature by a constant which is more or less material-independent. It can be expressed as

$$\frac{\kappa}{T\sigma} = \frac{\pi^2}{3e^2} = L_0 \ , \tag{1.2}$$

where e is the electron charge. The constant of proportionality L_0 is known as the Lorenz number.

Observing the properties of conductors and insulators, Drude assumed that the energy should be carried by the same conduction electrons which are responsible of charge transport and that are absent in the insulator. The relation of proportionality

in Eq. (1.2) would be nothing else but the transcription of the aforementioned Drude's statement.

In the following section, we will see that this proportionality is conserved even considering interactions between electrons as foreseen by Landau theory.

1.2 Landau hypothesis and Boltzmann equation

In 1928, Davisson and Germer proved the wave nature of electrons by means of interference phenomena experiments, [Schwabl92]; the results were in agreement with de Broglie hypothesis of 1923, where he supposed that to each particle could be assigned a frequency $\omega = E/\hbar$ and a wavelength $\lambda = 2\pi\hbar/p$; E being the energy of particle, and p its momentum.

Quantum mechanics allows the description of electrons as a wave packet obtained by the superposition of plane waves

$$\psi(\mathbf{r}, t) = \int \frac{d\mathbf{p}}{(2\pi)^3} u_p(\mathbf{r}) \exp\left[i\left(\mathbf{p}\cdot\mathbf{r} - \varepsilon(\mathbf{p})t\right)\right] . \tag{1.3}$$

$u_p(\mathbf{r})$ is the function that modulates the plane waves, and it can be, for example, a Bloch periodic function for electrons propagating in a periodic potential in bulk metals. The wave packet has its maximum value for $r \approx (\partial\varepsilon/\partial\mathbf{p})t$, and it propagates with velocity $v = \partial\varepsilon/\partial\mathbf{p}$.

Quantum mechanics replaces the hard spheres of Drude model with more complex objects having a well defined quantum mechanical phase. It is the existance of such a quantum mechanical phase that gives rise to the interference phenomena which we will speak of below. Of course, these quantum particles feel the mutual interactions, and a complete description of such interacting electrons gas is a complicated task.

Nevertheless, the formulation of a new theory taking into account, at least partially, the interactions among electrons was strongly wanted. A very important step was represented by the Landau theory of Fermi liquids.

It represents a deep evolution of Drude approach since it takes into account the

quantum mechanical nature of particles and, partially, the interactions among them, which were completely neglected until that moment. Since the first theories, scientists wanted to understand the limit of validity of independent particles assumption. Particularly, they wondered how successful this hypothesis could be in the presence of a dense electron gas as, for instance, in bulk metals, where particles interact by means of long range Coulomb forces.

Landau has shown that it is still possible to describe the system in terms of independent particles; the latter are no longer the real electrons, but a more complicated quantities, which nevertheless conserve the fermionic nature. Then, one can find for different physical quantities exactly the same expression as for an ideal Fermi gas, but with renormalised parameters.

In the following section, we show the fundamental phenomenological ideas of Landau theory, and how they allow the description of an interacting electronic gas. Of course, we do not want to present the theory in details, for which there are several textbooks, [Abrikosov88, Akkerman94, Pines89], but just to stress some important points that have been cornerstones in transport theory.

1.2.1 Independent particles and fermionic quasi-particles

The Landau theory of Fermi liquids bases itself on the properties of an ideal Fermi gas. We begin by reminding briefly some important points for a non-interacting fermionic particles system.

For a non-interacting and translationally invariant system, the single particles eigenstates are plane waves, whose energy is quantized, and it is equal to $\varepsilon_{\mathbf{k}} = \mathbf{k}^2/2m$. The ground state of N particles is the Fermi sea and the energy of the last occupied state is the Fermi energy $E_F = \mathbf{k}_F^2/2m$. The elementary excitations for such a gas are

- Adding a particle with wave vector $\mathbf{k}$. It is demanded $|\mathbf{k}| > \mathbf{k}_F$, and the energy of excitation is $\varepsilon_{\mathbf{k}} - \mu > 0$, μ being the chemical potential.

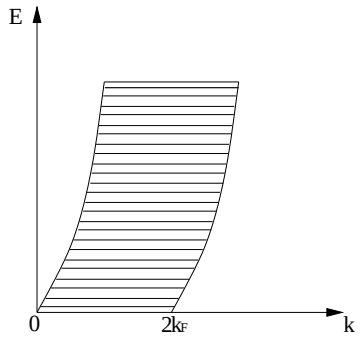

Figure 1.2: Particle-hole spectrum for system with dimension $D = 2$. There is a continuum of states different from 1D systems where it is not possible to have low-energy axcitations between 0 and $2k_F$, see Fig. 2.1(b).

- Annihilation of a particle with wave vector $\mathbf{k}$, or, equivalently, creation of a hole. In this case it is demanded $|\mathbf{k}| < \mathbf{k}_F$, and the energy of excitation is $\mu - \varepsilon_{\mathbf{k}} > 0$.

The previous kinds of excitations change the total number of particles. To build a state conserving the number, one has to take a particle with wave vector $\mathbf{k}$, such that $|\mathbf{k}| < \mathbf{k}_F$, and move it in state with wave vector $\mathbf{k}'$, with $|\mathbf{k}'| > \mathbf{k}_F$. This kind of excitation, of particle-hole type, is characterised by the two quantum numbers $\{\mathbf{k}, \mathbf{k}'\}$ and they form a continuum of states as shown in Fig. 1.2.

The fundamental idea of Landau theory, [Abrikosov88, Akkerman94, Pines89], is the existance of one-to-one correspondence between the eigenstates of the system without interactions, and the eigenstates of the same system supposed to be made up of interacting particles. Landau postulated that the ideas of Drude theory could be still used, but considering the systems to be formed of the above-mentioned interacting particles that are generally called *quasi-particles*. In other words, the spectrum of quasi-particles in a Fermi liquid with interactions between the particles can be constructed in the same way as for the ideal gas.

Let $|0, N\rangle$ be the ground state of N non-interacting fermions; let us imagine to add a particle with momentum $|\mathbf{p}| > \mathbf{k}_F$; we will indicate the new state as $|\mathbf{p}, N+1\rangle = a^\dagger_{\mathbf{p}}|0, N\rangle$, $a^\dagger_{\mathbf{p}}$ being the creation operator for a particle with momentum $\mathbf{p}$. Let us suppose, now, to switch on the interactions. If the system is translationally invariant,

interactions will conserve the total momentum, and the new state will always have the same momentum $\mathbf{p}$. For the energy, it is more complicated. Interactions among the added particle and the ones making up the Fermi sea, and the interactions among the electrons already present, will modify the distribution in the $\mathbf{k}$-space, and they will change the energy of the state. The ensemble made up by the particle with momentum $\mathbf{p}$ and the perturbated distribution of the others is the so-called *quasi-particle*.

The limit in using the concept of quasi-particle is represented by the need that it has a well defined life-time. It is possible to show that it is finite for each quasi-particle; particularly, for excitations close to $\mathbf{k}_F$, the relaxation time behaves as $1/\tau \propto (\varepsilon - E_F)^2 + T^2$. Then, the quasi-particles are well defined close to Fermi energy and for relatively low temperatures. From the latter expression, one realises that the Landau theory is useful for phenomena which happen on an energy scale much smaller than the Fermi energy.

The energy of a single quasi-particle can be easily evaluated.

Let us consider the ground state made up by the ensemble of quasi-particles and that is characterised by the following distribution

$$n_0(\mathbf{k}) = \begin{cases} 1 & : \quad |\mathbf{k}| < \mathbf{k}_F \\ 0 & : \quad |\mathbf{k}| > \mathbf{k}_F \end{cases} \tag{1.4}$$

The variation in the occupation number for a quasi-particle can be written as $n_0(\mathbf{k}) \rightarrow n_0(\mathbf{k}) + \delta n(\mathbf{k})$, where $\delta n(\mathbf{k}) = 1$ corresponds to the creation of a quasi-particle, while $\delta n(\mathbf{k}) = -1$ of a quasi-hole. At the lowest order in $\mathbf{k}$, since we are mainly interested in phenomena in the vicinity of $\mathbf{k}_F$, the energy of a single quasy-particle in the system can be written as

$$\varepsilon^0_{\mathbf{k}} = \frac{\mathbf{k}_F}{m^*}(|\mathbf{k}| - \mathbf{k}_F), \tag{1.5}$$

where m^* is the effective mass, and it takes into account the renormalization due to interactions in the electron gas.

Because of the interactions, if one adds a particle, a work shall be done, and the energy of an added particle will be no longer simply given by Eq. (1.5), but by a more

complicated expression depending on the form of interactions between quasi-particles, [Akkermans94],

$$\varepsilon_{\mathbf{k}} \propto \varepsilon^0_{\mathbf{k}} + \sum_{\mathbf{k}'} f(\mathbf{k}, \mathbf{k}')\delta n(\mathbf{k}'). \tag{1.6}$$

$\varepsilon^0_{\mathbf{k}}$ is defined in Eq. (1.5), while $f(\mathbf{k}, \mathbf{k}')$ takes into account the presence of the others quasi-particles, and the interactions between them; see [Akkermans94] for a more detailed discussion on the expression of the f-function.

In accordance with Landau hypothesis, since the non-interacting particles obey Fermi-Dirac statistics, the quasi-particles will obey to the same statistics, too; then, the occupation probabilty is,

$$n(\mathbf{k}) = \frac{1}{e^{\beta\varepsilon_{\mathbf{k}}} + 1}\ , \tag{1.7}$$

where $\varepsilon_{\mathbf{k}}$ is the energy of an added quasi-particle and not the bare energy $\varepsilon^0_{\mathbf{k}}$ given in Eq. (1.5). By means of Eq. (1.7), one can evaluate all the physical quantities. The difference that will arise with respect to the values for non interacting particles, is that some parameters as the mass will be renormalised because of the interactions. At higher temperatures, higher order corrections are demanded; anyway, in this case, the lifetime of particles is no longer well defined.

Landau theory was originally formulated for the ^{3}He, and then extended to other systems, as for example, the conduction electrons of a metal.

Quantitave calculations using Landau theory are not always correct, since it does not take into account some possible phenomena as electron-phonon interactions, for instance. This is not the case for Coulomb interactions which are correctely taken into account, including screening effects, as shown by Abrikosov by means of Green's functions, [Abrikosov75].

To conclude, if we can describe the metallic systems in terms of non-interacting (quasi-)particles, we can use a semi-classical equation, as the Boltzmann equation, to describe the transport.

1.2.2 Boltzmann equation

Quasi-classical theory of transport foresees the use of a non-equilibrium distribution function $g(\mathbf{r}, \mathbf{k}, t)$ able to describe the average occupation number of quasi-particles per state and energy; it is defined such that the quantity $g(\mathbf{r}, \mathbf{k}, t)d\mathbf{r}d\mathbf{k}/4\pi^3$ represents the number of electrons at time t, in the phase space in the element of volume $d\mathbf{r}d\mathbf{k}$ centered in $(\mathbf{r}, \mathbf{k})$. At equilibrium, $g(\mathbf{r}, \mathbf{k}, t)$ corresponds to the Fermi distribution in Eq. (1.7). Generally, in the quasi-classical distribution, it is demanded that the characteristic length of spatial variation in the system is much larger than the Fermi wavelength.

Let us consider a bulk metal to which a small gradient of potential and temperature are applied. After a while, in the system a stationary regime state will be reached; that is, there will be a balance between the external gradient which tends to perturb the system and the diffusion processes which oppose to the perturbation. There is a competition between these two phenomena. The distribution function $g(\mathbf{r}, \mathbf{k}, t)$ satisfies the Boltzmann equation

$$\frac{\partial g}{\partial t} + \mathbf{v}\frac{\partial g}{\partial \mathbf{r}} + \mathbf{F}\frac{\partial g}{\partial \mathbf{k}} = -\frac{g - f}{\tau} \ , \tag{1.8}$$

where $\mathbf{F}$ is the force on each quasi-particle, which generally depends on the applied external fields, and $\mathbf{v} = \dot{\mathbf{r}}$ is the velocity of the particles. From Eq. (1.8), it is possible to obtain all the information concerning the evolution of the system and of the quantities that allow its description. If we apply an electrical field $\mathcal{E}$ and a temperature gradient ∇T, for the electrical and thermal current densities the following expressions hold, [Ashcroft87]

$$\mathbf{j} = L^{11}\vec{\mathcal{E}} + L^{12}(-\nabla T) \ , \tag{1.9a}$$

$$\mathbf{q} = L^{21}\vec{\mathcal{E}} + L^{22}(-\nabla T) \ , \tag{1.9b}$$

where L^{ij} are the so-called transport coefficients that can be found from Eq. (1.8). We stress that the previous densities are local quantities, exactly as in Eq. (4) in the Introduction. Eqs. (1.9a) and (1.9b) link the external fields with the charge and heat density currents at the same time in the same position. This is a crucial point, since,

as we will see, for mesoscopic systems there will be no longer a local dependence.

For the transport coefficients, one gets the following results

$$L^{11} = \frac{ne^2\tau}{m} \equiv \sigma, \;\; L^{21} = TL^{12} = -\frac{(\pi T)^2\sigma'}{3e}, \;\; L^{22} = \frac{\pi^2 T}{3e^2}\sigma \equiv \kappa \; , \tag{1.10}$$

where $\sigma' = \partial\sigma(\varepsilon)/\partial\varepsilon|_{\varepsilon=\varepsilon_F}$ and

$$\sigma(\varepsilon) = e^2\tau(\varepsilon) \int \frac{d\mathbf{k}}{4\pi^3}\delta(\varepsilon - \varepsilon(\mathbf{k}))\mathbf{v}(\mathbf{k})\mathbf{v}(\mathbf{k}) \; . \tag{1.11}$$

The expression for electrical conductivity coincides with the one found by Drude. The existance of such an equality represents a further proof that Landau image of the electron sea made up by independent quasi-particles is correct. The expression of L^{22} shows the existance of a relation of proportionality between σ and κ, which is exactly the Wiedemann-Franz (WF) law, mentioned before and generally written as

$$\frac{\kappa}{\sigma T} = \frac{\pi^2}{3e^2} = L_0 \; , \tag{1.12}$$

where L_0 is the Lorenz number. The latter plays a very important role, since it is a signature of the Fermi liquid behaviour, and then the signature of well defined transport properties. The validity of Eq. (1.12) has been confirmed in the case of arbitrary impurity scattering, [Chester61]

Being able to evaluate for a system, under well defined conditions, the behaviour of Lorenz number means understanding whether or not a Fermi liquid description for charge and heat transfer is appropriate. On the contrary, the possible deviation gives a measure of how much the system is far from a Fermi liquid state.

This is the reason why, in the last years, more and more works investigated the behaviour of the Lorenz number and its possible variations for various systems, to test its robustness in very different conditions, [Castellani87, Kane96, Fazio98, Niven02, Beloborodov05, Biagini05, Ferone].

Drude claimed that the charge and heat carriers were the same, and this was proved by the WF law. Now, in accordance with the Landau theory, we can state that the carriers are the same, and they are the Landau fermionic quasi-particles.

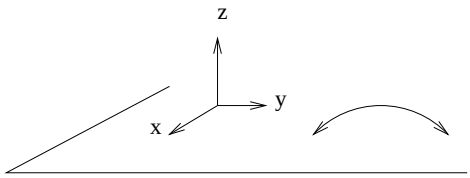

Figure 1.3: In low-dimensional systems, there is always a direction along which the strong Coulomb interactions are no longer negligible. For example, in the figure, for a 2D-gas, along the z-direction no screening effect can be imagined, unless a gate electrode is used along the surface of the gas.

1.3 Low temperatures and low-dimensional systems: quantum effects

The theories we have presented treat the electrons, more or less, as non-interacting hard spheres. We want to go beyond such a description.

There are particular situations where the Landau theory would produce wrong results; particularly, in many cases, the phenomenological foundations are no longer valid.

In the previous sections, we stated that the Landau theory was originally formulated for ^{3}He which is characterised by short-range interactions. With respect to its original formulation, the theory was then extended to several different systems, particularly the conduction electrons in metals. The problem was then solved for such a system, taking into account the Coulomb interactions, which are long-range interactions. That was possible, considering the screening effects due to the presence of the electron sea.

For low-dimensional systems, the screening effects change drastically, as simply shown in Fig. 1.3. In this case, along z-direction, it is not possible to consider any screening effect, except in presence of a possible gate electrode. Phenomenologically, the Landau theory is no longer appropriate to still describe the systems as composed by non interacting quasi-particles.

If the Landau theory is no longer useful, one may expect different dominating transport properties in the sample. Particularly, one can wonder whether the WF

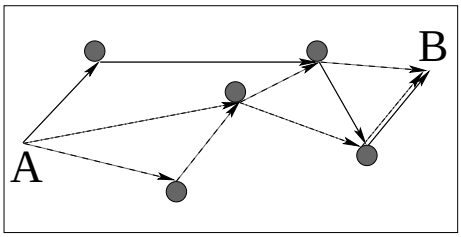

Figure 1.4: In a real cristal, impurities and defects are randomly distributed. The length for various trajectories from a point A to a point B is different, and non-constructive interference effects can rise.

law is still valid, or, on the contrary, the charge and heat transfer is now differently characterised. In principle, different mechanisms could contribute separately to their transfer.

The strongly reduced screening for low-dimensional systems is the first point that makes the Landau theory not useful in some conditions. It is not the only one.

When we have discussed the Drude model, we pointed out that before and after each collision, there were no correlations between the velocities of ingoing (i) and emerging (f) particle; that is $\langle v_f v_i \rangle = 0$, in agreement with the kinetic theory of gases. We wonder what happens for the quantum mechanical phase of a particle.

Let us consider all the possible trajectories for a particle propagating from a point A to a point B in a quasi-1D or in a higher dimensional system, as shown in Fig. 1.4.

In a very general way, the intensity of transport from point A to point B can be written as

$$I(A \to B) = \sum_{i,j} u_i u_j^* = \sum_i |u_i|^2 + \sum_{i \neq j} u_i u_j^* \ , \tag{1.13}$$

where u is a generic propagating amplitude.

The first term on the rhs of Eq. (1.13) corresponds to the contribution of each trajectory, while the second one represents the interference effects between the trajectories. In a real crystal, different sources of scattering exist: impurities or defects randomly distributed, phonons, interactions with the other electrons. Two different cases should be considered:

- Diffusive processes are caused by static elements, as impurities or defects.

- Diffusive processes are caused by dynamical elements, as lattice vibrations (phonons), and other electrons.

In the first case, the processes are always elastic, and a well defined relationship concerning the phase difference between the two different patterns exists. This difference can conserves for a long time, and such a time is called the coherence time τ_ϕ.

In the second case, because of the dynamic of diffusing processes, the phase difference changes randomly in time; then, the coherence is destroyed, and no interference effects can rise.

Let us suppose, now, that the temperature goes to zero; then, the system tends to go into its ground state. All the dynamical processes strongly reduce; the vibrational lattice modes freeze, and even the electron-electron interactions diminish, with a relaxation time which behaves as $\sim T^2$, as mentioned in Section 1.2.1. Indeed, the diffusion rate depends on the energy of the electron with respect the Fermi one; this difference is small, because of the low temperatures, then, the diffusion rate lowers, since the most of the states will be already occupied. Then, at low temperatures, even the electron-electron diffusions, which represent the most important contribution in this regime, become less and less important. We point out that electron-electron interactions can modify τ_ϕ, but not the mean free path l_e, since the Coulomb forces do not change the total momentum.

Then, at low temperatures, since the system is in its ground state, all the processes become elastic and the dynamical contributions, the only ones which could destroy the information about the phase, disappear.

If the scattering processes are elastic, then a well defined phase correlation exists before and after the collisions. The length along which an electron is able to conserve information about its phase is generally called coherence length L_ϕ.

If we are in a regime where the phase-relaxation time τ_ϕ is of the same order as

the mean free time τ_e, as in the high-mobility semiconductors, then

$$L_\phi = v_F \tau_\phi \ , \tag{1.14}$$

v_F being the Fermi velocity. In the opposite limit $\tau_\phi \gg \tau_e$, electron undergoes several collisions, each of them after an average time τ_e, before loosing the phase. After each collision, the velocity is completely randomised. If $v_F \tau_e$ is the average path between two following collisions, then the root mean squared distance along the θ-direction is

$$L_\phi^2 = \frac{\tau_\phi}{\tau_e}(v_F \tau_e)^2 \langle \cos^2 \theta \rangle \ , \tag{1.15}$$

where the ratio τ_ϕ/τ_e represents the number of collisions in the time τ_ϕ. From the previous equation,

$$L_\phi^2 = \frac{1}{2} v_F^2 \tau_e \tau_\phi \ . \tag{1.16}$$

Since $D = v_F^2 \tau_e/2$ defines the diffusion constant, the coherence length reads

$$L_\phi = \sqrt{D\tau_\phi} \ . \tag{1.17}$$

The existance of the coherence length introduces a *non-local* dependence of the physical quantities, since, their state at time t depends on all previous moments, that is on history. Then, the *relaxation-time approximation* used in Drude model and characterizing Landau theory too, can be no longer used.

Today, the technological development allows to make samples whose size is of the order of some micrometer. These kind of systems, which can be really clean, are often characterised, at very low temperatures, by a coherence length L_ϕ which largely exceeds the size of the sample. These systems are generally called mesoscopic systems.

In the macroscopic world, the size of the systems is generally much larger than L_ϕ, and the quantum effects are not visible. To understand why it happens, one can think, for such bulk systems, of a sample divided in several microscopic domains, each of them characterised by a coherence length producing independent interference patterns. By averaging over the whole sample, quantum effects disappear, and the electrical conductivity, just to give an example, is determined by the Drude value. One

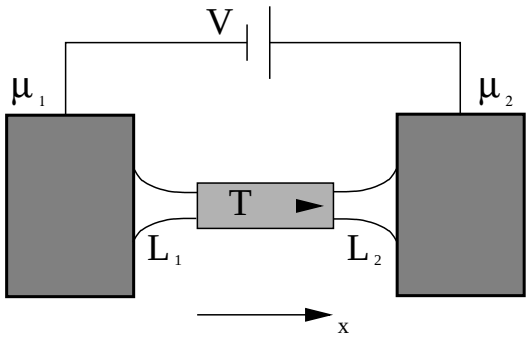

Figure 1.5: The current in a conductor can be evaluated in the framework of Landauer approach, where each particle has an average probability T to propagate through the conductor. Under the assumption that such a probability is one for an open transport channel, the conductance is quantised and it reads $G = 2e^2/h$ for a one-mode conductor.

speaks then of self-averaging systems. This is no longer the situation for a mesoscopic system, where interference effects can be well visible since $L < L_\phi$.

One of the most common effects of the mesoscopic regime, are, for example, the universal conductance fluctuations, [Imry02]. These phenomena have been called universal since the observed fluctuations for electrical conductance are independent from the size of the system, from the nature of the disorder, and from the dimension of the sample. Evaluating the root mean square of the conductivity fluctuations, $\delta g = \sqrt{\langle g^2 \rangle - \langle g \rangle^2}$, for N samples which are characterised by a different realization of the disorder, one finds that the amplitude of the fluctuations does not depend on the details of the system, as mentioned above. We stress that this is strictly true just for the amplitude. One finds that such fluctuations take up a value of the order $\sim e^2/h$. Of course, for each sample, the interference patterns will be different depending on the disorder configuration. Then, the mesoscopic samples are not self-averaging systems.

1.3.1 Non-interacting quantum particles: theory and experiments

In the seventies, Landauer proposed an approach to describe mesoscopic systems which revealed very useful, [Landauer70]. In term of this approach, the current prop-

agating through a conductor is written in function of the average probability electrons have to diffuse through it. The fundamental idea is quite simple and we show some details, because of the importance of such theory in treating the mesoscopic transport.

Refering to Fig. 1.5, we want to evaluate the current through a conductor which is characterised by an average probability T that an electron propagate through it. Let the conductor be connected to two reservoirs, characterised by distribution functions f_1 and f_2, by means of two ballistic leads L_1 and L_2. We suppose that the leads are reflectionless; it means that the probability to be reflected for a particle coming out from the lead to the reservoir is negligeable, [Datta97]. Let μ_1 and μ_2 be the Fermi level in the two reservoirs, with $\mu_1 > \mu_2$, and let us suppose that we are at zero temperature. In this case, since no energy fluctuations can be present, the transport will take place just in the energy range $\mu_2 < E < \mu_1$.

Let I_1^+ be the current transmitting from lead L_1 into the conductor; then, if T is the average transmission probability, the current in the lead L_2 will be $I_2^+ = TI_1^+$, while the current reflected in L_1 is $I_1^- = (1-T)I_1^+$. In each moment, the net current flowing in the system is $I = I_1^+ - I_1^- = I_2^+ = TI_1^+$. Then all the problem is to evaluate I_1^+.

Since the contacts are reflectionless, the current from left reservoir in lead L_1 will be carried by particles characterised by a positive wave vector $+k_x$. Such a current can be written as

$$I^+ = \frac{e}{L}\sum_k v_k f_1(E_k) = \frac{e}{L}\sum_k \frac{\partial E}{\partial k} f_1(E_k)\ , \tag{1.18}$$

where env_k is the current for an electron gas with electron density $n \propto L^{-1}$, and where each particle propagates with velocity v_k. L is the length of the conductor. At zero temperature, the distribution will not depend on temperature, but it will be characterised just by the value μ, that is by the applied voltage. Then, the net current will read

$$I_1^+ = I^+ - I^- = \frac{2e}{h}\int_{-\infty}^{\infty} M(E)\left[f_1(E) - f_2(E)\right] dE\ , \tag{1.19}$$

where $M(E)$ is the number of mode contributing to the transport, that is the number of energy levels involved in the transport, and inclused in the energy window $\mu_1 - \mu_2$. In the following, a more formal definition of modes will be given. At zero temperature, and if the number of modes is supposed to be constant between μ_2 and μ_1, Eq. (1.19) will read as

$$I_1^+ = \frac{2e^2}{h} M \frac{\mu_1 - \mu_2}{e} \ . \tag{1.20}$$

Finally, the net current in the conductor in Fig. 1.5 is

$$I = \frac{2e}{h} MT(\mu_1 - \mu_2) \ , \tag{1.21}$$

and the conductance reads

$$G = \frac{2e^2}{h} MT \ . \tag{1.22}$$

In terms of resistance, the latter equation can be written as

$$G^{-1} = \frac{h}{2e^2 M} \frac{1}{T} = G_C^{-1} + G_S^{-1} \ , \tag{1.23}$$

where G_C^{-1} is the contact resistance and G_S^{-1} reads

$$G_S^{-1} = \frac{h}{2e^2 M} \frac{1-T}{T} \ , \tag{1.24}$$

and it represents the resistance due to the presence of the scatterers inside the conductor.

1.3.2 Thermo-electric transport at finite temperature

In the same context, but with a more general hypothesis about temperature, the problem of thermo-electric transport of non-interacting quantum particles has been solved by Sivan and Imry, [Sivan86]. They have considered a disordered sample connected to two reservoirs which present a very small potential and temperature gradient, $\delta\mu$ and δT respectively, between them. In the sample, all the scattering processes are

elastic, while the inelastic ones take place only in the reservoirs. They evaluate the electrical and heat current between the two reservoirs, finding

$$\begin{pmatrix} \mathbf{J} \\ \mathbf{Q} \end{pmatrix} \propto \int dE \begin{pmatrix} e \\ E \end{pmatrix} \mathcal{T}(E)[f_l(E) - f_r(E)] \, , \tag{1.25}$$

where e and E represent the electronic charge and the heat transported, while $\mathcal{T}(E)$ is the transmission coefficient. The latter depends on the energy transported through the different channels, and f_l and f_r are the Fermi distributions for the left and right reservoirs. The charge and heat current, in terms of the external field, read

$$\mathbf{J} = G\frac{\delta\mu}{e} + \beta\delta T \, , \tag{1.26a}$$

$$\mathbf{Q} = -\beta T\frac{\delta\mu}{e} + Z\delta T \, . \tag{1.26b}$$

Eqs. (1.26a) and (1.26b) are formally the same we have found before, Eqs. (1.9a) and (1.9b), but they are non-local, that is the current depends on the electric field not in the same point, but upon integration on all the possible points. The currents do not depend on positions as in the previous ones. In Eq. (1.25), they show a dependence on the global quantities characterizing the system. The transport coefficients in Eqs. (1.26a) and (1.26b) can be evaluated, and in the linear regime, they read

$$G = \frac{2e^2}{h}T(E_F), \;\; \beta = \frac{2\pi^2 eT}{3h}T(E_F), \;\; Z = \frac{2\pi^2 T}{3h}T(E_F) \, , \tag{1.27}$$

If we suppose that the transmission coefficient is constant over the energy range where the transport occurs, then $\mathcal{T}(E_F) \sim \mathcal{T}$, and one finds the expression in Eq. (1.22) for a one-mode conductor. By writing the total transmission coefficient as the sum over the single mode transmission coefficient $\mathcal{T}_i$, one observes that for a single channel, the conductance is quantised in unity of $2e^2/h$, where the factor two takes into account the spin degeneracy.

In 1988, the conductance of a quantum point contact (QPC) made by means of a 2D electron gas confined at the interface of GaAs/AlGaAs heterostructure has been measured, [Vanwees88]. The point contacts were defined by electrostatic depletion of the gas underneath a gate electrode. The maximum width of the device was about

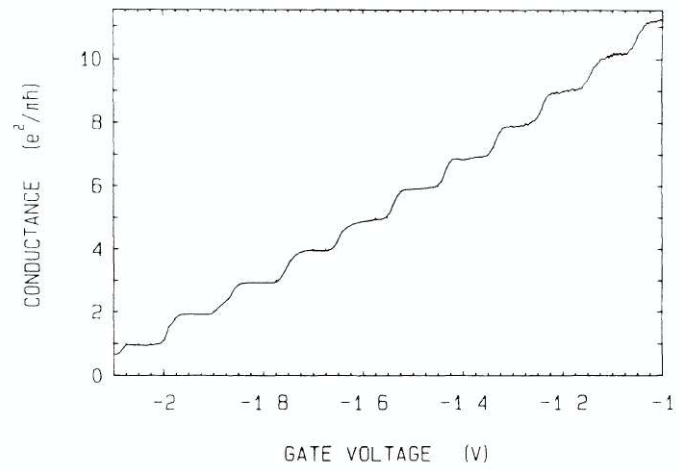

Figure 1.6: Quantised conductance of a ballistic quantum point contact. Each step represents the activation of a mode controlled by means of the gate electrode. The width of the constriction is about $\sim$ 250nm, and the transport is completely ballistic, [Vanwees88].

$\sim$ 250nm, while the mean free path was estimated being $l_e = 8.5\mu$m. The conductance in function of the gate voltage is ploted in Fig. 1.6. The strong confining potential is the cause of the quantization of transverse momentum in the contact constriction. Such a strong confinement makes that just the electrons of lowest energy subbands participate to transport. The other modes are separated by large energy gap of the order of $\sim eV$. They can be activated by means of a gate potential, exactly as they did in the above-mentioned experiment. The above quantization can be seen as a special case of the multichannel Landauer formula

$$G = \frac{e^2}{\pi} \sum_{n,m=1}^{N} |\mathcal{T}_{nm}|^2, \tag{1.28}$$

for transmission coefficients $|\mathcal{T}_{nm}|^2 = \delta_{nm}$ corresponding to ballistic transport with no channel mixing. Then, in the QPC, just one mode per time can be activated to contribute to the transport. The other modes can be controlled by means of the gate potential. The same results were found simultaneously in [Wharam88].

If the electrical conductance is quantised, one can wonder what happens for the thermal conductance. The WF law, that can be written in term of transport coefficients presented in Eq. (1.27), claims that such a quantization should be found for the

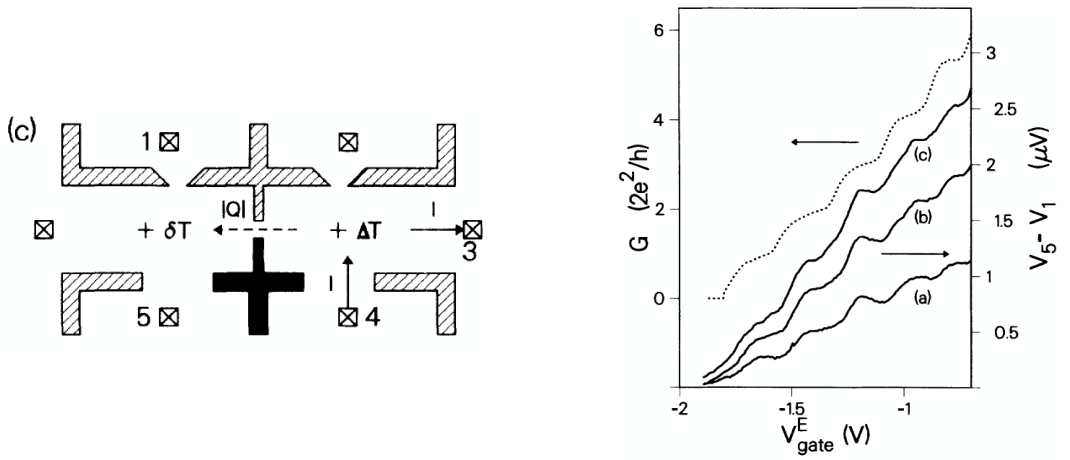

Figure 1.7: *Left*: Experimental apparatus used to measure the thermal conductance of a QPC. The central QPC is the one whose conductance has been measured, while the two lateral adjoining QPC are used as real sensible thermometers. *Right*: Solid lines represent the thermal conductance for different samples. They are quite well visible the steps of quantization in correspondence of the jump of the electrical conductance (dotted line), [Molenkamp92]

thermal transport too. Indeed, it is what was found in 1992, [Molenkamp92].

They were able to measure the thermal conductance of a QPC, using two adjoining QPC as real sensible thermometers. The system they used, made by means of a 2D gas confined in a AlGaAs/GaAs heterostructure, is presented in Fig. 1.7-left. They used Ohmic contacts numbered as 3 and 4 as current source and drain. This current caused the heating of the 2D electron gas at the right of the central QPC. The temperature difference between the left and the right side of the central QPC gave rise to a heat flow Q. The latter caused a small temperature rise in the left side of central QPC, and this rise could be detected by means of the thermovoltage $V_5 - V_1$ which is proportional to the thermal conductance. The measurements are plotted in Fig. 1.7-right. The classical steps are quite well visible, and they occur in correspondence with the jump for electrical conductance.

After showing the most important achievements of the transport theories which have been formulated in the last century, we can better understand the need of different approach for particular systems, and then, their characteristic behaviour. Other important elements will be given in the remaining chapters.

Résumé en français du chapitre 1

Le premier chapitre est dédié aux principes phénoménologiques fondamentaux de la théorie de transport: du transport classique au transport quantique. Nous présentons tout au long du chapitre, comment les différentes théories qui se sont succédées ont apporté, petit à petit, les briques nécessaires à la compréhension des phénomènes de transport, et donc de la nature microscopique des métaux.

D'abord, nous présentons les principes énoncées par Drude qui ne font pas du tout intervenir la nature quantique de l'électron, qui, lui, fut traité, au début du XX siècle, comme une sphère n'ayant pas d'interactions avec les autres électrons. Pour étudier les propriétés de transport des électrons dans un métal, Drude n'utilisa que la théorie cinétique des gaz. A l'aide de cette théorie Drude fut capable d'obtenir même des résultats quantitatifs, dont notamment l'expression de la conductivité électrique, qui porte aujourd'hui son nom. En observant les propriétés de transport des métaux et des isolants, Drude imagina que la charge et la chaleur devaient être transportées par les mêmes entités. Cette proportionnalité est exprimée par la loi de Wiedemann-Franz qui lie les conductivités électrique et thermique.

Les résultats obtenus par Drude à l'aide d'une théorie purement classique furent confirmés ensuite par la théorie de Landau; celle-ci prend en compte la nature quantique de l'électron, et partiellement la présence des interactions parmi les électrons dans un métal. Cependant, la théorie affirme qu'à condition que l'écrantage entre deux électrons donnés soit fort, à cause de la présence des autres électrons, alors, le système peut continuer à être décrit comme étant composé par des particules indépendantes, mais qui ne sont plus les vrais électrons, mais des particules beaucoup plus complexes,

appelés quasi-particules qui conservent leur caractère fermionique.

Les hypothèses de fort écrantage ne sont pas pertinantes pour les systèmes de taille réduite. Cela comporte qu'une nouvelle approche doit être envisagée. En plus, à très basse température, les systèmes sont caractérisés par une longueur ayant une nature purement quantique, la longueur de cohérence, L_ϕ. La présence d'une telle longueur change de façon drastique le comportement des grandeurs physiques décrivant le transport dans l'échantillon, et la nature quantique des électrons; aussi, les interactions de nature coulombiennes avec les autres électrons ne peuvent plus être négligés.

En fin de chapitre, d'importants résultats concernant le transport électrique et thermique pour des particules quantiques sont présentés.

PART I

DISORDERED QUANTUM WIRES

Chapter 2

LUTTINGER LIQUID THEORY

The inadequacy of Landau theory to describe low-dimensional systems forces to consider new and more suitable models which can take into account the phenomena that characterise them.

One of the most studied system which does not present a typical Fermi liquid behaviour is the one-dimensional gas of interacting electrons (1DEG). In accordance with a model proposed by Tomonaga and Luttinger, concerning spinless interacting fermions, generally one speaks of Tomonaga-Luttinger liquids and Tomonaga-Luttinger liquid theory, [Tomonaga50, Luttinger63, Mahan00].

In the following of this thesis, we will discuss particularly of the version proposed in 1963 by Luttinger, and for a sake of simplicity, we will speak of Luttinger liquids (LL). The first steps for a complete and correct solution were made in 1965 by Mattis and Lieb, [Mattis65].

In the following sections, we will present the foundations of such a model, writing the Hamiltonian and finding the eigenstates, pointing out the differences with respect to a Fermi liquid. To better understand the characteristics of our system, we start from the properties of a one-dimensional system. It presents some interesting and very particular aspects. The description of such peculiarities will lead to the formal definition of a Luttinger liquid. For detailed reviews, see [Mahan00, Schulz95, Haldane81, Voit94].

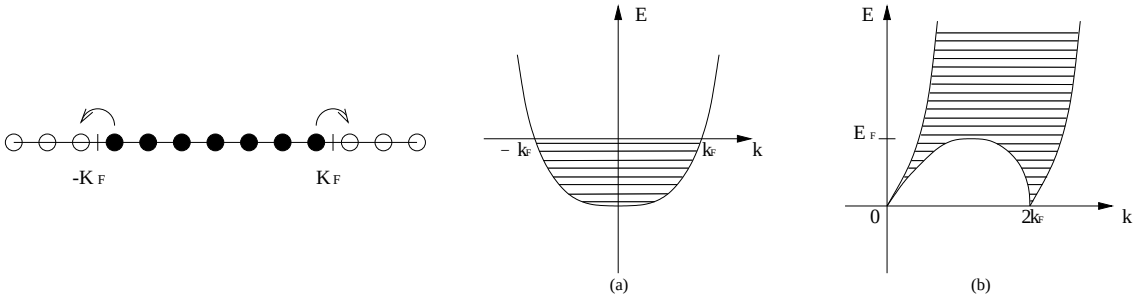

Figure 2.1: 1D Fermi gas. *Left*: The Fermi surface reduces to two points and the ground state is constituted by the particles included between $-k_F$ and k_F. A particle-hole excitation has bosonic character. *Right*: (a) Single particle spectrum. (b) Particle-hole spectrum. 1D systems are characterised by the lack of low energy excitations for value of k included between zero and $2k_F$.

2.1 1D Fermi gas and Luttinger liquid Hamiltonian

A 1D gas of non-interacting electrons presents some characteristics which are different with respect to higher-dimensional systems, since the Fermi surface reduces to two discrete points. Such a peculiarity can be observed in Fig. 2.1, where the dispersion relations for a single particle and for a particle-hole pair are shown. From Fig. 2.1-right(b), one observes the absence of low energy excitations for values of k included between zero and $2k_F$. This is not the case, for instance, for 2D systems as shown in Fig. 1.2.

For energies much smaller than the Fermi energy, the spectrum is divided into two different regions, where the dispersion relation can be described as linear. This is a very important point, since it allows the analytical solution of the problem. We will use the opportunity to linearize the dispersion relation for the fermions to solve exactly the model.

First of all, we observe that for a 1D system, the ground state is made up by the ensemble of particles included between $-k_F$ and k_F, as shown in Fig. 2.1-left. In such a system, an excitation is equivalent to move an electron in one of the available states characterised by a momenum $|k| > k_F$. Such a process involves two fermionic particles: a particle-hole pair, and then has a bosonic character. No transversal mode can alter such an excitation. Consequently, one can expect a similar behaviour for the

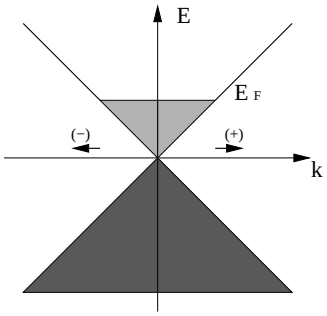

Figure 2.2: Single particle spectrum for a Luttinger liquid. The dispersion relation is linearized; the darker area represents non-physical states added to the system to make it solvable.

wave function, too.

The hypothesis behind the Luttinger model is that the electronic system is composed by two different kinds of fermions: the ones whose energy spectrum is given by $\varepsilon_k = kv_F$, generally called right-moving $(+)$, and the left-moving $(-)$, whose energy spectrum reads $\varepsilon_k = -kv_F$. In other words, the Hilbert space of a Luttinger liquid is not the usual for an electronic system, but it is extended to include a portion of positrons, too. They represent non-real physical states for the system, but they are necessary to make the model mathematically solvable. From a physical point of view, since such an excitation would require a large excitation energy, one can think they will not influence the low-energy spectrum of the system. Finally, the single-particle spectrum is given in Fig. 2.2.

At this point, we can write the non-interacting Hamiltonian; let a and b be the fermionic operators for right-moving and left-moving particles, respectively; the free Hamiltonian reads

$$H_0 = v_F \sum_k k(a_k^\dagger a_k - b_k^\dagger b_k) \,, \tag{2.1}$$

where a and b satisfy the usual fermionic commutation relations

$$a_\alpha a_{\alpha'}^\dagger + a_{\alpha'}^\dagger a_\alpha = \delta_{\alpha\alpha'}, \qquad\qquad a_\alpha a_{\alpha'} + a_{\alpha'} a_\alpha = 0. \tag{2.2}$$

Let us point out that we are, at the moment, considering spinless fermions; as already said, in our work, we considered just charge density waves contribution. In the following, we will see what the presence of spin indices would involve.

We introduce the density operators for the two kinds of particles

$$\rho_+(q) = \sum_k a^\dagger_{k+q} a_k \ , \qquad\qquad \rho_+(-q) = \sum_k a^\dagger_k a_{k+q} \ , \tag{2.3}$$

where $q > 0$, and equivalent expressions for operator b.

In order to write the Hamiltonian H_0 in Eq. (2.1), in term of the density operators defined in Eq. (2.3), we observe that they satisfy the following commutation relations:

$$[\rho_+(-q), \rho_+(q')] = [\rho_-(q), \rho_-(-q')] = \delta_{qq'} \frac{qL}{2\pi} \ , \tag{2.4a}$$

$$[\rho_+(q), \rho_-(q')] = 0 \ . \tag{2.4b}$$

The evaluation of previous commutation relations is quite easy, except than for the one in Eq. (2.4a), if $q \neq q'$. One finds

$$[\rho_+(-q), \rho_+(q)] = \sum_k (\hat{n}_{k-q} - \hat{n}_k) \ . \tag{2.5}$$

To evaluate the right-hand term, we consider a state with all the levels below a given value $k_0 < k_F$ occupied, but with a non-defined number of electron-hole excited pairs elsewhere, [Schulz95]. Then,

$$\begin{aligned} \sum_k (\hat{n}_{k-q} - \hat{n}_k) &= \left(\sum_{k \geq k_0} + \sum_{k < k_0} \right) (\hat{n}_{k-q} - \hat{n}_k) \\ &= \sum_{k \geq k_0} (\hat{n}_{k-q} - \hat{n}_k) \\ &= \sum_{k \geq k_0 - q} \hat{n}_k - \sum_{k \geq k_0} \hat{n}_k \\ &= \sum_{k_0 - q \leq k < k_0} \hat{n}_k = \frac{Lq}{2\pi} \ . \end{aligned} \tag{2.6}$$

Eqs. (2.4a) and (2.4b) define bosonic commutation relations, and they mirror the bosonic character of the action of operators ρ. Let us explain better this point.

The operator $\rho_+(q)$, with $q > 0$, describes the destruction of one particle in the state with wavevector k, and the creation of another particle in the state with wave

vector $k+q$. Particularly, if $k < k_F$ and $q+k > k_F$, then an electron-hole excitation with momentum q and energy $v_F q$ has been created. Equivalently, the operator $\rho_-(-q)$, with $q > 0$, will create bosonic excitations for the left-moving particles; it moves a particle from the state with wave vector $k + q > -k_F$ to one with wave vector $k < k_F$. The excitations created by the two operators always have a bosonic character.

In a very similar way, one can evaluate the commutators of the density operators with Hamiltonian H_0:

$$[H_0, \rho_+(q)] = v_F q \rho_+(q), \qquad [H_0, \rho_-(q)] = -v_F q \rho_-(q) \; . \tag{2.7}$$

Finally, in term of the density operators, the Hamiltonian H_0 can be written as

$$H_0 = \frac{2\pi v_F}{L} \sum_{q>0} [\rho_+(q)\rho_+(-q) + \rho_-(-q)\rho_-(q)] \; . \tag{2.8}$$

Starting from a Hamiltonian written in terms of fermionic operators, Eq. (2.1), we came to an expression in function of bosonic operators in Eq. (2.8).

The density operators can be written directly, for the sake of simplicity, in terms of creation and annihilation bosonic operators

$$\rho_+(q) = c_{1q}^\dagger \left(\frac{qL}{2\pi}\right)^{1/2} , \qquad \rho_+(-q) = c_{1q} \left(\frac{qL}{2\pi}\right)^{1/2} , \tag{2.9a}$$

$$\rho_-(q) = c_{2,-q} \left(\frac{qL}{2\pi}\right)^{1/2} , \qquad \rho_-(-q) = c_{2,-q}^\dagger \left(\frac{qL}{2\pi}\right)^{1/2} . \tag{2.9b}$$

As a function of bosonic operators c and $c^\dagger$, the Hamiltonian in Eq. (2.8) reads

$$H_0 = \sum_{q>0} q v_F (c_{1q}^\dagger c_{1q} + c_{2,-q}^\dagger c_{2,-q}) \; . \tag{2.10}$$

2.2 Interaction Hamiltonian and diagonalization

Hamiltonians in Eqs. (2.8) or (2.10) describe a non-interacting electron gas. In real systems, electrons interact because of long-range Coulomb forces.

The model conserves perfectly solvable if one takes into account the possible

interaction terms due to Coulomb interactions. Particularly, for spinless electrons, interactions are represented by the two forward scattering processes

$$(k_F, -k_F) \longrightarrow (k_F, -k_F), \qquad (k_F, k_F) \longrightarrow (k_F, k_F) \; . \tag{2.11}$$

The Hamiltonian describing such processes, in term of density operators, reads

$$H_{\rm int} = \frac{1}{2L} \sum_q \{ V_{1q} [\rho_+(q)\rho_+(-q) + \rho_-(-q)\rho_-(q)] + V_{2q} \rho_+(q)\rho_-(-q) \} \; . \tag{2.12}$$

The first term V_1 describes processes where an excitation, no matter if one speaks for right or left moving particles, is created, and another one, of the same kind is distroyed to preserve the total momentum: second process in Eq. (2.11). The second term V_2 describes processes where two excitations are created: first process in Eq. (2.11).

Finally, the total Hamiltonian is given by the sum of three terms

$$H = H_0 + V_1 + V_2 \; , \tag{2.13}$$

and, as a function of bosonic operators c, it reads

$$H = \sum_{q>0} \varepsilon_1 (c^\dagger_{1q} c_{1q} + c^\dagger_{2,-q} c_{2,-q}) + \sum_{q>0} \varepsilon_2 (c_{1q} c_{2,-q} + c^\dagger_{1q} c^\dagger_{2,-q}) \; , \tag{2.14}$$

where, for the sake of simplicity, we set $\varepsilon_1 = q(v_F + V_{1q}/2\pi)$, and $\varepsilon_2 = qV_{2q}/2\pi$.

Eq. (2.14) can be diagonalised by means of the following Bogoliubov transformation

$$c_{1q} = \alpha^*_q \gamma_{1q} - \beta_q \gamma^\dagger_{2q} \; , \tag{2.15}$$

$$c^\dagger_{2,-q} = -\beta^*_q \gamma_{1q} + \alpha_q \gamma^\dagger_{2q} \; . \tag{2.16}$$

The first condition on coefficients α_q and β_q is given by the bosonic nature of operators γ. In order to have the correct commutation relations for such operators, the coefficients have to satisfy the condition

$$|\alpha_q|^2 - |\beta_q|^2 = 1 \; . \tag{2.17}$$

The second condition is given by the cancellation of the non-diagonal terms

$$\varepsilon_2(|\alpha_q|^2 + |\beta_q|^2) - 2\varepsilon_1\alpha_q\beta_q = 0 \ , \tag{2.18}$$

with a similar equation for the hermitian conjugate terms.

By solving with respect the modulus square, and by means of Eq. (2.17), one finds for the coefficients α_q and β_q the following solutions

$$|\alpha_q|^2 = \frac{\varepsilon_2^2}{2\varepsilon_2^2 - 2\varepsilon_1^2 + 2\varepsilon_1\omega} \ , \tag{2.19a}$$

$$|\beta_q|^2 = \frac{2\varepsilon_1^2 - \varepsilon_2^2 - 2\varepsilon_1\omega}{2\varepsilon_2^2 - 2\varepsilon_1^2 + 2\varepsilon_1\omega} \ , \tag{2.19b}$$

with

$$\omega = \omega_q = (\varepsilon_1^2 - \varepsilon_2^2)^{1/2} \ . \tag{2.20}$$

Finally, the diagonalised hamiltonian reads

$$H = \sum_{q>0} \omega_q(\gamma_{1q}^\dagger\gamma_{1q} + \gamma_{2q}^\dagger\gamma_{2q}) \ , \tag{2.21}$$

where ω_q defines the spectrum, and it is given by Eq. (2.20), and can be written explicitly as

$$\omega_q = |q|[(v_F + V_{1q}/2\pi)^2 - (V_{2q}/2\pi)^2]^{1/2} \ . \tag{2.22}$$

What is the nature of the eigenmodes of the system, whose spectrum is given by the last equation?

The bosonic operators γ are linear combinations of density operators $\rho_\pm$. Then, the eigenmodes are collective oscillations of charge density. Their energy depends both on the kinetic term and on the interactions between the particles, as shown in Eq. (2.22).

2.3 Hamiltonian in term of bosonic operators in real space

Some of the properties we have shown in the previous sections can be reformulated in a different way. In order to evaluate some important quantities, as the single particle Green's function which will be useful for the calculation of conductance, we want to show how a fermionic operator, representing a single particle, can be written in term of Bose operators by mean of bosonization technique. The mathematical formulation of bosonization technique has solid foundations. We just want to discuss some of their characteristics. For a detailed review, see [Vondelft98, Mahan00].

The bosonization technique allows to write a fermionic field operator $\psi_\eta(x)$ in function of bosonic field $\phi_\eta(x)$; the fermionic field is expressed as $\psi_\eta \sim U_\eta e^{-i\phi_\eta}$, where U_η is the so called Klein factor which allows to raise or lower the number of fermions and which assures that the fermionic operator satisfies the correct commutation relations. Physically, bosonization is simply justified by the bosonic nature of excitations in 1D system, as mentioned before.

In order to write differently the Luttinger liquid Hamiltonian, we introduce the two bosonic fields, [Schulz95, Haldane81, Voit94]

$$\phi(x) = -\frac{i\pi}{L}\sum_{q\neq 0}\frac{1}{q}e^{-\alpha|q|/2-iqx}[\rho_+(q)+\rho_-(q)] - N\frac{\pi x}{L}\,, \tag{2.23}$$

$$\Pi(x) = \frac{1}{L}\sum_{q\neq 0}e^{-\alpha|q|/2-iqx}[\rho_+(q)-\rho_-(q)] + J/L\,, \tag{2.24}$$

with $N = N_+ + N_-$ and $J = N_+ - N_-$, $N_\pm$ being the number of added left or right-moving particles, respectively, and α a small cut-off parameter. The operators ϕ and Π satisfy the canonical commutation relation: $[\phi(x), \Pi(y)] = i\delta(x-y)$.

In terms of ϕ and Π operators, the fermionic field operator reads

$$\psi_\pm = \lim_{\alpha\to 0}\frac{1}{\sqrt{2\pi\alpha}}U_\pm \exp[\pm ik_F x \mp i\phi(x) + i\theta(x)]\,, \tag{2.25}$$

with $\theta(x) = \pi\int_{-\infty}^{x}\Pi(x')dx'$, and $U_\pm$ being the above-mentioned Klein factors.

The total Hamiltonian in Eq. (2.13) can be now written in terms of ϕ and Π

operators:

$$H = \int \left[\frac{\pi v g_{LL}}{2} \Pi^2(x) + \frac{v}{2\pi g_{LL}} (\partial_x \phi)^2 \right] , \tag{2.26}$$

where

$$v = [(v_F + V_{1q}/2\pi)^2 - (V_{2q}/2\pi)^2]^{1/2} , \qquad g_{LL} = \left[\frac{2\pi v_F + V_{1q} - V_{2q}}{2\pi v_F + V_{1q} + V_{2q}} \right]^{1/2} . \tag{2.27}$$

The Hamiltonian in Eq. (2.26) is exactly the one describing an elastic string, whose eigenmodes correspond to density fluctuations for the Luttinger liquid. The spectrum is given by Eq. (2.22); v in Eq. (2.27) is the renormalised velocity of plasmons, and g_{LL} gives the information about the interactions inside the conductor.

We stress again that there are no single particle excitations. This can be understood by thinking intuitively to what happens for a 1D systems. If one imagines that a particle is slightly moved from its equilibrium position, it will start interacting with its nearest neighbours, transferring part of its momentum to them. Its neighbours will behave anologously with their neighbours, giving rise to the propagation through the whole system of initial excitation. This is true only for 1D systems, since for higher-dimensional ones, such propagating modes are accompained by transversal modes demanding an appropriate description.

2.3.1 LL Hamiltonian from semi-classical equation of motion

In this section, we want to discuss, without presenting all the details which are given in Appendix A, how it is possible obtaining the same expression as in Eq. (2.26), starting from the semi-classical equation of motion, [Gramada97]. Such a discussion will allow to understand, from a different point of view, the physical meaning of all the terms in the Hamiltonian in Eq. (2.26).

The semi-classical equation of the motion in the wire, treated as a real liquid, is given by the Euler equation

$$mn \frac{d^2 u}{dt^2} = -en\mathcal{E} - \frac{dP}{dx} , \tag{2.28}$$

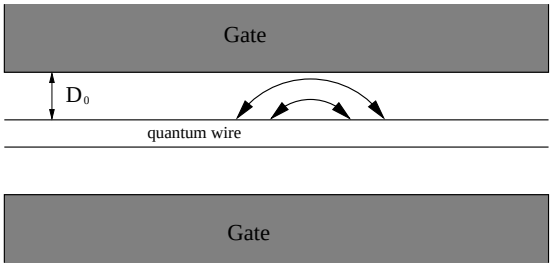

Figure 2.3: Experimentally, the conductor is never isolated. It is always screened by means of a gate electrode at a distance $D_0 \gg \lambda_F$. In this way, only the the short-range interactions, short with respect to the length of the wire, are selected. Then, the interaction potential in the wire can be written as $V(x, x') = V_0\delta(x - x')$.

where m is the mass of an electron; $u(x,t)$ is the displacement in the fermionic system; $n(x,t)$ describes the electronic density: $n(x,t) = n_0(x) + n_1(x,t)$, where n_1 describes the temporal fluctuations; $\mathcal{E}(x,t) = \mathcal{E}_0(x) + \mathcal{E}_1(x,t)$ is the electric field which we can imagine to write as the sum of a static and a dynamic term; $P = \pi^2\hbar^2 n^3/3m$ is the hydrostatic pressure.

As studied in the previous sections, there are two terms taking into account the electron-electron interactions, as written in Eq. (2.12). Since the nature of these interactions is the same, one can set $V_{1q} = V_{2q}$.

Let $V(x)$ be the electron-electon interaction potential. Then, the dynamical components of the electric field $\mathcal{E}_1$ can be thought as generated by the charge density fluctuations represented by $n_1(x,t)$

$$e\mathcal{E}_1 = -\frac{d}{dx}\int dx' V(x - x')n_1(x', t) \ . \tag{2.29}$$

The problem in Eq. (2.29) is represented by the form of the interaction potential $V(x)$. From an experimental point of view, the conductor is never isolated. It is always screened at a distance $D_0 \gg \lambda_F$, see Fig. 2.3. Such a physical constriction select just some components of interactions, since the long range interactions will be cut-off. As a result, one just conserves interactions which are short-ranged with respect to the length of the wire d which is much larger than D_0. This condition allows to write the

interaction potential in the wire in the simple form

$$V(x,x') = V_0\delta(x-x') \ , \tag{2.30}$$

with $V_{1q} = V_{2q} = V_0$. Of course, one could imagine to work on different scales, but then the potential in Eq. (2.30) would assume a more complicated form.

Under the previous assumption, the Eq. (2.29) is easily evaluable

$$e\mathcal{E}_1 = -V_0\frac{dn_1(x,t)}{dx} \ . \tag{2.31}$$

Linearizing the equation of motion with respect to $n_1(x,t)$, and imposing the energy conservation law, skipping all the details, presented in the Appendix A, one finds for the Luttinger liquid Hamiltonian

$$H_0 = \int dx \left[\frac{\hat{p}^2(x)}{2mn(x)} + \frac{1}{2}\left(V_0 + \frac{\pi^2}{m}n(x)\right)(\vec{\nabla}n(x)\hat{u})^2\right] \ , \tag{2.32}$$

where the displacement $u(x)$ has been treated as an operator, and $\hat{p}$ is its conjugate momentum; they satisfy the canonical commutation relation $[\hat{u}(x), \hat{p}(x')] = i\hbar\delta(x-x')$.

Eq. (2.32) is formally identical to Eq. (2.26); from Eq. (2.32), we see that the Luttinger liquid Hamiltonian is made up of a pure kinetic term, and a potential term. The latter can be identified as an harmonic potential describing the oscillations of a particle around its equilibrium position.

2.4 Spin-1/2 fermions and spin-charge separation

We finish this chapter, by considering spin-1/2 fermions Luttinger liquid.

The Hamiltonian for a 1D interacting spin-1/2 fermions, together with the charge density waves, has one more collective excitations: spin density waves. The charge density waves respond to external perturbation as the electrical fields. The spin density waves respond to magnetic perturbation. In 1965, Overhauser has shown that the spectrum is completely described by the sum of the two different excitations, [Mahan00].

In the same way we have described the charge density waves, one can defines again the density operators as follows

$$\rho_{+,s}(q) = \sum_k s a^\dagger_{k+q,s} a_{k,s} \ , \qquad \rho_{+,s}(-q) = \sum_{k,s} s a^\dagger_{k,s} a_{k+q,s} \ , \tag{2.33}$$

where $s = \pm$ is the spin index; of course, there are equivalent relations for left-moving particles.

For spin-1/2 fermions, it is not possible to write a backward scattering process as a forward one for different indices: $(k_F, s; -k_F, t) \to (-k_F, s; k_F, t)$.

The Hamiltonian reads

$$\begin{aligned} H &= \sum_{s,q>0} \omega_q (c^\dagger_{1,s,q} c_{1,s,q} + c^\dagger_{2,s,-q} c_{2,s,-q}) + \sum_{q>0} \left[\frac{qV'_{1q}}{4\pi} (c^\dagger_{1,s,q} c_{1,s,q} + c^\dagger_{2,s,-q} c_{2,s,-q}) \right. \\ &+ \frac{qV_{1q}}{4\pi} (c^\dagger_{1,s,q} c_{1,-s,q} + c^\dagger_{2,s,-q} c_{2,-s,-q}) \\ &\left. + \frac{qV_{2q}}{4\pi} \sum_{s'} (c_{1,s,q} c_{2,s',-q} + c^\dagger_{2,s,-q} c^\dagger_{1,s',q}) \right] . \end{aligned} \tag{2.34}$$

The exchange contribution is taken into account in the previous Hamiltonian, since the interaction potentials are assumed different.

The Hamiltonian can be diagonalised by means of bosonic coordinates, R_q and Σ_q, to describe the charge and spin oscillations, respectively. It can be written as the sum of two terms

$$H = H_\rho + H_\sigma \ , \tag{2.35}$$

$$H_\sigma = \sum_{q>0} \left[\bar{\omega}_q^2 - \left(\frac{qV_{1q}}{4\pi} \right)^2 \right]^{1/2} (\Sigma^\dagger_q \Sigma_q + \overline{\Sigma}^\dagger_q \overline{\Sigma}_q) \ , \tag{2.36}$$

$$H_\rho = \sum_{q>0} \left[\left(\bar{\omega}_q + \frac{qV_{1q}}{4\pi} \right) (R^\dagger_q R_q + \overline{R}^\dagger_q \overline{R}_q) + \frac{qV_{2q}}{2\pi} (R_q \overline{R}_q + R^\dagger_q \overline{R}^\dagger_q) \right] \ , \tag{2.37}$$

where $\bar{\omega}_q = q v_F$.

H_σ is diagonal, while H_ρ can become diagonalised by means of a Bogoliubov

transformation; then, one finds

$$H_\rho = \sum_{q>0} E_q(\gamma_{1q}^\dagger\gamma_{1q} + \gamma_{2q}^\dagger\gamma_{2q}) , \tag{2.38}$$

$$E_q = \left[\left(\bar{\omega}_q + \frac{qV_{1q}}{2\pi}\right)^2 - \left(\frac{qV_{2q}}{2\pi}\right)^2\right]^{1/2} . \tag{2.39}$$

In real space, the fermionic field can be written in a form analogous to Eq. (2.25), but with a supplementary index

$$\psi_{\pm,s} = \lim_{\alpha\to 0}\frac{1}{\sqrt{2\pi\alpha}}U_{\pm,s}\exp[\pm ik_F x - i(\pm(\phi_\rho(x)+s\phi_\sigma(x))+(\theta_\rho(x)+s\theta_\sigma(x)))\sqrt{2}] , \tag{2.40}$$

where we introduced the field $\phi(x)$ for the two spin projections separately

$$\phi_{\rho,\sigma} = \frac{1}{\sqrt{2}}(\phi_\uparrow \pm \phi_\downarrow) . \tag{2.41}$$

The full Hamiltonian takes the form

$$H = H_\rho + H_\sigma + \frac{2V'_{1q}}{(2\pi\alpha)^2}\int dx\cos(\sqrt{8}\phi_\sigma) , \tag{2.42}$$

where H_ρ and H_σ have the same form as in Eq. (2.26), with the only difference that the velocity v and the operator ϕ and Π have a supplementary subscript identifying either charge propagation or spin propagation. Particularly, the velocity for charge and spin density waves read

$$v_\sigma = \left[v_F^2 - \left(\frac{V'_{1q}}{4\pi}\right)^2\right]^{1/2} , \tag{2.43a}$$

$$v_\rho = \left[\left(v_F + \frac{V_{1q}}{2\pi}\right)^2 - \left(\frac{V_{2q}}{2\pi}\right)^2\right]^{1/2} . \tag{2.43b}$$

Once we got the spectrum, we can show a very important and general feature of a 1D interacting gas.

Let us suppose to create a particle in the fundamental state at the time $t = 0$ in the point x_0:

$$\langle 0|\psi_+(x_0)\rho(x)\psi_+^\dagger(x_0)|0\rangle = \delta(x - x_0) , \tag{2.44}$$

$$\langle 0|\psi_+(x_0)\sigma(x)\psi_+^\dagger(x_0)|0\rangle = \delta(x - x_0) . \tag{2.45}$$

Let us consider the time evolution of charge and spin distributions; the time dependence can be, of course, obtained by means of respective Hamiltonian. One gets

$$\begin{aligned}\langle 0|\psi_+(x_0)\rho(x,t)\psi_+^\dagger(x_0)|0\rangle &= \delta(x-x_0-v_\rho t)\frac{1+g_{LL}^\rho}{2}+\delta(x-x_0+v_\rho t)\frac{1-g_{LL}^\rho}{2}\ ,\\ \langle 0|\psi_+(x_0)\sigma(x,t)\psi_+^\dagger(x_0)|0\rangle &= \delta(x-x_0-v_\sigma t)\ .\end{aligned}$$

Since, the velocities are completely distinct, after a while the charge and spin modes will be completely separated in the space. Then, one speaks of spin-charge separation, which is a characteristic of such a system.

Résumé en français du chapitre 2

L'inadéquation de la théorie de Landau à décrire des systèmes de taille réduite oblige à considérer des modèles pouvants prendre en compte les phénomènes qui les caractérisent. Parmi les systèmes les plus étudiés, et qui ne présentent pas un comportement type liquide de Fermi, il y a le gaz uni-dimensionnel d'électrons en interactions. Ces types de systèmes sont généralement étudiés dans le contexte de la théorie des liquides de Luttinger.

D'abord, il est nécessaire de noter que pour un système uni-dimensionnel la surface de Fermi se réduit à deux points. Une excitation correspond au déplacement d'un électron d'un état avec vecteur d'onde $|k| < k_F$ vers un autre état caractérisé par un vecteur d'onde $|k| > k_F$. Un tel processus entraîne deux particules fermioniques, et donc a un caractère bosonique.

La théorie de liquides de Luttinger permet d'écrire en termes d'opérateurs bosoniques un Hamiltonien décrivant les modes propres d'un système uni-dimensionnel: les ondes de densité de charge, et les ondes de densité de spin. Dans notre travail, nous n'avons considéré que la contribution des ondes de densité de charge.

Dans ce chapitre, nous montrons comment il est possible d'écrire l'Hamiltonien de notre système uni-dimensionnel, puis nous calculons ses états propres. Cela nous servira dans le chapitre suivant, où nous allons évaluer les contributions de ces modes propres au transport électrique et thermique.

Chapter 3

QUANTUM WIRES AND LORENZ NUMBER

In the previous chapter, we have presented the basic concepts allowing the description, under well defined assumptions, of a 1D interacting system. Particularly, we have seen that the low-energy excitations are no longer single-particle excitations but collective modes: the charge density waves, also called plasmons, which have linear spectrum.

In this chapter, we introduce the concept of quantum wire presenting the way to model it, in accordance with Luttinger liquid theory, which allows to evaluate its transport properties.

First, we will show the results for a clean quantum wire, that is a wire without impurities; the different scattering properties between electrons and plasmons yield drastic effects: the Lorenz number is strongly renormalised. Such results will be, then, the starting point to tackle the problem of corrections induced by disorder.

The important role played by disorder in the transport properties in one-dimensional conductors was brought out by Tarucha *et al.* in 1995, [Tarucha95]. They have studied the conductance of semiconductor quantum wires in function of the gate voltage for different samples. Some results are shown in Fig. 3.1. The dependence of

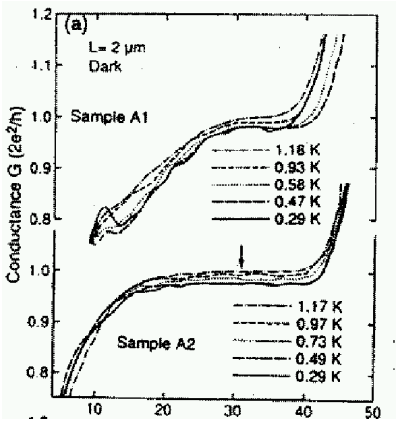

Figure 3.1: The conductance of two samples is plotted as a function of the gate voltage measured in mV, [Tarucha95]. The plateaux region depends on temperature, and such a dependence points out the role played by disorder. Coulomb interactions cannot explain alone such a dependence; they do not affect the mean free path and then the conductance. It is the presence of the disorder and of the interactions which renormalise the transmission through the conductors, and then the conductance in function of the temperature.

the plateaux on temperature is well visible. For clean samples, the tranport is supposed to be ballistic; the Coulomb interactions do not affect the electron mean free path, since they conserve the total momentum. Then, the transport cannot depend on temperature, and one will recover the quantum of conductance e^2/h. In presence of disorder, the system is no longer translationally invariant. Impurities scatter off electrons, and the mean free path reduces. At higher temperatures, the kinetic energy of electrons close to the Fermi level rises, and the transmission is advantaged. At lower temperatures the transmission will be no longer unitary, and the conductance lowers, as shown in Fig. 3.1. Higher mobility electrons in 1D gases do not show such a strong dependence on temperature variations, [Tarucha95]. Another experiment where the dependence of the conductance plateau on the temperature is well visible is shown in [Yacoby96].

In our work we investigate the behaviour of thermal and electrical conductance, in presence of disorder and as a function of the temperature.

The expression of the conductances are given in term of the Green's function describing the transport in the system. Then, a large part of the chapter will be de-

voted to its evaluation.

To make the reading fluent, we report the calculations in dedicated appendixes, where most of them are developped in details for the interested reader.

3.1 Clean quantum wires

Let us consider the propagation of a particle in a 2D conductor, which is homogeneus along the x-axis and with a confining potential along the y-axis. Particularly, to get a simple analytic solutions, one can imagine a parabolic confining potential,

$$U(y) = \frac{1}{2} m\omega_0^2 y^2 \ . \tag{3.1}$$

Then, by solving the corresponding Scrhödinger equation, the spectrum is found to be given by the sum of two terms

$$E(n,k) = \frac{\hbar^2 k^2}{2m} + \hbar\omega_0 \left(n + \frac{1}{2} \right) \ . \tag{3.2}$$

Along the x-axis, one has plane waves, whose eigenvalues are represented by the first term in the rhs of Eq. (3.2); along the transversal y-direction, the confining potential strongly influences the transport. Indeed, each value of n in Eq. (3.2) identifies a different transversal mode, where the distance between two following subbands is $\hbar\omega_0$. The larger ω_0, the stronger is the confinement, and further in energy are the different modes. Then, at low energies, only the first subband contributes to the transport. Such modes are the same already introduced in Section 1.3.1. Experimentally, examples of 1D conductors, are given by AlGaAs/GaAs heterostructures, [Tarucha95, Levy05], and carbon nanotubes, [Tans97, Wildoer98, Odom98]. In the latter, the energy separation between two subbands can achieve the order of $\sim eV$. Experimentally, such systems behave as an electron waveguide, since the transversal dimension can be of the order of some nanometer, then, comparable to Fermi wavelength λ_F. Such experimental systems behaving as 1D conductors are generally called quantum wires.

Before discussing the role played by disorder, we present the results which are already known for a clean quantum wire connected adiabatically to two two-dimensional

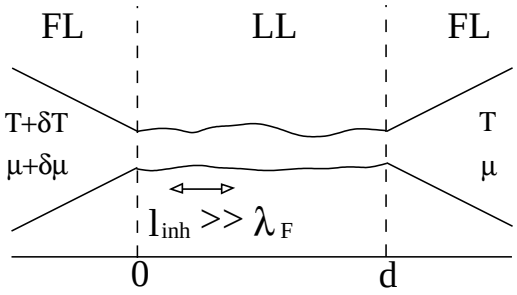

Figure 3.2: Disordered quantum wire connected to two FL reservoirs. All the inhomogeneities are supposed to have a characteristic spatial length scale $l_{\rm dis} \gg \lambda_F$. The different scattering properties of electrons and low-energy long-wavelength excitations (plasmons) yield drastic effects on charge and heat transport. The flow of charge and energy current is assured by the gradient of the chemical potential $\delta\mu$ and temperature δT, respectively.

reservoirs. They will be the starting point for our own work.

A quantum wire can be roughly represented as in Fig. 3.2. T and μ are the temperature and the chemical potential, respectively. In the figure, a disordered quantum wire is shown, and the disorder is represented as undulations on the side-walls of the wire. Indeed, this represents a real experimental set-up; see Fig. 3 in the Introduction.

In Fig. 3.2, all kind of inhomogeneitis in the wire are supposed to have a typical spatial length which is much larger than λ_F. Particularly, this is true for the disorder represented by the connections to reservoirs; of course, for a clean quantum wire, such connections represent the only source of disorder.

As we have already seen, the hamiltonian of a LL can be written as

$$H_0 = \int dx \left[\frac{\hat{p}^2(x)}{2mn(x)} + \frac{1}{2}\left(V_0 + \frac{\pi^2}{m} n(x) \right) (\nabla n(x)\hat{u})^2 \right] , \tag{3.3}$$

where the displacement $u(x)$ has been treated as an operator, and $\hat{p}$ is its conjugate momentum; they satisfy the canonical commutation relation $[\hat{u}(x), \hat{p}(x')] = i\hbar\delta(x-x')$; $n(x)$ is the electronic density, which we take constant: $n(x) = n_0 = mv_F/\pi$.

It has been shown, first experimentally, then theoretically, that for a clean one-mode quantum wire connected to two FL reservoirs the electrical conductance is not renormalised by the interactions inside the wire, with respect to the universal value e^2/h per spin, [Safi95, Safi97, Maslov95, Maslov95b, VanWees88, Wharam88], where the last two references concerne more specifically quantum point contact. For charge

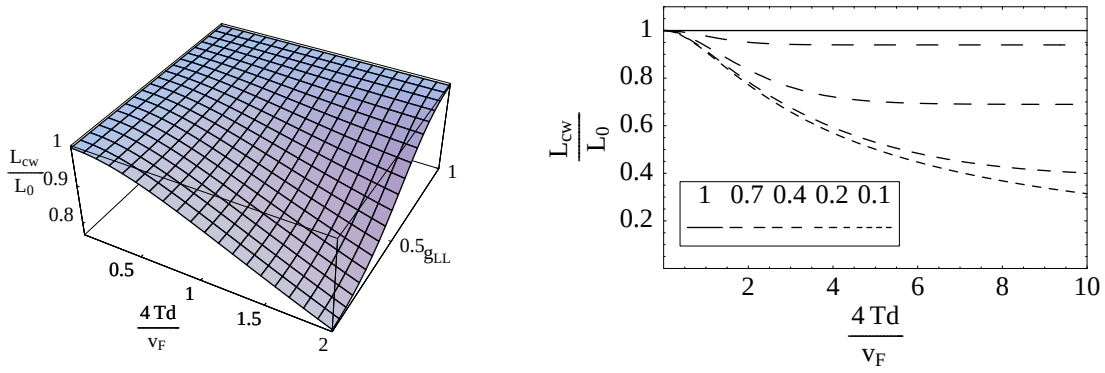

Figure 3.3: Lorenz number for a clean quantum wire. *Left*: 3D plot of Lorenz number for a clean quantum wire renormalised with respect to the classical value L_0 in function of dimensionless temperature $4Td/v_F$ and interactions strength g_{LL}. *Right*: Lorenz number for a clean quantum wire renormalised with respect to the classical value L_0 in function of dimensionless temperature $4Td/v_F$ for different values of g_{LL}.

transport, only the contact resistance plays an important role. There are no other renormalizing scattering processes taking place in the wire, and the universal value follows from the Landauer approach.

For the thermal conductance, the behaviour changes drastically. In Fig. 3.3, the Lorenz number as a function of temperature and interactions strength is plotted, [Fazio98, Krive98]. Up to a constant, it represents the behaviour of thermal conductance, too. The Fig. 3.3 shows a very different behaviour with respect to the classical theory. First of all, the classical value of the Lorenz number is recovered just in two different cases:

- The Luttinger parameter g_{LL} is equal to one.
- The temperature goes to zero.

Let us discuss the two previous points.

g_{LL} is the so called Luttinger parameter; it describes the strength of interactions inside the wire: $g_{LL} = 1$ stands for non-interacting particles, $g_{LL} < 1$ stands for repulsive interactions. g_{LL} will be defined analytically later.

For non-interacting electrons, at high temperatures, the system tends to behave as an ensemble of classical particles. The quantization of conductance no longer holds,

or at least is strongly smeared out by temperature; then, the transport properties are well described by the Boltzman equation, and by the classical value of Lorenz number L_0. For non-interacting quantum particles, as mentioned, the problem has been solved by Sivan and Imry in the context of Landauer approach, [Sivan86]; again, one finds the classical value from Eq. (1.27).

Instead, if the temperature goes to zero, then, statistically, the dominant contribution is given by long-wavelength plasmons. Particularly, if $T = 0$, then, at least in principle, just the infinite wavelength plasmons will contribute to the transport. The latter will not perceive the presence of the constriction represented by the wire, then they will have a perfect transmission; in other words, in this limit, the system reduces to an infinite FL reservoir and, again, the classical value L_0 is recovered.

What about the renormalization for $T \neq 0$?

We have mentioned that all the inhomogeneities in the wire are characterised by a spatial length scale $l_{\text{inh}} \gg \lambda_F$, as shown in Fig. 3.2. Electric transport will be not affected by such a presence; electrons, which can be seen as the responsible of the charge transport, will not perceive it at all, since they have a characteristic spatial length scale of the order of λ_F. This is no longer the case for the plasmons: there will always exist a value ω^* of the energy, whose corresponding wavelength can be comparable to l_{inh}; such excitations can suffer backscattering processes at the edges of the wire. This is the reason why the thermal conductance, and then the Lorenz number, present a strongly renormalization as show in Fig. 3.3.

Such a peculiar behaviour of plasmons gives rise to what is sometimes called *energy-charge separation*: the electron can propagate easily through the wire, but not all the energy can do it as well. The dissipated energy is given to the reservoirs.

For a clean quantum wire, then, there is a strong deviation with respect to a Fermi liquids behaviour. In the following of this chapter, we will justify analytically all the previous statements about electrical and thermal conductance.

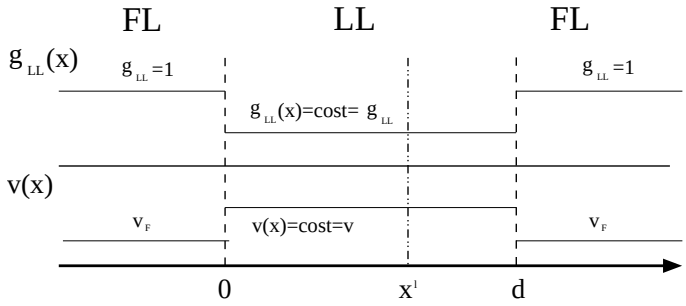

Figure 3.4: The physical system is replaced by an effective 1D model described by the effective interaction parameter $g_{LL}(x)$. It is equal to one in the reservoirs, signaling the absence of interactions in the FL state, and different than one but constant in the wire. An analogous condition holds for the velocity $v(x)$ of excitations: it is equal to v_F in the reservoirs, and equal to $v = v_F/g_{LL}$=constant in the wire.

3.2 Electrical and thermal conductance

In this chapter, we show that all the physical quantities in which we are interested can be written in terms of an appropriate Green's function describing the transport in the system. Then, we will evaluate such a function and the equation it satifies to get its analytical expression.

We begin with replacing the physical system containing the one-dimensional quantum wire connected adiabatically to two-dimensional reservoirs by an effective one-dimensional system, as shown in Fig. 3.4. Such a system is described by the Luttinger parameter $g_{LL}(x)$. It is equal to one as $x < 0$ and $x > d$, that is in the FL reservoirs, signaling the absence of interactions; it is less than one but constant as $0 < x < d$, that is in the interacting wire. $v(x)$ represents the velocity of propagation of the charge density waves in the wire; in the reservoirs, it reduces to v_F. The points whose coordinates are $x = 0, x', d$ represent the points where the boundary conditions have to be satisfied to get the correct Green's function.

In the following section, we show how the conductances can be expressed in term of the above-mentioned Green's function.

3.2.1 Electrical conductance

In time domaine, the expression for the electric current is the following

$$I(x,t) = \int \sigma(x,x';t,t')E(x',t')\,dx'\,dt' \ , \tag{3.4}$$

$\sigma(x,x';t,t')$ being the non-local ac conductivity, and $E(x',t')$ the electric field.

The following relations hold

$$\frac{1}{2\pi}\int \sigma(x,x';t-t')E(x',t')\,dt' = \mathcal{F}[\sigma_\omega(x,x')\bar{E}_\omega(x')] = \frac{1}{2\pi}\int e^{-i\omega t}\sigma_\omega(x,x')\bar{E}_\omega(x')\,d\omega \ , \tag{3.5}$$

$\mathcal{F}$ being the Fourier transform operator, and $\bar{E}_\omega(x')$ the Fourier transform of the electric field. Then, Eq. (3.4) can be written as

$$I(x,t) = \int_0^d dx' \frac{1}{2\pi}\int d\omega\, e^{-i\omega t}\sigma_\omega(x,x')\bar{E}_\omega(x') \ , \tag{3.6}$$

In linear response theory, [Mahan00, Rickayzen80], the electrical conductivity reads

$$\sigma_\omega(x,x') = \frac{e^2 i\omega_\nu^2}{\pi\omega} G_{i\omega_\nu}(x,x')\Big|_{i\omega_\nu\to\omega+i0} \ . \tag{3.7}$$

We used the Matsubara representation with imaginary time, ω_ν being the Matsubara bosonic frequency and

$$G_{i\omega_\nu}(x,x') = \pi n_0^2 \int_0^\beta d\tau \langle T_\tau \hat{u}(x,\tau)\hat{u}(x',0)\rangle e^{i\omega_\nu\tau} \ , \tag{3.8}$$

is the Fourier transform of the temperature Green's function describing the excitations propagation. T_τ is the time ordering operator, $\langle \ldots \rangle$ stands for thermodynamic average and $\hat{u}$ is the operator identifing the displacement in the wire.

The conductance of the wire is then obtained in the zero-frequency limit, $g = \sigma_{\omega\to 0}(x,x')$, where σ depends no longer on x and x'.

3.2.2 Thermal conductance

The thermal conductance K can be obtained analogously in the zero-frequency limit from the thermal conductivity, $K = \kappa_{\omega\to 0}(x,x')$, where $\kappa_\omega(x,x')$ can be written,

in linear response regime, by means of the corresponding Kubo formula

$$\begin{aligned}\kappa_\omega(x,x') &= \frac{i}{\omega T}\chi(x,x';i\omega_\nu)\Big|_{i\omega_\nu\to\omega+i0} \\ &= \frac{i}{\omega T}\int_0^\beta d\tau\langle T_\tau j_{\rm th}(x,\tau)j_{\rm th}(x',0)\rangle e^{i\omega_\nu\tau}\Big|_{i\omega_\nu\to\omega+i0}\,, \end{aligned} \tag{3.9}$$

where $j_{\rm th}$ is the thermal current density. Eq. (3.7) shows clearly the link between the electrical conductivity and the Green's function defined in Eq. (3.8). The expression for the thermal current density $j_{\rm th}$, and for the thermal conductance in terms of Green's function defined in Eq. (3.8) can be obtained as follows.

The Hamiltonian of the system, Eq. (3.3), can be generally writen as $H = \int dx\mathcal{H}(x)$, $\mathcal{H}(x)$ being the energy density. Since the total energy flowing in the system has to be conserved, by means of continuity equation

$$\partial_x j_{\rm th}(x) + \partial_t\mathcal{H} = 0\,, \tag{3.10}$$

it is possible to write the energy current $j_{\rm th}(x)$ in term of $\hat{u}(x)$ and $\hat{p}(x)$ operators, by a direct calculation of the commutator $[H,\mathcal{H}]$. Finally, the thermal current density reads

$$j_{\rm th}(x) = -\frac{v_F^2}{2}\{\hat{p}(x),\partial_x\hat{u}\}\,, \tag{3.11}$$

where $\{\cdots,\cdots\}$ denotes anticommutator, and $\hat{p}(x) = m\,n_0\,\partial_t\hat{u}$ is the conjugate momentum of the displacement operator $\hat{u}(x)$. Eq. (3.11) has been written under the assumption $x < 0$ or $x > d$. Since we are interested in the zero-frequency limit of thermal conductivity $\kappa_{\omega\to0}(x,x')$, which does not depend on coordinates x and x', it is convenient to choose $x < 0$ and $x' > d$, *i.e.*, in the noninteracting reservoirs.

The current-current correlation function in Eq. (3.9) can be written in term of the Green's function $G(x,x';\tau)$ with x and x' in the reservoirs as described in Appendix B. Finally, it reads

$$\begin{aligned}&\langle T_\tau j_{\rm th}(x,\tau)j_{\rm th}(x',0)\rangle \\ &\quad= v_F^2\left[\partial_\tau^2 G(x,x';\tau)\partial_{x,x'}^2 G(x,x';\tau) + \partial_{\tau,x}^2 G(x,x';\tau)\partial_{\tau,x'}^2 G(x,x';\tau)\right]\,. \end{aligned} \tag{3.12}$$

From Eq. (3.8), $G(x,x';\tau) = \pi n_0^2 \langle T_\tau \hat{u}(x,\tau)\hat{u}(x',0)\rangle$. Upon Fourier transform,

$$\begin{aligned}&\int_0^\beta d\tau \langle T_\tau j_{\rm th}(x,\tau) j_{\rm th}(x',0)\rangle e^{i\omega_\nu \tau} \\ &= -T\sum_{i\omega_\mu} G_{i\omega_\mu}(x',x) G_{i\omega_\nu + i\omega_\mu}(x,x') \left[(\omega_\nu+\omega_\mu)^2|\omega_\mu|^2 - \omega_\mu(\omega_\nu+\omega_\mu)|\omega_\mu||\omega_\nu+\omega_\mu|\right] \quad (3.13)\end{aligned}$$

In the latter equation, ω_ν represents the external Matsubara frequency of the field, and we shall consider the limit $\omega \to 0$, upon analytical continuation $i\omega_\nu \to \omega + i0$. Eq. (3.13) has been obtained using the fact that in the reservoirs, $\partial_x G_{i\omega_\mu}(x,x') = -\partial_{x'} G_{i\omega_\mu}(x,x') = (|\omega_\mu|/v_F) G_{i\omega_\mu}(x,x')$. As shown in Appendix B, the sum over ω_μ can be written as a contour integral in the complex frequency plane; performing analytical continuation and taking the limit $\omega \to 0$, one finds the thermal conductance

$$K = \frac{1}{2\pi T^2}\int_0^\infty d\omega \frac{\omega^4}{\sinh^2(\beta\omega/2)} |G_{\omega+i0}(0,d)|^2 \,, \quad (3.14)$$

where we used the continuity of Green's function at the interface $x = 0$ and $x' = d$, to express the thermal conductance in terms of Green's function *within* the wire.

This result is formally identical to the one found in [Fazio98], where a scattering approach was used to obtain thermal conductance. The contribution to thermal conductivity is given by excitations with frequencies up to temperature T, *i.e.* of wavelengths of the order of v/T up to infinity, $v = v_F/g_{LL}$ being the propagation velocity of plasmons in the wire. Generally, wavelengths comparable to the scale $l_{\rm inh}$ will play a role, too. They will suffer backscattering on the edges of wire, causing a renormalization of thermal conductivity and hence a variation of Lorenz number, as shown in Fig. 3.3, [Fazio98].

3.3 Equation of motion for a clean wire

In this section, starting from the single particle Green's function, we will come to its equation of motion; this equation will allow the analytical determination of such a function, and then of the electrical and thermal conductances in Eqs. (3.7) and

(3.14). The details of calculations are reported in the Appendix C. The single-particle temperature Green's function, in the Matsubara imaginary time τ, is defined as

$$G^0(x,x';\tau) = \pi n_0^2 \langle T_\tau \hat{u}(x,\tau)\hat{u}'(x',0)\rangle \ , \tag{3.15}$$

where the superscript 0 indicates that we are considering a clean wire, and the average is evaluated in absence of disorder.

The equation of motion can be written by taking the derivative of Green's function with respect to time

$$\frac{\partial}{\partial\tau}G^0(x,x';\tau) = \pi n_0^2 \left[\frac{\partial}{\partial\tau}\langle\hat{u}\hat{u}'\rangle\theta(\tau) + \frac{\partial}{\partial\tau}\langle\hat{u}'\hat{u}\rangle\theta(-\tau)\right] \ , \tag{3.16}$$

where, for the sake of simplicity, we set $\hat{u} = \hat{u}(x,\tau)$, $\hat{u}' = (x',0)$ and $\theta(\tau)$ is the step function. The previous equation reads

$$\frac{\partial}{\partial\tau}G^0(x,x';\tau) = -\frac{i\pi n_0}{m}\langle T_\tau \hat{p}(x,\tau)\hat{u}(x',0)\rangle \ . \tag{3.17}$$

In Eq. (3.17), the derivative of Green's function is not proportional to the same Green's function, but to another not well defined function; then, we need at least the second derivative to close the equation

$$\frac{\partial^2}{\partial\tau^2}G^0(x,x';\tau) = -\frac{i\pi n_0}{m}\left\{\partial_\tau\langle\hat{p}\hat{u}'\rangle\ \theta(\tau) + \partial_\tau\langle\hat{u}'\hat{p}\rangle\theta(-\tau)\right\} \ . \tag{3.18}$$

Evaluating separately the two terms in the rhs of Eq. (3.18), the equation of motion reads

$$\partial_\tau^2 G^0(x,x';\tau) + \frac{n_0}{m}\partial_x\left\{\left[V_0 + \frac{\pi^2 n_0}{m}\right]\partial_x G^0(x,x';\tau)\right\} = -\frac{\pi n_0}{m}\delta(x-x')\delta(\tau) \ . \tag{3.19}$$

The quantity in the square brackets in the second term of the lhs of Eq. (3.19) can be written as

$$\left(V_0 + \frac{\pi^2 n_0}{m}\right) = \frac{\pi^2 n_0}{m}\left(1 + \frac{mV_0}{\pi^2 n_0}\right) = \frac{\pi^2 n_0}{m}\frac{1}{g_{LL}^2(x)} \ . \tag{3.20}$$

The definition of the Luttinger parameter g_{LL} follows from the second equality in the latter equation. Besides, to write Eq. (3.20), we used the definition of the total number

of particles: $N = \frac{L}{\pi}k_F \Rightarrow \frac{N}{L} = \frac{mv_F}{\pi} = n_0$; if the velocity depends on x, so does the denstity, and one can write: $n(x) = mv(x)/\pi$. Then, the Eq. (3.20) can be written as

$$\frac{\pi^2 n_0}{m}\frac{1}{g_{LL}^2(x)} = \pi\frac{v(x)}{g_{LL}(x)} \,, \tag{3.21}$$

where $v(x) = s(x)/g_{LL}(x)$ is the velocity of plasmons inside the wire, and it is renormalised by the interactions described by $g_{LL}(x)$. Then, by means of Eq. (3.21) the Eq. (3.19) reads

$$\left\{\partial_\tau^2 + s(x)\partial_x\left(\frac{v(x)}{g_{LL}(x)}\partial_x\right)\right\} G^0(x,x';\tau) = -s(x)\delta(x-x')\delta(\tau) \,. \tag{3.22}$$

Considering the relation between $v(x)$ and $s(x)$, one finds the equation of motion in time domain

$$\left\{\frac{1}{v(x)g_{LL}(x)}\partial_\tau^2 + \partial_x\left(\frac{v(x)}{g_{LL}(x)}\partial_x\right)\right\} G^0(x,x';\tau) = -\delta(x-x')\delta(\tau) \,. \tag{3.23}$$

In frequency space, it reads

$$\left\{-\partial_x\left(\frac{v(x)}{g_{LL}(x)}\partial_x\right) + \frac{\omega_\nu^2}{v(x)g_{LL}(x)}\right\} G^0_{i\omega_\nu}(x,x') = \delta(x-x') \,. \tag{3.24}$$

The explicit calculation of the Green's function is reported in the Appendix D. If the propagation velocity is supposed constant in the wire, as in our model, then the solution of Eq. (3.24) inside the wire reads

$$G^0_{i\omega_\nu}(x,x') = A_{\omega_\nu}(x')e^{\alpha_\nu x} + B_{\omega_\nu}(x')e^{-\alpha_\nu x} \,, \tag{3.25}$$

where we defined $\alpha_\nu \equiv |\omega_\nu|/v$. The functions A_{ω_ν} and B_{ω_ν} are proportional to each other,

$$B_{\omega_\nu} = \gamma A_{\omega_\nu}, \tag{3.26}$$

where we defined the constant $\gamma \equiv (1-g_{LL})/(1+g_{LL})$. The explicit form of the function A_{ω_ν} is

$$A_{\omega_\nu}(x) = \frac{\cosh[\alpha_\nu(d-x)]\,(1+g_{LL}\tanh[\alpha_\nu(d-x)])}{|\omega_\nu|\,(e^{\alpha_\nu d}+\gamma e^{-\alpha_\nu d}) + \frac{|\omega_\nu|}{g_{LL}}\,(e^{\alpha_\nu d}-\gamma e^{-\alpha_\nu d})}. \tag{3.27}$$

In the wire, if $x = x'$, Green's function reads

$$G^0_{i\omega_\nu}(x,x) = \frac{g_{LL}}{2|\omega_\nu|}\frac{1}{1-\gamma^2 e^{-2\alpha_\nu d}}\left\{1+\gamma^2 e^{-2\alpha_\nu d}+\gamma e^{-2\alpha_\nu x}+\gamma e^{-2\alpha_\nu (d-x)}\right\}. \quad (3.28)$$

The importance of Eq. (3.28) will be clear in the following.

The expression of Green's function valid within the wire can be obtained immediately substituting $x = 0$ and $x' = d$ in Eq. (3.25). One finds

$$G^{(0)}_{i\omega_\nu}(0,d) = (1+\gamma)A_{\omega_\nu}(d) = \frac{2}{|\omega_\nu|}\frac{g_{LL}}{(1+g_{LL})^2 e^{\alpha_\nu d}-(1-g_{LL})^2 e^{-\alpha_\nu d}}. \quad (3.29)$$

3.4 Results for a clean quantum wire

By means of Eq. (3.29), the behaviour for a clean wire is easily recovered.

The Green's function valid within the wire, from Eq. (3.29), performing analytical continuation, reads

$$G^{(0)}_{\omega+i0}(0,d) = i\frac{2}{\omega}\frac{g_{LL}}{(1+g_{LL})^2 e^{-i\omega d/v}-(1-g_{LL})^2 e^{i\omega d/v}}. \quad (3.30)$$

Substituting Eq. (3.30) into Eq. (3.7) and taking the limit $\omega \to 0$, one finds the conductance for a clean one-mode quantum wire $g_{\mathrm{cw}} = e^2/h$.

From Eq. (3.30),

$$|G^{(0)}_{\omega+i0}(0,d)|^2 = \frac{2}{\omega^2}\frac{g^2_{LL}}{1+6g^2_{LL}+g^4_{LL}-(1-g^2_{LL})^2\cos(2\omega d/v)}. \quad (3.31)$$

Comparing the latter equation with the results in [Safi95, Fazio98] for the thermal conductance, one gets the expression for the so-called plasmons transmission coefficient of a clean wire,

$$T_{pl}(\omega) = 4\omega^2|G^{(0)}_{\omega+i0}(0,d)|^2 = \frac{8g^2_{LL}}{1+6g^2_{LL}+g^4_{LL}-(1-g^2_{LL})^2\cos(2\omega d/v)}. \quad (3.32)$$

The behaviour of the transmission coefficient, Eq. (3.32), is plotted in Fig. 3.5, in function of dimensionless energy $\omega d/v_F$ and interactions strength g_{LL}.

If $g_{LL} = 1$, that is for non-interacting electrons, then $T_{pl}(\omega) = 1$; from Eqs. (3.14) and (3.31) one gets the classical value for thermal conductance $K = (\pi/6)T$,

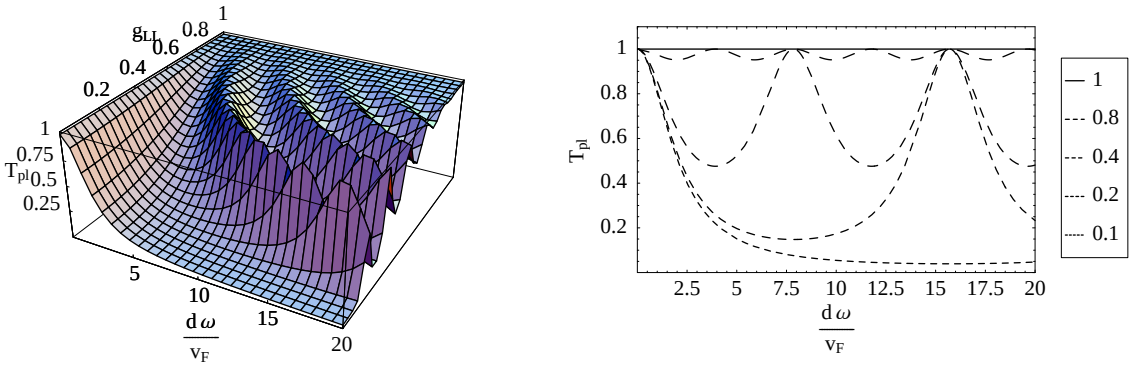

Figure 3.5: Transmission coefficient for a clean quantum wire. *Left*: 3D plot of transmission coefficient for a clean quantum wire in function of dimensionless energy $\omega d/v_F$ and the interaction strength g_{LL}. *Right*: Transmission coefficient for a clean quantum wire in function of dimensionless energy $\omega d/v_F$ for different value of the interaction strength g_{LL}. Resonance picks are well visible when $\omega d/v_F = \pi k/g_{LL}$. For each value of k a collective mode is excited.

and, consequently, the classical value L_0 for the Lorenz number, too, see Fig. 3.3. As mentioned, the same classical value, is recovered at low temperatures $T \ll v/d$, for any value of Luttinger parameter g_{LL}.

The plot of $T_{pl}(\omega)$ shown in Fig. 3.5 for different values of interactions strength, allows us to better understand phenomenologically how the collective modes are excited inside the wire.

For non interacting particles, the transmission coefficient is constantly equal to one; particles can transmit easily through the wire, because no repulsive forces are present. As long as g_{LL} lowers, the system becomes more and more rigid, and resonances peaks appear.

From Eq. (3.32), one has the maxima for the transmission coefficient for values of dimensionless energy given by

$$\frac{\omega d}{v_F} = \frac{\pi}{g_{LL}} k \,, \tag{3.33}$$

where k is an integer, zero included. Each peak corresponds to an excitation of a collective mode whose wavelength has a well defined value

$$\lambda = \frac{2d}{k} \,. \tag{3.34}$$

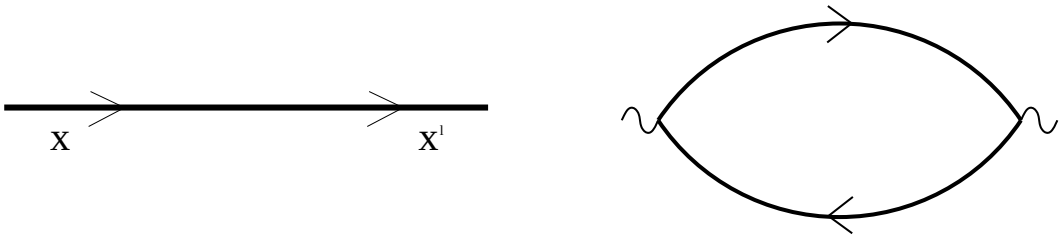

Figure 3.6: Diagrams for conductance in a clean wire. *Left*: Electrical conductance in bosonised form is proportional to single-particle Green's function, Eq. (3.7). Then, the only contributing diagram is represented by a straight line, where the arrows indicate the direction of propagation. *Right*: The thermal density current operator, Eq. (3.11), is bilinear in the displacement operator $\hat{u}$. Then, even in bosonised form, the simplest diagram contributing to thermal conductance in a clean wire is still represented by a bubble diagram. Each branch of the diagram is equivalent to the straight-line diagram on the left. Wavy lines represent interactions with the external field.

At very low temperatures, the contribution to energy transport is determined by those excitations whose wavelength largely exceeds the length of the wire. For $k = 2$ the corresponding mode has a wavelength equal to the wire length, then, for increasing values of k smaller wavelength modes are excited. For each supplementary mode a larger amount of energy is demanded. The stronger the interactions, the lower the average value of transmission coefficient, and the larger the energy to excite even a single mode. Of course, if $g_{LL} = 0$, then an infinite amount of energy is demanded to excite even the lowest modes.

In Fig. 3.6, the two diagrams contributing to electrical and thermal conductance are shown. In the bosonized form, the electrical conductance is represented by a simple straight line diagram, since it is proportional to the single-particle Green's function, Eq. (3.7). No bubble diagram contributes. On the contrary, since the thermal current density operator is bilinear in the displacement operator $\hat{u}$, Eq. (3.11), the simplest diagram contributing to thermal conductance for a clean wire is still a bubble diagram.

As we will see in the following sections, this difference will play a very important role in the evaluation of the corrections due to disorder. This evaluation will be the aim of the next sections. Because of the different structure of electrical and thermal conductance, Eqs. (3.7) and (3.14), the corrections to the aforementioned diagrams,

and then to the conductances, cannot be evaluated in the same identical way. We anticipate that for the electrical conductance the equation of motion for the single-particle Green's function can be used to evaluate the correction to the Green's function and then to the conductance. For the thermal conductance, a diagrammatic approach will be followed to recover correctly all the contributing analytical terms.

3.5 Corrections induced by disorder

The Green's function $G^0_{i\omega_\nu}(x,x')$ in Eq. (3.25), solution of the equation of motion in Eq. (3.24), has been used to find the results for a clean one-mode quantum wire presented in the previous section. Notwithstanding the fact that the structure of electrical and thermal conductance in terms of Green's function is profoundly different, Eqs. (3.7) and (3.14), they just depend on $G^0_{i\omega_\nu}(x,x')$, in the case of charge transport, or on $|G^0_{i\omega_\nu}(x,x')|^2$ for the energy transport. As we have mentioned, this difference goes back to the distinct structure of current density operator, which is linear in the operator $\hat{u}$ for the charge transport, $j_{\rm el} = -i\sqrt{\pi}n_0\partial_\tau\hat{u}$, [Maslov95], and bilinear for the energy transport, Eq. (3.11).

While for a clean wire, the above-mentioned different structure of electrical and thermal conductance does not prevent from using the same equation of motion, this is no longer true in presence of impurities.

Under the assumption of weak disorder, one can study the linear response of the system to such a perturbation by writing the electrical and thermal conductances as the sum of two terms

$$g_{\rm dw} = g_{\rm cw} + \delta g_{\rm dw}\ , \qquad\qquad K_{\rm dw} = K_{\rm cw} + \delta K_{\rm dw}\ . \tag{3.35}$$

The first terms in the rhs of these equations, are the values for a clean wire, and they are given by Eqs. (3.7) and (3.14), respectively; δg_{dw} and δK_{dw} are the corrections due to the perturbative potential. From Eq. (3.35), the correction to Lorenz number can

be evaluated, and, at the lowest order in the corrections, it reads

$$L_{\rm dw} \simeq \frac{K_{\rm cw}}{T g_{\rm cw}} \left[1 - \frac{\delta g_{\rm dw}}{g_{\rm cw}} + \frac{\delta K_{\rm dw}}{K_{\rm cw}} \right] = L_{\rm cw} \left[1 - \frac{\delta g_{\rm dw}}{g_{\rm cw}} + \frac{\delta K_{\rm dw}}{K_{\rm cw}} \right] , \tag{3.36}$$

Eq. (3.36) shows that the correction to Lorenz number depends on the corrections to the conductances which appear with opposite sign. So far, to our knowledge, few works exist which allow to determine the behaviour of the above-mentioned correction, [Li02, Ferone]. In [Li02], the behaviour of the Lorenz number is not explicitly presented. No information can be deduced about the sign of the correction, and particularly, the limit of high temperatures is not discussed at all.

3.6 Correction to g_{cw} and generalised equation of motion

The correction to the electrical conductance in the first equation in Eq. (3.35) can be written in terms of the correction to the Green's function.

In linear response regime, one can write

$$G_{\rm dw}(x, x'; \tau) = G^0(x, x'; \tau) + \delta G_{\rm dw}(x, x'; \tau) , \tag{3.37}$$

where $G^0(x, x'; \tau)$ is the expression of the Green's function for a clean wire, and it is the solution of Eq. (3.23), while $\delta G_{\rm dw}$ the correction due to disorder. Such a correction, we stress, is the correction to the single-particle Green's function.

From Eqs. (3.7) and (3.37) the correction induced by disorder to electrical conductivity can be written as

$$\delta\sigma_\omega(x, x') = \frac{e^2 i\omega_\nu^2}{\pi\omega} \delta G_{i\omega_\nu}(x, x') \Big|_{i\omega_\nu \to \omega + i0} . \tag{3.38}$$

The evaluation of $\delta G_{i\omega_\nu}(x, x')$, and then, of $\delta\sigma_\omega(x, x')$ is equivalent to the evaluation of the self-energy Σ_1, shown in Fig. 3.7-left, which dresses the bare Green's function, [Abrikosov75, Rickayzen80]. The form of Σ_1 will be discussed in details later. Here, we point out that since from Eq. (3.38) $\delta\sigma_\omega(x, x')$ is proportional to $\delta G_{i\omega_\nu}(x, x')$, the

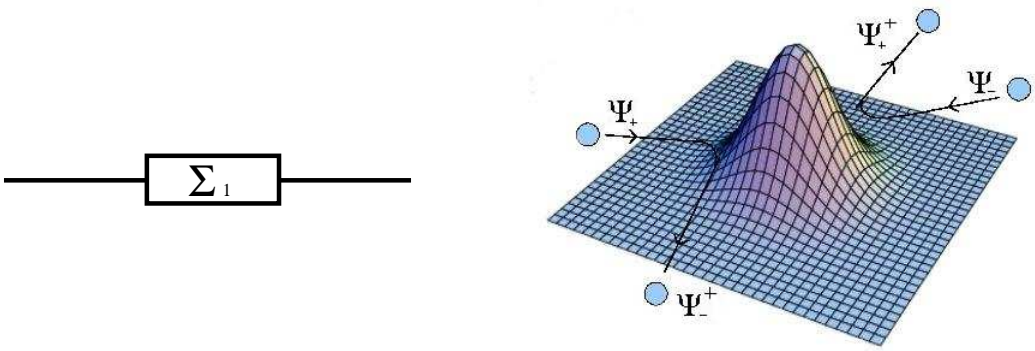

Figure 3.7: *Left*: Single particle Green's function self-energy contributing to electrical conductance. *Right*: The only terms giving information about the action of perturbative potential in Eq. (3.40) and shown in the figure are $\psi_-^+\psi_+$ and $\psi_+^+\psi_-$; the first term describes a right-moving state, ψ_+, scattered off by the potential in a left-moving state, ψ_-^+. On the contrary, the second term describes a left-moving state ψ_- scattered off in a right-moving state ψ_+^+. Both terms are used to write the expression of the perturbative Hamiltonian $H_{\rm imp}$ in Eq. (3.42).

self-energy Σ_1 is all what one has to evaluate for the electrical conductance. No other possible correlation functions appear in the evaluation.

In the following sections, we write the equation of motion for the single particle Green's function in presence of disorder. It will allow us to evaluate the correction $\delta G_{i\omega_\nu}(x,x')$, and then the electrical conductance.

The Hamiltonian we have used until now, Eq. (3.3), describes a clean quantum wire. To tackle the problem of a disordered 1D conductor, the first step is understanding the way to modify correctly the Hamiltonian in order to describe the effects of disorder.

In second quantification formalism, [Rickayzen80, Mahan00], the Hamiltonian describing the effect of impurities reads

$$H_{\rm imp} = \int d^3\mathbf{r}\, \psi^\dagger(\mathbf{r}) V(\mathbf{r}) \psi(\mathbf{r}) \ , \tag{3.39}$$

where $V(\mathbf{r})$ is the perturbative potential, and ψ a fermionic field.

The product of fermionic operators can be decomposed in contributions concerning right, $(+)$, and left, $(-)$, movers, respectively:

$$\psi^\dagger\psi = \psi_+^\dagger\psi_+ + \psi_-^\dagger\psi_- + \psi_+^\dagger\psi_- + \psi_-^\dagger\psi_+ \ . \tag{3.40}$$

Physically, the only terms giving information about the action of the perturbative potential are the third and the fourth ones in the rhs of Eq. (3.40), that is the mixed one; they are the only ones to give an information about the particles reflected by the potential, see Fig. 3.7-right. As we have seen in Section 2.3, the bosonization technique allows to write a fermionic operator as

$$\psi_{\pm} \sim \exp[\pm ik_F x \mp i\phi(x) + \theta(x)] \; . \tag{3.41}$$

where ϕ and θ are bosonic operators. By taking just the terms giving a contribution to conductance as mentioned before, the Hamiltonian describing the effect of disorder reads

$$H_{\text{imp}} = \frac{2}{a} \int dx V(x) \cos(2k_F x - 2\pi n_0 \hat{u}) \; , \tag{3.42}$$

where a is a microscopic cut-off length. The equation of motion with respect to the Hamiltonian $H_0 + H_{\text{imp}}$ can be now evaluated. As for the clean case, all the calculations are reported in details in the Appendix E. The equation of motion reads

$$\left\{ \frac{1}{v(x) g_{LL}(x)} \partial_\tau^2 + \partial_x \left(\frac{v(x)}{g_{LL}(x)} \partial_x \right) \right\} G(x, x'; \tau) = \\ -\delta(x - x')\delta(\tau) + \frac{4\pi}{a} n_0 V(x) \langle T_\tau \sin(2k_F x - 2\pi n_0 \hat{u}) \hat{u}' \rangle \; . \tag{3.43}$$

From the previous equation it is possible, at least in principle, to determine the complete evolution of the perturbed system provided that one is able to evaluate the average in the second term in the rhs. We will see that it is analytically possible under the assumption of weak disorder. Particularly, the calculation of the above-mentioned average allows to evaluate the correction to Green's function, and consequently, to the electrical conductance.

3.6.1 First order corrections

We want to recover the analytical expression of the correction to Green's function. From Eqs. (3.23), (3.37) and (3.43), the equation of motion for such a correction

reads

$$\left\{-\partial_x\left(\frac{v(x)}{g(x)}\partial_x\right)+\frac{{\omega_\nu}^2}{v(x)g(x)}\right\}\delta G_{i\omega_\nu}(x,x')= \\ =-\frac{4\pi}{a}n_0V(x)\langle T_\tau\sin(2k_Fx-2\pi n_0\hat{u})\,\hat{u}'\rangle\ . \qquad (3.44)$$

In order to study the system perturbatively in the potential $V(x)$, at the lowest order in the aforesaid potential, the rhs of Eq. (3.44) being already linear in $V(x)$, the average can be evaluated with respect to the unperturbed Hamiltonian H_0.

The perturbative approach in this case is possible if the strength of the potential $V(x)$ is much smaller than the characteristic energy scale v/d of the wire. This point will be discussed in details later.

To evaluate the average, we observe that the Hamiltonian in Eq. (3.3) can be diagonalised by means of linear transformations; they allow to write the aforesaid Hamiltonian in a bilinear form with respect to bosonic operators, [Fazio98]. Under these assumptions, it is shown that the following equation holds

$$\left\langle e^{\hat{B}}\right\rangle = e^{\frac{1}{2}\langle\hat{B}^2\rangle}\ . \qquad (3.45)$$

To evaluate the average $\langle T_\tau\sin(2K_Fx-2\pi n_0\hat{u})\hat{u}'\rangle_{H_0}$, we observe that one can decompose it by means of trigonometric formula; the averages to evaluate, then, can be written as

$$\langle\cos(2\pi n_0\hat{u})\hat{u}'\rangle=\frac{1}{2}\left\{\left\langle e^{-i2\pi n_0\hat{u}}\hat{u}'\right\rangle+\left\langle e^{i2\pi n_0\hat{u}}\hat{u}'\right\rangle\right\}\ . \qquad (3.46)$$

Each of the single term in the rhs of the Eq. (3.46) can be evaluated by means of Eq. (3.45). Calculating each term, for the average one finds

$$\langle T_\tau\sin(2K_Fx-2\pi n_0\hat{u})\hat{u}'\rangle_{H_0}=-\frac{2}{n_0}\cos(2K_Fx)G^0(x,\tau;x',0)e^{-2\pi G^0(x,\tau;x,\tau)}\ . \qquad (3.47)$$

The Green's function appearing in the exponential function does not depend on time; in fact, the general properties of Green's functions state, provided that the Hamiltonian does not depend on time, that they depend just on the difference of the time argument. In this case, the two values are equal. By means of Eq. (3.47), the

equation of motion for the correction to Green's function in Eq. (3.44) reads

$$\left\{-\partial_x\left(\frac{v(x)}{g_{LL}(x)}\partial_x\right)+\frac{\omega_\nu^2}{v(x)g_{LL}(x)}\right\}\delta G_{i\omega_\nu}(x,x') = \\ = \frac{8\pi}{a}V(x)\cos(2k_Fx)G^0_{i\omega_\nu}(x,x')e^{-2\pi G^0(x,\tau;x\tau)} = f(x,x';\omega_\nu)\ . \quad (3.48)$$

The general theory of Green's functions allows to write immediately the solution of the previous differential equation

$$\delta G_{i\omega_\nu}(x,x') = \int dx'' G^0_{i\omega_\nu}(x,x'')f(x'',x',\omega_\nu)\ . \quad (3.49)$$

Finally, the correction can be written as

$$\delta G_{i\omega_\nu}(x,x') = \frac{8\pi}{a}\int dx'' V(x'')\cos(2k_Fx'')G^0_{i\omega_\nu}(x,x'')G^0_{i\omega_\nu}(x'',x')e^{-2\pi G^0(x'',\tau'';x''\tau'')}\ . \quad (3.50)$$

We studied the case of a white noise potential, that is for a potential $V(x)$ such that $\langle V(x)\rangle = 0$ and $\langle V(x_1)V(x_2)\rangle = n_i u^2\delta(x_1-x_2)$, where n_i is the density of impurities in the wire, u their strength, and, for the potential, $\langle\cdots\rangle$ stands for the average over disorder realizations. For a perturbative approach, the condition $u \ll v/d$ must holds.

Since $\langle V(x)\rangle = 0$, from Eqs. (3.38) and (3.50), no information on the behaviour of electrical conductance can be obtained at this step, and higher order corrections have to be evaluated. Besides, we stress that even for a different perturbative potential, Eqs. (3.38) and (3.50) just give rise to an inductive correction. Then, no real resistive contribution exists.

3.6.2 Second order corrections

The average in Eq. (3.44) should be evaluated with respect the total Hamiltonian $H_0 + H_{\rm imp}$, where H_0 and $H_{\rm imp}$ are given by Eqs. (3.3) and (3.42), respectively. Since the rhs of Eq. (3.44) is already linear in the potential $V(x)$, one has to consider all the first order contributions in the perturbative Hamiltonian $H_{\rm imp}$.

Let $H = H_0 + H_{\rm imp}$ be the total Hamiltonian. One can write

$$\langle f_1 f_2 \rangle_H = \frac{1}{\mathcal{Z}} \mathrm{Tr}\; e^{-\beta H} f_1 f_2 \;, \tag{3.51}$$

where f_1 and f_2 are two operators functions, and $\mathcal{Z}$ the partition function.

If the perturbation is small, as it is in our case, the density matrix reads

$$\rho = \rho_0 \left[1 - \beta H_{\rm imp}\right] \;, \tag{3.52}$$

where ρ_0 is the unperturbed density matrix. In the same way, the partition function can be written as

$$\mathcal{Z} = \mathcal{Z}_0 \left[1 - \langle \beta H_{\rm imp} \rangle_0\right] \;. \tag{3.53}$$

By using the two previous equations, the average in Eq. (3.51) will assume the following expression

$$\langle f_1 f_2 \rangle_H = \frac{1}{\left[1 - \langle \beta H_{\rm imp} \rangle_0\right]} \left\{ \langle f_1 f_2 \rangle_0 - \langle \beta H_{\rm imp} f_1 f_2 \rangle_0 \right\} \;, \tag{3.54}$$

and consequently,

$$\langle f_1 f_2 \rangle_H \simeq \left\{1 + \langle \beta H_{\rm imp} \rangle_0\right\} \cdot \left\{ \langle f_1 f_2 \rangle_0 \right\} - \langle \beta H_{\rm imp} f_1 f_2 \rangle_0 \right\} \;. \tag{3.55}$$

At the first order in $H_{\rm imp}$, the contributions read

$$\langle f_1 f_2 \rangle^{(I)} = \langle \beta H_{\rm imp} \rangle_0 \langle f_1 f_2 \rangle_0 - \langle \beta H_{\rm imp} f_1 f_2 \rangle_0 \;. \tag{3.56}$$

In the latter equation, all the averages are to be evaluated with respect the unperturbed Hamiltonian H_0. For our problem, the functions in Eq. (3.56) read

$$f_1 = f(x_1, \tau_1) = \sin(2k_F x_1 - 2\pi n_0 \hat{u}(x_1, \tau_1)) \;, \tag{3.57}$$

$$f_2 = f(x_2, \tau_2) = -2\sqrt{\pi} n_0 \hat{u}(x_2, \tau_2) \;, \tag{3.58}$$

$$H_{\rm imp} = \frac{2}{a} \int dx_3 V(x_3) \cos(2k_F x_3 - 2\pi n_0 \hat{u}(x_3, \tau_3)) \;. \tag{3.59}$$

For the sake of simplicity, we call $(x_1, \tau_1) = (x, \tau)$, $(x_2, \tau_2) = (x', 0)$, and $\hat{u}(x_i, \tau_i) = \hat{u}_i$. From Eqs. (3.44), (3.56), (3.57), (3.58) and (3.59), the contribution, at

the first order in the perturbative Hamiltonian, will read

$$\begin{aligned}\sqrt{\pi}n_0\langle T_\tau \sin(2k_F x - 2\pi n_0\hat{u})\hat{u}'\rangle^{(I)} = \\ = -\frac{2}{a}\int d\tau_3 dx_3 V(x_3)\langle T_\tau \sin(2k_F x_1 - 2\pi n_0\hat{u}_1)\hat{u}_2\cos(2k_F x_3 - 2\pi n_0\hat{u}_3)\rangle_0 \\ -\frac{2}{a}\int d\tau_3 dx_3 V(x_3)\langle\cos(2k_F x_3 - 2\pi n_0\hat{u}_3)\rangle_0\langle T_\tau \sin(2k_F x_1 - 2\pi n_0\hat{u}_1)\hat{u}_2\rangle_0 \quad (3.60)\end{aligned}$$

Evaluating the different contributions, which are reported in the Appendix F, one gets

$$\begin{aligned}\sqrt{\pi}n_0\langle T_\tau \sin(2k_F x - 2\pi n_0\hat{u})\hat{u}'\rangle^{(I)} = \\ = \frac{2\sqrt{\pi}}{a}\int d\tau_3 dx_3 V(x_3) \\ \times\Bigg\{\left[G^0_{12}e^{-2\sqrt{\pi}(G^0_{11}+G^0_{33})}\left[e^{-4\pi G^0_{13}}-1\right]+G^0_{23}e^{-2\pi(G^0_{11}+G^0_{33}+2G^0_{13})}\right]\cos[2k_F(x_1+x_3)] \\ +\left[G^0_{12}e^{-2\sqrt{\pi}(G^0_{11}+G^0_{33})}\left[e^{4\pi G^0_{13}}-1\right]-G^0_{23}e^{-2\pi(G^0_{11}+G^0_{33}-2G^0_{13})}\right]\cos[2k_F(x_1-x_3)]\Bigg\} \\ = G^{(I)}(X_1,X_2)\ , \quad (3.61)\end{aligned}$$

where: $X_i = (x_i, \tau_i)$.

We can write immediately the equation of motion for the second order corretion to the Green's function

$$\begin{aligned}\left\{\frac{1}{v(x_1)g_{LL}(x_1)}\partial_\tau^2 + \partial_{x_1}\left(\frac{v(x_1)}{g_{LL}(x_1)}\partial_{x_1}\right)\right\}\delta^{(II)}G_{12} = \\ \frac{4\sqrt{\pi}}{a}V(x_1)G^{(I)}(X_1,X_2) = f(X_1,X_2)\ . \quad (3.62)\end{aligned}$$

where $G^0_{ij} = G^0(X_i, X_j)$. Green's functions theory allows to write the solution of the previous equation, thanks to the knowledge of the Green's function associated to the differential operator

$$\delta^{(II)}G_{12} = \int dX_4 G^0(X_1,X_4)f(X_4,X_2)\ . \quad (3.63)$$

Keeping just the terms giving a non vanishing contribution, the correction finally reads

$$\begin{aligned}\delta^{(II)}G_{12} = -\frac{8\pi}{a^2}\int dX_3 dX_4 V(x_3)V(x_4)G^0(X_1,X_4) \\ \times\left[G^0_{42}e^{-2\pi(G^0_{44}+G^0_{33}-2G^0_{43})} - G^0_{23}e^{-2\pi(G^0_{44}+G^0_{33}-2G^0_{43})}\right]\cos[2k_F(x_4-x_3)]\ . \quad (3.64)\end{aligned}$$

We can write the expression of the correction we have found for a white noise potential; then, the correction to the Green's function reads

$$\delta G^{wn}_{i\omega_\nu} = -\frac{8\pi}{a^2} n_{\rm i} u^2 \int_0^d dx_0 G^0_{i\omega_\nu}(x_1, x_0) G^0_{i\omega_\nu}(x_0, x_2) \left[F_0(x_0) - F_{i\omega_\nu}(x_0)\right] \ , \qquad (3.65)$$

where $F_{i\omega_\nu}$ is the Fourier transform of

$$F(x,\tau) = \exp\left\{ \frac{-4\pi}{\beta} \sum_{\omega_\nu} (1 - e^{-i\omega_\nu \tau}) G^0_{i\omega_\nu}(x,x) \right\} \ . \qquad (3.66)$$

The latter equation requires, specifically, the knowledge of Green's function in the wire with $x = x'$, whose expression is given by Eq.(3.28).

By means of Eqs.(3.65) and (3.66), one can evaluate the corrections to Green's function and then to electrical conductance at any temperature. Eq. (3.66) can be evaluated at any temperature by performing exactly the sum; one gets the general expression $F(y,\tau) = \exp\{\chi(y,\tau)\}$, where

$$\begin{aligned} \chi(y,\tau) \ &= \ -g \sum_{k=0}^{\infty} \gamma^{2k} \Bigg\{ \ln\left[1 + \frac{\sin^2\left(\frac{\pi}{\beta}\tau\right) + \alpha^2}{\sinh^2\left(\frac{\pi d}{\beta v} 2(k+\alpha)\right)}\right] + \gamma^2 \ln\left[1 + \frac{\sin^2\left(\frac{\pi}{\beta}\tau\right) + \alpha^2}{\sinh^2\left(\frac{\pi d}{\beta v} 2(k+1)\right)}\right] \\ &+ \ \gamma \ln\left[1 + \frac{\sin^2\left(\frac{\pi}{\beta}\tau\right) + \alpha^2}{\sinh^2\left(\frac{\pi d}{\beta v} 2(k+y)\right)}\right] + \gamma \ln\left[1 + \frac{\sin^2\left(\frac{\pi}{\beta}\tau\right) + \alpha^2}{\sinh^2\left(\frac{\pi d}{\beta v} 2(k+1-y)\right)}\right] \Bigg\} \qquad (3.67) \end{aligned}$$

where $y = x/d$ is the renormalized position of impurities in the wire, and α an infrared cut-off. In the following, we will study the case of low and high temperatures, where "low" and "high" refer here to the characteristic energy scale of the system v/d. In this limit, the analytical expression of $F_{i\omega_\nu}$ can be obtained.

The correction to Green's function in Eq. (3.65), can be written in a more suitable way. Using the property $G^0_{i\omega_\nu}(x_1,x_2) G^0_{i\omega_\nu}(x_2,x_3) = G^0_{i\omega_\nu}(x_1,x_3) G^0_{i\omega_\nu}(x_2,x_2)$, it reads

$$\delta G^{wn}_{i\omega_\nu}(x_1,x_2) = -\frac{8\pi}{a^2} n_{\rm i} u^2 G^0_{i\omega_\nu}(x_1,x_2) \int_0^d dx_0 G^0_{i\omega_\nu}(x_0,x_0) \left[F_0(x_0) - F_{i\omega_\nu}(x_0)\right] . \qquad (3.68)$$

Substituting this result into Eq. (3.38), one finds the corrections to the electrical conductance

$$\delta g_{\rm dw} = -g_{\rm cw} \frac{8\pi}{a^2} n_{\rm i} u^2 \int_0^d dx G^0_{i\omega_\nu}(x,x) \left[F_0(x) - F_{i\omega_\nu}(x)\right] \Big|_{i\omega_\nu \to 0+i0} \ . \qquad (3.69)$$

In the following section, we present the result for the electrical conductance in the limit of low and high temperatures. Then, we will develop the diagrammatic approach to recover all the diagrams contributing to thermal conductance.

3.7 Electrical conductance. Low temperature limit: $T \ll v/d$

By taking the limit $\beta \to \infty$ in Eq. (3.67), one finds the expression for the correlation function at zero temperature. Taking this limit in Eq. (3.67) is equivalent to replacing the sum over Matsubara frequencies in Eq. (3.66) by an integral. The result reads

$$\chi(y,\tau) = -g\Bigg\{ \ln[1+(\omega_F\tau)^2] \;+\; \sum_{\substack{m\in\mathbb{Z}_{even}\\ m\neq 0}} \gamma^{|m|} \ln\left[\frac{m^2+(\tau v/d)^2}{m^2}\right] + \sum_{m\in\mathbb{Z}_{odd}} \gamma^{|m|} \ln\left[\frac{(m+1-2y)^2+(\tau v/d)^2}{(m+1-2y)^2}\right] \Bigg\} \tag{3.70}$$

which coincides with the result obtained in [Safi97, Dolcini03].

Since we are interested in the response at low frequencies $\omega \ll v/d$, the main contribution comes from the long-time region $v\tau/d \gg 1$ such that we can use the corresponding long-time asymptotic form of Eq. (3.70). Then $F(x,\tau)$, in Eq. (3.66), reads

$$F(x,\tau) = \frac{1}{[1+(\omega_F\tau)^2]^{g_{LL}}} \left(\frac{v\tau}{d}\right)^{2(g_{LL}-1)}, \tag{3.71}$$

valid in the limit $\tau \gg d/v$.

We need the Fourier transform of $F(x,\tau)$ which is found from the integral

$$F_0(x) - F_{i\omega_\nu}(x) = \int_{-\beta/2}^{\beta/2} d\tau \frac{1-\cos(\omega_\nu\tau)}{[1+(\omega_F\tau)^2]^{g_{LL}}} \left(\frac{v\tau}{d}\right)^{2(g_{LL}-1)}. \tag{3.72}$$

In the relevant limit (low-temperature and $\omega_\nu \to 0$), it can be written as

$$F_0(x) - F_{i\omega_\nu}(x) = \frac{\omega_\nu}{\omega_F^2} \left(\frac{v}{\omega_F d}\right)^{2(g_{LL}-1)} \int_{-\infty}^{\infty} dz \frac{1-\cos z}{z^2}. \tag{3.73}$$

Upon integration over z and analytical continuation, this reads

$$F_0(x) - F_{i\omega_\nu \to \omega + i0}(x) \simeq \frac{-i\pi\omega}{\omega_F^2} \left(\frac{v}{\omega_F d} \right)^{2(g_{LL}-1)} . \tag{3.74}$$

We now turn to the calculation of the disordered-induced correction δg_{dw} to the zero-temperature conductance of the quantum wire. In the limit $\omega_\nu \to 0$, we can approximate, from Eq. (3.25), $G^0_{i\omega_\nu} \simeq 1/2|\omega_\nu|$. With the help of Eqs. (3.38), (3.68), and (3.74), one obtains the same behaviour as in [Maslov95b]

$$\delta g_{\rm dw} = -g_{\rm cw} \frac{d}{l} \left[\frac{\omega_F d}{v} \right]^{2(1-g_{LL})} , \tag{3.75}$$

where we defined the inverse effective mean free path

$$\frac{1}{l} = \frac{4\pi^2 n_{\rm i} u^2}{a^2 \omega_F^2}. \tag{3.76}$$

The behaviour of electrical conductance in Eq. (3.75) was very recently confirmed experimentally, [Levy05].

The validity of the perturbative approach can be inferred from the condition that the zero-temperature correction $\delta g_{\rm dw} \ll g_{\rm cw} = e^2/h$. This yields the condition

$$\frac{d}{l} \left[\frac{\omega_F d}{v} \right]^{2(1-g_{LL})} \ll 1. \tag{3.77}$$

Defining the energy scale $T_0 = \omega_F (d/l)^{1/2(1-g_{LL})}$, characteristic of the interplay between disorder and interactions, the correction $\delta g_{\rm dw}$ can also be written as

$$\delta g_{\rm dw} = -g_{\rm cw} \left(\frac{T_0 d}{v} \right)^{2(1-g_{LL})} . \tag{3.78}$$

The condition that this correction be small can then also be written as $T_0 d/v \ll 1$. In order for disorder effects to be weak, the energy scale T_0, should be much smaller than the energy separation v/d between subsequent plasma modes in the wire. This condition will be met generally by simultaneously limiting the strength of the disorder potential, via the condition $l \gg d$, and the interaction strength such that $1 - g_{LL} \ll 1$.

3.8 Electrical conductance. High temperature limit: $v/d \ll T \ll \omega_F$

In this limit, Eq. (3.66) has to be analyzed using Eq. (3.67). Note that this limit corresponds to a long quantum wire, such that the dominant term in Green's function in Eq. (3.25) is $G_{i\omega_\nu} \simeq g/2|\omega_\nu|$. Then we find, as in [Maslov95b],

$$F(x,\tau) = \left[\frac{(\pi/\beta\omega_F)^2}{\sin^2(\pi\tau/\beta)}\right]^{g_{LL}} . \tag{3.79}$$

The result for the Fourier transform of F is obtained by direct integration. This yields

$$F_0(x) - F_{i\omega_\nu}(x)|_{i\omega_\nu\to\omega+i0} = \left[\frac{2\pi}{\omega_F\beta}\right]^{2g_{LL}} \frac{\beta}{\pi}\overline{F}(\omega), \tag{3.80}$$

where

$$\overline{F}(\omega) = \sin(\pi g_{LL})\left[B(g_{LL}, 1-2g_{LL}) - B(g_{LL} - i\frac{\omega\beta}{2\pi}, 1-2g_{LL})\right], \tag{3.81}$$

with $B(x,y)$ the Beta function.

In order to calculate the conductance, we need the Fourier transform of $F(x,\tau)$ in the low-frequency limit $\omega \to 0$. Direct expansion of the Beta function yields

$$F_0(x) - F_{i\omega_\nu}(x)|_{i\omega_\nu\to\omega+i0} = -\frac{i\omega\sqrt{\pi}}{2\omega_F^2}\sin(\pi g_{LL})\left(\frac{\omega_F}{\pi T}\right)^{2(1-g_{LL})}\frac{\Gamma(1-g_{LL})}{\Gamma\left(\frac{1}{2}+g_{LL}\right)}\left[\Gamma(g_{LL})\right]^2 \tag{3.82}$$

Using Eqs. (3.38), (3.68), (3.82), we can evaluate the correction $\delta g_{\rm dw}$ to electrical conductance

$$\begin{aligned}\delta g_{\rm dw} &= -g_{\rm cw}C(g_{LL})\frac{d}{l}\left(\frac{\omega_F}{\pi T}\right)^{2(1-g_{LL})} \\ &= -g_{\rm cw}C(g_{LL})\left(\frac{T_0}{\pi T}\right)^{2(1-g_{LL})},\end{aligned} \tag{3.83}$$

where the function $C(g_{LL})$ is

$$C(g_{LL}) = \frac{\sqrt{\pi}}{2}\frac{\Gamma(g_{LL})}{\Gamma\left(\frac{1}{2}+g_{LL}\right)}. \tag{3.84}$$

The behaviour of the correction is shown in Fig. 3.8. The higher is the temperature,

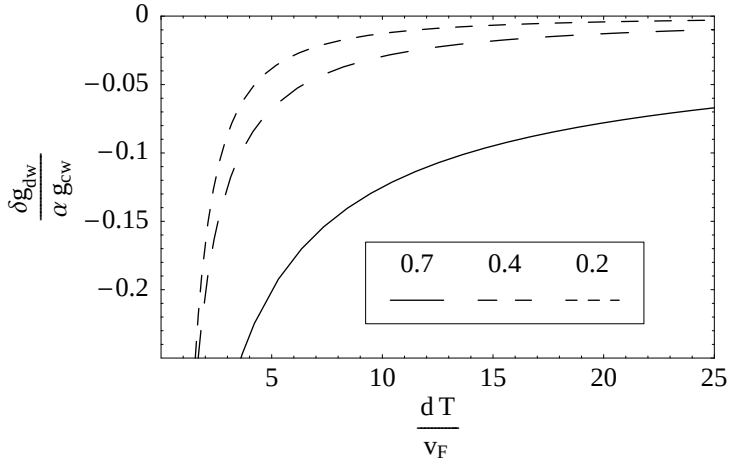

Figure 3.8: The behaviour of the correction to electrical conductance at high temperatures is shown in function of the reduced temperature Td/v_F in arbitrary units. The constant α is defined as $\alpha \equiv (d/l)x_F^{2(1-g_{LL})}$, and $x_F \equiv \omega_F d/v_F$.

the larger is the thermal activation and the smaller is the correction. If $g_{LL} = 1$, we find $\delta g_{\rm dw} = -g_{\rm cw}(d/l)$ both at low and high temperatures. In order for the perturbative approach to be valid for electrical conductance, we demand that $T \gg T_0$, which is satisfied for any $T \gg v/d$ in view of the condition $T_0 \ll v/d$ discussed above.

3.9 Correction to K_{cw} and diagrammatic approach

We have mentioned the fact that because of the different structure of current density operator for charge and heat transport, the diagrams contributing to the electrical and thermal conductance are very different.

The electrical conductance is directly proportional to Green's function, and the diagram contributing to charge transport for a clean quantum wire is just a straight line diagram, as shown in Fig. 3.6-left. In the previous sections, we have evaluated the correction to g_{cw} due to the presence of disorder. To do that, we have written the equation of motion for the Green's function in presence of disorder, and we have evaluated the correction to Green's function in Eq. (3.64) which allows to get the correction δg_{dw} in Eq. (3.69). We stress that the correction in Eq. (3.64) is the correction to

single-particle Green's function.

The thermal current density operator is bilinear in the displacement operator $\hat{u}$, Eq. (3.11); then, the simplest diagram contributing to heat transport is represented by the bubble diagram in Fig. 3.6-right.

The thermal conductance is described by the two-particles Green's function. Consequently, the correction to K_{cw} due to the presence of disorder cannot be correctly inferred from the equation of motion for the single-particle Green's function.

The complete dependence on the perturbative potential can be obtained by means of the perturbation theory, [Abrikosov75, Rickayzen80]. At the second order in the potential $V(x)$, the two-particles response function can be written as

$$\begin{aligned}\langle T_\tau j_{\rm th}(x_1,\tau_1) j_{\rm th}(x_2,\tau_2)\rangle = & \frac{1}{\langle 1 - H_{\rm imp}(x',\tau') + (1/2) H_{\rm imp}(x',\tau') H_{\rm imp}(x'',\tau'')\rangle} \\ & \times [\langle T_\tau j_{\rm th}(x_1,\tau_1) j_{\rm th}(x_2,\tau_2)\rangle - \langle T_\tau j_{\rm th}(x_1,\tau_1) j_{\rm th}(x_2,\tau_2) H_{\rm imp}(x',\tau')\rangle \\ & + (1/2)\langle T_\tau j_{\rm th}(x_1,\tau_1) j_{\rm th}(x_2,\tau_2) H_{\rm imp}(x',\tau') H_{\rm imp}(x'',\tau'')\rangle] \ . \end{aligned} \tag{3.85}$$

The latter equation gives rise to the contributions in the perturbative potential $V(x)$. As we will show in the following, such contributions correspond to all possible connected diagrams for the two-particles response function.

We are intrested in developing the third term in the numerator in the rhs of Eq. (3.85), since it is this term to give rise to the second order contributions in the perturbative potential $V(x)$. Remembering the definitions of the current operator $j_{\rm th}$, Eq. (3.11), and the Hamiltonian describing the effect of disorder, Eq. (3.42), one can write

$$\begin{aligned} & \frac{1}{2}\int d\,\tau_5 d\,\tau_6 \langle T_\tau j_{\rm th}(x_1,\tau_1) j_{\rm th}(x_2,\tau_2) H_{\rm imp}(x_5,\tau_5) H_{\rm imp}(x_6,\tau_6)\rangle \\ & \quad = \frac{v_F^4}{2}(m n_0)^2 \partial_{\tau_1}\partial_{\tau_3}\partial_{x_2}\partial_{x_4} \int d\,\tau_5 d\,\tau_6 \langle T_\tau \hat{u}_1\hat{u}_2\hat{u}_3\hat{u}_4 H_{\rm imp}(x_5,\tau_5) H_{\rm imp}(x_6,\tau_6)\rangle \\ & \quad = \frac{v_F^4}{2}(m n_0)^2 \left(\frac{2}{a}\right)^2 \partial_{\tau_1}\partial_{\tau_3}\partial_{x_2}\partial_{x_4} \int d\,X_5 d\,X_6 \,[\cos 2k_F x_5 \cos 2k_F x_6 \\ & \quad \times \langle T_\tau \hat{u}_1\hat{u}_2\hat{u}_3\hat{u}_4 \cos\pi n_0\hat{u}_5 \cos\pi n_0\hat{u}_6\rangle + \sin 2k_F x_5 \sin 2k_F x_6 \\ & \quad \times \langle T_\tau \hat{u}_1\hat{u}_2\hat{u}_3\hat{u}_4 \sin\pi n_0\hat{u}_5 \sin\pi n_0\hat{u}_6\rangle] \ , \end{aligned} \tag{3.86}$$

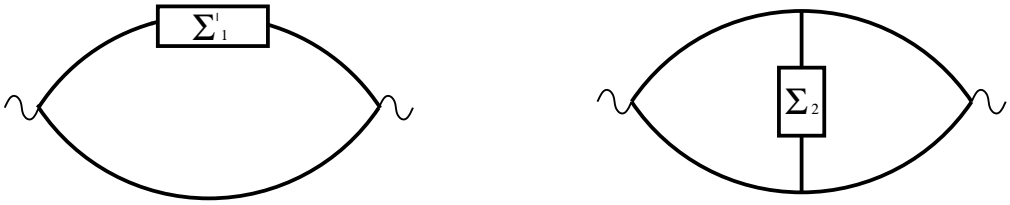

Figure 3.9: *Left*: First-class diagram. It is characterised by the presence of disorder on just one of two branches of bubble diagram. Σ_1' is the self-energy related to the presence of disorder. *Right*: Second-class diagram. It is characterised by the presence of disorder on both branches, and Σ_2 is the related self-energy. In both diagrams, solid lines are bosonic Green's function, and the wavy lines describe the interactions with the external field.

where (x_i, τ_i) $\forall i \in \{1, 2, 3, 4\}$ are just auxiliary variables, $\hat{u}_i = \hat{u}(x_i, \tau_i)$ and $X_i = (x_i, \tau_i)$.

All the connected contributing diagrams are obtained by means of Wick's theorem applied to the average values in the latter equation. Such diagrams can be divided into two different classes: we call first-class diagrams the contributions characterised by the presence of disorder Hamiltonians on just one of the two branches of the bubble diagram. The corresponding diagram is shown in Fig. 3.9-left, where Σ_1' is the self-energy related to the correction due to disorder. We call second-class diagrams the contributions characterised by the presence of disorder Hamiltonians on both branches of bubble diagram, and corresponding to the diagram in Fig. 3.9-right.

3.9.1 First-class diagram

The response function for a white noise potential corresponding to diagram in Fig. 3.9-left, from Eq. (3.86) reads

$$\chi(x, x'; i\omega_\nu) = 2\pi \left(\frac{2}{a}\right)^2 n_i u_0^2 \int d\, x_0\, T \sum_{i\omega_\mu} G_{i\omega_\nu + i\omega_\mu}(x, x_0) G_{i\omega_\nu + i\omega_\mu}(x_0, x') G_{i\omega_\mu}(x' x) \times \left[(\omega_\nu + \omega_\mu)^2 \omega_\mu^2 - \omega_\mu(\omega_\nu + \omega_\mu)|\omega_\mu||\omega_\nu + \omega_\mu|\right] \left[F_0(x_0) - F_{i\omega_\nu + i\omega_\mu}(x_0)\right] \quad (3.87)$$

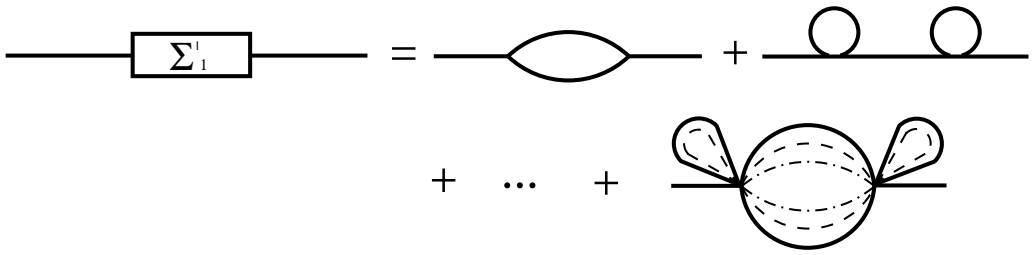

Figure 3.10: Diagrams infinite series contributing to the self-energy Σ_1'. They represent the only contributing terms to the electrical conductance.

The function $F_{i\omega_\nu}(x)$ is the Fourier transform of

$$\begin{aligned} F(x_1,\tau_1;x_2,\tau_2) &= \langle \sin\pi n_0\hat{u}_1 \sin\pi n_0\hat{u}_2\rangle + \langle \cos\pi n_0\hat{u}_1 \cos\pi n_0\hat{u}_2\rangle_{\rm CON} \\ &= \langle \sin\pi n_0\hat{u}_1 \sin\pi n_0\hat{u}_2\rangle + \langle \cos\pi n_0\hat{u}_1 \cos\pi n_0\hat{u}_2\rangle \\ &\quad -\langle \cos\pi n_0\hat{u}_1\rangle\langle \cos\pi n_0\hat{u}_2\rangle \ . \end{aligned} \tag{3.88}$$

The function $F_{i\omega_\nu}(x)$ filters all the connected diagrams by the deconnected ones, and it is the same function F in Eq. (3.66). CON in the latter equation stands for connected. In Eq. (3.87), the function $G_{i\omega_\mu}(x'x)$ describes the lower branch in the diagram in Fig. 3.9-left; the two remaining Green's functions, and the difference between the two F-functions describe the upper branch taking into account the correction due to disorder and then giving rise to the self-energy Σ_1'. From a diagrammatic point of view, the evaluation of Σ_1' corresponds to the sum, at any order, over all the dressed single-particle Green's functions contributing to transport, as shown in Fig. 3.10.

The analytical structure of Eq. (3.87) and the diagrams in Fig. 3.10 allow to understand how the contributions to energy transport take place. The response function $\chi(x,x';i\omega_\nu)$ is built summing over all the possible virtual states, indicated with solid and dashed lines in Fig. 3.10, each of which has energy ω_μ. Then, the external frequency ω_ν is coupled to each of these virtual states contributing to tranport. Such a complicated expression is a direct consequence of the strongly non-linear character of impurities Hamiltonian defined in Eq. (3.42). Transforming the sum into an integral in the complex plane, as already done in Appendix B for the thermal conductance for a clean wire, one recovers the first-class contribution to the correction to thermal

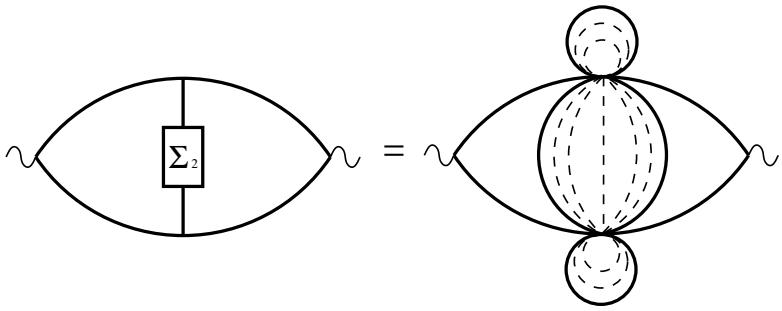

Figure 3.11: Second-class diagrams contributing to the self-energy Σ_2. They are related to two-particles Green's function, and do not exist for the charge transport.

conductance

$$\delta K^{\rm I}_{\rm dw} = -\frac{2n_{\rm i}u^2}{T^2a^2}\int_0^\infty d\omega \frac{\omega^2 T_{\rm pl}(\omega)}{\sinh^2(\beta\omega/2)} \Re{\rm e}\left\{\int_0^d dx G^{(0)}_{\omega+i0}(x,x)\left[F_0(x)-F_{\omega+i0}(x)\right]\right\}, \quad (3.89)$$

where the superscript I stands for first-class contribution. Of course, in the latter equation, we took into account the multiplicity due to the possibility that the disorder can also act on the lower branch of the diagram.

The self-energy Σ_1', from Fig. 3.9-left, takes into account the renormalization, due to disorder, of the single-particle Green's function. That is the first-class contribution to thermal conductance can be evaluated starting from the correction to the Green's function evaluated by means of the equation of motion in Eq. (3.64). The two self-energies Σ_1 and Σ_1' coincide.

3.9.2 Second-class diagrams

The second-class diagrams take into account the possibility that the two disorder Hamiltonians in the lhs of Eq. (3.86) are coupled each to one of the braches. In Fig. 3.11, all the second-class diagrams contributing to the self-energy Σ_2 are shown. These diagrams give rise to four distinct contributions. The corresponding response functions read

$$\chi_1(x,x';i\omega_\nu) = -8\pi^2\left(\frac{2}{a}\right)^2 n_i u_0^2 \int d\,x_0 T^2 \sum_{i\omega_\lambda, i\omega_\mu} (\omega_\nu+\omega_\lambda)(\omega_\nu+\omega_\mu)|\omega_\lambda||\omega_\mu| F_0(x_0)$$
$$\times G_{i\omega_\nu+i\omega_\lambda}(x,x_0)G_{i\omega_\lambda}(x_0,x)G_{i\omega_\nu+i\omega_\mu}(x_0,x')G_{i\omega_\mu}(x',x_0)\;, \qquad (3.90a)$$

$$\chi_2(x,x';i\omega_\nu) = -8\pi^2\left(\frac{2}{a}\right)^2 n_i u_0^2 \int d\,x_0 T^2 \sum_{i\omega_\lambda, i\omega_\mu} (\omega_\nu+\omega_\lambda)(\omega_\nu+\omega_\mu)|\omega_\lambda||\omega_\mu| F_{i\omega_\nu}(x_0)$$
$$\times G_{i\omega_\nu+i\omega_\lambda}(x,x_0)G_{i\omega_\lambda}(x_0,x)G_{i\omega_\nu+i\omega_\mu}(x_0,x')G_{i\omega_\mu}(x',x_0)\;, \qquad (3.90b)$$

$$\chi_3(x,x';i\omega_\nu) = -8\pi^2\left(\frac{2}{a}\right)^2 n_i u_0^2 \int d\,x_0 T^2 \sum_{i\omega_\lambda, i\omega_\mu} F_{i\omega_\lambda - i\omega_\mu}(x_0)$$
$$\times(\omega_\nu+\omega_\lambda)|\omega_\lambda|[(\omega_\nu+\omega_\mu)|\omega_\mu| - |\omega_\nu+\omega_\mu|\omega_\mu]$$
$$\times G_{i\omega_\nu+i\omega_\lambda}(x,x_0)G_{i\omega_\lambda}(x_0,x)G_{i\omega_\nu+i\omega_\mu}(x_0,x')G_{i\omega_\mu}(x',x_0)\;, \qquad (3.90c)$$

$$\chi_4(x,x';i\omega_\nu) = 8\pi^2\left(\frac{2}{a}\right)^2 n_i u_0^2 \int d\,x_0 T^2 \sum_{i\omega_\lambda, i\omega_\mu} (\omega_\nu+\omega_\lambda)(\omega_\nu+\omega_\mu)|\omega_\lambda||\omega_\mu|$$
$$\times G_{i\omega_\nu+i\omega_\lambda}(x,x_0)G_{i\omega_\lambda}(x_0,x)G_{i\omega_\nu+i\omega_\mu}(x_0,x')G_{i\omega_\mu}(x'x_0)$$
$$\times[F_{i\omega_\mu}(x_0)+F_{i\omega_\lambda}(x_0)+F_{i\omega_\nu+i\omega_\mu}(x_0)+F_{i\omega_\nu+i\omega_\lambda}(x_0)]\;. \qquad (3.90d)$$

The analytical structure of the above-mentioned response functions is even more complicated than the one evaluated in Eq. (3.87). Particularly, in their structure a double sum appears. One of the sums can be interpreted as we did in the previous section. The second one appears since one has to consider this time all the virtual states concerning the exchange energy between the two branches of the bubble, as shown in Fig. 3.11. First, one has to consider the possible coupling between the external frequency ω_ν with all the virtual states chracterised by an energy ω_μ; then, for each of them, one has to consider the possible coupling with the virtual states with energy ω_λ. All these processes contributing to thermal transport, and shown in Fig. 3.11, do not exist at all for the charge transport.

3.10 Lorenz number for a non-interacting system

The first test on the correctness of the linear response functions in Eqs. (3.89), (3.90a), (3.90b), (3.90c) and (3.90d) has been done calculating the Lorenz number for

$g_{LL} = 1$. As it has been shown by Chester and Tellung, even in presence of arbitrary impurity scattering, the Wiedemman-Franz law for a non-interacting system is fullfilled, [Chester61].

The expression of correction to Lorenz number is given by Eq. (3.36). The contributions given by the first-class diagrams to electrical and thermal conductance can be easily evaluated by means of Eqs. (3.75) and (3.89); they are well-behaved, and for $g_{LL} = 1$ they read

$$\frac{\delta g_{\rm dw}}{g_{\rm cw}} = -\frac{d}{l} \, , \qquad\qquad \frac{\delta K^{\rm I}_{\rm dw}}{K_{\rm cw}} = -2\frac{d}{l} \, . \tag{3.91}$$

The contributions of second-class diagrams for $g_{LL} = 1$ can be evaluated from Eqs. (3.90a), (3.90b), (3.90c) and (3.90d), and, albeit lengthy, the sum of the response functions reads

$$\chi_1(\omega) + \chi_2(\omega) + \chi_3(\omega) + \chi_4(\omega) = -(i\omega T) \left\{ \frac{d}{l} K_{\rm cw} + \frac{1}{2}\frac{d}{l}\omega_F \right\} \, . \tag{3.92}$$

The corresponding contribution to the thermal conductance follows from Eq. (3.9), and it reads

$$\frac{\delta K^{\rm II}_{\rm dw}}{K_{\rm cw}} = \left\{ \frac{d}{l} + \frac{1}{2}\frac{d}{l}\frac{\omega_F}{K_{\rm cw}} \right\} \, . \tag{3.93}$$

Unlike the contributions given by the firts-class diagrams, the correction in Eq. (3.93) is not well-behaved, giving rise to an ultraviolet divergence. Of course, such a divergence is completely unphysical, and it must be removed. No contributions to thermal conductance can exist as $T = 0$. No diagram has been neglected since, from Eqs. (3.36), (3.91) and (3.93), removing the non-physical terms, the Wiedemann-Franz law is fulfilled. And this results is robust.

The evaluation of contributions from second-class diagrams in presence of the interactions has been slowed down by our attempt to understand the origin of such unphysical ultraviolet divergence. It will be very important, for the calculations for any value of g_{LL} being able to discriminate the terms giving physical and unphysical contributions.

This will allow us to evaluate the correction to thermal conductance, and then

to Lorenz number. Of course, the total correction to heat transfer has to be negative because of the presence of disorder. Nothing can be said about the behaviour of the Lorenz number. Of course, as $T \to 0$, one expects to find again the classical value L_0 because of the dominant contribution of long wave-length plasmons, which will no longer perceive the presence of the constriction.

3.11 First-class contribution to thermal conductance in presence of interactions

We have mentioned that the evaluation of the second-class diagrams for any value g_{LL} is very cumbersome. In the meantime, the behaviour of the first-class diagram contribution to thermal conductance in Eq. (3.89) can be shown. It can be evaluated analytically in the limit of low and high temperatures, as previously did for the electrical conductance.

3.11.1 Low temperature limit: $T \ll v/d$

According to Eq. (3.89), we need to calculate the zero frequency limit of

$$\int_0^d dx \Re\mathrm{e}\left\{G^{(0)}_{i\omega_\nu\to\omega+i0}(x,x)\left[F_0(x)-F_{i\omega_\nu\to\omega+i0}(x)\right]\right\} = \frac{\pi d}{2\omega_F^2}\left(\frac{v}{\omega_F d}\right)^{2(g_{LL}-1)} . \quad (3.94)$$

The latter limit was easily performed by means of Eq. (3.74), and since in the zero frequency limit, as already mentioned, the Green's function reads $G^0_{i\omega_\nu} \simeq 1/2|\omega_\nu|$. Then, by means of Eq. (3.89), one finds the first contribution to the correction δK_{dw} to thermal conductance in the limit of vanishing temperature $T \to 0$,

$$\begin{aligned} \delta K^{\mathrm{I}}_{\mathrm{dw}} &= -2K_{\mathrm{cw}}\frac{d}{l}\left(\frac{\omega_F d}{v}\right)^{2(1-g_{LL})} \\ &= -2K_{\mathrm{cw}}\left(\frac{T_0 d}{v}\right)^{2(1-g_{LL})} \end{aligned} \quad (3.95)$$

Similar to the correction to electrical conductance, the correction to thermal conductance is negative and governed by the ratio $T_0 d/v$. Then, for Eq. (3.95) the same assumptions as for the corrections to electrical conductance in Eq. (3.78) hold.

3.11.2 High temperature limit: $v/d \ll T \ll \omega_F$

In order to evaluate the thermal conductance, we note that the Fourier transform of F in Eqs. (3.80) and (3.81) does not depend on the position x along the wire. As a result the integral over x in Eq. (3.89) only involves $G^{(0)}_{i\omega_\nu}(x,x)$,

$$\int_0^d dx G^{(0)}_{i\omega_\nu \to \omega + i0}(x,x) = d\overline{G}(\omega), \tag{3.96}$$

where

$$\overline{G}(\omega) = \frac{g}{2\omega}\frac{1+\gamma^2 e^{2i\omega d/v}}{1-\gamma^2 e^{2i\omega d/v}}\left(i - \frac{v\gamma}{\omega d}\frac{1-e^{2i\omega d/v}}{1+\gamma^2 e^{2i\omega d/v}}\right). \tag{3.97}$$

The correction $\delta K^{\rm I}_{\rm dw}$ to thermal conductance then can be written as

$$\delta K^{\rm I}_{\rm dw} = -\frac{1}{8\pi T^2}\int_0^\infty d\omega \frac{\omega^2}{\sinh^2(\beta\omega/2)}\delta T_{\rm pl}(\omega), \tag{3.98}$$

with

$$\delta T_{\rm pl}(\omega) = T\frac{16d}{l}T_{\rm pl}(\omega)\left(\frac{\omega_F}{2\pi T}\right)^{2(1-g_{LL})}\Re{\rm e}[\overline{F}(\omega)\overline{G}(\omega)]. \tag{3.99}$$

As a first test on the correctness of Eqs. (3.98) and (3.99) we calculate $\delta K_{\rm dw}$ for $g_{LL} = 1$, which must be equal to the result found at low temperatures, since the energy scale v_F/d for a non-interacting system is meaningless. In this case, $\overline{F}(\omega) = -i\beta\omega/4$ and $\overline{G}(\omega) = i/2\omega$, hence we find the expected result

$$\delta K^{\rm I}(g_{LL}=1) = -\frac{\pi}{3}\frac{dT}{l}T = -2K_{\rm cw}\frac{d}{l}. \tag{3.100}$$

Analytical evaluation of correction for arbitrary value of g_{LL} is very difficult for thermal

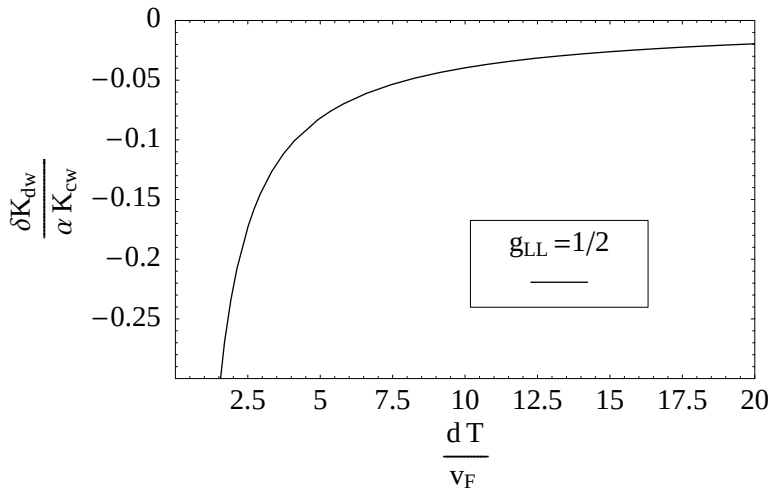

Figure 3.12: The behaviour of the first-class correction to thermal conductance at high temperatures and $g_{LL} = 1/2$ is shown in function of the reduced temperature Td/v_F in arbitrary units. The constant α is defined as $\alpha \equiv (d/l)x_F$, and $x_F \equiv \omega_F d/v_F$.

conductance, because of complicated expression of $\overline{F}$. For $g_{LL} = 1/2$, the real and imaginary part of $\overline{F}$ in Eq. (3.99), $\overline{F}_R$ and $\overline{F}_I$, respectively, have a simpler expression

$$\overline{F}_R = \Re\mathrm{e}\left[\Psi\left(\frac{1}{2} + i\frac{\omega}{2\pi T}\right)\right] + \gamma + 2\ln 2\,, \tag{3.101}$$

$$\overline{F}_I = \frac{\pi}{2}\tanh\left(\frac{\omega}{2T}\right)\,, \tag{3.102}$$

where $\Psi(z)$ is the digamma function. The first-class correction to thermal conductance, $\delta K^{\mathrm{I}}_{dw}/K_{cw}$ can be evaluated numerically, and its behaviour for $g_{LL} = 1/2$ is shown in Fig. 3.12. It behaves as $\sim T^{-1}$; the higher is the temperature, the larger the thermal activation, and the smaller is the correction, as in the case of the electrical conductance.

3.12 Conclusions

We are studying the thermal conductance for a one-mode disordered quantum wire connected adiabatically to two reservoirs. The physical system has been modeled by means of a finite length Luttinger liquid, and the disorder as a white noise potential.

First, we have reproduced the behaviour for a clean quantum wire. The electrical

conductance is not renormalised unlike the thermal conductance. Such a renormalisation takes place since the plasmons, which can be seen as responsible of heat transfer, suffer backscattering at the edges of the wire because of the connection to reservoirs. If $l_{\rm inh} \gg \lambda_F$ is the characteristic spatial scale of any inhomogeneities in the conductor, then electrons will not perceive at all the one-dimensional constriction, and the universal value for the electrical conductance is recovered, $g_{\rm cw} = e^2/h$. This is no longer true for plasmons which can have any wavelength. Then, for particular values, such a wavelength can be comparable to $l_{\rm inh}$, and plasmons are scattered off by leads. This gives rise to a strong renormalization of thermal conductance and of Lorenz number.

In presence of disorder, an interplay between disorder and interactions exists. Such an interplay is contained in the energy scale T_0 we have introduced in Section 3.7.

Because of the analytical structure of electrical current density operator, the correction to electrical conductance can be evaluated by means of the correction to the bare single-particle Green's function. This has been done solving the equation of the motion for the above-mentioned Green's function and its correction that allows to write immediately the correction to electrical conductance. The charge transport has been studied in the limit of low and high temperatures. Particularly, for finite temperatures, it behaves as $\sim T^{-2(1-g_{LL})}$. The effects of disorder is as smaller as temperature increases.

For the thermal conductance, the evaluation is more cumbersome.

In this case, the thermal conductance is proportional to two-particles Green's function. A diagrammatic approach has been developed in the perturbative theory framework to take into account all the diagrams contributing to heat transport. As we have discussed, some of these diagrams could be evaluated by means of single-particle Green function. For the remaining ones, a different approach is mandatory.

Unlike what happens for electrical conductance, because of the structure of thermal current density operator, two different kind of contributions exist. The ones called first-class contributions where the disorder acts on just one branch of the bubble diagram, and the so-called second-class contributions, where the disorder acts on both

branches. The first-class diagrams are well-behaved. They give rise to a contribution which has been evaluated in the limit of high and low temperatures, and which behaves qualitatively as the correction to electrical conductance. On the contrary, the second-class diagrams are not-well behaved, and they give rise to an ultraviolet divergence. Our work has been slowed down by the need to understand the nature of such a divergence. At the moment, we verified that the aforementioned diagrams give rise to, for a non-interacting system, $g_{LL} = 1$, the correct result to thermal conductance in order for the Wiedemann-Franz law to be respected. Understanding the nature of the above-mentioned divergence is a fundamental step to be able to tackle the problem for any value of interaction strength.

Once the correction to thermal conductance will be calculated, the behaviour of the Lorenz number for the interacting system will be able to be evaluated. At the moment, one cannot say, whether the presence of impurities affects equally the charge and heat transport; that is, one cannot say whether the correction to the Lorenz number, with respect to a clean wire, is negative or positive.

Conclusions

Nous étudions la conductance thermique pour un fil quantique connecté de façon adiabatique à deux réservoirs. Le système physique a été modélisé comme un liquide de Luttinger de taille finie, et le désordre comme un potentiel du type bruit blanc.

D'abord, nous avons reproduit le comportement d'un fil quantique propre. La conductance électrique n'est pas renormalisée, à la différence de la conductance thermique. Une telle renormalisation a lieu car les plasmons, qui peuvent être vus comme les responsables du transport de chaleur, sont diffusés aux bords du fil à cause de la connexion aux réservoirs. Si $l_{\mathrm{inh}} \gg \lambda_F$ est l'échelle spatiale typique de toutes les inhomogénéités à l'intérieur du fil, alors les électrons n'apercevront pas du tout la présence du fil, et la valeur universelle pour la conductance électrique est retrouvée, $g_{\mathrm{cw}} = e^2/h$. Cela n'est plus vrai pour les plasmons qui peuvent avoir n'importe quelle longueur

d'onde. Alors, pour certaines valeurs, une telle longueur d'onde peut être comparable à $l_{\rm inh}$ et les plasmons peuvent être diffusés. Cela donne lieu à une forte renormalisation de la conductance thermique et ensuite du nombre de Lorenz.

En présence de désordre, une compétition entre le désordre et les interactions existe. Une telle compétition est décrite par le paramètre T_0 que nous avons introduit dans la Section 3.7.

A cause de la structure analytique de l'opérateur densité de courant électrique, la correction à la conductance électrique peut être évaluée à l'aide de la correction à la fonction de Green à une particule. Cela a été fait, en résolvant l'équation du mouvement pour la fonction de Green en question et pour sa correction qui permet d'écrire immédiatement la correction à la conductance électrique. Le transport de charge a été étudié dans les limites de basse et de haute températures. En particulier, à température finie, elle se comporte comme $\sim T^{-2(1-g_{LL})}$. Les effets du désordre sont de plus en plus faibles pour des températures croissantes.

En ce qui concerne la conductance thermique, l'évaluation est beaucoup plus lourde.

Dans ce cas, la conductance thermique est proportionnelle à la fonction de Green à deux particules. Une approche diagrammatique a été développée dans le contexte de la théorie perturbative pour prendre en compte tous les diagrammes contribuants au transport de chaleur. Comme nous l'avons discuté, certains de ces diagrammes peuvent être évalué à l'aide de la fonction de Green à une particule. Pour les restants, une approche différente est obligatoire.

A la différence de ce qu'il se passe pour la conductance électrique, à cause de la structure de l'opérateur densité de courant, deux types de contribution existent. Celles que nous avons appelés diagrammes de première classe où le désordre agit seulement sur une branche du diagramme à bulle, et les dits diagrammes de deuxième classe, où le désordre agit sur les deux branches de la bulle. Les diagrammes de première classe ont un comportement régulier. Ils donnent lieu à une contribution qui a été évaluée à les basses et à hautes températures, et qui se comporte qualitativement comme la correc-

tion à la conductance électrique. En revanche, les diagrammes de deuxième classe ont un comportement singulier, et ils donnent lieu à une divergence ultraviolette. Notre travail, a été ralenti par la nécessité de comprendre la nature de ces divergences. Pour le moment, nous avons vérifié que les susdits diagrammes donnent lieu, pour un système sans interaction, $g_{LL} = 1$, au résultat correct pour la conductance thermique de façon à ce que la loi de Wiedemann-Franz soit respectée. Comprendre la nature des susdites divergences constitue un pas fondamental en vue d'aborder le problème pour n'importe quelle valeur des interactions dans le fil.

Une fois les corrections à la conductance thermique calculées, le comportement du nombre de Lorenz pour un système en interaction pourra être évalué. Pour l'instant, personne ne peut dire si la présence des impuretés affecte également le transport de la charge et de la chaleur; c'est à dire que personne ne peut prévoir si la correction au nombre de Lorenz par rapport à un fil propre est négative ou positive.

Résumé en français du chapitre 3

A l'aide de la théorie des liquides de Luttinger, dans ce chapitre nous étudions le transport électrique et thermique pour un système uni-dimensionnel.

D'abord, nous montrons les résultats pour un fil propre. Comme nous l'avons mentionné dans l'Introduction, dans ce cas, la seule forme de désordre présente à l'intérieur du système est représentée par les connexions aux réservoirs. De telles inhomogénéités sont caractérisées par une échelle spatiale typique $l_{inh} \gg \lambda_F$. Les électrons, responsables du transport de la charge, ne sont pas sensible à une telle présence car ils sont caractérisés par une échelle spatiale de l'ordre de λ_F. En revanche, les ondes de densité de charge, ou plasmons, peuvent avoir n'importe quelle longueur d'onde. Ceci étant, pour des valeurs bien définies et comparables à l_{inh}, les plasmons seront diffusés au bords du fil. Cela donne lieu à une forte renormalisation de la conductance thermique et ensuite du nombre de Lorenz.

L'évaluation des corrections aux susdites conductances en présence d'impuretés à été accomplie pour un désordre de type bruit blanc. A cause de la nature différente des électrons et des plasmons, la méthode suivie dans l'évaluation des corrections est différente aussi.

Pour la correction à la conductance électrique, nous écrivons l'équation du mouvement pour la fonction de Green à une particule en terme de laquelle la conductance électrique peut être écrite. Une telle équation en présence de désordre ne peut être résolue que de façon perturbative par rapport à l'amplitude de la force des impuretés. Cela permet de retrouver correctement toutes les contributions à la conductance électrique. La correction a été étudiée dans le régime des basses et hautes températures.

La conductance thermique, quant à elle, est décrite en termes de la fonction de Green à deux particules. Ceci-étant, la susdite solution à l'équation du mouvement ne peut pas être utilisée. Nous avons donc suivi une approche diagrammatique permettant de récupérer tous les diagrammes nécessaires afin d'évaluer correctement la conductance. Les fonctions de réponse associés à chacun de ces diagrammes ont des expressions très compliquées demandant une analyse attentive est adéquate.

Pour l'instant, nous avons vérifié, pour la conductance thermique, que les susdites contributions pour un système sans interactions donnent la valeur correcte de la conductance thermique de sorte que la loi de Wiedemann-Franz est respectée, ainsi que prévu pour des particules sans interaction en présence de désordre.

PART II

GRANULAR METALS

Chapter 4

SUPERCONDUCTIVITY AND FLUCTUATIONS

In this second part of the thesis, we present the evaluation of the corrections, due to superconducting fluctuations, to thermal conductivity in granular metals.

Thermodynamical fluctuations play an important role in phase transitions close to the critical temperature, giving rise to measurable effects. We will discuss the influence of such effects in the case of superconducting transition on electrical and thermal transport in the normal state. Because of such fluctuations, the transport properties of superconducting state are mixed with the properties of the normal one. We will show that the fluctuations of order parameter give rise to important contributions which are both classical and quantum mechanical.

In this first chapter, we will give some reminders of BCS theory, presenting particularly the so-called BCS Hamiltonian, which will be used later, and showing the fundamental results; then, we will discuss phenomenologically the importance of thermodynamical fluctuations, giving some elements to better understand the role they play in phase transitions. The importance of superconducting fluctuations will be pointed out, first from a phenomenological point of view, then from a microscopic one. We will focus on the microscopic approach, which is the way we have followed in our study.

Known results are presented to define a coherent context where illustrate our own work.

4.1 BCS theory of superconductivity

In this section, we want to recall the most important results of BCS theory. For a complete review, see [Tinkham96, DeGennes99].

When Bardeen, Cooper and Shrieffer presented the microscopic theory of superconductivity in 1957, such a phenomenon was known since nearly fifty years; already in 1911, Kamerlingh-Onnes had discovered that below the temperature of 4.2 K mercury presents a strong suppression of electrical resistance. The same behaviour was then discovered for other metals. The temperature at which the superconducting transition occurs is called *critical temperature* T_c.

Between 1911 and 1957, a great number of efforts were made to describe such a phenomenon, both from a phenomenological and microscopic point of view.

The discovery of isotopic effect in 1950, showing the dependence of T_c on the mass of ions in the lattice, $T_c \propto M^{-1/2}$, pointed out the importance played by the lattice vibrations, also called phonons. Such a discovery represented perhaps the decisive step for a deeper comprehension from a microscopic point of view.

In fact, it was later shown that electrons in a lattice can interact by means of an attractive force, and that such an attractive force can be correctly described by means of an effective electron-phonon interaction, inducing the formation of a bound electron-electron state at temperatures lower than T_c. Bardeen, Cooper and Shrieffer in their description imagined that the effective potential describing the attractive interaction could be considered constant until a cut-off value given by the Debye frequency ω_D. Under these assumptions, the system can be described by the following BCS Hamiltonian

$$H_{BCS} = \sum_{\mathbf{k},\sigma} \varepsilon_{\mathbf{k}} c^{\dagger}_{\mathbf{k},\sigma} c_{\mathbf{k},\sigma} - g \sum_{\substack{\mathbf{kl} \\ \epsilon_{\mathbf{k}},\epsilon_{\mathbf{l}} < \omega_D}} c^{\dagger}_{\mathbf{k}\uparrow} c^{\dagger}_{-\mathbf{k}\downarrow} c_{-\mathbf{l}\downarrow} c_{\mathbf{l}\uparrow} \ , \tag{4.1}$$

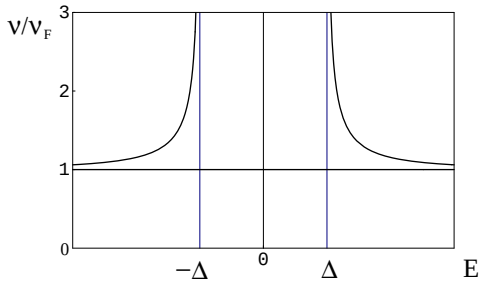

Figure 4.1: BCS density of states in superconducting metals. The superconducting instability concerns just a layer around the Fermi level, and it is characterised by the opening of a gap Δ in the density of states and in the spectrum of quasi-particles excitations.

where $\varepsilon_{\mathbf{k}}$ is the energy of an electron of wave vector $\mathbf{k}$, σ is the spin index, $c^\dagger$ and c the creation and annihilation operators respectively, and g the positive constant describing the effective attractive interaction between electrons; the second term in the rhs of Eq. (4.1) is a two-body interacting potential.

Phenomenologically, at very low temperatures, Fermi's sphere has most of the states occupied. As it generally happens for transport properties, the superconducting instability, that is the possibility for electrons to form Cooper pairs, just concerns a narrow layer around the Fermi level.

The superconducting transition is characterised by the opening of an energy gap Δ in the density of state around the Fermi level, as shown in Fig. 4.1, and in the spectrum of quasi-particles excitations in the condensate; such a spectrum was found by Cooper to be $\epsilon = [\xi^2 + \Delta^2]^{1/2}$, $\xi = \varepsilon - \mu$ being the energy of electronic quasi-particles measured with respect to the Fermi level μ.

The length ξ_c which defines the spatial extension of Cooper pairs is the so-called *correlation length*, and it can be estimated to be of the order

$$\xi_c \sim \frac{v}{\Delta}, \tag{4.2}$$

v being the velocity of the quasi-particle in the normal state. In most of the pure bulk metals, the correlation length is of the order $\sim 10^{-5}$cm.

The expression for the gap at zero temperature is given by BCS theory, and it

reads

$$\Delta(T=0) = 2\omega_D \exp\left(-\frac{2}{g\nu_F}\right) , \tag{4.3}$$

where ν_F is the density of states at Fermi energy. The value of the gap is related to the critical temperature

$$\Delta(T=0) = \frac{\pi}{\gamma_E} T_c , \tag{4.4}$$

where $\gamma_E = e^{\gamma}$, γ being the Euler constant. The dependence on temperature of the correlation length reads

$$\xi_c(T) = \frac{v}{\pi\Delta(T)} , \tag{4.5}$$

and, if $T = T_c$, then ξ_c reads

$$\xi_0 \equiv \xi_c(0) \approx 0.18 \frac{v}{T_c} . \tag{4.6}$$

4.2 Superconducting fluctuations

In this and in the following sections, we discuss superconducting fluctuations, particularly from a microscopic point of view; we want to understand the role they play in the transport properties of normal state in metals, and what kind of physical and mathematical tools we need to study such phenomena.

Second order phase transitions are characterised by the presence of an order parameter which vanishes in the normal state, and it is different than zero below the critical temperature T_c, [Huang87]. For example, in the ferromagnetic transition, the order parameter can be the spontaneous magnetization vector $\mathbf{M}$; in the superconducting transition, the order parameter is a complex scalar quantity: the coherent wave function of Cooper pair in the condensate state.

The phenomenological Landau theory of phase transition states that close to T_c, where the order parameter becomes smaller and smaller, the generic thermodynamic potential Φ can be developed in term of the order parameter, here indicated with φ, as

$$\Phi = \Phi_0 + \frac{1}{2}\alpha V \epsilon \varphi^2 + \frac{1}{4} b V \varphi^4 - h\varphi V , \tag{4.7}$$

where $\epsilon = (T - T_c)/T_c$ is the reduced temperature, V the volume of the system, α and b the development coefficients, and h an external field. From the potential Φ, several thermodynamical quantities can be evaluated, as, for instance, the entropy $S = -(\partial\Phi/\partial T)_\varphi$, and then the heat capacity $C_p = (T/V)(\partial S/\partial T)_p$, p being the pressure. The heat capacity presents a jump in correspondece with the transition, as usual for the second order phase transition.

The evaluation of different physical quantities shows that the critical exponents controlling their behaviour do not match exactly with the experimental results. Landau theory does not provide the truly correct behaviour, since it does not take into account the fluctuations of order parameter. Such fluctuations, very close to T_c, give rise to measurable effects.

If ΔE is the total variation of energy due to onset of just one fluctuation, then the probability that such a fluctuation takes place is, [Larkin04]

$$W \propto \exp\left(\frac{-\Delta E}{T}\right) \ . \tag{4.8}$$

From Eq. (4.8), the smaller the variation of energy associated to fluctuation, the larger is the probability it takes place. Close to T_c, the difference between the two phases is so small, that the fluctuations of order parameter are associated to very small variations of energy. Then, they can give large contributions to the thermodynamical quantities. Consequently, the potential in Eq. (4.7) has to be modified to take correctly into account such phenomena. The new potential can be written as

$$\Phi(\varphi) = \Phi_0 + \int d\,V \left[\frac{1}{2}c(\nabla\varphi)^2 + \frac{1}{2}\alpha\epsilon\varphi^2 + \frac{1}{4}b\varphi^4 - h\varphi\right] \ , \tag{4.9}$$

where we supposed that $\varphi = \varphi(r)$ is a function and no longer a simple number. The first term in the integral in the rhs of Eq. (4.9) is the term allowing to take into account the fluctuations of order parameter. Eq. (4.9) is a very general expression holding for any second order phase transition. Particularly, discussing the superconducting transition, the free energy functional for a superconductor reads

$$\mathcal{F}_s = \mathcal{F}_n + \int d\,V \left[\alpha\epsilon|\Psi|^2 + \frac{1}{2}b|\Psi|^4 + \frac{1}{4m}\left|\left(-i\nabla - \frac{2e}{c}\mathbf{A}\right)\Psi\right|^2 + \frac{H}{8\pi}\right] \ , \tag{4.10}$$

where $\mathcal{F}_n$ is the free energy in the normal state, H is an external magnetic field, $\mathbf{A}$ the vector potential, and Ψ is the order parameter for the superconducting state. It is generally defined as

$$\Psi = \sqrt{\frac{n_s}{2}} e^{i\phi} \,, \tag{4.11}$$

where n_s is the superconducting electrons density, and ϕ the phase of the wave function describing the condensate of Cooper pairs. From Eq. (4.10) the Ginzburg-Landau theory allows to determine different thermodynamical quantities; for a complete review, see [Larkin04, Thinkam96]. Here, we just point out a result which we will be useful later; Ginzburg-Landau theory allows to define a characteristic length, which is the correlation length of the fluctuations of order parameter Ψ, and it is defined as

$$\xi_{GL}(T) = \frac{1}{2(m\alpha|\epsilon|)^{1/2}} \,. \tag{4.12}$$

ξ_{GL} in Eq. (4.12) can be related to the correlation length in Eq. (4.5) of BCS theory

$$\xi_{GL}(T) = 0.74\,\xi_0 \left(\frac{T_c}{T_c - T}\right)^{1/2} \qquad \text{clean case} \,, \tag{4.13a}$$

$$\xi_{GL}(T) = 0.85 \left(\frac{\xi_0 l T_c}{T_c - T}\right)^{1/2} \qquad \text{dirty case} \,, \tag{4.13b}$$

where l is the mean free path.

4.3 Microscopic approach

We have spoken of thermodynamical fluctuations, and we have pointed out that such phenomena are more relevant as one gets closer to T_c. We gave some brief reminder about the phenomenological approach typical of the Landau-Ginzburg theory; particularly, we presented the Landau functional, Eq. (4.10), which allows the evaluation of several physical quantities for the superconducting state, at least under the hypothesis that one is not too far from T_c. The functional allows not only the evaluation of the above-mentioned physical quantities, but also the corrections due to the fluctuations of order parameter.

The approach we will follow to determine such corrections will be different. We will try to understand how such corrections can be described by a microscopic point of view.

Fluctuations of order parameter in superconducting transition manifests themselves with the appearance of Cooper pairs above the critical temperature T_c. One may say that such pairs anticipate the superconducting transition, or, at least, some features of the superconducting state, modifing the transport properties of the normal one. This is observable in the behaviour of different physical quantities such as the conductivity and the heat capacity, [Varlamov99]. Particularly, for the heat capacity, the characteristic jump of second order phase transition can be strongly smeared.

Without entering in details, we point out that the precursor effects of superconductivity due to fluctuations are much more observable in the high temperature superconductors (HTS), or very dirty samples, [Larkin04]. HTS and dirty superconductors are characterised by a correlation length ξ_c of Cooper pairs much smaller than in bulk metals. This is due to low-dimension effective spectrum for electrons in the first case, and to the diffusive nature of propagation in the second one. Above T_c, many spatial regions, whose typical dimension is ξ_c, can undergo fluctuations to superconducting state, and the transition is strongly smeared.

The first estimation of the contribution of superconducting fluctuations was made by Ginzburg in 1960, and he showed, as anticipated before, that fluctuations smear the typical jump foreseen by Landau theory of phase transition, [Ginzburg60, Larkin04]. Ginzburg also estimated the range of temperature where the fluctuations corrections are relevant, and he found for a 3D-system

$$\frac{\delta T}{T_c} \sim \left(\frac{a}{\xi_0}\right)^4 \sim 10^{-12} - 10^{-14} \,, \tag{4.14}$$

where a is the interatomic distance, and ξ_0 the superconducting coherence length at zero temperature, already defined in Eq. (4.6). Of course, the interval defined in Eq. (4.14) is below the accessible range in experiments. This is the reason why the fluctuations contributions in transport properties were for long time neglected.

The same estimation as the one presented by Ginzburg was then made by Aslamazov and Larkin by means of a microscopic approach in 1968, [Aslamazov68]; they also found the dependence on the dimension of the sample of the exponent of the ratio a/ξ_0 in Eq. (4.14); for 2D electron spectrum, it reduces to 1, providing a more accesible range in experiments.

In the following, we consider the effects of fluctuations on electrical and thermal conductivity, describing qualitatively what happens for bulk metals from a microscopic point of view.

The presence of fluctuations of order parameter gives rise to three different contributions that we analyse distinctly in the following.

As we have mentioned, the fluctuations of order parameter manifest themselves with the appearance of Cooper pairs above the critical temperature T_c. The time dependent Ginzburg-Landau theory, (TDGL), foresees that the lifetime of such pairs is the so-called Ginzburg-Landau time $\tau_{GL} \sim 1/(T - T_c)$, which shows that the aforementioned Cooper pairs are well defined close to the critical temperature. Of course, below T_c they are in excess with respect to the fermionic quasi-particles composing the normal state. In other words, fluctuations of order parameter open in the normal state a new transport channel called the Cooper channel; such a channel is described by an appropriate propagator, generally called *Cooper pair fluctuation propagator*. In the next chapter, we will study the form of such a propagator which plays a fundamental role in the microscopic description.

The attitude of Cooper pairs to propagate easily through the system makes the correction due to their presence in the normal state positive: both electrical and thermal conductivity are enhanced by fluctuating Cooper pairs, [Larkin04, Niven02]. This correction is usually called Aslamazov-Larkin contribution, (AL), or paraconductivity. Particularly, one finds for bulk metals the following dependence on temperaure

$$\sigma_{AL} \sim (T - T_c)^{d/2-2} , \tag{4.15a}$$

$$T\,\kappa_{AL} \sim (T - T_c)^{d/2} , \tag{4.15b}$$

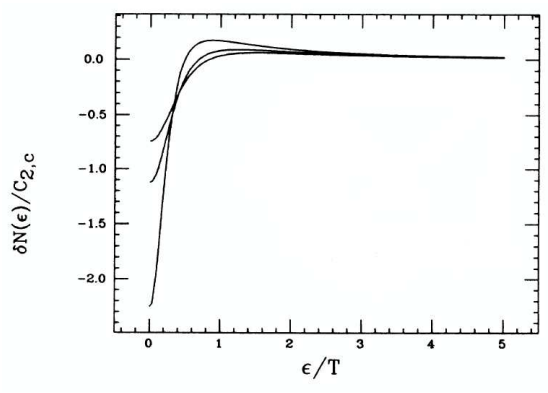

Figure 4.2: Single-particle DOS correction for a two-dimensional sample in the case of a clean superconductor, [DiCastro90].

where d is the dimension of the sample. The AL contribution to electrical conductivity is strongly divergent as $T \to T_c$, while the contribution to thermal conductivity is not. Qualitatively, this behaviour can be understood by means of Cooper pairs features: they can easily transport charge, but they do not carry heat, at least, at a first approximation. Then, close to the critical temperature, where the number of Cooper pairs strongly increases, the contribution of pairs to electrical transport is much larger than to the thermal one.

Electrons forming Cooper pairs are no longer available for single-particle transport. The number of electronic states being well defined, the density of states close the Fermi level has to change. This reduction of single-particle density of states is described by the so-called DOS contribution, and for a clean superconductor, its behaviour is shown in Fig. 4.2, [DiCastro90]. The decrease of single-particle density of states leads to negative contribution to electrical and thermal conductivity. Both of them behave, for bulk metals, as $\sim -(T - T_c)^{d/2-1}$ in three and one dimension. In two dimension, the behaviour is logarithmic. The DOS contribution is divergent for $d \leq 2$, but it diverges more slowly than the AL contribution. Because of this weaker divergency, for the electrical conductivity, it is often neglected except for the case where the other diverging contributions are suppressed or far from T_c, [Varlamov99].

For thermal conductivity, it is different. As shown recently by Niven and Smith,

always in bulk metals, the DOS contribution is exactly canceled by the third and last contribution to transport properties that fluctuations give rise: Maki-Thompson contribution (MT), [Niven02].

This latter contribution can be seen as the result of Andreev reflection of the electrons by the fluctuating Cooper Pairs, [Maki68, Thompson70, Larkin04]. As explained in [Niven02], because of the fluctuations, and then of Cooper attractive interaction, electrons can scatter into a hole. The latter carry the same heat current as an electron, but the opposite charge. The probability amplitude of Andreev reflection is the same as for an electron to form a fluctuating Cooper pair, and then is the same as the probability that the single-particle density of states is reduced. Since, as mentioned, the heat current contribution is the same for an electron and for a hole, for the thermal conductivity in bulk metals, DOS and MT contributions cancel exactly. This is not the case for the electrical conductivity, since holes carry opposite charge with respect to the electrons; then, for electric transport, DOS and MT corrections have the same sign and they reinforce.

The temperature dependence of MT close to the critical temperature T_c and for bulk metals is the same as for the DOS. MT correction is also described sometimes as generated by the coherent scattering of electrons forming Cooper pairs on the same elastic impurities. Then, MT is extremely sentitive to all electron phase-breaking processes.

Résumé en français du chapitre 4

Dans ce chapitre, nous donnons un bref rappel des principaux résultats de la théorie BCS de la supraconductivité. Certains seront utilisés pour discuter des propriétés de métaux granulaires.

Puis, nous abordons le problème des fluctuations supraconductrices. Elles jouent un rôle fondamental dans les transitions de phase, et elles influencent énormément les propriétés de transport près de la température de transition T_c, où les propriétés typiques de la phase normale se mélangent avec celles de la phase supraconductrice. Nous présentons, d'abord, le phénomène de fluctuations d'un point de vue thermodynamique. La théorie de Ginzburg-Landau permet d'écrire la fonctionnel énergie libre à partir de laquelle toutes les grandeurs physiques peuvent être évaluées, en prenant en compte les contributions dues aux fluctuations.

Nous, nous avons suivi une approche microscopique qui fut proposée pour la première fois en 1968 par Aslamazov et Larkin, [Aslamazov68]. Comme nous les avons mentionnés dans l'Introduction, nous présentons les différentes contributions microscopiques dues aux fluctuations: la contribution Aslamazov-Larkin, qui prend en compte la possibilité que deux électrons puissent former une paire de Cooper même dans la phase normale près de la température critique; les électrons qui forment une paire de Cooper ne sont plus disponible pour le transport à une particule. Cela implique qu'il doit y avoir une redistribution au niveau de Fermi des états disponibles à une particule; cette redistribution est prise en compte par la contribution dite Densité d'états, DOS. Enfin, un terme de nature purement quantique apparaît: la contribution Maki-Thompson; elle considère la possibilité que les deux électrons formant une paire

de Cooper soient diffusés de façon cohérente par la même impureté.

Chapter 5

GRANULAR METALS

In the first section of this chapter, we motivate the interest for such systems; we define what a granular metal is, and we introduce the characteristic energy scales which allow to define different working regimes, and some important physical quantities.

Then, we illustrate particularly the known results concerning the electrical transport. As for other kinds of mesoscopic systems, the charge transport has been more studied at the moment than the thermal transport. We will show how different the behaviour of a granular system can be, passing from truly metallic to insulating behaviour. This will allow us to have a larger vision of granular metals characteristics before introducing in details our work.

Finally, we study the influence of superconducting fluctuations on thermal conductivity; we evaluate, by means of the diagrammatic technique, the three different contributions which have been introduced in the previous chapter, pointing out the difference existing between the bulk and the granular case. At the end, we present the results and the conclusions.

As we did for quantum wires, most of the calculation are presented in details, for the interested reader, in dedicated appendices to make the reading fluent.

5.1 Normal granular metals

Since many years, the interest in understanding the transport properties of granular metals represents a great deal of research in mesoscopic physics, both theoretically and experimentally, [Abeles77, Dynes78, Orr86, Imry81, Shapira83, Barber94, Gerber97, Efetov03, Beloborodov00, Beloborodov03, Beloborodov05]. The reason resides both in the fact that their properties are general for a wealth of disordered systems and in the fact that granular metals represent, from an experimental point of view, systems where the interaction strength and the disorder can be partially controlled, [Barber94, Gerber97].

Granular metals can be considered as a d-dimensional array of metallic grains embedded in an insulating amorphous matrix, with impurities on the surface and inside each grain. In Fig. 5.1-left, Al grains are embedded in Ge matrix, [Shapira83]. Each Al grain has an average dimension of 120±20 , and the sample has linear dimension of the order of mm.

The highly disordered granular structure of real samples can be detected experimentally by studying the resistance of the samples in function of their thickness. This was one of the first techniques to reveal the granular nature of the samples, [Dynes78]. In Fig 5.1-right, it is reported the behaviour of the resistance for different metals deposited, in extremely thin monolayers per time, on thin films. The figure shows how the decrease of resistance is very rapid for very small increase of thickness, and it is described approximately by an exponential behaviour. It implies that the morphology is not uniform, but granular. Qualitatively, one can think of a model, where each deposition reduces the average distance between the already deposited grains or island, increasing the tunneling, and then the conductivity.

In each grain, the energy levels have no longer the classical band structure typical of bulk metals; because of the small size of the grains, they are discrete. The smallest energy scale is the mean level spacing

$$\delta = \frac{1}{\nu_F V} , \tag{5.1}$$

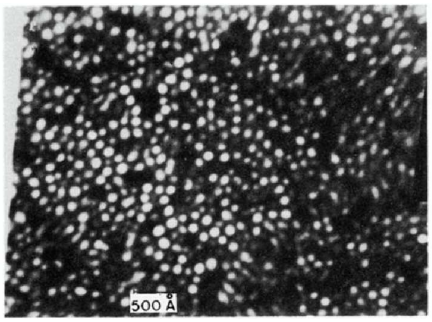

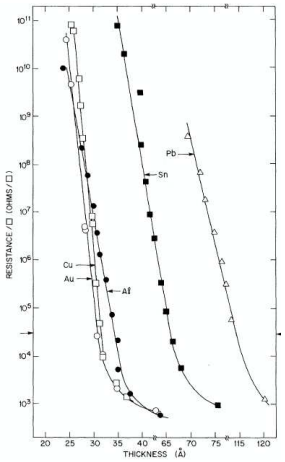

Figure 5.1: *Left*: Image of a granular film composed of Al grains on amorphous Ge background. The typical size of the grains is ~ 120, [Shapira83]. *Right*: The granular structure of thin samples can be revelaled studing the behaviour of the resistance in function of the thickness of the film. The nearly exponential behaviour shown in the figure can be justified only by a strongly non-uniform morphology typical of granular metals.

where $V = a^d$ is the volume of the grain, a being the size of the single grain, and ν_F the density of states at the Fermi level. The size of the grain defines the Thouless energy $E_T = D/a^2$, $D = v_F^2\tau/3$ being the diffusion constant, v_F the Fermi velocity and τ the mean free path between two collisions. Each grain is characterised by a local dimensionless conductance

$$g = \frac{E_T}{\delta} \,, \tag{5.2}$$

while the macroscopic tunnelling conductance is defined as

$$g_T = \left(\frac{\pi}{2}\frac{t}{\delta}\right)^2 \,, \tag{5.3}$$

where t is the hopping energy. Generally, it is supposed $g_T \ll g$, signaling the condition that an electron propagates easier in the grain than in the macroscopic sample because of tunneling among grains. In other words, the granular structure is important, and the largest contribution to resistance comes from the contact resistance.

The value of macroscopic tunneling conductance g_T plays a fundamental role, since it allows to define different regimes. In the following, we report some known results for normal granular metals in two cases: $g_T \ll 1$ and $g_T \gg 1$, and for temperatures $T \ll g_T\delta$ and $T \gg g_T\delta$. In both cases, the effects of long-range Coulomb

interactions have been taken into account, and the corrections to the electrical and thermal conductivity have been evaluated.

It has been shown by Beloborodov et al. that in the limits $T \gg g_T\delta$, corresponding to not very low temperatures, the weak localizations effects are suppressed, leading to incoherent motion of electrons in the grains, [Beloborodov01]. In this limit, for large tunneling conductance g_T, the electrical conductivity behaves, in the limit of zero-frequency, as

$$\sigma = \sigma_0 \left[1 - \frac{1}{2\pi d g_T} \ln \left(\frac{g_T E_c}{T} \right) \right] , \tag{5.4}$$

where $\sigma_0 = e^2(8/\pi) g_T a^{2-d}$ is the electrical conductivity of the granular metal per spin, and $E_c = e^2/2C$ is the charging energy taking into account the Coulomb interactions inside and among grains, [Efetov03]. As mentioned above, the correction due to Coulomb interactions is essentially independent of the dimensionality d. That is the tunneling of electrons is completely incoherent; the granular structure dominates the physics.

On the other side, if the temperature lowers, always for large value of g_T, one finds corrections due to the coherent motions of electrons on scales which can be larger of the size a of a single grain. In this case, the corrections read

$$\frac{\delta\sigma}{\sigma_0} = \begin{cases} \frac{\alpha}{12\pi^2 g_T} \sqrt{\frac{T}{g_T\delta}} & d = 3 \\ -\frac{1}{4\pi^2 g_T} \ln \frac{g_T\delta}{T} & d = 2 \\ -\frac{\beta}{4\pi} \sqrt{\frac{\delta}{T g_T}} & d = 1 \end{cases} \tag{5.5}$$

α and β are two numerical constants of order unity, [Beloborodov03]. Corrections in Eq. (5.5) are similar to those obtained for bulk metals by Altshuler and Aronov, [Altshuler85].

In the limit of low coupling among grains, the charging energy becomes important, and the electrical conductivity, because of a finite charging energy, behaves as, [Efetov03]

$$\sigma = 2\sigma_0 \exp\left(-\frac{E_c}{T} \right) . \tag{5.6}$$

The macroscopic conductivity is strongly reduced, and the sample behaves as an insulator, or, in other words, the conduction becomes activated, as confirmed later

by Meyer et al., [Meyer04].

The thermal transport has been studied for not too low temperatures, and for large coupling. The Coulomb interactions renormalise the thermal conductivity, too. For a two-dimensional samples, it reads

$$\kappa = \kappa_0 - \frac{\pi - 2}{6} T \ln\left(\frac{g_T E_c}{T}\right) , \tag{5.7}$$

where $\kappa_0 = L_0 \sigma_0 T$ is the thermal conductivity for the granular metal, [Beloborodov05]. Contrary to the electrical conductivity, κ depends on the dimensionality of the system even for high temperatures $T \gg g_T \delta$. This can be qualitatively explained, thinking of what happens in consequence of local charge fluctuations. For local charge fluctuations, electrical conductivity is not affected, since the net current does not change, while energy distribution is, giving rise to contributions which do not exist for charge transport. In other words, one may think of two different transport mechanisms; energy transport would involve low-energy long wavelength modes, which even in presence of incoherent motion of electrons give rise to dimension-dependent corrections to thermal conductivity.

The correction to Lorenz number δL is constant if $d = 3$, while it behaves as $\delta L \sim \ln(g_T E_c/T)$ and it is positive in two dimensions, indicating that interactions suppress charge transport more than heat transport.

5.2 Superconducting granular metals

Granular metals can exhibit superconducting phase transition. In Fig. 5.2, it is shown the behaviour close to critical temperature T_c for a quasi-bulk lead sample, solid lines, and for a granular lead sample. The former exibits a complete superconducting transition at the temperature of 6.6 K, while the latter shows a much more broadened transition, starting from T_c, [Dynes78].

Before discussing the behaviour close to the superconducting transition, we point out that it has been shown that samples having high normal-state resistance, do not

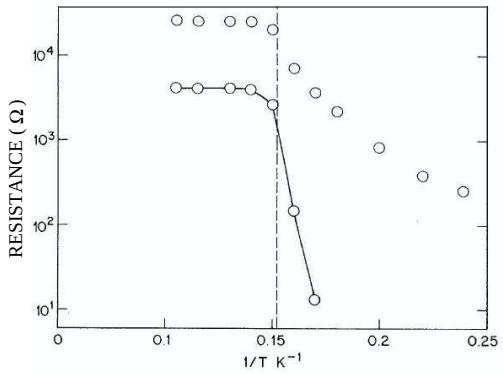

Figure 5.2: At a temperature of 6.6 K, a quasi-bulk lead sample, solid line, shows a complete superconducting transition. A granular lead sample shows a much more broadened transition, starting from T_c. It is supposed that the superconducting state starts appearing in the single grains, but no global phase coherence exists.

exibit the superconducting transition at all. Their resistance even increases with respect to the normal state starting from T_c, [Strongin70, Barber94]. The limit of high normal-state resistance occurs when the electronic mean free path is equal to the Fermi wavelength, [Dynes78, Ioffe60]. Beyond this condition, the conduction becomes activated and no longer metallic. In bulk metals, such a high resistance cannot be reached, since the Fermi wavelength is comparable to the lattice spacing. Then, experimentally, the metal has to be strongly non-uniform to present high resistances, and the single grain can be spatially placed very far from the other. Under this condition, below the critical temperature T_c, it is supposed that the single grains are superconducting, but the tunneling among them is very inefficient. The opening of an energy gap in the density of states, makes the tunneling even more difficult for voltage below the gap if the Josephson tunneling is not set up yet.

In our work, we consider the range of temperatures such that $T \gtrsim T_c$, where T_c is the critical temperature for the grains. Then, we suppose to be in the region of phase transition where the superconducting state just starts appearing in each grain by means of order parameter fluctuations, but there not exists a global phase coherence. The sample is not supposed to undergo a complete phase transition; similar experimental conditions have been observed in different experiences, [Dynes78, Orr86, Gerber97].

Electrons can diffuse through the system thanks to tunneling among the grains. We point out that we speak of single electron tunneling, and not Josephson tunneling which occurs just at lower temperatures, and that would contribute to set up the global superconducting state.

With respect to the bulk metals, the interest in studying thermal transport in granular metals is in the completely different behaviour one can expect, depending on the temperature regime. We will see that in granular superconductors, there exists a temperature region close to T_c in which a singular correction due to superconducting fluctuations dominates the behaviour of the thermal conductivity; such a correction can be either negative or positive, depending on the ratio between the tunneling barrier transparency and the critical temperature T_c. When the temperature approaches even more T_c, the behaviour observed in homogeneous systems is recovered, and the divergence will be cut-off to cross over to the regular behaviour. Moreover, a significant difference with respect to the homogeneous systems is present, the constant correction at $T = T_c$ being either negative or positive depending on the above-mentioned ratio. For some choice of the parameter, a non-monotonic temperature-dependent behaviour of the correction is possible.

We will see that the above different behaviour is due to the fact that the three different contributions to thermal conductivity, AL, MT and DOS corrections, depend differently on the tunneling because of their different nature.

5.3 The model

We consider a $d-$dimensional array of metallic grains embedded in an insulating amorphous matrix as described in Sec. 5.1, with impurities on the surface and inside each grain, and schematized as in Fig. 5.3.

Even if the model we use is for a perfectly ordered d-dimensional matrix, the results still hold for an amorphous one. Indeed, one can imagine different possible configurations of spatial position of grains in the lattice, that is different disordered

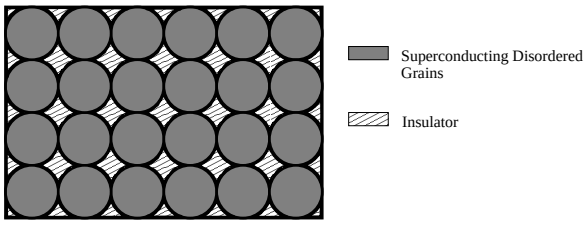

Figure 5.3: Even if the analytical model we use is for a perfectly ordered d-dimensional matrix, as represented in the figure, the results we found still hold for an amorphous one; indeed, our description is correct till the system can be described by a dimensionless tunneling conductance g_T on a scale which is much larger than the typical linear dimension of the grains a, but smaller than the macroscopic size of the whole sample.

configurations. Consequently, the hopping matrix shall vary for each sample. By performing the average over disorder, one gets a model with the same value of the coordination number and hopping energy, t, for different configurations. In other words, our description is correct till the system can be described by a dimensionless tunneling conductance on a scale which is much larger than the typical linear dimension of the grains, a, but smaller than the macroscopic size of the whole sample.

The Hamiltonian of the system reads

$$\hat{H} = \hat{H}_0 + \hat{H}_P + \hat{H}_T \ . \tag{5.8}$$

$\hat{H}_0$ and $\hat{H}_P$ describe the free electron gas and the BCS pairing Hamiltonian inside each grain, respectively

$$\hat{H}_0 = \sum_{i,k} \varepsilon_{i,k} \hat{a}^\dagger_{i,k} \hat{a}_{i,k} + \hat{H}_{\rm imp} \ , \tag{5.9a}$$

$$\hat{H}_P = -\lambda \sum_{i,kk'} \hat{a}^\dagger_{i,k} \hat{a}^\dagger_{i,-k} \hat{a}_{i,-k'} \hat{a}_{i,k'} \ , \tag{5.9b}$$

where i is the grain index, and $\hat{a}^\dagger_{i,k}$ ($\hat{a}_{i,k}$) stands for creation (annihilation) operator of an electron in the state $k = (\mathbf{k}, \uparrow)$ or $-k = (-\mathbf{k}, \downarrow)$. The term $\hat{H}_{\rm imp}$ describes the electron elastic scattering with impurities.

The interaction term in Eq. (5.8) contains only diagonal terms. This simple description is correct under the condition that the off-diagonal terms are really small. It can be shown that for granular systems, such terms are proportional to rapidly

oscillating functions, giving a contribution of the order $1/g = \delta/E_T$, [Kurland00]. For highly conducting grains, as in our case, such a contribution is extremely small. This condition is included in the following important inequality

$$\delta \ll \Delta \ll E_T \ , \tag{5.10}$$

where δ is the mean level spacing defined in Eq. (5.1), Δ is the BCS superconducting gap of a single grain, supposed equal for each of them, and E_T is the Thouless energy.

The first inequality, $\delta \ll \Delta$, is the fundamental condition in order for the superconductivity to exist, more or less as in bulk samples, in a single grain, [Imry81]. The second one, $\Delta \ll E_T$, is equivalent to the condition $a \ll \xi_0$, $\xi_0 = \sqrt{D/T_c}$ being the GL dirty superconducting coherence length. The condition $a \ll \xi_0$ states that each grain behaves as a zero-dimensional system, so that the order parameter is approximately uniform inside each grain. Finally, $\delta \ll E_T$ is the necessary condition in order for the off-diagonal terms to be negligeable. Eq. (5.10) shows that the mean level spacing δ is the smallest energy scale in our problem, while the Thouless energy the largest one.

The grains are coupled by single electron tunneling, and the tunneling Hamiltonian $\hat{H}_T$ in Eq. (5.8) reads

$$\hat{H}_T = \sum_{\langle i,j \rangle} \sum_{\mathbf{pq},\sigma} \left[t_{ij}^{pq} \hat{a}_{i,\mathbf{p}\sigma}^{\dagger} \hat{a}_{j,\mathbf{q}\sigma} + \text{H.c.} \right] \ . \tag{5.11}$$

It is assumed that the momentum of an electron is completely randomized after the tunneling. Besides, we assume that the sample is a good metal, that is $g_T \gg 1$; then, we are not in Coulomb blockade regime, and the long range Coulomb interactions can be safely neglected. Finally, we assume that the temperature is larger than $g_T\delta$, so that weak localization effects are completely smeared, and can be neglected, [Beloborodov01].

5.4 Conductivity in normal granular metals

In linear response regime, the expressions of electrical and thermal conductivity can be evaluated by means of the electromagnetic response operator $\mathcal{Q}(\mathbf{r}, \mathbf{r}', t, t')$,

[Abrikosov75, Rickayzen80, Larkin04]. The expression between the current density $\mathbf{j}(\mathbf{r},t)$ and the vector-potential $\mathbf{A}(\mathbf{r}',t')$ reads

$$\mathbf{j}(\mathbf{r},t) = -\int \mathcal{Q}(\mathbf{r},\mathbf{r}',t,t')\mathbf{A}(\mathbf{r}',t')d\mathbf{r}'dt' \; . \tag{5.12}$$

Comparing the Fourier components of Eq. (5.12) with the definition of conductivity $\mathbf{j}(\mathbf{r},t) = \sigma\mathcal{E}(\mathbf{r},t)$, $\mathcal{E}$ being the electrical field, one can write the electrical conductivity as

$$\sigma(\omega) = \lim_{\omega\to 0}\left[\frac{\mathcal{Q}^{(elec)}(i\omega_\nu)}{\omega_\nu}\right]_{i\omega_\nu\to\omega+i0^+} , \tag{5.13}$$

where $\omega_\nu = 2\pi T\nu$ is the bosonic frequency of the external field in the Matsubara representation, [Abrikosov75, Rickayzen80, Fetter03]. Analogously, the thermal conductivity reads

$$\kappa = \lim_{\omega\to 0}\left[\frac{\mathcal{Q}^{(heat)}_{ret}\,(i\omega_\nu)}{\omega_\nu T}\right]_{i\omega_\nu\to\omega+i0^+} , \tag{5.14}$$

where $\mathcal{Q}^{(heat)}(i\omega_\nu)$ is the linear response operator to an applied temperature gradient.

The diagrammatic technique we have used in our work allows to write the linear response operator quite easily; for a complete review, see [Abrikosov75, Larkin04, Fetter03].

Before evaluating the corrections to thermal conductivity, in this section we calculate the electrical and the thermal conductivity of the granular metal in the normal state. It will be such conductivities which will be renormalised by the presence of superconducting fluctuations.

For a normal granular metal, the diagram which provides the electrical and thermal conductivity is represented in Fig. 5.4. Solid lines are impurity-averaged single-electron Green's functions with the specified momentum and Matsubara's frequency; they describe the propagation of an electron in the disordered i-th grain, and an anti-particle or hole in the j-th grain, respectively. The crossed circles represent tunnelling vertices. In diagrammatic technique, to each vertex is associated a contribution j_{vertex}, representing the electron microscopic contribution to electrical or thermal conductivity. Vertex contributions can have different representations. Of course, they

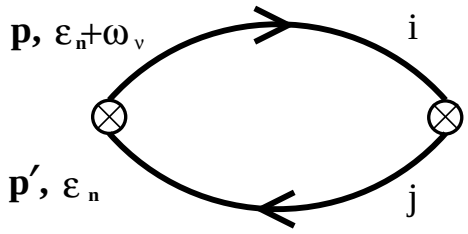

Figure 5.4: Diagram for the thermal conductivity in a granular metal. The solid lines are impurity-averaged single-electron Green's functions with the specified momentum and Matsubara's frequency, and belonging to the grain i and j. Crossed circles represent tunneling vertices, and each of them contributes as $j^Q_{vertex} = i2at(\varepsilon_n + \omega_\nu/2)$.

are equivalent, giving the same results, but their diagrammatic representation is different, [Langer62, Ussishkin03]. In our case, the tunnelling heat current operator is given by

$$\mathbf{j}^{(heat)} = ia \sum_j \sum_{\mathbf{pp}'\sigma} \left[\varepsilon_n t_{ij}^{pp'} \hat{a}^\dagger_{i,\mathbf{p}\sigma} \hat{a}_{j,\mathbf{p}'\sigma} - h.c. \right] , \tag{5.15}$$

where $\varepsilon_n = \pi T(2n+1)$ is the Matsubara frequency of the electron involved in the transport. Eq. (5.15) has been obtained by means of Lagrangian approach. For Hamiltonian representations examples, see [Varlamov90, Ussishkin03, Beloborodov00, Larkin04].

From Eq. (5.15), vertex contributions to thermal conductivity reads

$$j^Q_{vertex} = i2at(\varepsilon_n + \omega_\nu/2) , \tag{5.16}$$

where we took into account the interactions with the field, represented by ω_ν, and we considered the tunneling amplitude uniform and momentum-independent, $t_{ij}^{pp'} \equiv t$, which is as a good approximation as one is closer to Fermi level. Eq. (5.16) can be qualitatively understood as follows: each time an electron jumps from one grain to another, its transmission probability is given by t; for each electron tunneling from the i-th grain to j-th grain, one has to consider not only such a contribution to thermal conductivity, but also the energy transported by the hole tunneling from j-th grain to i-th grain. To the electron contribution, one has to sum the contribution given by the photons of the electromagnetic field and represented by the frequencies ω_ν, too.

As we mentioned above, diagrammatic technique allows to write easily the linear

response operator $\mathcal{Q}(i\omega_\nu)$; it will contain a sum over all discrete electron frequencies ε_n, the integration over the momentum of electrons involved in the transport, and the vertex contributions.

For diagram in Fig. 5.4, the linear response operator will read

$$\mathcal{Q}^{(heat)}(i\omega_\nu) = -a^2 t\, t^* T \sum_{i,j} \sum_{\varepsilon_n} (2\varepsilon_n + \omega_\nu)^2\, I(\varepsilon_n, \omega_\nu)\ , \tag{5.17a}$$

$$I(\varepsilon_n, \omega_\nu) = \int (dp) G\left(\tilde{\varepsilon}_{n+\nu}, \mathbf{p}\right) \int (dp') G\left(\tilde{\varepsilon}_n, \mathbf{p}'\right)\ . \tag{5.17b}$$

$t^* = -t$ is the tunneling amplitude for an electron tunneling from j-th grain to i-th grain; $(dp) = d^d p/(2\pi)^d$, $\tilde{\varepsilon}_n$ and $\varepsilon_{n+\nu}$ are shorthand notations for $\varepsilon_n + (1/2\tau)\mathrm{sign}(\varepsilon_n)$ and $\varepsilon_n + \omega_\nu$, respectively. $G\left(\tilde{\varepsilon}_n, \mathbf{p}\right)$ is the Matsubara Green's function of an electron in a disordered grain

$$G\left(\tilde{\varepsilon}_n, \mathbf{p}\right) = \frac{1}{i\varepsilon_n + i\frac{1}{2\tau}\mathrm{sgn}(\varepsilon_n) - \xi(\mathbf{p})}\ . \tag{5.18}$$

As usual, $\xi(\mathbf{p}) = p^2/2m - \mu$, μ being the Fermi level, and $(1/2\tau)\mathrm{sgn}(\varepsilon_n)$ is the self-energy taking into account the coherent scattering of electron on impurities in the bulk metal, [Altshuler85]. Particularly, in diffusive regime, provided that the energy scale τ^{-1} is much larger than the energy ε_n of the quasi-particles involved in transport

$$G\left(\tilde{\varepsilon}_n, \mathbf{p}\right) \simeq \frac{1}{i\frac{1}{2\tau}\mathrm{sgn}(\varepsilon_n) - \xi(\mathbf{p})}\ . \tag{5.19}$$

Let us evaluate $I(\varepsilon_n, \omega_\nu)$ in Eq. (5.17b); first, we observe that the integral over the momentum, can be written as an integral over the energy since

$$d\xi = \frac{p}{m} dp\ , \tag{5.20a}$$

$$d^3 p = p m d\xi d\Omega\ , \tag{5.20b}$$

where $d\Omega = \sin\theta d\theta d\phi$ is the measure in spherical coordinates. Then,

$$\int \frac{d^3 p}{(2\pi)^3} G(\tilde{\varepsilon}_n, \mathbf{p}) = \nu_F \int d\xi G(\tilde{\varepsilon}_n, \mathbf{p})\ , \tag{5.21}$$

where $\nu_F = pm/2\pi^2$ is the density of states at Fermi level. To evaluate the integrals in $I(\varepsilon_n, \omega_\nu)$, by means of Eq. (5.21), we observe that

$$\begin{aligned}\nu_F^2 \int d\xi \frac{1}{i\frac{1}{2\tau}\mathrm{sgn}(\varepsilon_n+\omega_\nu)-\xi} \int d\xi' \frac{1}{i\frac{1}{2\tau}\mathrm{sgn}(\varepsilon_n)-\xi'} \\ = 2\nu_F^2 \int d\theta d\chi \frac{1}{\theta+\chi-i\frac{1}{2\tau}\mathrm{sgn}(\varepsilon_n)} \frac{1}{\theta-\chi-i\frac{1}{2\tau}\mathrm{sgn}(\varepsilon_n+\omega_\nu)} \,,\end{aligned} \tag{5.22}$$

where we defined

$$\theta = \frac{\xi+\xi'}{2}, \qquad\qquad \chi = \frac{\xi-\xi'}{2} \,. \tag{5.23}$$

In order for the integral in the rhs of Eq. (5.22) to not vanish, the two poles have to be in the two different half-planes. This condition is fullfilled if and only if $\varepsilon_n < 0$ and $\varepsilon_n + \omega_\nu > 0$. Using contour integration, one finds

$$I(\varepsilon_n, \omega_\nu) = \nu_F^2 \pi^2 \Big|_{\substack{\varepsilon_n<0 \\ \varepsilon_n+\omega_\nu>0}} \,. \tag{5.24}$$

From Eq. (5.17a), the linear response operator reads

$$\mathcal{Q}^{(heat)}(i\omega_\nu) = (\pi\nu_F a t)^2 T \sum_j \sum_{\varepsilon_n} (2\varepsilon_n+\omega_\nu)^2 \,. \tag{5.25}$$

Since the Green's functions do not depend on the site, no term depends on site indices, and the sum over $\{j\}$ can be performed immediately; it turns out to be z, where z is the coordination number, that is the number of neighbours of each grain. In the expression of conductivity, we will not consider such a factor, since we will consider a quantity per unit volume. The sum over ε_n can be written as

$$\sum_{\substack{\varepsilon_n<0 \\ \varepsilon_n+\omega_\nu>0}} (2\varepsilon_n+\omega_\nu)^2 = \sum_{0<\varepsilon_n<\omega_\nu} (2\varepsilon_n-\omega_\nu)^2 \simeq -\frac{2}{3}\pi T\omega_\nu \,. \tag{5.26}$$

In the sum, we just conserved the terms linear in ω_ν. All the other higher order terms will disappear taking the limit in Eq. (5.14). Finally, from Eqs. (5.3), (5.14) and (5.25), the thermal conductivity for a granular metal reads

$$\kappa_0 = \frac{8}{3}\pi a^2 g_T T \,. \tag{5.27}$$

Analogously, one can evaluate the electrical conductivity. In this case, each vertex contributes as

$$j^e_{vertex} = i\,2\,e\,a\,t\ . \tag{5.28}$$

The energy is replaced by the charge, and the field does not contribute directly to charge transport. From Eq. (5.13), one finds

$$\sigma_0 = \frac{8}{\pi} e^2 a^2 g_T\ . \tag{5.29}$$

From Eqs. (5.27) and (5.29) the Lorenz number for a granular metal is

$$L_0 = \frac{\kappa_0}{\sigma_0 T} = \frac{\pi^2}{3e^2}\ , \tag{5.30}$$

and the Wiedemann-Franz law is fullfilled.

5.5 Electron coherence effects on transport

The superconducting fluctuations, as we have mentioned, manifest themselves allowing the creation of Cooper pairs at temperatures above but close to the critical one T_c. This new transport channel is generally called *Cooper pair fluctuation propagator*. The presence of Cooper pairs above T_c strongly affects transport properties of the normal state. To evaluate the correction to thermal conductivity κ_0 in Eq. (5.27), one needs the analytical expression of fluctuations propagator. Such a propagator is nothing else but the fingerprint of the coherence between the electrons forming Cooper pairs.

This is not the only effect of the coherence introduced by the fluctuations of order parameter. One has to consider, in diffusive regime, the renormalization due to coherent scattering on the same impurity by both electrons forming the Cooper pairs. Such a renormalization to conductivity is called Cooperon or vertex correction.

This latter contribution is largely known and studied for several systems; one can find in several books detailed calculations. We will discuss the physical meaning of Cooperon correction, and will give directly its analytical expression. This will give us

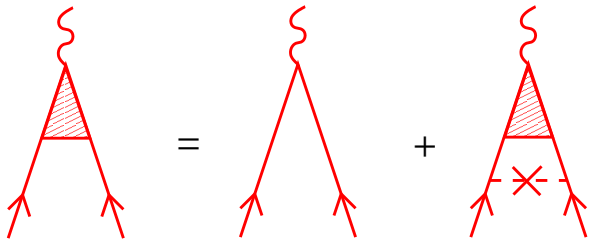

Figure 5.5: Cooperon vertex correction. It takes into account the possibility of coherent scattering by both the electrons forming the Cooper pair on the same imputiies. Solid lines are one-electron Green's functions, while the dashed lines indicate the scattering by both the electrons on the same impurity represented by the cross.

the opportunity to concentrate on the evaluation of fluctuation propagator for granular system, which present interesting points to discuss.

The aim of most of this section is evaluating explicitly the fluctuation propagator for our specific problem. As we will see, the deep difference with respect to bulk metals is represented by the renormalization due to the presence of the tunneling.

Finally, by means of analytical expression of fluctuation propagator, we will be able to evaluate the three corrections to thermal conductivity.

5.5.1 Vertex correction

In section 5.4, when we introduced the one-electron Green's function in Eq. (5.18), we mentioned the self-energy taking into account the coherent scattering of an electron on the impurities in the sample. Now, the existence of BCS pairing potential and then the possibility for two electrons to form a Cooper pair introduces a new correction. The latter takes into account the coherent scattering by both the electrons forming the Cooper pair on the same impurity. The renormalized vertex, generally indicated as $\lambda(\mathbf{q}, \varepsilon_1, \varepsilon_2)$, can be determined by a graphical Dyson's equation, as shown in Fig. 5.5.

Diagrams in Fig. 5.5 correspond to Dyson's equation

$$\lambda = 1 + \Sigma\,\lambda\ , \tag{5.31}$$

where Σ is the self-energy. Analytically, Eq. (5.31) reads

$$\lambda(\mathbf{q},\varepsilon_1,\varepsilon_2) = 1 + \frac{1}{2\pi\nu\tau}\int \frac{d\,\mathbf{p}}{(2\pi)^3}\lambda(\mathbf{q},\varepsilon_1,\varepsilon_2)G(\mathbf{p}+\mathbf{q},\tilde{\varepsilon}_1)G(-\mathbf{p},\tilde{\varepsilon}_2)\ . \tag{5.32}$$

The first term in the rhs of Eq. (5.32) corresponds to the "bare" diagram in Fig. 5.5. The numerical factor $1/2\pi\nu_F\tau = \langle U^2\rangle$ is the strength of impurity. Solid lines in the diagrams are one-electron Green's functions, while the dashed lines indicate the scattering by both the electrons on the same impurity represented by the cross; we neglect the diagrams with crossed dashed lines giving rise to a negligeable contribution in the parameter $(1/k_F l)$, l being the mean free path. Then, one speaks of ladder approximation. For a complete review, see [Abrikosov75, Altshuler85, Larkin04, Akkermans04]

For our sample, the vertex correction reads

$$\lambda(\mathbf{q},\varepsilon_1,\varepsilon_2) = \frac{1}{\tau}\frac{1}{|\varepsilon_1-\varepsilon_2| + D\mathbf{q}^2}\ , \tag{5.33}$$

where ε_1 and ε_2 are the energies of the electrons involved in the Cooper pair, $\mathbf{q}$ is the momentum of the pair and D the diffusion constant. Particularly, as stated in section 5.3, since we are in the approximation of an ensemble of zero dimensional grains, $a \ll \xi_0$, the Cooperon $\lambda(\mathbf{q},\varepsilon_1,\varepsilon_2)$ provides the main contribution as $\mathbf{q}\to 0$, and the vertex correction reads

$$\lambda(\varepsilon_1,\varepsilon_2) = \frac{1}{\tau}\frac{1}{|\varepsilon_1-\varepsilon_2|}\ . \tag{5.34}$$

5.5.2 Cooper pair fluctuation propagator

The propagator is generally defined by means of the diagrams in Fig. 5.6: the first diagram in the rhs in the top line represents the BCS electron-electron interaction, and it is expressed by a constant $g > 0$. The second and third diagrams take into account the corrections induced by the fluctuations. All these diagrams can be summed up as shown in the bottom line, allowing to write a Dyson's equation for the flucuation propagator

$$L^{-1}_{\mathbf{K}}(\Omega_\mu) = g^{-1} - \Pi_{\mathbf{K}}(\Omega_\mu)\ , \tag{5.35}$$

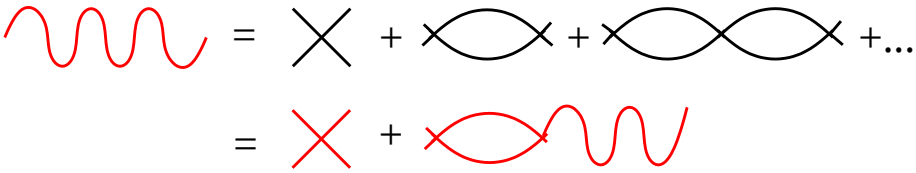

Figure 5.6: Diagrams providing the Cooper pair fluctuation propagator in absence of tunneling. The first diagram in the rhs in the top line represents the BCS electron-electron interaction, and it is expressed by a constant $g > 0$. The second and third diagrams take into account the corrections induced by the fluctuations. The diagrams in the bottom line represent graphically Dyson's equation for the fluctuation propagator, Eq. (5.35).

where $\mathbf{K}$ is the wave vector associated with the lattice grains, and Ω_μ is the bosonic Matsubara's frequency reflecting the bosonic nature of Cooper pairs. From Eq. (5.35), one needs to evaluate the so-called polarization operator

$$\Pi_{\mathbf{K}}(\Omega_\mu) = T\sum_{\varepsilon_n}\int \frac{d\,\mathbf{p}}{(2\pi)^3} G(\mathbf{K}+\mathbf{p}, \varepsilon_n + \Omega_\mu) G(-\mathbf{p}, -\varepsilon_n)\ , \tag{5.36}$$

to find the expression of $L^{-1}_{\mathbf{K}}(\Omega_\mu)$.

The diagrams in Fig. 5.6 allow to have an intuitive idea of the meaning of the fluctuation propagator and of the physical processes it describes; besides, the evaluation of Dyson's equation is the way generally followed for bulk metals; see [Larkin04] for a complete review.

Neverthless, for granular systems the diagrams shown in Fig. 5.6 do not take into account at all the renormalization due to tunnelling. Why does the tunneling renormalize the propagator?

As mentioned above, the fluctuation propagator describes the coherent motion of electrons forming Cooper pairs and the effects of the fluctuations of order parameter. In a granular system, because of the finite probability for each electron to tunnel from one grain to another, one has to consider the possibility that each electron forming the Cooper pair can tunnel during the lifetime τ_{GL} of the Cooper pair itself without loosing the coherence. At the lowest order in tunneling two different physical situations can take place: in the first one, both the electrons forming the Cooper pair tunnel coherently from one grain to another; in the second case, one electron tunnels back and forth; in

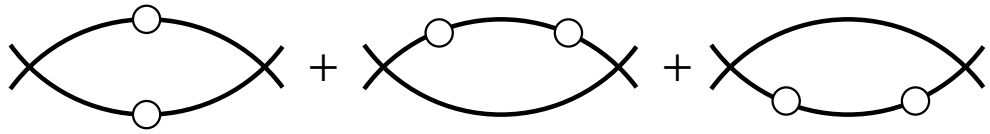

Figure 5.7: Diagrams providing the renormalization of fluctuation propagator in Fig. 5.6. The first one describes the physical process where both the electrons forming the Cooper pair tunnel from one grain to another. The second and the third diagram describe the processes where just one electron forming the Cooper pair tunnels back and forth from one grain to another.

this case, one has a double multiplicity since this event can take place for both the electrons of the Cooper pair. Such processes are represented by the diagrams shown in Fig. 5.7.

To take correctly into account the tunneling renormalization, we evaluate the fluctuation propagator using the characteristic properties of gaussian integrals. In the following, we show the principal steps of such a calculation; most of the details can be found in Appendices G and H.

We write the Hamiltonian in Eq. (5.8) in real space, by means of fermionic field operator Ψ_i and $\Psi_i^\dagger$ for each grain

$$\hat{H}_0 = \sum_i \Psi_i^\dagger(\mathbf{r}) \left(-\frac{\nabla_i^2}{2m} \right) \Psi_i(\mathbf{r}) \,, \tag{5.37a}$$

$$\hat{H}_P = -g \sum_i \int \Psi_{i\uparrow}^\dagger(\mathbf{r}) \Psi_{i\downarrow}^\dagger(\mathbf{r}) \Psi_{i\downarrow}(\mathbf{r}) \Psi_{i\uparrow}(\mathbf{r}) d\,\mathbf{r} \,, \tag{5.37b}$$

$$\hat{H}_T = \frac{1}{2} \sum_{i,j} \sum_\sigma t_{ij} \int \Psi_{i\sigma}^\dagger(\mathbf{r}) \Psi_{j\sigma}(\mathbf{r}') d\,\mathbf{r} d\,\mathbf{r}' + \text{H.c.} \,. \tag{5.37c}$$

By means of interaction representation and time ordering operator T_τ, one can evaluate the partition function of our system as

$$\begin{aligned} \mathcal{Z} &= \text{Tr} \; e^{-\int_0^\beta \hat{H}(\tau) d\tau} \\ &= \text{Tr} \left\{ e^{-\int_0^\beta \hat{H}_0(\tau) d\tau} T_\tau e^{-\int_0^\beta [H_P(\tau) + H_T(\tau)] d\tau} \right\} \,. \end{aligned} \tag{5.38}$$

The latter expression is not quadratic in the field operators. To get a quadratic form to be able to use properties of Gaussian integrals, we introduce a new field operator Δ

by means of Hubbard-Stratonovich transformation. Let us observe that

$$e^{g\sum_i \int d\tau d\mathbf{r} P_i^\dagger(\mathbf{r},\tau)P_i(\mathbf{r},\tau)} = \prod_{\Delta x} e^{g\sum_i P_i^\dagger(\mathbf{r},\tau)P_i(\mathbf{r},\tau)\Delta x} , \tag{5.39}$$

where $P_i(\mathbf{r},\tau) = \Psi_{i\downarrow}(\mathbf{r},\tau)\Psi_{i\uparrow}(\mathbf{r},\tau)$. Each term of Eq. (5.39) can be written as a quadratic integral

$$e^{g\sum_i P_i^\dagger(\mathbf{r},\tau)P_i(\mathbf{r},\tau)\Delta x} = \int d^2\Delta(\mathbf{r},\tau) e^{\sum_i \int_0^\beta \left[-\frac{|\Delta_i(\mathbf{r},\tau)|^2}{g} - \Delta_i^*(\mathbf{r},\tau)P_i(\mathbf{r},\tau) - \Delta_i(\mathbf{r},\tau)P_i^\dagger(\mathbf{r},\tau)\right]\Delta x} . \tag{5.40}$$

The product of all these terms is a functional integral and the partition function reads

$$\mathcal{Z} = \mathrm{Tr}\Bigg\{ e^{-\int_0^\beta H_0(\tau)d\tau} T_\tau \int \mathcal{D}\Delta(\mathbf{r},\tau)\mathcal{D}\Delta^*(\mathbf{r},\tau) \times e^{\sum_i \int_0^\beta \left[-\frac{|\Delta_i(\mathbf{r},\tau)|^2}{g} - \Delta_i^*(\mathbf{r},\tau)P_i(\mathbf{r},\tau) - \Delta_i(\mathbf{r},\tau)P_i^\dagger(\mathbf{r},\tau)\right] - H_T(\tau)} \Bigg\} . \tag{5.41}$$

The latter equation allows to know the action for our granular system, since the partition function can be written as

$$\mathcal{Z} = e^{-S_0} \int \mathcal{D}\Delta(\mathbf{r},\tau)\mathcal{D}\Delta^*(\mathbf{r},\tau) \exp\{-S[\Delta(\mathbf{r},\tau)]\} , \tag{5.42}$$

where $S[\Delta(\mathbf{r},\tau)]$ represents the fluctuation contribution in the total action, [Larkin04]. $S[\Delta(\mathbf{r},\tau)]$ can be presented as a series over the BCS parameter $\Delta(\mathbf{r},\tau)$ and the tunneling amplitude t. The Cooper pair fluctuation propagator is given exactly by the coefficient of the second order term in the development, [Larkin04].

By means of Taylor's expansion in the field Δ and in the tunneling amplitude t, one can develop the two terms $\exp\left\{\sum_i \int_0^\beta \left[-\Delta_i^*(\mathbf{r},\tau)P_i(\mathbf{r},\tau) - \Delta_i(\mathbf{r},\tau)P_i^\dagger(\mathbf{r},\tau)\right]\right\}$ and $\exp\{-H_T(\tau)\}$. The expansion is justified by our assumption to be close but above to the critical temperature where the mean field (BCS) value of order parameter is still zero; moreover, one can expand in t, in the region $t \ll 1/\tau \ll E_T$.

From the development, most of the terms of the product gives no contribution since they are not diagonal; just two terms give a non-vanishing contributions, corresponding to the typical action of superconducting fluctuations, and to the tunneling correction, respectively

$$S_{eff} = S_{eff}^0 + S_{eff}^t . \tag{5.43}$$

The first term in the rhs of Eq. (5.43) reads, see the Appendix G for all details,

$$S^0_{eff} = -\frac{T}{V}\sum_{\Omega_\mu} |\Delta_i(\Omega_\mu)|^2 \left[\frac{1}{g} - 4\pi\nu_F T\tau \sum_{2\varepsilon_n > \Omega_\mu} \lambda(\varepsilon_n, \varepsilon_{\mu-n})\right] . \tag{5.44}$$

In the approximation of zero dimensional grains, one can neglect the dependence on spatial coordinate in the field Δ_i. The sum over the fermionic frequencies in Eq. (5.44) is logarithmically divergent and must be cut-off at Debye's frequency, [Larkin04]; using the definition of superconducting critical temperature

$$\frac{1}{g} = \nu\left[\log\frac{\omega_D}{2\pi T_C} - \Psi\left(\frac{1}{2}\right)\right] , \tag{5.45}$$

one obtains

$$S^0_{eff} = -\nu_F\frac{T}{V}\sum_{\Omega_\mu} |\Delta_i(\Omega_\mu)|^2 \left[\ln\frac{T}{T_c} + \Psi\left(\frac{1}{2} + \frac{|\Omega_\mu|}{4\pi T_c}\right) - \Psi\left(\frac{1}{2}\right)\right] . \tag{5.46}$$

$\Psi(x)$ is the digamma function, defined as the logarithmic derivative of gamma function. Close to critical temperature, $T \simeq T_c$, the main contribution to singular behaviour comes from "classical" frequencies, $|\Omega_\mu| \ll T_c$; see the end of this Section for some more comments. Then, we can expand the Ψ function in the small parameter $|\Omega_\mu|/T_c$:

$$S^0_{eff} = -\nu_F\frac{T}{V}\sum_{\mathbf{K},\Omega_\mu} \left[\ln\frac{T}{T_c} + \frac{\pi|\Omega_\mu|}{8T_c}\right] |\Delta_{\mathbf{K}}(\Omega_\mu)|^2 . \tag{5.47}$$

In the last expression, we considered the lattice Fourier transform: $\mathbf{K}$ belongs to the first Brillouin zone of reciprocal grain lattice.

The tunneling-dependent part of the action can be evaluated starting from diagrams in Fig. 5.8.

The calculation of diagram in Fig. 5.8(a) gives the contribution due to the possibility of tunneling of both electrons during the lifetime of the fluctuating Cooper pair, i.e. the Ginzburg-Landau time $\tau_{GL} = \pi/8(T - T_c)$; it is equal to

$$S^{t,(a)}_{eff} = z g_T \sum_{\mathbf{K},\Omega_\mu} \gamma_{\mathbf{K}} |\Delta_{\mathbf{K}}(\Omega_\mu)|^2 , \tag{5.48}$$

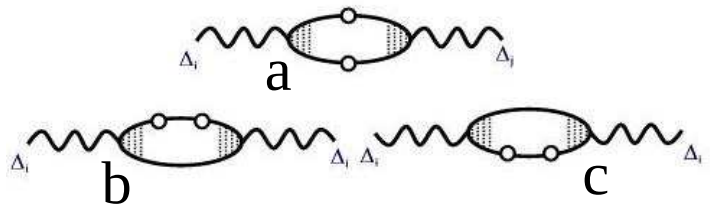

Figure 5.8: Total tunneling correction to the fluctuation propagator. The upper diagram is related to the possibility of tunneling of both electrons forming the fluctuating Cooper pair during its lifetime τ_{GL}. The other two diagrams consider the renormalization of the intra-grain fluctuation propagator. Shadowed areas represent vertices corrections.

where, as mentioned, z is the number of nearest neighbors, and the function $\gamma_{\mathbf{K}} = (1/z)\sum_{\mathbf{a}} \exp\{i\mathbf{K}\cdot\mathbf{a}\}$ is the so-called lattice structure factor, where $\mathbf{a}$ is a vector connecting nearest neighbor grains.

The diagrams in Fig. 5.8(b) and Fig. 5.8(c) give an identical contribution, which is related to the probability that a single electron, participating in the fluctuating Cooper pair, undergoes a double tunneling, back and forth, during the Ginzburg-Landau time. Such a contribution reads

$$S_{eff}^{t,(b+c)} = -z g_T \sum_{\mathbf{K},\Omega_\mu} \left|\Delta_{\mathbf{K}}\left(\Omega_\mu\right)\right|^2 . \tag{5.49}$$

The final result for fluctuation propagator at every order in tunneling in the ladder approximation is, [Beloborodov00, Biagini05]

$$L_{\mathbf{K}}\left(\Omega_\mu\right) = -\frac{1}{\nu_F}\frac{1}{\ln\frac{T}{T_c} + \frac{\pi|\Omega_\mu|}{8T_c} + z\frac{g_T\delta}{T_c}\left(1-\gamma_{\mathbf{K}}\right)}. \tag{5.50}$$

We point out that the propagator in Eq. (5.50) corresponds to the sum of the diagrams in Fig. 5.6 and in Fig. 5.7. Of course, from Eq. (5.50), without the tunneling correction, one finds again the propagator for a single grain.

Since we are interested in the behaviour of conductivity close to critical temperature, from Eq. (5.50), one can see that as $T \to T_c$, the most diverging contribution is given by $\Omega_\mu = 0$. Such a limit is often called static limit. One can imagine such a contribution as given by very long wavelength modes of Cooper channel. As one as gets further from T_c, finite wavelength modes starts playing an important role, and the

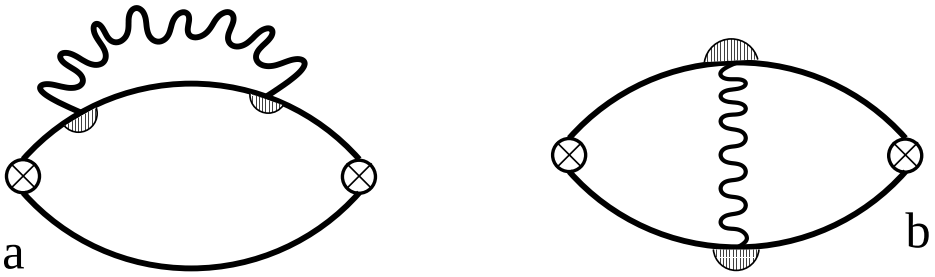

Figure 5.9: (a) Density of states and (b) Maki-Thompson diagrams. The solid lines are impurity-averaged single-electron Green's functions, wavy lines represent fluctuation propagator and the shadowed areas are Cooperon vertex corrections. Crossed circles represent tunneling vertices.

so-called dynamical contribution appears.

The contribution as $\Omega_\mu = 0$ is also called classical limit; physically, it means that the product of Heisenberg field operator $\Psi_{i\downarrow}(\mathbf{r})\Psi_{i\uparrow}(\mathbf{r})$ in Eq. (5.37b) behaves as a classical field describing the Cooper pair wave function, and proportional to the fluctuation order parameter close to T_c.

5.6 Superconducting fluctuation corrections

In this section, we evaluate the corrections to thermal conductivity due to superconducting fluctuations. We present the evaluation of the three different contributions, the Aslamazov-Larkin (AL) correction, the Maky-Thompson (MT) correction and the density of states (DOS) contribution, addressing the interested reader to the appendix for detailed calculations. Finally, we will discuss the behaviour of total correction showing its dependence on the ratio between the barrier transparency and the critical temperature T_c. The knowledge of thermal conductivity will allow us to evaluate the Lorenz number thanks to the known results for the electrical conductivity, [Beloborodov00].

5.6.1 Density of states correction

The diagram describing the DOS correction is shown in Fig. 5.9(a). Solid

lines are impurity-averaged single-electron Green's functions; wavy line represents the fluctuation propagator and the shadowed areas are Cooperon vertex corrections. As usual, crossed circles represent tunneling vertices.

At the lowest order in tunneling in the fluctuation propagator, the DOS contribution involves two electrons forming a fluctuating Cooper pairs inside one given grain, contrary to what happens for MT or AL diagrams in Fig. 5.9(b) and Fig. 5.10. It means that the DOS correction is the only contribution which is present even in absence of tunneling. Then, in temperature regions far from the critical temperature, namely $T - T_c \gg g_T \delta$, where the coherence length does not increase excessively, one can expect this term to give a significant contribution to thermal conductivity stressing the granular nature of the sample.

The contribution to thermal conductivity can be evaluated by means of Eq. (5.14). The corresponding response function operator reads

$$\mathcal{Q}^{(DOS)}(\omega_\nu) = T^2 t^2 a^2 \sum_j \sum_{\Omega_\mu} L_{ij}(\Omega_\mu)\, \Sigma(\Omega_\mu, \omega_\nu) \ , \tag{5.51}$$

where

$$\Sigma(\Omega_\mu, \omega_\nu) = \sum_{\varepsilon_n} (\varepsilon_n + \varepsilon_{n+\nu})^2 \lambda^2(\varepsilon_{n+\nu}, \varepsilon_{-n-\nu+\mu})\, I(\varepsilon_n, \Omega_\mu, \omega_\nu) \ , \tag{5.52}$$

and

$$I(\varepsilon_n, \Omega_\mu, \omega_\nu) = \int (dp)\, G^2(\mathbf{p}, \varepsilon_{n+\nu})\, G(\mathbf{p}, \varepsilon_{-n-\nu+\mu}) \int (dp')\, G(\mathbf{p}', \varepsilon_n) \, . \tag{5.53}$$

In Eq. (5.51), $L_{ij}(\Omega_\mu)$ is the Fourier transform with respect to the grains lattice of the propagator in Eq. (5.50). It is defined as

$$L_{ij}(\Omega_\mu) = \sum_{\mathbf{K}} e^{i\mathbf{R}_{ij}\cdot\mathbf{K}} L_{\mathbf{K}}(\Omega_\mu) \ , \tag{5.54}$$

where $\mathbf{R}_{ij}$ is the vector between two sites; for DOS diagram, $\mathbf{R}_{ij} = \mathbf{R}_{ii}$. As already mentioned, the main contribution to singular behaviour comes from classical frequencies $|\Omega_\mu| \ll T_c$; then, we will take the so-called static limit $\Omega_\mu = 0$. The product of integrals in Eq. (5.53) can be evaluated by means of contour integration

$$I(\varepsilon_n, 0, \omega_\nu) = -2(\pi\nu_F\tau)^2 \left[\theta(\varepsilon_n\varepsilon_{n+\nu}) - \theta(-\varepsilon_n\varepsilon_{n+\nu})\right] \ , \tag{5.55}$$

where $\theta(x)$ is the step function.

Thanks to previous equation, the sum in Eq. (5.52) can be evaluated, and the only linear contribution in ω_ν turns to be

$$\Sigma\left(0,\omega_\nu\right) \simeq -\omega_\nu \pi \nu_F^2 \ . \tag{5.56}$$

Finally, the DOS response function can be evaluated from Eqs. (5.51) and (5.56)

$$\mathcal{Q}^{(DOS)}\left(\omega_\nu\right) = \left(\omega_\nu\right) \frac{8}{\pi} g_T T a^2 \sum_j L_{ij}\left(0\right) \ , \tag{5.57}$$

where we also took into account the double multiplicity of DOS diagram, since the fluctuation propagator can involve the lower branch of the diagram in Fig. 5.9(a). The DOS correction to thermal conductivity reads, [Biagini05]

$$\frac{\delta\kappa^{(DoS)}}{\kappa_0} = -\frac{3}{\pi^2}\frac{1}{g_T}\frac{g_T\delta}{T_c}\int_{BZ}(dK)\frac{1}{\epsilon + z\frac{g_T\delta}{T_c}\left(1-\gamma_{\mathbf{K}}\right)}. \tag{5.58}$$

We took the lattice Fourier transform and defined the reduced temperature $\epsilon = \ln(T/T_c) \simeq (T-T_c)/T_c$. $(dK) = [a^d/(2\pi)^d]d^dK$ is the dimensionless measure of the first Brillouin zone.

Before discussing the behaviour of correction in Eq. (5.58), we calculate the other corrections too; in this way, we will be able to compare the different contribution and evaluate their weight in function of the temperature.

5.6.2 Maki-Thompson correction

Maki-Thompson diagram is shown in Fig. 5.9(b). With respect the DOS diagram, there is an important difference. In the case of DOS diagram, the bubble represents the propagation of a particle and its corresponding hole, and the tunnelling coefficients for vertices are t_{ij} and $t_{ij}^* = t_{ji} = -t_{ij}$. In MT diagrams, one has two incoming particles, and the tunnelling coefficients are the same. Besides, the electrons entering the diagram from opposite side contribute with opposite sign energies.

The linear response operator reads

$$\mathcal{Q}^{(MT)}\left(\omega_\nu\right) = T^2 t^2 a^2 \sum_j \sum_{\Omega_\mu} L_{ij}\left(\Omega_\mu\right) \Sigma\left(\Omega_\mu,\omega_\nu\right) \ , \tag{5.59}$$

where

$$\Sigma\left(\Omega_\mu,\omega_\nu\right)=\sum_{\varepsilon_n}\left(\varepsilon_n+\varepsilon_{n+\nu}\right)^2\lambda\left(\varepsilon_{n+\nu},\varepsilon_{-n-\nu+\mu}\right)\lambda\left(\varepsilon_n,\varepsilon_{-n+\mu}\right)I\left(\varepsilon_n,\Omega_\mu,\omega_\nu\right)\ , \quad (5.60)$$

and

$$I\left(\varepsilon_n,\Omega_\mu,\omega_\nu\right) = \int\left(dp\right)G\left(\mathbf{p},\varepsilon_{n+\nu}\right)G\left(\mathbf{p},\varepsilon_{-n-\nu+\mu}\right)\int\left(dp'\right)G\left(\mathbf{p}',\varepsilon_n\right)G\left(\mathbf{p}',\varepsilon_{-n+\mu}\right). \quad (5.61)$$

Eqs. (5.60) and (5.61) can be evaluated in the same way as for DOS correction, see Appendix J for details, and the correction to thermal conductivity reads, [Biagini05]

$$\frac{\delta\kappa^{(MT)}}{\kappa_0}=\frac{3}{\pi^2}\frac{1}{g_T}\frac{g_T\delta}{T_c}\int_{BZ}(dK)\frac{\gamma_{\mathbf{K}}}{\epsilon+z\frac{g_T\delta}{T_c}\left(1-\gamma_{\mathbf{K}}\right)}. \quad (5.62)$$

As expected from bulk behaviour, the MT correction has the same singular behaviour as the DOS but opposite sign. On the other hand, because such a correction involves the coherent tunneling of the fluctuating Cooper pair from one site to the nearest neighbors, it is proportional to the lattice structure factor $\gamma_{\mathbf{K}}$: due to this proportionality, in the regime $T-T_c\gg g_T\delta$, the correction vanishes because $\int_{BZ}(dK)\gamma_{\mathbf{K}}=0$. Such a behaviour mirrors the condition that in such a regime, the granular structure is important, and the tunneling is not efficient. Let us stress that this is not the case for the DOS correction, which in this regime behaves as $\sim-(1/g)(E_T/T_c)(1/\epsilon)$, giving a non-vanishing contribution.

5.6.3 Aslamazov-Larkin correction

The AL diagrams for a granular system can be built up by means of blocks in Fig. 5.10, by considering all their possible combinations in pairs. For the sake of simplicity, we will call the first block, Fig. 5.10(a), B_1, and the second one B_2. Finally, one has three different kind of diagrams: the first one, with two B_1-type blocks; the second one with two B_2-type blocks, and the latter, with both of them. Because of the double multiplicity of B_2-type block, totally, one has nine diagrams contributing to

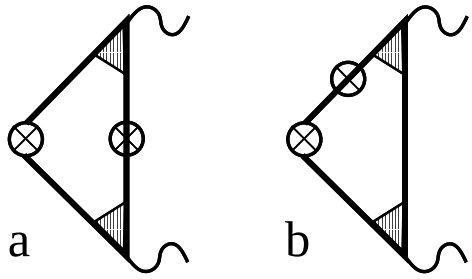

Figure 5.10: Diagrams of the blocks appearing in the Aslamazov-Larkin contribution to thermal conductivity. The AL diagrams for a granular system can be built up by means of the shown blocks, by considering all their possible combinations in pairs. Diagram (b) has a double molteplicity, since the bare tunnel vertex can stay on both side of the block.

thermal conductivity. In the following, we evaluate the analytical expression of B_1 and B_2 in the static approximation, as for the two previous corrections; we will see that for the AL correction, one needs to go beyond the static approximation to find a first non-vanishing contribution.

The general expression of linear response function for the AL diagrams reads

$$\mathcal{Q}^{(AL)}(\omega_\nu) = T^2 t^4 a^2 \sum_{l,j} \sum_{\Omega_\mu} L_{ij}(\Omega_{\mu+\nu}) L_{ml}(\Omega_\mu) B_{left}(\omega_\nu, \Omega_\mu) B_{right}(\omega_\nu, \Omega_\mu) \ , \quad (5.63)$$

where B_{left} and B_{right} can be either B_1 or B_2-type. We point out that in Eq. (5.63), contrary to what happens for DOS and MT corrections, there is a factor t^4 due to the presence of four tunneling vertices. For granular metals, it is not possible to build AL diagrams of lower order. Among them, two are tunneling vertices which interact with the external electromagnetic field and which contribute, as usual, as $j^Q_{vertex} = i2at(\varepsilon_n + \omega_\nu/2)$; the other two ones just contribute as pure tunneling vertices with a factor t.

B_1 block reads

$$B_1(\omega_\nu, \Omega_\mu) = \sum_{\varepsilon_n} (\varepsilon_n + \varepsilon_{n+\nu}) \lambda(\varepsilon_{n+\nu}, \varepsilon_{\mu-n}) \lambda(\varepsilon_n, \varepsilon_{\mu-n}) \times \int (dp) G(\mathbf{p}, \varepsilon_{n+\nu}) G(\mathbf{p}, \varepsilon_{\mu-n}) \int (dp') G(\mathbf{p}', \varepsilon_{\mu-n}) G(\mathbf{p}', \varepsilon_n) \ . \quad (5.64)$$

Taking the integrals over the Fermi surface, in the static approximation, we get

$$\begin{aligned} B_1(\omega_\nu, 0) &= (2\pi\nu_F\tau)^2 \sum_{\varepsilon_n} \theta(\varepsilon_{n+\nu}\varepsilon_n)(\varepsilon_n + \varepsilon_{n+\nu})\lambda(\varepsilon_{n+\nu}, -\varepsilon_n)\lambda(\varepsilon_n, -\varepsilon_n) \\ &= (2\pi\nu_F)^2 \left[\sum_{\varepsilon_n<-\omega_\nu} + \sum_{\varepsilon_n>0}\right] \frac{\varepsilon_n + \varepsilon_{n+\nu}}{|\varepsilon_{n+\nu} + \varepsilon_n|} \frac{1}{|2\varepsilon_n|} . \end{aligned} \tag{5.65}$$

Manipulating the sum, it is easy to see that

$$\begin{aligned} B_1(\omega_\nu, 0) &= (2\pi\nu_F)^2 \sum_{0<\varepsilon_n<\omega_\nu} \frac{1}{2\varepsilon_n} \\ &= (2\pi\nu_F)^2 \left[\psi\left(\frac{\omega_\nu}{2\pi T} + \frac{1}{2}\right) - \psi\left(\frac{1}{2}\right)\right] \\ &\approx \left(\frac{\pi\nu_F}{2}\right)^2 \frac{\omega_\nu}{T} . \end{aligned} \tag{5.66}$$

In the same way as sketched above, one can show, always in the static approximation, that the block B_2 vanishes identically. Then, all the diagrams containing B_2-type blocks do not give any contribution. Since the only AL diagram with two B_1-type block is proportional to the square of Eq. (5.66), it is quadratic in the external frequency ω, and therefore vanishes identically in the limit $\omega \to 0$.

To evaluate the first non vanishing AL correction, one has to consider the dynamical contribution. In such a case, the B_2 block, for instance, reads

$$\begin{aligned} B_2(\omega_\nu, \Omega_\mu) = \sum_{\varepsilon_n} (\varepsilon_n + \varepsilon_{n+\nu})\lambda(\varepsilon_{n+\nu}, \varepsilon_{\mu-n})\lambda(\varepsilon_n, \varepsilon_{\mu-n}) \\ \int (dp') G(\mathbf{p}', \varepsilon_{\mu-n}) G(\mathbf{p}', \varepsilon_n) G(\mathbf{p}', \varepsilon_{n+\nu}) \int (dp) G(\mathbf{p}, \varepsilon_{n+\nu}) . \end{aligned} \tag{5.67}$$

In the evaluation of the block, because of the pole structure of fluctuation propagator, one can neglect the ω_ν dependence, and keeps just the one in Ω_μ, [Larkin04]. The calculation of the integrals and the sums in the latter equation is, in the dynamical approximation, a little bit more cumbersome. One has to take into account the different possible signs of Ω_μ and ε_n, see Appendix K. Finally, Eq. (5.67) reads

$$\begin{aligned} B_2(0, \Omega_\mu) = -2(\pi\nu_F)^2 \sum_{\varepsilon_n} \frac{2\varepsilon_n}{(2\varepsilon_n - \Omega_\mu)^2} \\ \times\{\theta(\Omega_\mu)[\theta(\varepsilon_n - \Omega_\mu) + \theta(-\varepsilon_n)] + \theta(-\Omega_\mu)[\theta(\Omega_\mu - \varepsilon_n) + \theta(\varepsilon_n)]\} . \end{aligned} \tag{5.68}$$

By taking the lowest order in the bosonic frequency Ω_μ, one gets the result for the block

$$B_2\left(0,\Omega_\mu\right)=-\frac{1}{2}\left(\frac{\pi\nu_F}{2T}\right)^2\Omega_\mu\ . \tag{5.69}$$

In the same way, one can evaluate also B_1-type block, with the result

$$B_1\left(0,\Omega_\mu\right)=-2B_2\left(0,\Omega_\mu\right)\ , \tag{5.70}$$

which is consistent with the homogeneous case, [Larkin04]. The sum over Ω_μ in the response function can be performed by writing the sum as an integral, [Larkin04], and exploiting the properties of the pair correlators. All the details are reported in Appendix K.

Finally, the AL dynamical correction to thermal conductivity reads, [Biagini05]

$$\frac{\delta\kappa^{(AL)}}{\kappa_0}=\frac{9}{2\pi}\frac{1}{g_T}\left(\frac{g_T\delta}{T_c}\right)^2\int_{BZ}(dK)\frac{(1-\gamma_{\mathbf{k}})^2}{\epsilon+z\frac{g_T\delta}{T_c}\left(1-\gamma_{\mathbf{K}}\right)}\ . \tag{5.71}$$

Latter equation is the first non vanishing correction due to AL channel. Such a correction is always positive, and it depends, as in the MT, on the lattice structure factor $\gamma_{\mathbf{K}}$, but it does not vanishes in the regime $T-T_c\gg g_T\delta$. This is a good feature of the system, since far from T_c, the dynamical contribution plays an important role; in this region, one has to compare such a correction with DOS contribution, as discussed in the following section. Here, we just observe that since the corrections, Eqs. (5.58), (5.62) and (5.71), have different signs, non-monotonic behaviour in the total correction is expected, depending on the ratio $g_T\delta/T_c$.

5.7 Conclusions

The total correction to thermal conductivity close to the critical temperature can be immediately written by means of Eqs. (5.58), (5.62) and (5.71), [Biagini05]. It reads

$$\frac{\delta\kappa}{\kappa_0}=\frac{3}{\pi^2}\frac{1}{g_T}\frac{g_T\delta}{T_c}\int_{BZ}(dK)\frac{(1-\gamma_{\mathbf{K}})\left[\frac{3\pi}{2}\frac{g_T\delta}{T_c}\left(1-\gamma_{\mathbf{K}}\right)-1\right]}{\epsilon+z\frac{g_T\delta}{T_c}\left(1-\gamma_{\mathbf{K}}\right)}. \tag{5.72}$$

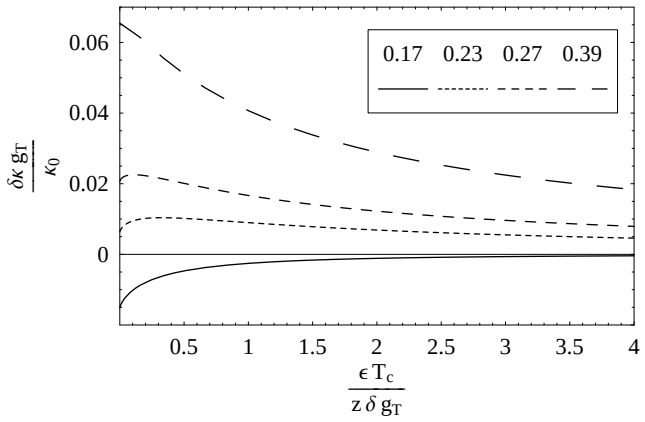

Figure 5.11: Total correction to the thermal conductivity due to superconducting fluctuations for different values of $g_T\delta/T_c$ for a two-dimensional system. A $1/\epsilon-$suppression is observed at high temperatures, with a sign depending on the above-mentioned ratio. At low temperatures, a finite correction, inversely proportional to the coordination number z, is reached at $\epsilon = 0$. In a finite interval of values of $g_T\delta/T_c$, a non-monotonic behaviour of the correction is observed, where the correction is positive and increasing with decreasing temperature, reaches a maximum and then goes to a smaller (possibly negative) value at the critical temperature, [Biagini05].

This correction has been obtained at all orders in the tunneling amplitude in the ladder approximation. Its behaviour is plotted in Fig. 5.12, as a function of the reduced temperature for the case of a two dimensional sample, and for different values of the ratio $g_T\delta/T_c$. We can recognize two different regimes of temperatures: far from T_c, $\epsilon \gg g_T\delta/T_c$, and close to T_c, $\epsilon \ll g_T\delta/T_c$. For the sake of simplicity, we will identify these two regimes as "high temperatures" and "low temperatures", respectively. The energy scale that separates the two regions, $g_T\delta$, can be recognized as the inverse tunneling time for a single electron, giving information on barrier transparency, [Beloborodov01].

5.7.1 High temperature regime: $\epsilon \gg g_T\delta/T_c$

The condition $\epsilon \gg g_T\delta/T_c$ is equivalent to the condition $\tau_{GL} \ll \tau_{dwell} = (g_T\delta)^{-1}$. That is the lifetime of a Cooper pair is smaller than the time the electrons spend in the grain before tunneling. Then, the tunneling is not efficient, and the system behaves as

an ensemble of real zero-dimensional grains.

As a consequence, only the DOS and the AL terms contribute significantly to the superconducting fluctuations; the correction to heat conductivity reads

$$\frac{\delta\kappa}{\kappa_0} \approx \frac{3}{\pi^2}\frac{1}{g_T}\frac{g_T\delta}{T_c}\frac{1}{\epsilon}\left[\frac{3\pi}{2}\frac{g_T\delta}{T_c}\left(1+\frac{1}{z}\right)-1\right] . \tag{5.73}$$

This expression shows a $1/\epsilon$ singularity and it can have either positive or negative sign, depending on the ratio $g_T\delta/T_c$; let γ_1 be the value of the above-mentioned ratio solution of Eq. (5.77). In the absence of renormalization due to tunnelling, the correction is negative and corresponds to the typical singularity of the quasi-zero-dimensional density of state. On the other hand, increasing the barrier transparency $g_T\delta$, the correction grows due to the presence of the direct channel, i.e., the AL term, which becomes more and more important, till the correction itself vanishes at γ_1, afterwhich it becomes positive.

A direct comparison with the behaviour of the electrical conductivity, [Beloborodov00], shows that there is a positive violation of the Wiedemann-Franz law,

$$\frac{\delta L}{L_0} = \frac{\delta\kappa}{\kappa_0} - \frac{\delta\sigma}{\sigma_0} \approx \left[-\frac{3}{\pi^2} + \frac{9}{2\pi}\frac{g_T\delta}{T_c}\frac{z+1}{z} + \frac{7\zeta(3)}{\pi^2}\right]\frac{\delta}{T_c}\frac{1}{\epsilon} . \tag{5.74}$$

5.7.2 Low temperature regime: $\epsilon \ll g_T\delta/T_c$

In this regime the tunneling is effective and there is a crossover to the typical behaviour of a homogeneous system, as $T \to T_c$, from the point of view of the fluctuating Cooper pairs. Physically, the bulk behaviour is recovered, and one gets a non divergent correction even at $\epsilon = 0$, where it equals

$$\frac{\delta\kappa\,(\epsilon=0)}{\kappa_0} = \frac{3}{z\pi^2}\frac{1}{g_T}\left(\frac{3\pi}{2}\frac{g_T\delta}{T_c}-1\right) . \tag{5.75}$$

The latter equation gives the saturation value in any dimension. Again, the value of the constant can be either negative or positive. The correction vanishes at a value $g_T\delta/T_c = \gamma_2$ which is independent on the dimensionality and larger than γ_1. In the interval $\gamma_1 < g_T\delta/T_c < \gamma_2$, the correction has a non-monotonic behaviour, being positive and increasing with decreasing temperatures and negative for low temperatures.

In the above-mentioned interval, the barrier transparency is enough large in order for the correction to be positive because of AL and MT positive contributions, but the negative correction given by DOS contribution yet plays a role giving rise to a non-monotonic behaviour. For larger values of barrier transparency, the sample behaves as a real bulk system, and the DOS correction is completely cut off by the MT one. Such a behaviour has been plotted, for the case of $d = 2$, in Fig. 5.12.

The deviation from the Wiedemann-Franz law in the low temperature region is much more evident than in the high temperature one, because of the pronounced singular behaviour of the electrical conductivity, due to the increasing number of Cooper pairs, close to the critical temperature, [Beloborodov00].

Conclusion

La correction totale à la conductivité thermique près de la température critique peu être immédiatement écrite à l'aide des Eqs. (5.58), (5.62) et (5.71), [Biagini05]. Elle s'écrit

$$\frac{\delta\kappa}{\kappa_0} = \frac{3}{\pi^2}\frac{1}{g_T}\frac{g_T\delta}{T_c}\int_{BZ}(dK)\frac{(1-\gamma_{\mathbf{K}})\left[\frac{3\pi}{2}\frac{g_T\delta}{T_c}(1-\gamma_{\mathbf{K}})-1\right]}{\epsilon + z\frac{g_T\delta}{T_c}(1-\gamma_{\mathbf{K}})}. \tag{5.76}$$

Cette correction a été obtenue à tous les ordres en l'amplitude du tunnelling dans l'approximation soi-disant *ladder*. Son comportement est montré sur la Fig. 5.12, en fonction de la température réduite, et pour différentes valeurs du rapport $g_T\delta/T_c$. On peut reconnaître deux régimes différents: loin de T_c, $\epsilon \gg g_T\delta/T_c$, et près de T_c, $\epsilon \ll g_T\delta/T_c$. Pour une question de simplicité, nous identifions ces deux régimes comme "hautes" et "basses" températures, respectivement. L'échelle d'énergie qui sépare les deux régions, $g_T\delta$, peut être vue comme l'inverse du temps de tunnelling, donnant des informations sur la transparence de la barrière, [Beloborodov01].

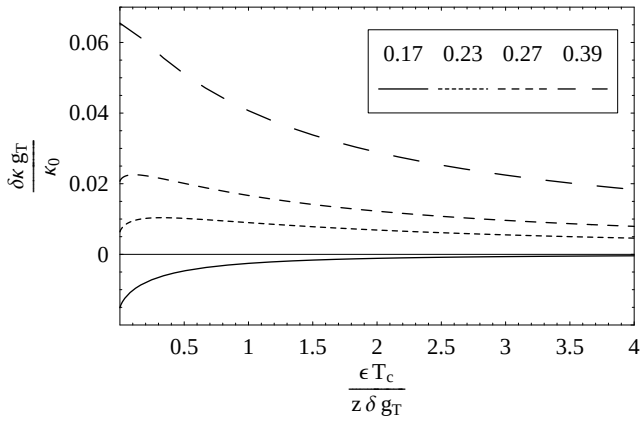

Figure 5.12: Correction totale à la conductivité thermique due aux fluctuations supraconductrices pour différentes valeurs du rapport $g_T\delta/T_c$ pour un système deux-dimensionnel. Une suppression se comportant comme $1/\epsilon$ est observée à hautes températures, avec un signe qui dépend du susdit rapport. A basse températures, une correction finie, inversement proportionnelle au nombre de coordination z, est atteinte à $\epsilon = 0$. Dans un intervalle de valeurs de $g_T\delta/T_c$, un comportement non monotone est observé, où la correction est positive et croissante avec la diminution de la température, atteint le maximum et puis décroît vers des valeurs plus petites à la température critique, [Biagini05].

5.7.3 Régime des hautes temperatures: $\epsilon \gg g_T\delta/T_c$

La condition $\epsilon \gg g_T\delta/T_c$ est équivalente à la condition $\tau_{GL} \ll \tau_{dwell} = (g_T\delta)^{-1}$. C'est à dire que le temps de vie d'une paire de Cooper est plus petit que le temps que les électrons passent dans les grains avant de tunneler. Donc, le tunnelling n'est pas efficace, et le système se comporte comme un ensemble de grains uni-dimensionnels.

Par consequant, juste les termes DOS et AL contribuent significativement aux fluctuations supraconductrice; la correction à la conductivité thermique s'écrit

$$\frac{\delta\kappa}{\kappa_0} \approx \frac{3}{\pi^2}\frac{1}{g_T}\frac{g_T\delta}{T_c}\frac{1}{\epsilon}\left[\frac{3\pi}{2}\frac{g_T\delta}{T_c}\left(1+\frac{1}{z}\right)-1\right] . \tag{5.77}$$

Cette dernière expression montre une singularité $1/\epsilon$ et peut être soit positive soit négative; elle dépend du rapport $g_T\delta/T_c$. Soit γ_1 la valeur du rapport ci-dessus qui est solution de l'Eq. (5.77). En absence de renormalisation due au tunnelling, la correction est négative et correspond à la singularité typique pour la densité d'états. En augmentant la transparence de la barrière $g_T\delta$, la correction croît à cause de la présence du canal direct, i.e., le terme AL, qui devient de plus en plus important jusqu'à ce que

la correction disparaît lorsque la valeur γ_1 est atteinte, pour enfin devenir positive.

Une comparaison directe avec le comportement de la conductivité électrique, [Beloborodov00], montre qu'il y a une violation positive de la loi de Wiedemann-Franz,

$$\frac{\delta L}{L_0} = \frac{\delta\kappa}{\kappa_0} - \frac{\delta\sigma}{\sigma_0} \approx \left[-\frac{3}{\pi^2} + \frac{9}{2\pi}\frac{g_T\delta}{T_c}\frac{z+1}{z} + \frac{7\zeta(3)}{\pi^2} \right] \frac{\delta}{T_c}\frac{1}{\epsilon} \, . \tag{5.78}$$

5.7.4 Régime des basses températures: $\epsilon \ll g_T\delta/T_c$

Dans ce régime, le tunnelling est efficace et il y a un crossover au comportement typique pour un système homogène, pour $T \to T_c$, du point de vue des paires de Cooper. Physiquement, le comportement d'un métal massif est retrouvé, et on obtient une correction non divergeante même pour $\epsilon = 0$, où elle s'écrit

$$\frac{\delta\kappa\,(\epsilon=0)}{\kappa_0} = \frac{3}{z\pi^2}\frac{1}{g_T}\left(\frac{3\pi}{2}\frac{g_T\delta}{T_c} - 1\right) \, . \tag{5.79}$$

La dernière équation donne la valeur de saturation dans n'importe quelle dimension. Ici aussi, la valeur de la constante peut être positive ou négative. La correction s'annule à la valeur $g_T\delta/T_c = \gamma_2$ qui ne dépend pas de la dimensionalité, et qui est plus grande que γ_1. Dans l'intervalle $\gamma_1 < g_T\delta/T_c < \gamma_2$, la correction a un comportement non monotone, elle est positive et croît lorsque la température décroît, et négative à basses températures. Dans le susdit intervalle, la transparence de la barrière est assez grande de sorte que la correction est positive à cause des corrections AL et MT, mais la correction négative donnée par la contribution DOS joue encore un rôle donnant lieu à un comportement non monotone. Pour des valeurs plus grandes de la transparence de la barrière, l'échantillon se comporte comme un système massif, et le terme DOS est complètement coupé par le terme MT. Un tel comportement est montré, pour le cas $d = 2$ sur la Fig. 5.12.

La déviation à la loi de Wiedemann-Franz dans le régime des basses températures est encore plus évidente encore à cause du comportement fortement singulier de la conductivité électrique, due au nombre croissant de paires de Cooper près de la température critique, [Beloborodov00].

Résumé en français du chapitre 5

Dans la première partie de ce chapitre, nous présentons les propriétés fondamentales des métaux granulaires normaux.

Nous montrons comment dans les années 70, à l'aide d'études sur la résistivité, leur structure fortement non-uniforme fut révélée. Nous introduisons les plus importantes échelles d'énergie qui permettent de définir de différents régimes de travail. En particulier, comme nous l'avons mentionné, nous supposons que les métaux granulaires sont de bons conducteurs ce qui équivaut à affirmer que la conductivité tunnel sans dimension entre les grains est beaucoup plus grande qu'un. Cependant, nous supposons aussi que la plus grande contribution à la résistance vient du tunnelling entre les grains. C'est à dire que les électrons se déplacent beaucoup plus facilement à l'intérieur d'un grain qu'entre deux grains.

Sous ses conditions, nous montrons les résultats les plus importants pour le métaux normaux concernant le transport électrique et thermique.

Puis, nous abordons le problème des métaux supraconducteurs. Nous présentons le modèle que nous avons utilisé et calculons le courant thermique entre les grains. L'approche que nous avons utilisée afin d'évaluer les différentes contributions à la conductance thermique est l'approche diagrammatique. L'expression du courant thermique nous permet de connaître les contributions de chaque vertex des diagrammes.

Par rapport au cas d'un métal massif, la présence du tunnelling comporte un profond changement de comportement. La possibilité que deux électrons formant une paire de Cooper puissent tunneler sans perdre leur corrélation entraîne une correction importante dans l'expression du propagateur du canal direct de Cooper, et donc dans

les corrections aux conductivités.

Pour les contributions MT et DOS, il a été suffisant d'évaluer la contribution dite statique. Pour le terme AL, la première contribution dynamique a été calculé.

APPENDICES

Appendix A

LL Hamiltonian: semi-classical approach

We want to write the Hamiltonian of a LL by means of a semi-classical approach, that is by considering the electrons gas as a real fluid, and using the Euler equation, [Gramada97].

Let us consider the semi-classical equation of motion

$$mn(x,t)\frac{d^2u(x,t)}{dt^2} = -en(x,t)\mathcal{E}(x,t) - \frac{dP}{dx}\ , \tag{A.1}$$

where m is the mass of an electron, and $u(x,t)$ the displacement in the fluid; $n(x,t)$ is the electron density: $n(x,t) = n_0 + n_1(x,t)$, where $n_1(x,t)$ describes the time fluctuations; $\mathcal{E}(x,t) = \mathcal{E}_0(x) + \mathcal{E}_1(x,t)$ is the electric field, which can be imagined as composed by a steady part and a dynamical one; $P = \pi^2\hbar^2 n^3/3m$ is the hydrostatic pressure.

The steady component of the electric field can be cancelled by the equation of motion, using the equilibrium condition

$$e\mathcal{E}_0 n_0 = -\left.\frac{dP}{dx}\right|_{n=n_0}\ . \tag{A.2}$$

Replacing Eq. (A.2) in the equation of motion, Eq. (A.1), and linearizing the latter with respect to $n_1(x,t)$, one gets

$$mn_0\frac{d^2u}{dt^2} = -en_0\mathcal{E}_1 - \frac{\pi^2\hbar^2}{m}\left(n_0^2\frac{dn_1}{dx} + n_0 n_1\frac{dn_0}{dx}\right)\ . \tag{A.3}$$

Let $V(x)$ be the electron-electron interaction potential. The electric field $\mathcal{E}_1$ can be imagined to be generated by the fluctuations of the density $n_1(x,t)$; then,

$$e\mathcal{E}_1 = -\frac{d}{dx}\int dx' V(x-x')n_1(x',t)\ . \tag{A.4}$$

By means of the fundamental hypotesis on quantum wire, Eq. (2.30), Eq. (A.4) can be written as $e\mathcal{E}_1 = -V_0(dn_1(x,t)/dx)$. The density n_1 can be written in terms of the displacement $\hat{u}$ by means of the continuity equation: $n_1 = -d(n_0u)/dx$. To obtain the energy conservation law, one can multiply Eq. (A.3) by du/dt. Thanks to Eq. (A.4), the first term in the rhs of Eq. (A.3) reads

$$-\frac{V_0}{2}\frac{d}{dt}\left[\frac{d(n_0u)}{dx}\right]^2 + V_0\left(\frac{d}{dx}\right)\left[\frac{d(n_0u)}{dx}\frac{d(n_0u)}{dt}\right]\ , \tag{A.5}$$

and the remaining terms

$$\frac{\pi^2\hbar^2}{2m}\frac{d}{dt}\left\{\frac{d}{dx}\left[n_0\frac{d(n_0u)^2}{dx}\right] - n_0\left[\frac{d(n_0u)^2}{dx}\right]^2\right\}\ . \tag{A.6}$$

Integrating over x, Eq. (A.3) reads $dE/dt = 0$, where the energy is

$$E = \int dx\left[\frac{mn_0}{2}\left(\frac{du}{dt}\right)^2 + \frac{1}{2}\left(V_0 + \frac{\pi^2\hbar^2}{m}n_0\right)(\vec{\nabla}n_0u)^2\right]\ . \tag{A.7}$$

The latter expression for the energy allows to write the corresponding Hamiltonian. Let us consider the displacement $u(x)$ as an operator $\hat{u}(x)$; let $\hat{p}(x)$ be the conjugate momentum, with $[\hat{u}(x),\hat{p}(x)] = i\hbar\delta(x-x')$. Finally, the Hamiltonian reads

$$H_{0_{\hat{u}}} = \int dx\left[\frac{\hat{p}^2(x)}{2mn_0} + \frac{1}{2}\left(V_0 + \frac{\pi^2\hbar^2}{m}n_0\right)(\nabla n_0\hat{u})^2\right]\ . \tag{A.8}$$

Appendix B

Thermal conductance for a clean wire

To evaluate the thermal conductance for a clean wire, we start from the current-current correlation function in Eq. (3.9), and the expression of current density operator in Eq. (3.11).

$$\begin{aligned}
&\langle T_\tau j_{\rm th}(x,\tau) j_{\rm th}(x',0)\rangle \\
&\quad = \left(\frac{v_F^4 m^2 n_0^2}{4}\right) \langle T_\tau \left[\partial_{\tau_1}\hat{u}(x_1,\tau_1)\partial_{x_2}\hat{u}(x_2,\tau_2) + \partial_{x_2}\hat{u}(x_2,\tau_2)\partial_{\tau_1}\hat{u}(x_1,\tau_1)\right] \\
&\quad \times \left[\partial_{\tau_3}\hat{u}(x_3,\tau_3)\partial_{x_4}\hat{u}(x_4,\tau_4) + \partial_{x_4}\hat{u}(x_4,\tau_4)\partial_{\tau_3}\hat{u}(x_3,\tau_3)\right]\rangle \\
&\quad = v_F^4 m^2 n_0^2 \left(\partial_{\tau_1}\partial_{\tau_3}\partial_{x_2}\partial_{x_4}\right) \langle T_\tau \hat{u}_1\hat{u}_2\hat{u}_3\hat{u}_4\rangle \,, \qquad \text{(B.1)}
\end{aligned}$$

where, for the sake of simplicity, $\hat{u}_i = \hat{u}(x_i,\tau_i)$. From the latter equality, it is easy to get the expression in Eq. (3.12). By means of Fourier transform of Green's function, the correlation function can be written as

$$\begin{aligned}
\langle T_\tau j_{\rm th}(x,\tau) j_{\rm th}(x',0)\rangle = v_F^2 &\left(\partial_{\tau_1}\partial_{\tau_3}\partial_{x_2}\partial_{x_4}\right) \\
\times \quad T^2 &\left[\sum_{i\omega_1, i\omega_2} e^{-i\omega_1(\tau_1-\tau_3)} e^{-i\omega_2(\tau_4-\tau_2)} G^0(x_1,x_3;i\omega_1) G^0(x_4,x_2;i\omega_2)\right. \\
+ \quad &\left.\sum_{i\omega_3, i\omega_4} e^{-i\omega_3(\tau_1-\tau_4)} e^{-i\omega_4(\tau_3-\tau_2)} G^0(x_1,x_4;i\omega_3) G^0(x_3,x_2;i\omega_4)\right]. \qquad \text{(B.2)}
\end{aligned}$$

Remembering that

$$\partial_x G_{i\omega_\mu}(x,x') = -\partial_{x'} G_{i\omega_\mu}(x,x') = (|\omega_\mu|/v_F) G_{i\omega_\mu}(x,x') \ , \tag{B.3}$$

Eq. (B.2) can be written as

$$\begin{aligned}
&\langle T_\tau j_{\rm th}(x,\tau) j_{\rm th}(x',0)\rangle \\
&= -T^2 \Bigg[\sum_{i\omega_1, i\omega_2} \omega_1^2 |\omega_2|^2 e^{-i\omega_1(\tau_1-\tau_3)} e^{-i\omega_2(\tau_4-\tau_2)} G^0(x_1,x_3;i\omega_1) G^0(x_4,x_2;i\omega_2) \\
&- \sum_{i\omega_3, i\omega_4} \omega_3\omega_4 |\omega_3||\omega_4| e^{-i\omega_3(\tau_1-\tau_4)} e^{-i\omega_4(\tau_3-\tau_2)} G^0(x_1,x_4;i\omega_3) G^0(x_3,x_2;i\omega_4) \Bigg] .
\end{aligned} \tag{B.4}$$

Now, one can take the correct limits for the different variables: $(x_1,x_2)\to x$, $(x_3,x_4)\to x'$, $(\tau_1,\tau_2)\to\tau$ and $(\tau_3,\tau_4)\to 0$. Eq. (B.4), then, reads

$$\begin{aligned}
&\langle T_\tau j_{\rm th}(x,\tau) j_{\rm th}(x',0)\rangle \\
&\qquad = -T^2 \Bigg[\sum_{i\omega_1, i\omega_2} \omega_1^2 |\omega_2|^2 e^{-i(\omega_1-\omega_2)\tau} G^0(x,x';i\omega_1) G^0(x',x;i\omega_2) \\
&\qquad - \sum_{i\omega_3, i\omega_4} \omega_3\omega_4 |\omega_3||\omega_4| e^{-i(\omega_3-\omega_4)\tau} G^0(x,x';i\omega_3) G^0(x',x;i\omega_4) \Bigg] .
\end{aligned} \tag{B.5}$$

Defining $\omega_\nu = \omega_1 - \omega_2$ in the first term, and $\omega_\nu = \omega_3 - \omega_4$ in the second, and by means of Fourier tranform, one gets Eq. (3.13),

$$\begin{aligned}
&\int_0^\beta d\tau \langle T_\tau j_{\rm th}(x,\tau) j_{\rm th}(x',0)\rangle e^{i\omega_\nu\tau} \\
&= -T \sum_{i\omega_\mu} G_{i\omega_\mu}(x',x) G_{i\omega_\nu + i\omega_\mu}(x,x') \left[(\omega_\mu+\omega_\nu)^2 |\omega_\mu|^2 - \omega_\mu(\omega_\nu+\omega_\mu)|\omega_\mu||\omega_\nu+\omega_\mu| \right]
\end{aligned} \tag{B.6}$$

where we set $\omega_2 = \omega_4 = \omega_\mu$. The latter equation gives rise to a non vanishing contribution only for values of ω_μ such that $-\omega_\nu < \omega_\mu < 0$. The sum in the latter equation can be rewritten as a contour integral in the complex plane by means of the Eliashberg formula, [Eliashberg61]

$$T \sum_{\Omega_\mu} f(\Omega_\mu) = \frac{1}{4\pi i} \oint_{C_0} dz \coth\left(\frac{z}{2T}\right) f(-iz) \ , \tag{B.7}$$

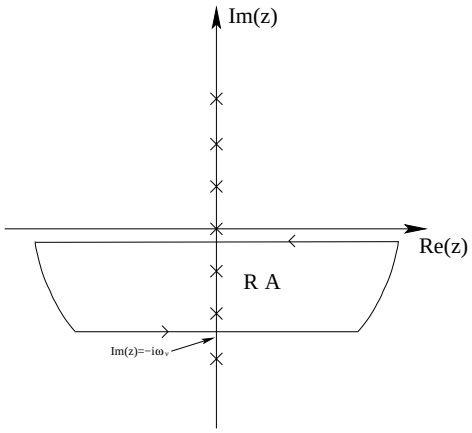

Figure B.1: The sum over ω_μ in Eq. (B.6) can be performed transforming the sum into an integral along the indicated integration contour. The function in the integral is not analytical at $\Im\mathrm{m}(z) = 0$ and $\Im\mathrm{m}(z) = -i\omega_\nu$. Crosses represent the poles of $\coth(z/2T)$, and A and R stand for advanced and retarded, respectively.

with $z = i\omega_\mu$; then,

$$\int_0^\beta d\tau \langle T_\tau j_{\rm th}(x,\tau) j_{\rm th}(x',0)\rangle e^{i\omega_\nu \tau}$$
$$= -\frac{2}{4\pi i}\oint_{C_0} dz \coth\left(\frac{z}{2T}\right) G^0(x',x;z) G^0(x,x';i\omega_\nu + z)(-iz)^2(\omega_\nu - iz)^2 \ . \quad \text{(B.8)}$$

The contour of integration is shown in Fig. B.1. The rhs of Eq. (B.8) can be written as

$$-\frac{1}{2\pi i}\left\{\int_{-\infty-i\omega_\nu}^{\infty-i\omega_\nu} dz \coth\left(\frac{z}{2T}\right) z^2(i\omega_\nu + z)^2 G^R(x,x';i\omega_\nu + z) G^A(x',x;z) \right.$$
$$\left. + \int_{+\infty}^{-\infty} dz \coth\left(\frac{z}{2T}\right) z^2(i\omega_\nu + z)^2 G^R(x,x';i\omega_\nu + z) G^A(x',x;z)\right\} \ , \quad \text{(B.9)}$$

where the superscripts A and R stand for advanced and retarded, respectively. Setting $z' = z + i\omega_\nu$ in the first integral, Eq. (B.9) reads

$$-\frac{1}{2\pi i}\left\{\int_{-\infty}^{+\infty} dz' \coth\left(\frac{z'}{2T}\right)(z')^2(z' - i\omega_\nu)^2 G^R(x,x';z') G^A(x',x;z' - i\omega_\nu) \right.$$
$$\left. - \int_{-\infty}^{+\infty} dz \coth\left(\frac{z}{2T}\right) z^2(i\omega_\nu + z)^2 G^R(x,x';z + i\omega_\nu) G^A(x',x;z)\right\} \ . \quad \text{(B.10)}$$

Performing analytical continuation $\omega_\nu \to -i\omega$, and setting $z' = z + \omega$ in the second integral

$$
\begin{aligned}
&-\frac{1}{2\pi i}\left\{\int_{-\infty}^{+\infty} dz \coth\left(\frac{z}{2T}\right) z^2(z-\omega)^2 G^R(x,x';z)G^A(x',x;z-\omega)\right. \\
&\left.-\int_{-\infty}^{+\infty} dz' \coth\left(\frac{z'-\omega}{2T}\right)(z')^2(z'-\omega)^2 G^R(x,x';z')G^A(x',x;z'-\omega)\right\} \\
&= -\frac{1}{2\pi i}\int_{-\infty}^{+\infty} dz \coth\left[\coth\left(\frac{z}{2T}\right) - \coth\left(\frac{z-\omega}{2T}\right)\right] \\
&\qquad\qquad \times z^2(z-\omega)^2 G^R(x,x';z)G^A(x',x;z-\omega)\ . \qquad \text{(B.11)}
\end{aligned}
$$

In the limit $\omega \to 0$, one gets the expression for the thermal conductance in Eq. (3.14), G^A being the hermitian conjugate of G^R.

Appendix C

Equation of motion for the Green's function

For the sake of simplicity, we consider the bosonic operator $\hat{\phi}(x,\tau)$, in terms of which the density of current is written as, [Maslov95, Maslov95b]

$$\hat{j}(x,\tau) = -\partial_\tau \frac{\hat{\phi}(x,\tau)}{\sqrt{\pi}}. \tag{C.1}$$

By means of the current continuity equation, the operator $\hat{\phi}(x,\tau)$ can be written in function of the displacement $\hat{u}(x,\tau)$ as

$$\hat{\phi}(x,\tau) = -\sqrt{\pi}[n_0 \hat{u}(x,\tau)] \ . \tag{C.2}$$

The relation of commutation between $\hat{\phi}$ and $\hat{p}$, its conjugate momentum, reads

$$[\hat{\phi}(x,\tau), \hat{p}(x',\tau)] = -\sqrt{\pi} i n_0 \delta(x-x') \ . \tag{C.3}$$

The Luttinger liquids Hamiltonian in Eq. (3.3) in terms of operator $\hat{\phi}$ reads

$$H_{0_{\hat{\phi}}} = \int dx \left[\frac{\hat{p}^2(x)}{2mn_0} + \frac{1}{2\pi}\left(V_0 + \frac{\pi^2}{m} n_0\right)(\nabla\hat{\phi})^2 \right] \ . \tag{C.4}$$

To evaluate the equation of motion, let us consider the temperature Green's function in time domain

$$G(x,x';\tau) = \langle T_\tau \hat{\phi}(x,\tau)\hat{\phi}(x',0)\rangle \ , \tag{C.5}$$

and let us evaluate $\partial_\tau G$:

$$\frac{\partial}{\partial\tau}G = \frac{\partial}{\partial\tau}\langle\phi\phi_\prime\rangle\theta(\tau) + \frac{\partial}{\partial\tau}\langle\phi_\prime\phi\rangle\theta(-\tau) \ . \tag{C.6}$$

For the sake of simplicity, we have indicated $\hat{\phi}(x,\tau) = \phi$, and $\hat{\phi}(x',0) = \phi_\prime$; $\theta(\tau)$ is the step function.

The first term in the rhs of Eq. (C.6) reads

$$\frac{\partial}{\partial\tau}\langle\phi\phi_\prime\rangle\theta(\tau) = \langle\phi\phi_\prime\rangle\delta(\tau) + \theta(\tau)\langle[H,\phi]\phi_\prime\rangle \ . \tag{C.7}$$

The commutator which appears in Eq. (C.7) reads

$$\begin{aligned}
[H,\phi] &= \int dx' \left\{ \frac{1}{2mn_0}[\hat{p}_\prime^2,\phi] + \frac{1}{2\pi}\left(V_0 + \frac{\pi^2}{m}n_0\right)[(\nabla_\prime\phi_\prime)^2,\phi] \right\} \\
&= \int dx' \frac{1}{2mn_0}[\hat{p}_\prime^2,\phi] \\
&= \int dx' \frac{1}{2mn_0}\left\{2\sqrt{\pi}in_0\delta(x-x')\hat{p}_\prime\right\} \\
&= \frac{i\sqrt{\pi}}{m}\hat{p}(x) \ .
\end{aligned} \tag{C.8}$$

By means of Eq. (C.8), Eq. (C.7) can be written as

$$\frac{\partial}{\partial\tau}\langle\phi\phi_\prime\rangle\theta(\tau) = \langle\phi\phi_\prime\rangle\delta(\tau) + \frac{i\sqrt{\pi}}{m}\langle\hat{p}\phi_\prime\rangle\theta(\tau) \ . \tag{C.9}$$

Analogously, developing the second term in the rhs of Eq. (C.6), one finds

$$\frac{\partial}{\partial\tau}\langle\phi_\prime\phi\rangle\theta(-\tau) = -\langle\phi\phi_\prime\rangle\delta(\tau) + \frac{i\sqrt{\pi}}{m}\langle\hat{p}\phi_\prime\rangle\theta(-\tau) \ . \tag{C.10}$$

The sum of Eqs. (C.9) and (C.10) reads

$$\frac{\partial}{\partial\tau}G(x,x';\tau) = \frac{i\sqrt{\pi}}{m}\langle T_\tau\hat{p}(x,\tau)\phi(x',0)\rangle \ . \tag{C.11}$$

Since we are interested in the equation of motion of $G(x,x';\tau)$, we need to evaluate the second derivative; the Green's function which appears in the rhs of Eq. (C.11) does not give any useful information.

$$\frac{\partial^2}{\partial\tau^2}G(x,x';\tau) = \frac{i\sqrt{\pi}}{m}\left\{\partial_\tau\langle\hat{p}\phi_\prime\rangle\ \theta(\tau) + \partial_\tau\langle\phi_\prime\hat{p}\rangle\theta(-\tau)\right\} \ . \tag{C.12}$$

Let us evaluate separately the two terms in the rhs of Eq. (C.12).

$$\partial_\tau \langle \hat{p}\phi_{\prime} \rangle \theta(\tau) = \langle \hat{p}\phi_{\prime} \rangle \delta(\tau) + \theta(\tau) \langle [H, \hat{p}]\phi_{\prime} \rangle \ . \tag{C.13}$$

It is necessary to evaluate the commutator between H and $\hat{p}$

$$[H, \hat{p}] = \int dx' \frac{1}{2\pi} \left(V_0 + \frac{\pi^2 \hbar^2}{m} n_0 \right) [(\nabla_{\prime}\phi_{\prime})^2, \hat{p}] \ , \tag{C.14}$$

$$[(\nabla_{\prime}\phi_{\prime})^2, \hat{p}] = -2\sqrt{\pi} i \nabla_{\prime} n_0 \delta(x - x') \nabla_{\prime}\phi_{\prime} \ . \tag{C.15}$$

By means of Eq. (C.15), Eq. (C.14) can be written as

$$[H, \hat{p}] = -\frac{iV_0}{\sqrt{\pi}} \int dx' \nabla_{\prime} n_0 \delta(x - x') \nabla_{\prime}\phi_{\prime} - \frac{i\pi^2 \hbar^2}{m\sqrt{\pi}} \int dx' n_0 \nabla_{\prime} n_0 \delta(x - x') \nabla_{\prime}\phi_{\prime} \ . \tag{C.16}$$

Integrals appearing in Eq. (C.16) can be evaluated by integration by parts, and exploiting the properties of Dirac δ function

$$\int dx' \nabla_{\prime} n_0 \delta(x - x') \nabla_{\prime}\phi_{\prime} = -n_0 \nabla^2 \phi(x) \ , \tag{C.17}$$

$$\int dx' n_0 \nabla_{\prime} n_0 \delta(x - x') \nabla_{\prime}\phi_{\prime} = -n_0 \nabla [n_0 \nabla \phi] \ . \tag{C.18}$$

Replacing Eqs. (C.17) and (C.18) in Eq. (C.16), one finds

$$[H, \hat{p}] = \frac{iV_0}{\sqrt{\pi}} n_0 \nabla^2 \phi(x) + \frac{i\pi^2}{m\sqrt{\pi}} n_0 \nabla [n_0 \nabla \phi] \ . \tag{C.19}$$

Eq. (C.13) by means of Eq. (C.19) reads

$$\begin{aligned} \partial_\tau \langle \hat{p}\phi_{\prime} \rangle \theta(\tau) &= \langle \hat{p}\phi_{\prime} \rangle \delta(\tau) \\ &+ \theta(\tau) \left\{ \frac{iV_0}{\sqrt{\pi}} \langle n_0 \nabla^2 \phi(x) \phi_{\prime} \rangle + \frac{i\pi^2}{m\sqrt{\pi}} \langle n_0 \nabla [n_0 \nabla \phi] \phi_{\prime} \rangle \right\} \ . \end{aligned} \tag{C.20}$$

The second term in the rhs of Eq. (C.12) can be evaluated as

$$\begin{aligned} \partial_\tau \langle \phi_{\prime} \hat{p} \rangle \theta(-\tau) &= -\langle -\sqrt{\pi} i n_0 \delta(x - x') + \hat{p}\phi_{\prime} \rangle \delta(\tau) \\ &+ \theta(-\tau) \partial_\tau \langle -\sqrt{\pi} i n_0 \delta(x - x') + \hat{p}\phi_{\prime} \rangle \\ &= i\sqrt{\pi} n_0 \delta(x - x') \delta(\tau) - \langle \hat{p}\phi_{\prime} \rangle \delta(\tau) + \theta(-\tau) \langle [H, \hat{p}]\phi_{\prime} \rangle \ . \end{aligned} \tag{C.21}$$

Eq. (C.21) can be evaluated by means of Eq. (C.19)

$$\begin{aligned}\partial_\tau\langle\phi_\prime\hat{p}\rangle\theta(-\tau) &= i\sqrt{\pi}n_0\delta(x-x')\delta(\tau)-\langle\hat{p}\phi_\prime\rangle\delta(\tau)\\ &\quad+\theta(-\tau)\Bigg\{\frac{iV_0}{\sqrt{\pi}}\langle n_0\nabla^2\phi(x)\phi_\prime\rangle\\ &\quad+\frac{i\pi^2}{m\sqrt{\pi}}\langle n_0\nabla[n_0\nabla\phi]\phi_\prime\rangle\Bigg\}\,. \end{aligned}\tag{C.22}$$

The sum of Eqs. (C.20) and (C.22) reads

$$\begin{aligned}\frac{\partial^2}{\partial\tau^2}G(x,x';\tau) &= -\Bigg\{\frac{\pi}{m}n_0\delta(x-x')\delta(\tau)+\frac{V_0}{m}n_0\nabla^2G(x,x';\tau)\\ &\quad+\frac{\pi^2}{m^2}n_0\nabla n_0\nabla G(x,x';\tau)+\frac{n_0^2\pi^2}{m^2}\nabla^2G(x,x';\tau)\Bigg\}\,. \end{aligned}\tag{C.23}$$

Eq. (C.23) can be written as

$$\partial_\tau^2G(x,x';\tau)+\frac{n_0}{m}\partial_x\left\{\left[V_0+\frac{\pi^2n_0}{m}\right]\partial_xG(x,x';\tau)\right\}=-\frac{\pi n_0}{m}\delta(x-x')\delta(\tau)\,.\tag{C.24}$$

Finally, the equation of motion reads

$$\left\{\frac{1}{v(x)g_{LL}(x)}\partial_\tau^2+\partial_x\left(\frac{v(x)}{g_{LL}(x)}\partial_x\right)\right\}G(x,x';\tau)=-\delta(x-x')\delta(\tau)\,,\tag{C.25}$$

In the frequency domain, Eq. (C.25) reads

$$\left\{-\partial_x\left(\frac{v(x)}{g_{LL}(x)}\partial_x\right)+\frac{{\omega_\nu}^2}{v(x)g_{LL}(x)}\right\}G^0_{i\omega_\nu}(x,x')=\delta(x-x')\,.\tag{C.26}$$

Appendix D

Green's function in a clean wire

We want to solve the equation of motion, Eq. (C.26). From Fig. 3.4, Eq. (C.26) can be written as

$$\partial_x^2 G^0(x,x';\tau) = \frac{{\omega_\nu}^2}{v^2} G^0(x,x'\tau) \ , \tag{D.1}$$

that is as a constant coefficients differential equation.

The general solution is

$$G^0_{i\omega_\nu}(x,x') = \begin{cases} Ee^{\frac{|\omega_\nu|}{v_F}x} & : \quad x \leq 0 & G_I \\ Ae^{\frac{|\omega_\nu|}{v}x} + Be^{-\frac{|\omega_\nu|}{v}x} & : \quad 0 < x \leq x' & G_{II} \\ Ce^{\frac{|\omega_\nu|}{v}x} + De^{-\frac{|\omega_\nu|}{v}x} & : \quad x' < x \leq L & G_{III} \\ Fe^{-\frac{|\omega_\nu|}{v_F}x} & : \quad x > L & G_{IV} \end{cases} \tag{D.2}$$

The evaluation of coefficient is done by means of boundary conditions

$$\begin{cases} G_I(0) = G_{II}(0) & : \\ G_{II}(x') = G_{III}(x') & : \\ G_{III}(d) = G_{IV}(d) & : \\ v_F G'_I(0) = \frac{v}{g_{LL}} G'_{II}(0) & : \\ \frac{v}{g_{LL}} G'_{III}(d) = v_F G'_{IV}(d) & : \\ -\frac{v}{g_{LL}} G'^0(x,x')\Big|_{x'-\epsilon}^{x'+\epsilon} = 1 & : \end{cases} \tag{D.3}$$

Easily, albeit slowly, one finds

$$B = \frac{\gamma-\omega}{\gamma+\omega}A\,, \tag{D.4a}$$

$$E = \frac{2\gamma}{\gamma+\omega}A\,, \tag{D.4b}$$

$$C = -\frac{e^{-\alpha x'}}{2\gamma}+A\,, \tag{D.4c}$$

$$D = \frac{e^{\alpha x'}}{2\gamma}+\frac{\gamma-\omega}{\gamma+\omega}A\,, \tag{D.4d}$$

$$F = -\frac{e^{\beta d}}{\gamma}\sinh[\alpha(d-x')]+e^{\beta d}\left(e^{\alpha d}+e^{-\alpha d}\frac{\gamma-\omega}{\gamma+\omega}\right)A\,, \tag{D.4e}$$

$$A = \frac{\cosh[\alpha(d-x')]\left(1+\frac{\omega}{\gamma}\tanh[\alpha(d-x')]\right)}{\omega\left(e^{\alpha d}+e^{-\alpha d}\frac{\gamma-\omega}{\gamma+\omega}\right)+\gamma\left(e^{\alpha d}-e^{-\alpha d}\frac{\gamma-\omega}{\gamma+\omega}\right)}\,, \tag{D.4f}$$

where

$$\omega=|\omega_\nu|\,,\qquad \alpha=|\omega_\nu|/v\,,\qquad \beta=|\omega_\nu|/v_F\,,\qquad \gamma=|\omega_\nu|/g_{LL}\,. \tag{D.5}$$

Appendix E

Generalised equation of motion

We want to write the equation of motion in presence of the perturbative potential

$$H_{\rm imp} = \frac{2}{a}\int dx V(x)\cos(2K_F x + 2\sqrt{\pi}\phi) \ . \tag{E.1}$$

The way to follow is the same as the one in Appendix C, with the difference that all the quantities have to be evaluated with respect to the total Hamiltonian, $\hat{H}_0 + \hat{H}_{\rm imp}$. Let us start from Eq. (C.5), and from the evaluation of the derivative. In Eq. (C.7), what has to be changed is the calculation of the commutator, which reads

$$[H,\phi] = [H_0,\phi] + [H_{\rm imp},\phi] = \frac{i\sqrt{\pi}}{m}\hat{p} + [H_{\rm imp},\phi] \ . \tag{E.2}$$

The commutator in the rhs of Eq. (E.2) reads

$$[H_{\rm imp},\phi] = \frac{1}{a}\int dx' V(x')\left\{\left[e^{i(2K_F x' + 2\sqrt{\pi}\phi_\prime)} + e^{-i(2K_F x' + 2\sqrt{\pi}\phi_\prime)},\phi\right]\right\} = 0 \ . \tag{E.3}$$

The commutator vanishes, since $\hat{\phi}$ commute with itself, and in general $[A, f(A)] = 0$. Then, the perturbative term does not give any contribution to the first derivative, and one gets the same expression as in Eq. (C.11).

One has to evaluate the second derivative. Let us evaluate the two terms in Eq. (C.12) separately. For the first one, Eq. (C.13), we need the value of the commutator $[H_{\rm imp},\hat{p}]$. It reads

$$[H_{\rm imp},\hat{p}] = \frac{1}{a}\int dx' V(x')\left\{e^{i(2K_F x')}\left[e^{i(2\sqrt{\pi}\phi_\prime)},\hat{p}\right] + e^{-i(2K_F x')}\left[e^{-i(2\sqrt{\pi}\phi_\prime)},\hat{p}\right]\right\} \ . \tag{E.4}$$

To evaluate the two commutators, one needs to use the relation of commutation between $\hat{\phi}$ and $\hat{p}$, and the following relation

$$[F(\phi_\prime), \hat{p}] = \frac{\partial F}{\partial \phi_\prime}[\phi_\prime, \hat{p}] \ . \tag{E.5}$$

By means of Eq. (E.5), one finds

$$\left[e^{i(2\sqrt{\pi}\phi_\prime)}, \hat{p}\right] = 2\pi n_0 e^{i(2\sqrt{\pi}\phi_\prime)}\delta(x - x') \ , \tag{E.6}$$

$$\left[e^{-i(2\sqrt{\pi}\phi_\prime)}, \hat{p}\right] = -2\pi n_0 e^{-i(2\sqrt{\pi}\phi_\prime)}\delta(x - x') \ . \tag{E.7}$$

By means of Eqs. (E.6) and (E.7), Eq. (E.4) can be written as

$$\begin{aligned} [H_{\rm imp}, \hat{p}] &= \frac{4\pi i}{a}\int dx' V(x') n_0 \sin(2K_F x' + 2\sqrt{\pi}\phi)\delta(x - x') \\ &= \frac{4\pi i}{a} V(x) n_0 \sin(2K_F x + 2\sqrt{\pi}\phi) \ . \end{aligned} \tag{E.8}$$

The latter equation allows to write Eq. (C.13) as

$$\begin{aligned} \partial_\tau \langle \hat{p}\phi_\prime\rangle\theta(\tau) &= \langle \hat{p}\phi_\prime\rangle\delta(\tau) + \theta(\tau)\Bigg\{ \frac{iV_0}{\sqrt{\pi}}\langle n_0 \nabla^2\phi(x)\phi_\prime\rangle \\ &\quad + \frac{i\pi^2}{m\sqrt{\pi}}\langle n_0 \nabla[n_0\nabla\phi]\phi_\prime\rangle \\ &\quad + \frac{4\pi i}{a} V(x) n_0 \langle \sin(2K_F x + 2\sqrt{\pi}\phi)\phi_\prime\rangle \Bigg\} \ . \end{aligned} \tag{E.9}$$

Developing the second term in Eq. (C.12), and using what we found for a clean wire

$$\begin{aligned} \partial_\tau \langle \phi_\prime \hat{p}\rangle\theta(-\tau) &= i\sqrt{\pi} n_0 \delta(x - x')\delta(\tau) - \langle \hat{p}\phi_\prime\rangle\delta(\tau) + \theta(-\tau)\Bigg\{ \frac{iV_0}{\sqrt{\pi}}\langle n_0 \nabla^2\phi(x)\phi_\prime\rangle \\ &\quad + \frac{i\pi^2}{m\sqrt{\pi}}\langle n_0 \nabla[n_0\nabla\phi]\phi_\prime\rangle \\ &\quad + \frac{4\pi i}{a} V(x) n_0 \langle \sin(2K_F x + 2\sqrt{\pi}\phi)\phi_\prime\rangle \Bigg\} \ . \end{aligned} \tag{E.10}$$

The sum of Eqs. (E.9) and (E.10) reads

$$\begin{aligned}\frac{\partial^2}{\partial\tau^2}G(x,x';\tau) &= -\Bigg\{\frac{\pi}{m}n_0\delta(x-x')\delta(\tau)+\frac{V_0}{m}n_0\nabla^2G(x,x';\tau)\\ &\quad+\frac{\pi^2}{m^2}n_0\nabla n_0\nabla G(x,x';\tau)+\frac{n_0^2\pi^2}{m^2}\nabla^2G(x,x';\tau)\\ &\quad+\frac{4\pi}{a}V(x)n_0\langle T_\tau^*\sin(2K_Fx+2\sqrt{\pi}\phi)\phi_\prime\rangle\Bigg\}\,. \end{aligned}\tag{E.11}$$

By means of Eq. (C.24), Eq. (E.11) can be written as

$$\begin{aligned}&\left\{\frac{1}{v(x)K(x)}\partial_\tau^2+\partial_x\left(\frac{v(x)}{K(x)}\partial_x\right)\right\}G_\phi=\\ &\quad-\delta(x-x')\delta(\tau)-\frac{4\sqrt{\pi}}{a}V(x)\langle T_\tau\sin(2K_Fx+2\sqrt{\pi}\phi)\phi_\prime\rangle\,.\end{aligned}\tag{E.12}$$

The latter equation represents the general equation of motion for the Green's function in time domain in presence of the perturbative potential Eq. (E.1).

Under the assumption of being able to evaluate the average in the rhs, Eq. (E.12) describes the evolution of the Green's function and of the whole system.

Appendix F

Second order correction in the perturbative potential

Let us start from Eq. (3.60) which in term of operator ϕ reads,

$$\begin{aligned}\langle T_\tau \sin(2K_F x + 2\sqrt{\pi}\phi)\phi_\prime\rangle^{(I)} = \\ = -\frac{2}{a}\int d\tau_3 dx_3 V(x_3)\langle T_\tau \sin(2K_F x_1 + 2\sqrt{\pi}\phi_1)\phi_2 \cos(2K_F x_3 + 2\sqrt{\pi}\phi_3)\rangle_0 \\ +\frac{2}{a}\int d\tau_3 dx_3 V(x_3)\langle\cos(2K_F x_3 + 2\sqrt{\pi}\phi_3)\rangle_0\langle T_\tau \sin(2K_F x_1 + 2\sqrt{\pi}\phi_1)\phi_2\rangle_0 .\end{aligned} \tag{F.1}$$

To evaluate the rhs of the latter equation, we need to evaluate the averages appearing in the integrals. The second average in the second integral in the rhs of Eq. (F.1) has been already evaluated in Eq. (3.47)

$$\langle T_\tau \sin(2K_F x_1 + 2\sqrt{\pi}\phi_1)\phi_2\rangle_0 = 2\sqrt{\pi}\cos(2K_F x_1) G(x_1,\tau_1;x_2,\tau_2) e^{-2\pi G(x_1,\tau_1;x_1,\tau_1)} \ . \tag{F.2}$$

We need to evaluate the term

$$\langle\cos(2K_F x_3 + 2\sqrt{\pi}\phi_3)\rangle_0 = \cos(2K_F x_3)\langle\cos(2\sqrt{\pi}\phi_3)\rangle_0 - \sin(2K_F x_3)\langle\sin(2\sqrt{\pi}\phi_3)\rangle_0 \ . \tag{F.3}$$

Writing the sin and cos function in terms of exponential function, and reminding that $\langle e^{\hat{B}}\rangle = e^{\frac{1}{2}\langle\hat{B}^2\rangle}$, one finds

$$\langle\cos(2K_F x_3 + 2\sqrt{\pi}\phi_3)\rangle_0 = e^{-2\pi G_{33}}\cos(2K_F x_3) \ . \tag{F.4}$$

The second integral in the rhs of Eq. (F.1) reads

$$\frac{4\sqrt{\pi}}{a}\int d\tau_3 dx_3 V(x_3) G_{12} e^{-2\pi(G_{11}+G_{33})}\cos(2K_F x_1)\cos(2K_F x_3)\ , \tag{F.5}$$

where $G_{12} = G(x_1,\tau_1;x_2,\tau_2)$.

The average in the first term in the rhs of Eq. (F.1) can be evaluated in a similar way

$$\begin{aligned}
&\langle T_\tau \sin(2K_F x_1 + 2\sqrt{\pi}\phi_1)\phi_2 \cos(2K_F x_3 + 2\sqrt{\pi}\phi_3)\rangle_0 = \\
&\quad \sin(2K_F x_1)\cos(2K_F x_3)\langle T_\tau \cos(2\sqrt{\pi}\phi_1)\phi_2 \cos(2\sqrt{\pi}\phi_3)\rangle_0 \\
&\quad - \sin(2K_F x_1)\sin(2K_F x_3)\langle T_\tau \cos(2\sqrt{\pi}\phi_1)\phi_2 \sin(2\sqrt{\pi}\phi_3)\rangle_0 \\
&\quad + \cos(2K_F x_1)\cos(2K_F x_3)\langle T_\tau \sin(2\sqrt{\pi}\phi_1)\phi_2 \cos(2\sqrt{\pi}\phi_3)\rangle_0 \\
&\quad - \cos(2K_F x_1)\sin(2K_F x_3)\langle T_\tau \sin(2\sqrt{\pi}\phi_1)\phi_2 \sin(2\sqrt{\pi}\phi_3)\rangle_0\ .
\end{aligned} \tag{F.6}$$

Among the four terms in the latter equation, the ones where the function inside is odd vanish. The other two ones can be evaluated in the usual way. Given the generating function

$$\langle T_\tau e^{i\lambda\phi_1} e^{i\mu\phi_2} e^{i\gamma\phi_3}\rangle = e^{-\frac{1}{2}(\lambda^2 G_{11}+\mu^2 G_{22}+\gamma^2 G_{33})} e^{-(\lambda\mu G_{12}+\lambda\gamma G_{13}+\mu\gamma G_{23})}\ , \tag{F.7}$$

each term in Eq. (F.6) can be written as a derivative of Eq. (F.7), with the correct values of λ, μ, and γ; one finds

$$\begin{aligned}
&\langle T_\tau \sin(2K_F x_1 + 2\sqrt{\pi}\phi_1)\phi_2 \cos(2K_F x_3 + 2\sqrt{\pi}\phi_3)\rangle_0 = \\
&\quad = \sqrt{\pi}\Big\{ (G_{12}+G_{23}) e^{-2\pi(G_{11}+G_{33}+2G_{13})}\cos[2K_F(x_1+x_3)] \\
&\quad + (G_{12}-G_{23}) e^{-2\pi(G_{11}+G_{33}-2G_{13})}\cos[2K_F(x_1-x_3)]\Big\}\ .
\end{aligned} \tag{F.8}$$

By means of Eqs. (F.5) and (F.8), the first order contribution in the perturbative

potential finally reads

$$\begin{aligned}
&\langle T_\tau \sin(2K_F x + 2\sqrt{\pi}\phi)\phi_{\prime}\rangle^{(I)} = \\
&\quad = -\frac{2\sqrt{\pi}}{a}\int d\tau_3 dx_3 V(x_3) \\
&\quad \times\Big\{ \left[G_{12}e^{-2\pi(G_{11}+G_{33})}\left[e^{-4\pi G_{13}}-1\right] + G_{23}e^{-2\pi(G_{11}+G_{33}+2G_{13})}\right]\cos[2K_F(x_1+x_3)] \\
&\quad + \left[G_{12}e^{-2\pi(G_{11}+G_{33})}\left[e^{4\pi G_{13}}-1\right] - G_{23}e^{-2\pi(G_{11}+G_{33}-2G_{13})}\right]\cos[2K_F(x_1-x_3)]\Big\} \\
&\quad = G^{(I)}(X_1,X_2)\ , \qquad\qquad (F.9)
\end{aligned}$$

where $X_i = (x_i, \tau_i)$.

Appendix G

Fluctuation propagator with tunneling

Our aim in this appendix is the analytical evaluation of the Cooper pair fluctuation propagator in presence of the tunneling. As we have seen in Sec. 5.5.2, the partition function can be written in terms of the action of the system, and the fluctuation propagator is represented by the coefficient of the second order term in the development in the field Δ and in the tunneling amplitude t. As already mentioned, the two terms to develop till the second order in Δ and t are

$$\exp\left\{\sum_i \int_0^\beta \left[-\Delta_i^*(\mathbf{r},\tau)P_i(\mathbf{r},\tau) - \Delta_i(\mathbf{r},\tau)P_i^\dagger(\mathbf{r},\tau)\right]\right\} , \tag{G.1}$$

and

$$\exp\{-H_T(\tau)\} . \tag{G.2}$$

where $P_i(\mathbf{r},\tau) = \Psi_{i\downarrow}(\mathbf{r},\tau)\Psi_{i\uparrow}(\mathbf{r},\tau)$. Using the kinetic term appearing in Eq. (5.41), $\exp\{-\int_0^\beta H_0(\tau)d\tau\}$, one can exploit the definition of mean value

$$\mathcal{Z}_0\langle A\rangle = \mathrm{Tr}\, \exp\{-H_0\} \tag{G.3}$$

where A is any physical quantity, to evaluate the non-vanishing contributions in the product of the terms coming out from Taylor's development of Eqs. (G.1) and (G.2).

Most of the terms gives no contribution since they are not diagonal. The only two ones which give a non-vanishing contribution are

$$\sum_{i,j,\sigma}[\Delta_i^*\Delta_j\Psi_{i,-\sigma}\Psi_{i,\sigma}\Psi^\dagger_{j,\sigma}\Psi^\dagger_{j,-\sigma}+\Delta_i\Delta_j^*\Psi^\dagger_{i,\sigma}\Psi^\dagger_{i,-\sigma}\Psi_{j,-\sigma}\Psi_{i,\sigma}]\ , \tag{G.4}$$

$$\left[\sum_{\substack{i,j,l\\m,a,b\\\sigma,\sigma',\sigma''}}\Delta_i^*\Delta_j t_{lm}t_{ab}\Psi_{i,-\sigma''}\Psi_{i,\sigma''}\Psi^\dagger_{j,\sigma''}\Psi^\dagger_{j,-\sigma''}\Psi^\dagger_{l\sigma}\Psi_{m\sigma}\Psi^\dagger_{a\sigma'}\Psi_{b\sigma'}\right.$$

$$\left.+\sum_{\substack{i,j,l\\m,a,b\\\sigma,\sigma',\sigma''}}\Delta_i\Delta_j^* t_{lm}t_{ab}\Psi^\dagger_{i,\sigma''}\Psi^\dagger_{i,-\sigma''}\Psi_{j-\sigma''}\Psi_{j,\sigma''}\Psi^\dagger_{l\sigma}\Psi_{m\sigma}\Psi^\dagger_{a\sigma'}\Psi_{b\sigma'}\right]\ . \tag{G.5}$$

The two latter expressions can be dealed by means of Wick's theorem to select correctly Green's functions. For the sake of clarity, as already done in Sec. 5.5.2, we write the effective action as in Eq. (5.43),

$$S_{eff}=S^0_{eff}+S^t_{eff}\ . \tag{G.6}$$

S^0_{eff} and S^t_{eff} describe the fluctuations in an isolated grain and the corrections due to tunneling, respectively. By means of Wick's theorem, Eq. (G.4) can be written as

$$\sum_{i,\sigma}[\Delta_i(\mathbf{r}_1,\tau_1)\Delta_i^*(\mathbf{r}_4,\tau_4)]G_{i,\sigma}(\mathbf{r}_4-\mathbf{r}_1,\tau_4-\tau_1)G_{i,-\sigma}(\mathbf{r}_4-\mathbf{r}_1,\tau_4-\tau_1)\ . \tag{G.7}$$

Then, the effective action for an isolated grain reads

$$S^0_{eff}=-\sum_{i,\sigma}\left[\frac{|\Delta_i(\mathbf{r}_1,\tau_1)|^2}{g}\right.$$

$$\left.-[\Delta_i(\mathbf{r}_1,\tau_1)\Delta_i^*(\mathbf{r}_4,\tau_4)+\text{H.c.}]G_{i,\sigma}(\mathbf{r}_4-\mathbf{r}_1,\tau_4-\tau_1)G_{i,-\sigma}(\mathbf{r}_4-\mathbf{r}_1,\tau_4-\tau_1)\right]. \tag{G.8}$$

where we took into account also the the first term in the sum in the second integral in the rhs of Eq. (5.41). If we suppose that the field Δ does not depend on space coordinates, by means of Fourier transform, Eq. (G.8) reads

$$S^0_{eff} = -\frac{T}{V}\sum_{\Omega_\mu} |\Delta_i(\Omega_\mu)|^2 \left[\frac{1}{g} - 4\pi\nu_F T\tau \sum_{2\varepsilon_n > \Omega_\mu} \lambda(\varepsilon_n, \varepsilon_{\mu-n})\right] . \tag{G.9}$$

$\lambda(\varepsilon_n, \varepsilon_{\mu-n})$ is the Cooperon, and the factor $1/V$ comes from the independence of the field Δ on space coordinates. Before evaluating analytically S^0_{eff}, let us see how the expression in Eq. (G.5) can be written. Such a term gives rise to the correction to fluctuation propagator due to tunneling. Using Wick's theorem, one can write, for instance

$$\langle T_\tau \Psi_{i\downarrow}\Psi_{i\uparrow}\Psi^\dagger_{j\uparrow}\Psi^\dagger_{j\downarrow}\Psi^\dagger_{l\uparrow}\Psi_{m\uparrow}\Psi^\dagger_{a\downarrow}\Psi_{b\downarrow}\rangle = -G_{i\uparrow}G_{i\downarrow}G_{j\uparrow}G_{j\downarrow} , \tag{G.10}$$

where we supposed that the tunneling process affects opposit-spin particles. In other words, Eq. (G.10) describes the physical situation where both particles tunnel from i-th grain to j-th grain without loosing their correlation. Then, Eq. (G.10) can be written as

$$\begin{aligned}\frac{1}{2}\sum_{i,j}[\Delta^*_i(\mathbf{r}_1,\tau_1)\Delta_j(\mathbf{r}_4,\tau_4) + \text{H.c.}]t_{ij}t^*_{ij}G_j(\mathbf{r}_4-\mathbf{r}_6,\tau_4-\tau_5) \\ \times G_j(\mathbf{r}_4-\mathbf{r}_3,\tau_4-\tau_2)G_i(\mathbf{r}_2-\mathbf{r}_1,\tau_2-\tau_1)G_i(\mathbf{r}_5-\mathbf{r}_1,\tau_5-\tau_1) ,\end{aligned} \tag{G.11}$$

where in the numerical prefactor we took into account the development coefficient, 1/16, the multiplicity of the physical process, 4, and the spin degeneracy. If a is the radius of a grain, then the tunneling element can be expressed as

$$t_{i(\mathbf{r}_1)j(\mathbf{r}_2)} = t_{ij}\int d\,\mathbf{a}\,\delta(|\mathbf{r}_1-\mathbf{a}|)\delta(\mathbf{r}_2-\mathbf{r}_1) , \tag{G.12}$$

where the latter expression means that the tunneling process happens between very

close points. In term of Fourier transform, just to give an example, Eq. (G.11) reads

$$\frac{1}{2}t^2T^6V^{-2}\sum_{i,j}\sum_{\Omega_{q_1},\Omega_{q_2}}[\Delta_i^*(\Omega_{q_1})\Delta_j(\Omega_{q_2})+\text{H.c.}]$$
$$\times\sum_{\varepsilon_1,\varepsilon_2\varepsilon_3,\varepsilon_4}\int\prod_{i=1}^{6}d\mathbf{r}_i d\tau_1 d\tau_2 d\tau_4 d\tau_5 d\mathbf{p}_1 d\mathbf{p}_2 d\mathbf{p}_3 d\mathbf{p}_4 d\mathbf{a} d\mathbf{a}' e^{i\mathbf{p}_1(\mathbf{r}_4-\mathbf{r}_6)}e^{i\mathbf{p}_2(\mathbf{r}_4-\mathbf{r}_3)}e^{i\mathbf{p}_3(\mathbf{r}_2-\mathbf{r}_1)}$$
$$\times e^{i\mathbf{p}_4(\mathbf{r}_5-\mathbf{r}_1)}e^{i\tau_1\Omega_{q_1}}e^{-i\tau_4\Omega_{q_2}}e^{-i\varepsilon_1(\tau_4-\tau_5)}e^{-i\varepsilon_2(\tau_4-\tau_2)}e^{-i\varepsilon_3(\tau_2-\tau_1)}e^{-i\varepsilon_4(\tau_5-\tau_1)}\delta(|\mathbf{r}_2-\mathbf{a}|)$$
$$\times\delta(|\mathbf{r}_5-\mathbf{a}'|)\delta(\mathbf{r}_2-\mathbf{r}_3)\delta(\mathbf{r}_5-\mathbf{r}_6)G_j(\mathbf{p}_1,\varepsilon_1)G_j(\mathbf{p}_2,\varepsilon_2)G_i(\mathbf{p}_3,\varepsilon_3)G_i(\mathbf{p}_4,\varepsilon_4)\,. \quad \text{(G.13)}$$

The evaluation of the latter equation reads

$$\frac{z}{2}\sum_{i,j}\sum_{\Omega_q,\varepsilon_n}[\Delta_i^*(\Omega_q)\Delta_j(\Omega_q)+\text{H.c.}]t^2T^2$$
$$\times\int d\mathbf{p}_i d\mathbf{p}_j G(\mathbf{p}_j,\varepsilon_n)G(\mathbf{p}_j,-\varepsilon_n)G(\mathbf{p}_i,-\varepsilon_n)G(\mathbf{p}_i,\varepsilon_n)\lambda^2(\varepsilon_n,\Omega_q-\varepsilon_n)\,, \quad \text{(G.14)}$$

and it corresponds to the diagram in Fig. 5.8(a)

In the same identical way, one can evaluate the contribution corresponding to the physical processes where just one electron tunnel back and forth from one grain to another, Fig. 5.8(b+c)

$$z\sum_i[\Delta_i^*(\mathbf{r}_1,\tau_1)\Delta_i(\mathbf{r}_4,\tau_4)+\text{H.c.}]t_{ij}t_{ij}^*G_i(\mathbf{r}_4-\mathbf{r}_1,\tau_4-\tau_1)$$
$$\times G_i(\mathbf{r}_4-\mathbf{r}_3,\tau_4-\tau_2)G_i(\mathbf{r}_5-\mathbf{r}_1,\tau_5-\tau_1)G_j(\mathbf{r}_2-\mathbf{r}_6,\tau_2-\tau_5)\,, \quad \text{(G.15)}$$

where we took into account the multiplicity due to equivalent diagram, represented by the H.c., and z is the correlation number, that is the number of the nearest neighbours. Performing again the Fourier transform, one gets

$$z\sum_i\sum_{\Omega_q,\varepsilon_n}[\Delta_i^*(\Omega_q)\Delta_i(\Omega_q)+\text{H.c.}]t^2T^2$$
$$\times\int d\mathbf{p}_i dp_j G(\mathbf{p}_i,\varepsilon_n)G(\mathbf{p}_i,-\varepsilon_n)G(\mathbf{p}_i,-\varepsilon_n)G(\mathbf{p}_j,-\varepsilon_n)\lambda^2(\varepsilon_n,\Omega_q-\varepsilon_n)\,. \quad \text{(G.16)}$$

To resume

$$S_{eff}^{t,(a)} = \frac{z}{2}\sum_{i,j}\sum_{\Omega_q,\varepsilon_n}[\Delta_i^*(\Omega_q)\Delta_j(\Omega_q) + \text{H.c.}]t^2T^2$$
$$\times \int d\mathbf{p}_i d\mathbf{p}_j G(\mathbf{p}_j,\varepsilon_n)G(\mathbf{p}_j,-\varepsilon_n)G(\mathbf{p}_i,-\varepsilon_n)G(\mathbf{p}_i,\varepsilon_n)\lambda^2(\varepsilon_n,\Omega_q-\varepsilon_n) \quad \text{(G.17)}$$

$$S_{eff}^{t,(b+c)} = z\sum_{i}\sum_{\Omega_q,\varepsilon_n}[\Delta_i^*(\Omega_q)\Delta_i(\Omega_q) + \text{H.c.}]t^2T^2$$
$$\times \int d\mathbf{p}_i d\mathbf{p}_j G(\mathbf{p}_i,\varepsilon_n)G(\mathbf{p}_i,-\varepsilon_n)G(\mathbf{p}_i,-\varepsilon_n)G(\mathbf{p}_j,-\varepsilon_n)\lambda^2(\varepsilon_n,\Omega_q-\varepsilon_n) \quad \text{(G.18)}$$

$$S_{eff}^{0} = -\frac{T}{V}\sum_{\Omega_\mu}|\Delta_i(\Omega_\mu)|^2\left[\frac{1}{g} - 4\pi\nu_F T\tau\sum_{2\varepsilon_n>\Omega_\mu}\lambda(\varepsilon_n,\varepsilon_{\mu-n})\right]. \quad \text{(G.19)}$$

Appendix H

Analytical evaluation of effective action

Let us start with $S_{eff}^{t,(a)}$. First, we have to evaluate the integral

$$\int d\mathbf{p}_i d\mathbf{p}_j G(\mathbf{p}_j,\varepsilon_n)G(\mathbf{p}_j,-\varepsilon_n)G(\mathbf{p}_i,-\varepsilon_n)G(\mathbf{p}_i,\varepsilon_n) = \left[\int d\mathbf{p}_i G(\mathbf{p}_i,-\varepsilon_n)G(\mathbf{p}_i,\varepsilon_n)\right]^2 , \tag{H.1}$$

in the diffusive limit, $\varepsilon_n \ll 1/\tau$. Using Cauchy's Theorem, one gets easily

$$\left[\int d\mathbf{p}_i G(\mathbf{p}_i,-\varepsilon_n)G(\mathbf{p}_i,\varepsilon_n)\right]^2 = (2\pi\nu_F\tau)^2 , \tag{H.2}$$

Then, one has to evaluate the sum

$$\sum_{\varepsilon_n} \lambda^2(\varepsilon_n,\Omega_q-\varepsilon_n) = \frac{1}{\tau^2}\sum_{\varepsilon_n}\frac{1}{(|2\varepsilon_n-\Omega_q|+Dq^2)^2} , \tag{H.3}$$

By considering individually the case of positive and negative values of ε_n, the sum can be written as

$$\sum_{\varepsilon_n}\frac{1}{(|2\varepsilon_n-\Omega_q|+Dq^2)^2} = 2\sum_{\varepsilon_n>0}\frac{1}{(2\varepsilon_n+Dq^2)^2} , \tag{H.4}$$

where we just considered the static approximation, $\Omega_q \to 0$. Since the sum diverges, one first considers a finite sum and then its asymptotic behavior.

$$\sum_{\varepsilon_n>0}^{M}\frac{1}{(2\varepsilon_n+Dq^2)^2} = -\sum_{\varepsilon_n>0}^{M}\frac{\partial}{\partial(Dq^2)}\left(\frac{1}{2\varepsilon_n+Dq^2}\right) . \tag{H.5}$$

The sum is known, and latter expression reads

$$-\sum_{\varepsilon_n>0}^{M}\frac{\partial}{\partial(Dq^2)}\left(\frac{1}{2\varepsilon_n+Dq^2}\right)=-\frac{1}{(4\pi T)^2}\left\{\Psi'\left(\frac{1}{2}+\frac{Dq^2}{4\pi T}+M\right)-\Psi'\left(\frac{1}{2}+\frac{Dq^2}{4\pi T}\right)\right\}\ . \tag{H.6}$$

Taking the limit as $M\to 0$, since $\Psi'(x)\overset{x\to\infty}{\to}1/2x$ then, definetively, in the static approximation,

$$\sum_{\varepsilon_n}\lambda^2(\varepsilon_n,\Omega_q-\varepsilon_n)=\frac{2}{(4\pi\tau T)^2}\Psi'\left(\frac{1}{2}+\frac{Dq^2}{4\pi T}\right)\ . \tag{H.7}$$

Then, the effective action for two-particles tunnelling reads

$$S_{eff}^{t,(a)}=\frac{1}{4}(\nu_F t)^2\sum_{i,j}\sum_{\Omega_q}[\Delta_i^*(\Omega_q)\Delta_j(\Omega_q)+\text{H.c.}]\Psi'\left(\frac{1}{2}+\frac{Dq^2}{4\pi T}\right)\ . \tag{H.8}$$

Now, we consider the representation in FT of the field Δ, too. First,

$$\Delta_i(\Omega_q)=\sum_{\mathbf{K}}\Delta_{\mathbf{K}}(\Omega_q)e^{i\mathbf{R}_i\cdot\mathbf{K}}\ , \tag{H.9}$$

Then, one can write

$$\sum_{i,j}[\Delta_i^*(\Omega_q)\Delta_j(\Omega_q)]=\sum_{ij}\sum_{\mathbf{K}_i,\mathbf{K}_j}\Delta_{\mathbf{K}_i}^*\Delta_{\mathbf{K}_j}e^{i\mathbf{R}_i\cdot(\mathbf{K}_j-\mathbf{K}_i)}e^{i\delta\cdot\mathbf{K}_j}\ , \tag{H.10}$$

with $\mathbf{R}_j=\mathbf{R}_i+\mathbf{a}$, $\mathbf{a}$ being the vector conneting the center of two close grains. Then,

$$\sum_{i,j}[\Delta_i^*(\Omega_q)\Delta_j(\Omega_q)]=z\sum_{\mathbf{K}}\gamma_{\mathbf{K}}\Delta_{\mathbf{K}}^*\Delta_{\mathbf{K}}\ , \tag{H.11}$$

where $\gamma_{\mathbf{K}}$ is the structure factor, defined as $\gamma_{\mathbf{K}}=z^{-1}\sum_{\mathbf{a}}e^{i\mathbf{K}\cdot\mathbf{a}}$

Then, one can write the contribution, Eq. (G.17), as

$$S_{eff}^{t,(a)}=\frac{z}{2}(\nu_F t)^2\Psi'\left(\frac{1}{2}+\frac{Dq^2}{4\pi T}\right)\sum_{\mathbf{K},\Omega_q}\gamma_{\mathbf{K}}|\Delta_{\mathbf{K}}|^2\ . \tag{H.12}$$

In the same identical way, we can evaluate the contribution given by Eq. (G.18). In this case, of course, the integral to evaluate is

$$\int d\mathbf{p}_i G(\mathbf{p}_i,\varepsilon_n)G(\mathbf{p}_i,-\varepsilon_n)G(\mathbf{p}_i,-\varepsilon_n)\int d\mathbf{p}_j G(\mathbf{p}_j,-\varepsilon_n)\ . \tag{H.13}$$

The second integral in last expression can be easily evaluated and it reads $-i\pi\nu_F \,\mathrm{sgn}(\varepsilon_n)$. Evaluating by means of Cauchy's theorem the first one, one gets, for the whole integral in Eq. (H.13), $-2(\pi\nu_F\tau)^2$. The sum appearing in Eq. (G.18) has been already evaluated, Eq. (H.7). Then, using the FT on the field Δ, the action taking into account the tunnelling between grains is

$$S_{eff}^{t,(b+c)} = -\frac{z}{2}(\nu_F t)^2 \Psi'\left(\frac{1}{2}+\frac{Dq^2}{4\pi T}\right)\sum_{\mathbf{K},\Omega_q}|\Delta_{\mathbf{K}}|^2 \,. \tag{H.14}$$

We can finally write the expression for the action S_{eff}^t,

$$S_{eff}^t = -\left(\frac{2}{\pi}\right)^2 \frac{z g_T}{2V^2}\Psi'\left(\frac{1}{2}+\frac{Dq^2}{4\pi T}\right)\sum_{\Omega_q}(1-\gamma_{\mathbf{K}})|\Delta_{\mathbf{K}}|^2 \,, \tag{H.15}$$

where g_T is the dimensionless conductance, $g_T = (\pi t/2\delta)^2$.

Now, in order to get the expression of propagator, we have to evaluate S_{eff}^0, Eq. (G.19). The only thing we need to evaluate this contribution is the sum over a single Cooperon. It can be performed in the same way as before, with the only difference that the upper limit of the sum will be Debye's energy. In the static approximation, one gets

$$\sum_{2\varepsilon_n>|\Omega_q|}\lambda(\varepsilon_n,\Omega_q-\varepsilon_n) = \frac{2}{\tau}\frac{1}{4\pi T}\left\{\Psi\left(\frac{1}{2}+\frac{Dq^2}{4\pi T}+\frac{\omega_D}{4\pi T}\right)-\Psi\left(\frac{1}{2}+\frac{Dq^2}{4\pi T}\right)\right\} \,, \tag{H.16}$$

Since the critical temperature is defined as the value of T for which the propagator has a pole, from the expression of fluctuation propagator inside a grain, on gets

$$\frac{1}{g} = \nu_F\left[\log\frac{\omega_D}{2\pi T_C} - \Psi\left(\frac{1}{2}\right)\right] \,. \tag{H.17}$$

Replacing latter expression in Eq. (G.19), and using Eq. (H.16), one gets for the action

$$S_{eff}^0 = -\frac{\nu_F T}{V}\sum_{\Omega_q,\mathbf{K}}\left[\log\frac{T}{T_C}+\Psi\left(\frac{1}{2}+\frac{Dq^2}{4\pi T}\right)-\Psi\left(\frac{1}{2}\right)\right]|\Delta_{\mathbf{K}}|^2 \,, \tag{H.18}$$

where we Fourier tranformed the field Δ, as usual.

Finally, from Eqs. (H.15) and (H.18), we can write the full expression of the

propagator, which reads

$$L_{\mathbf{K}}(\Omega_\mu) = -\nu_F^{-1}\Bigg\{ \left[\log\frac{T}{T_C} + \Psi\left(\frac{1}{2}+\frac{Dq^2}{4\pi T}\right) - \Psi\left(\frac{1}{2}\right)\right] + \left(\frac{2}{\pi}\right)^2 \frac{z g_T E_T}{2 g_0 T}\Psi'\left(\frac{1}{2}+\frac{Dq^2}{4\pi T}\right)(1-\gamma_{\mathbf{K}})\Bigg\}^{-1}. \tag{H.19}$$

In the limit of zero dimensional grain, $Dq^2 = 0$, from Eq. (H.19) one obtains the expression of the Cooper pair fluctuation propagator used in Eq. (5.50), where we did not take the static limit yet.

Appendix I

DOS correction without tunneling

In this appendix, we want to show how to evaluate the DOS correction to thermal conductivity for a granular metal without considering the tunneling: the correction we will evaluate is just given by the renormalization of the density of states due to pairing processes which do not involve tunneling.

The aim of this appendix is above all showing some calculations techniques which will allow to evaluate the results we have presented in the previous chapters.

We start from Fig. 5.9(a), for which the response function reads

$$\mathcal{Q}^{(DOS)}(\omega_\nu) = T^2 t^2 a^2 \sum_j \sum_{\Omega_\mu} L_{ij}(\Omega_\mu)\, \Sigma(\Omega_\mu, \omega_\nu) \ . \tag{I.1}$$

Eq. (I.1) is already written in the limit of zero dimensional grains. In the following, often this limit is considered just at the end of calculations; this because some mathematical steps can be easier to perform. Then, the limit will be performed at the end.

In Eq. (I.1)

$$\Sigma(\Omega_\mu, \omega_\nu) = \sum_{\varepsilon_n} (\varepsilon_n + \varepsilon_{n+\nu})^2\, \lambda^2(\varepsilon_{n+\nu}, \varepsilon_{-n-\nu+\mu})\, I(\varepsilon_n, \Omega_\mu, \omega_\nu) \ , \tag{I.2}$$

and

$$I(\varepsilon_n, \Omega_\mu, \omega_\nu) = \int (dp)\, G^2(\mathbf{p}, \varepsilon_{n+\nu})\, G(\mathbf{p}, \varepsilon_{-n-\nu+\mu}) \int (dp')\, G(\mathbf{p}', \varepsilon_n) \, . \tag{I.3}$$

By means of Cauchy's theorem, one gets

$$\int \frac{d\mathbf{p}'}{(2\pi)^3} G(\mathbf{p}', \varepsilon_n) = -i\pi\nu_F \,\mathrm{sgn}(\varepsilon_n) \;, \tag{I.4}$$

$$\begin{aligned} &\int \frac{d\mathbf{p}}{(2\pi)^3} G^2(\mathbf{p}, \varepsilon_n + \omega_\nu) G(\mathbf{q}-\mathbf{p}, \Omega_\mu - \varepsilon_n - \omega_\nu) \\ &\quad = \left[I_1'(\varepsilon_n > 0) + I_2'(\varepsilon_n < 0, \varepsilon_n + \omega_\nu > 0) + I_3'(\varepsilon_n < 0, \varepsilon_n + \omega_\nu < 0) \right] . \end{aligned} \tag{I.5}$$

with

$$I_1' = -2i\pi\nu_F\tau^2 \;, \qquad I_2' = -2i\pi\nu_F\tau^2 \;, \qquad I_3' = 2i\pi\nu_F\tau^2 \;. \tag{I.6}$$

The product of two integrals reads

$$I(\varepsilon_n, \Omega_\mu, \omega_\nu) = \left[I_1(\varepsilon_n > 0) + I_2(\varepsilon_n < 0, \varepsilon_n + \omega_\nu > 0) + I_3(\varepsilon_n < 0, \varepsilon_n + \omega_\nu < 0) \right] , \tag{I.7}$$

with

$$I_1 = -2(\pi\nu_F\tau)^2 \;, \qquad I_2 = 2(\pi\nu_F\tau)^2 \;, \qquad I_3 = -2(\pi\nu_F\tau)^2 \;. \tag{I.8}$$

We can write $\Sigma(\Omega_\mu, \omega_\nu)$ as a sum of three terms $\Sigma_1 + \Sigma_2 + \Sigma_3$, with

$$\Sigma_1 = -2(\pi\nu_F)^2 T \sum_{\varepsilon_n > 0} \frac{(2\varepsilon_n + \omega_\nu)^2}{(2\varepsilon_n + 2\omega_\nu + Dq^2)^2} \;, \tag{I.9}$$

$$\Sigma_2 = 2(\pi\nu_F)^2 T \sum_{0 < \varepsilon_n < \omega_\nu} \frac{(2\varepsilon_n - \omega_\nu)^2}{(2\varepsilon_n + Dq^2)^2} \;, \tag{I.10}$$

$$\Sigma_3 = -2(\pi\nu_F)^2 T \sum_{\varepsilon_n > 0} \frac{(2\varepsilon_n + \omega_\nu)^2}{(2\varepsilon_n + Dq^2)^2} \;, \tag{I.11}$$

where we just wrote the second and third sum differently, by exploiting conditions on the signs of ε_n in Eq. (I.7). Now, we show briefly how the sum can be performed, since Σ_1 and Σ_3 diverge. First of all, let us write $\Sigma_1 = -2(\pi\nu_F)^2 T S_1$ and $\Sigma_3 = -2(\pi\nu_F)^2 T S_3$, and we want to evaluate S_1 and S_3. They can be written as

$$S_1 = \sum_{\varepsilon_n > 0} \left[1 + \frac{(\omega_\nu + Dq^2)^2}{(2\varepsilon_n + 2\omega_\nu + Dq^2)^2} - \frac{2(\omega_\nu + Dq^2)}{(2\varepsilon_n + 2\omega_\nu + Dq^2)} \right] \;, \tag{I.12}$$

$$S_3 = \sum_{\varepsilon_n > 0} \left[1 + \frac{(\omega_\nu - Dq^2)^2}{(2\varepsilon_n + Dq^2)^2} + \frac{2(\omega_\nu - Dq^2)}{(2\varepsilon_n + Dq^2)} \right] \;, \tag{I.13}$$

The first two terms in the sum are purely real, then they give no contributions to conductivity, and we will no longer consider them. The other terms can be grouped like

$$
\begin{aligned}
- \quad & 2\omega_\nu \sum_{\varepsilon_n>0} \left(\frac{1}{2\varepsilon_n + 2\omega_\nu + Dq^2} - \frac{1}{2\varepsilon_n + Dq^2} \right) - 2Dq^2 \sum_{\varepsilon_n>0} \left(\frac{1}{2\varepsilon_n + 2\omega_\nu + Dq^2} \right. \\
+ \quad & \left. \frac{1}{2\varepsilon_n + Dq^2} \right) + 2\omega_\nu Dq^2 \sum_{\varepsilon_n>0} \left(\frac{1}{(2\varepsilon_n + 2\omega_\nu + Dq^2)^2} - \frac{1}{(2\varepsilon_n + Dq^2)^2} \right) \\
+ \quad & (\omega_\nu^2 + (Dq^2)^2) \sum_{\varepsilon_n>0} \left(\frac{1}{(2\varepsilon_n + 2\omega_\nu + Dq^2)^2} + \frac{1}{(2\varepsilon_n + Dq^2)^2} \right) . \qquad \text{(I.14)}
\end{aligned}
$$

The way we have written last expression allows us to evaluate correctely the sums, paying attention to the problems of convergence. Using the definition of digamma function, [Larkin04], the four terms can be evaluated as

$$
\begin{aligned}
- \quad & \frac{2\omega_\nu}{4\pi T} \left[\Psi\left(\frac{1}{2} + \frac{Dq^2}{4\pi T} \right) - \Psi\left(\frac{1}{2} + \frac{\omega_\nu}{2\pi T} + \frac{Dq^2}{4\pi T} \right) \right] \qquad \text{(I.15)} \\
- \quad & 2\frac{Dq^2}{4\pi T} \lim_{\Lambda\to\infty} \left[\Psi\left(\frac{1}{2} + \frac{\omega_\nu}{2\pi T} + \frac{Dq^2}{4\pi T} + \Lambda \right) - \Psi\left(\frac{1}{2} + \frac{\omega_\nu}{2\pi T} + \frac{Dq^2}{4\pi T} \right) \right. \\
+ \quad & \left. \Psi\left(\frac{1}{2} + \frac{Dq^2}{4\pi T} + \Lambda \right) - \Psi\left(\frac{1}{2} + \frac{Dq^2}{4\pi T} \right) \right] + \frac{2\omega_\nu Dq^2}{(4\pi T)^2} \left[\Psi'\left(\frac{1}{2} + \frac{\omega_\nu}{2\pi T} + \frac{Dq^2}{4\pi T} \right) \right. \\
- \quad & \left. \Psi'\left(\frac{1}{2} + \frac{Dq^2}{4\pi T} \right) \right] + \frac{\omega_\nu^2 + (Dq^2)^2}{(4\pi T)^2} \left[\Psi'\left(\frac{1}{2} + \frac{\omega_\nu}{2\pi T} + \frac{Dq^2}{4\pi T} \right) + \Psi'\left(\frac{1}{2} + \frac{Dq^2}{4\pi T} \right) \right] .
\end{aligned}
$$

The third and the fourth term in Eq. (I.14) have been evaluated as in Eq. (H.5).

By performing analitycal continuation $\omega_\nu \to -i\omega$, and taking the limit as $\omega \to 0$,

one gets

$$\begin{aligned}
\Sigma_1+\Sigma_3 = -\frac{\pi\nu^2}{2}\Bigg\{ & -\frac{\omega^2}{\pi T}\Psi'\left(\frac{1}{2}+\frac{Dq^2}{4\pi T}\right) - 2Dq^2 \lim_{\Lambda\to\infty}\Bigg[\Psi\left(\frac{1}{2}+\frac{Dq^2}{4\pi T}+\Lambda\right) \\
- & \Psi'\left(\frac{1}{2}+\frac{Dq^2}{4\pi T}+\Lambda\right)\frac{i\omega}{2\pi T} - \Psi\left(\frac{1}{2}+\frac{Dq^2}{4\pi T}\right) + \Psi'\left(\frac{1}{2}+\frac{Dq^2}{4\pi T}\right)\frac{i\omega}{2\pi T} \\
+ & \Psi\left(\frac{1}{2}+\frac{Dq^2}{4\pi T}+\Lambda\right) - \Psi\left(\frac{1}{2}+\frac{Dq^2}{4\pi T}\right)\Bigg] - \frac{2i\omega Dq^2}{4\pi T}\Bigg[\Psi'\left(\frac{1}{2}+\frac{Dq^2}{4\pi T}\right) \\
- & \Psi''\left(\frac{1}{2}+\frac{Dq^2}{4\pi T}\right)\frac{i\omega}{2\pi T} - \Psi'\left(\frac{1}{2}+\frac{Dq^2}{4\pi T}\right)\Bigg] + \frac{(Dq^2)^2-\omega^2}{4\pi T}\Bigg[\Psi'\left(\frac{1}{2}+\frac{Dq^2}{4\pi T}\right) \\
- & \Psi''\left(\frac{1}{2}+\frac{Dq^2}{4\pi T}\right)\frac{i\omega}{2\pi T} + \Psi'\left(\frac{1}{2}+\frac{Dq^2}{4\pi T}\right)\Bigg]\Bigg\} . \qquad \text{(I.16)}
\end{aligned}$$

The only non vanishing contributions are the ones which are linear in ω; then, neglecting the purely real terms, Eq. (I.16) reads

$$\Sigma_1+\Sigma_3 = -\frac{\pi\nu_F^2}{2}\Bigg\{ -\frac{i\omega}{\pi T}\Psi'\left(\frac{1}{2}+\frac{Dq^2}{4\pi T}\right)Dq^2 - \frac{i\omega}{8(\pi T)^2}\Psi''\left(\frac{1}{2}+\frac{Dq^2}{4\pi T}\right)(Dq^2)^2\Bigg\} . \qquad \text{(I.17)}$$

In the limit of zero dimensional grains, Dq^2 goes to zero, and the second term in latter expression is negligeable with respect the first one. Finally, the sum reads

$$\Sigma_1+\Sigma_3 = \frac{i\omega\nu_F^2}{2T}Dq^2\Psi'\left(\frac{1}{2}+\frac{Dq^2}{4\pi T}\right) . \qquad \text{(I.18)}$$

From Eq.(I.10), $\Sigma_2 = 2(\pi\nu_F)^2 T S_2$, and we want to evaluate S_2. As we did above, it can be written as

$$S_2 = \sum_{0<\varepsilon_n<\omega_\nu}\left[1+\frac{(\omega_\nu+Dq^2)^2}{(2\varepsilon_n+Dq^2)^2} - \frac{2(\omega_\nu+Dq^2)}{2\varepsilon_n+Dq^2}\right] . \qquad \text{(I.19)}$$

Of course, S_2 converges since it is finite. The first term in the sum just gives $\omega_\nu/2\pi T$. The seconde one reads

$$\begin{aligned}\sum_{0<\varepsilon_n<\omega_\nu}\frac{(\omega_\nu+Dq^2)^2}{(2\varepsilon_n+Dq^2)^2} &= -\frac{(\omega_\nu+Dq^2)^2}{4\pi T}\frac{\partial}{\partial(Dq^2)}\left[\Psi\left(\frac{1}{2}+\frac{\omega_\nu}{2\pi T}+\frac{Dq^2}{4\pi T}\right)\right.\\ &- \left.\Psi\left(\frac{1}{2}+\frac{Dq^2}{4\pi T}\right)\right]\\ &= -\frac{-\omega^2+(Dq^2)^2-i2\omega Dq^2}{(4\pi T)^2}\left[\Psi'\left(\frac{1}{2}-\frac{i\omega}{2\pi T}+\frac{Dq^2}{4\pi T}\right)\right.\\ &- \left.\Psi'\left(\frac{1}{2}+\frac{Dq^2}{4\pi T}\right)\right]\\ &= \frac{i\omega(Dq^2)^2}{2^4(\pi T)^3}\Psi''\left(\frac{1}{2}+\frac{Dq^2}{4\pi T}\right)\ , \end{aligned} \tag{I.20}$$

where we performed analytical continuation, developed over small ω, and took only contributing terms. Staightforward, one can evaluate the third term in Eq.(I.19). Finally, under the assumption $Dq^2 \to 0$,

$$\Sigma_2 \simeq 2(\pi\nu)^2 T\left[-\frac{i\omega}{2\pi T}\right]\ , \tag{I.21}$$

and the Eq.(I.2), in the limit of zero dimensional grains, turns out to be, by means of Eqs.(I.18) and (I.21)

$$\Sigma(q,\Omega_k,\omega_\nu) = -i\pi\omega\nu_F^2\ . \tag{I.22}$$

Finally, we can evaluate the response function, Eq.(I.1), where the fluctuation propagator, in diffusive regime and in the static approximation, $\Omega_\mu = 0$, reads

$$L^{-1}(\Omega_\mu=0) = -\nu_F\left[\ln\frac{T}{T_C}\right]\ . \tag{I.23}$$

The response function will read

$$Q(\omega) = -\frac{zTt^2a^2}{\nu_F}\left[-i\pi\omega\nu_F^2\frac{1}{\log(T/T_C)}\right]\ . \tag{I.24}$$

Then, by considering the topologically equivalent diagram, the correction to thermal conductivity given by the diagram in Fig. 5.9(a) is

$$\begin{aligned} \delta k_1^{DOS} &= \lim_{\omega\to 0} \frac{Q(i\omega_\nu)}{T\omega_\nu}\bigg|_{i\omega_\nu\to\omega+i\eta} \\ &= -2\pi\nu t^2 a^2 [\ln(T/T_C)]^{-1} \ . \end{aligned} \tag{I.25}$$

If one defines the dimensionless tunnelling conductance as $g_T = (\pi t/2\delta)^2$, and $\kappa_0 = 8g_T T a^2/3\pi$ is the thermal conductivity for the granular sample, then Eq.(I.25) can be written as

$$\frac{\delta k^{DOS}}{k_0} = -\frac{3}{\pi^2}\frac{1}{g_T}\frac{g_T\delta}{T_c}[\ln(T/T_C)]^{-1} \ . \tag{I.26}$$

Appendix J

Maki-Thompson correction

As we have seen in Sec. 5.6.2, the linear response operator corresponding to diagram in Fig. 5.9(b) reads

$$\mathcal{Q}^{(MT)}\left(\omega_\nu\right) = T^2 t^2 a^2 \sum_j \sum_{\Omega_\mu} L_{ij}\left(\Omega_\mu\right) \Sigma\left(\Omega_\mu, \omega_\nu\right) \ , \tag{J.1}$$

where

$$\Sigma\left(\Omega_\mu, \omega_\nu\right) = \sum_{\varepsilon_n} \left(\varepsilon_n + \varepsilon_{n+\nu}\right)^2 \lambda\left(\varepsilon_{n+\nu}, \varepsilon_{-n-\nu+\mu}\right) \lambda\left(\varepsilon_n, \varepsilon_{-n+\mu}\right) I\left(\varepsilon_n, \Omega_\mu, \omega_\nu\right) \ , \tag{J.2}$$

and

$$\begin{aligned} & I\left(\varepsilon_n, \Omega_\mu, \omega_\nu\right) \\ & \quad = \int (dp)\, G_0\left(\mathbf{p}, \varepsilon_{n+\nu}\right) G_0\left(\mathbf{p}, \varepsilon_{-n-\nu+\mu}\right) \int (dp')\, G_0\left(\mathbf{p}', \varepsilon_n\right) G_0\left(\mathbf{p}', \varepsilon_{-n+\mu}\right) . \end{aligned} \tag{J.3}$$

Both integrals in Eq. (J.3) read $2\pi\nu_F\tau$, and the sums to evaluate are

$$\Sigma_1 = (2\pi\nu_F)^2 T \sum_{\varepsilon_n > 0} \frac{(2\varepsilon_n + \omega_\nu)^2}{(2\varepsilon_n + 2\omega_\nu) 2\varepsilon_n} \ , \tag{J.4a}$$

$$\Sigma_2 = (2\pi\nu_F)^2 T \sum_{0 < \varepsilon_n < \omega_\nu} \frac{(2\varepsilon_n - \omega_\nu)^2}{2\varepsilon_n(-2\varepsilon_n + 2\omega_\nu)} \ , \tag{J.4b}$$

$$\Sigma_3 = (2\pi\nu_F)^2 T \sum_{\varepsilon_n > 0} \frac{(2\varepsilon_n + \omega_\nu)^2}{(2\varepsilon_n + 2\omega_\nu) 2\varepsilon_n} \ . \tag{J.4c}$$

The sums can be performed in the same way as we have seen before in the limit of zero dimensional grains. Σ_1 and Σ_3 just give real contributions, while one finds

$$\Sigma_2 = i2\pi\nu_F^2\omega \ . \tag{J.5}$$

Then, in the static limit, the response function in Eq. (J.1) reads

$$Q(\omega) = i2\pi(at\nu_F)^2\omega T\sum_j L_{ij}(\Omega_\mu = 0) \ . \tag{J.6}$$

To evaluate the sum in the latter equation, we consider the expression of the Cooper pair fluctuation propagator given in Eq. (5.50)

$$L_{\mathbf{K}}\left(\Omega_\mu\right) = -\frac{1}{\nu_F}\frac{1}{\ln\frac{T}{T_c} + \frac{\pi|\Omega_\mu|}{8T_c} + z\frac{g_T\delta}{T_c}\left(1-\gamma_{\mathbf{K}}\right)}. \tag{J.7}$$

By means of Fourier transform,

$$L_{ij} = \sum_{\mathbf{K}} e^{i\mathbf{R}_{ij}\cdot\mathbf{K}} L_{\mathbf{K}} \ , \tag{J.8}$$

where $\mathbf{R}_{ij}$ is the vector between two sites. Then

$$\sum_{\langle i,j\rangle} L_{ij} = -\frac{1}{\nu}\sum_{\langle i,j\rangle}\sum_{\mathbf{K}}\frac{e^{i(\mathbf{R}_i-\mathbf{R}_j)\cdot\mathbf{K}}}{\varepsilon + z\frac{g_T\delta}{T_c}(1-\gamma_{\mathbf{K}})} \ . \tag{J.9}$$

For MT ones $\mathbf{R}_{ij} = \mathbf{a}$, $\mathbf{a}$ being the distance between two sites. From the linear response operator in Eq. (J.6), the MT correction reads

$$\frac{\delta\kappa^{(MT)}}{\kappa_0} = \frac{3}{\pi^2}\frac{1}{g_T}\frac{g_T\delta}{T_c}\int_{BZ}(dK)\frac{\gamma_{\mathbf{K}}}{\epsilon + z\frac{g_T\delta}{T_c}\left(1-\gamma_{\mathbf{K}}\right)} \ , \tag{J.10}$$

where we have integrated over the first Brillouin zone.

The evaluation of DOS correction in presence of tunneling does not present many differences with respect to the calculation of MT contribution. It can be easily performed by means of Sections. I and J. With respect to MT correction, in Eq. (J.9), $\mathbf{R}_{ij} = \mathbf{R}_{ii}$.

Appendix K

Aslamazov-Larkin correction

The evaluation of the AL correction to thermal conductivity is quite cumbersome in the dynamical case. In the following, we report most of the steps necesessary to its evaluation.

As we have seen in Sec. 5.6.3, AL diagrams can be built up starting from the two blocks shown in Fig. 5.10, considering all their possible combination in pair. We have called B_1 the one in Fig. 5.10(a), and B_2 the other one. The general expression of the linear response operator is

$$\mathcal{Q}^{(AL)}\left(\omega_\nu\right) = Tt^4a^2 \sum_{j,l} \sum_{\Omega_\mu} L_{ij}\left(\Omega_{\mu+\nu}\right) L_{ml}\left(\Omega_\mu\right) B_{left}\left(\omega_\nu, \Omega_\mu\right) B_{right}\left(\omega_\nu, \Omega_\mu\right) \ , \quad \text{(K.1)}$$

In the latter equation, B_{left} and B_{right} can be either B_1 or B_2-type. The first problem is the evaluation of the two different blocks. Let us start with Fig. 5.10(b), that is the B_2-type.

$$B_2\left(\omega_\nu, \Omega_\mu\right) = T \sum_{\varepsilon_n} \left(\varepsilon_n + \varepsilon_{n+\nu}\right) \lambda\left(\varepsilon_{n+\nu}, \varepsilon_{\mu-n}\right) \lambda\left(\varepsilon_n, \varepsilon_{\mu-n}\right) I(\varepsilon_n, \Omega_\mu, \omega_\nu) \ , \quad \text{(K.2)}$$

where

$$\begin{aligned} I(\varepsilon_n, \Omega_\mu, \omega_\nu) &= \int (dp) G\left(\mathbf{p}, \varepsilon_{n+\nu}\right) \int (dp') G\left(\mathbf{p}', \varepsilon_{\mu-n}\right) G\left(\mathbf{p}', \varepsilon_n\right) G\left(\mathbf{p}', \varepsilon_{n+\nu}\right) \\ &= I_1 \cdot I_2 \ . \end{aligned} \quad \text{(K.3)}$$

As already mentioned, because of the pole structure of the fluctuation propagator in Eq. (5.50), one can neglect the ω_ν dependence and keep just the one in Ω_μ. The first integral is known, and it reads $I_1 = -i\pi\nu_F \mathrm{sgn}(\varepsilon_n)$. For I_2, one has to consider all the possible signs of Ω_μ and ε_n. The only non vanishing contributions are

$$\begin{aligned} I_2 = & \, i2\pi\nu_F\tau^2 \\ & \times\{\theta(-\Omega_\mu)[\theta(\Omega_\mu-\varepsilon_n)-\theta(\varepsilon_n)]+\theta(\Omega_\mu)[\theta(-\varepsilon_n)]-\theta(\varepsilon_n-\Omega_\mu)]\}\,, \end{aligned} \tag{K.4}$$

where $\theta(x)$ is the step function. By means of Eqs. (K.3) and (K.4), the expression of the block in Eq. (K.2) is

$$\begin{aligned} B_2\,(0,\Omega_\mu) = & -2(\pi\nu_F)^2 T\sum_{\varepsilon_n}\frac{2\varepsilon_n}{(2\varepsilon_n-\Omega_\mu)^2} \\ & \times\{\theta(\Omega_\mu)[\theta(\varepsilon_n-\Omega_\mu)+\theta(-\varepsilon_n)]+\theta(-\Omega_\mu)[\theta(\Omega_\mu-\varepsilon_n)+\theta(\varepsilon_n)]\}\,. \end{aligned} \tag{K.5}$$

Conditions on the signs of Ω_μ and ε_n in Eq. (K.5) allow to write the block as

$$\begin{aligned} B_2\,(0,\Omega_\mu) &= -4(\pi\nu_F)^2 T\Omega_\mu\left\{\theta(\Omega_\mu)\sum_{\varepsilon_n>0}\frac{1}{(2\varepsilon_n+\Omega_\mu)^2}+\theta(-\Omega_\mu)\sum_{\varepsilon_n>0}\frac{1}{(2\varepsilon_n-\Omega_\mu)^2}\right\} \\ &= -4(\pi\nu_F)^2 T\Omega_\mu\left\{[\theta(\Omega_\mu)+\theta(-\Omega_\mu)]\sum_{\varepsilon_n>0}\frac{1}{(2\varepsilon_n+|\Omega_\mu|)^2}\right\} \\ &= -4(\pi\nu_F)^2 T\Omega_\mu\frac{1}{(4\pi T)^2}\Psi'\left(\frac{1}{2}+\frac{|\Omega_\mu|}{4\pi T}\right) \\ &= -\frac{\pi^2}{8}\frac{\nu_F^2}{T}\Omega_\mu\,, \end{aligned} \tag{K.6}$$

where Ψ is the digamma function; we took the limit $\Omega_\mu \to 0$ in Ψ' to get the result in Eq. (K.6).

Now we have the expression of B_2-type block, we want to evaluate the other one. The B_1-type block reads

$$B_1\,(\omega_\nu,\Omega_\mu) = T\sum_{\varepsilon_n}(\varepsilon_n+\varepsilon_{n+\nu})\,\lambda\,(\varepsilon_{n+\nu},\varepsilon_{\mu-n})\,\lambda\,(\varepsilon_n,\varepsilon_{\mu-n})\,I(\varepsilon_n,\Omega_\mu,\omega_\nu)\,, \tag{K.7}$$

where, this time

$$\begin{aligned} I(\varepsilon_n,\Omega_\mu,\omega_\nu) &= \int(dp)G\,(\mathbf{p},\varepsilon_{n+\nu})\,G\,(-\mathbf{p},\varepsilon_{\mu-n})\int(dp')G\,(-\mathbf{p}',\varepsilon_{\mu-n})\,G\,(\mathbf{p}',\varepsilon_n) \\ &= I_1\cdot I_2\,. \end{aligned} \tag{K.8}$$

The product reads

$$I_1 \cdot I_2 = (2\pi\nu_F\tau)^2\{\theta(\Omega_\mu)[\theta(\varepsilon_n - \Omega_\mu) + \theta(-\varepsilon_n)] + \theta(-\Omega_\mu)[\theta(\varepsilon_n) + \theta(-\varepsilon_n + \Omega_\mu)]\} \quad \text{(K.9)}$$

and the B_1-type block reads

$$\begin{aligned} B_1(0,\Omega_\mu) &= (2\pi\nu_F)^2 T \sum_{\varepsilon_n} \frac{2\varepsilon_n}{(2\varepsilon_n - \Omega_\mu)^2} \\ &\quad \times[\theta(\Omega_\mu)[\theta(\varepsilon_n - \Omega_\mu) + \theta(-\varepsilon_n)] + \theta(-\Omega_\mu)[\theta(\varepsilon_n) + \theta(-\varepsilon_n + \Omega_\mu)]] \\ &= 8(\pi\nu_F)^2 T\Omega_\mu \left\{ [\theta(\Omega_\mu) + \theta(-\Omega_\mu)] \sum_{\varepsilon_n>0} \frac{1}{(2\varepsilon_n + |\Omega_\mu|)^2} \right\} \\ &= 8(\pi\nu_F)^2 T\Omega_\mu \frac{1}{(4\pi T)^2} \Psi'\left(\frac{1}{2} + \frac{|\Omega_\mu|}{4\pi T}\right) \\ &= \frac{\pi^2}{4}\frac{\nu_F^2}{T}\Omega_\mu \ . \end{aligned} \quad \text{(K.10)}$$

Then, we found the important relation between the two types of blocs

$$B_1(0,\Omega_\mu) = -2B_2(0,\Omega_\mu) \ . \quad \text{(K.11)}$$

To evaluate the AL correction, first of all, we observe that if we suppose that the blocks depend on two indices, then, by means of Fourier transform, one can write

$$B_{il} = \sum_{\mathbf{K}} e^{i(\mathbf{R}_i - \mathbf{R}_l)\mathbf{K}} B_{\mathbf{K}} \ , \quad \text{(K.12)}$$

where $\mathbf{R}_i = \mathbf{R}_l + \mathbf{a}$. Then, for the diagram with two B_1-type blocks, by means of Fourier transform

$$\sum_{j,l} L_{ij}L_{ml}B_{li}B_{jm} = \sum_{\mathbf{K}} \gamma_{\mathbf{K}}^2 L_{\mathbf{K}}L_{\mathbf{K}}B_{li}B_{jm} \ . \quad \text{(K.13)}$$

The latter equation for AL diagrams composed by two B_2-type blocks reads

$$\sum_{j,l} L_{jl}L_{lj}B_{ji}B_{lm} = \sum_{\mathbf{K}} L_{\mathbf{K}}L_{\mathbf{K}}B_{ji}B_{lm} \ . \quad \text{(K.14)}$$

For a diagram with both the two type of blocks

$$\sum_{j,l} L_{jl}L_{li}B_{ij}B_{lm} = \sum_{\mathbf{K}} \gamma_{\mathbf{K}} L_{\mathbf{K}}L_{\mathbf{K}}B_{ij}B_{lm} \ . \quad \text{(K.15)}$$

Taking into account that for the two last type of diagrams the multiplicity is four, and that B_1 and B_2 are bound by Eq. (K.11), the sum of Eqs. (K.13), (K.14) and (K.15) reads

$$4\sum_{\mathbf{K}}(\gamma_{\mathbf{K}}-1)^2 L_{\mathbf{K}} L_{\mathbf{K}} B_2 B_2 \; . \tag{K.16}$$

The total AL correction can be written as

$$\mathcal{Q}^{(AL)}\left(\omega_\nu\right) = 4Tt^4a^2\sum_{\mathbf{K}}\sum_{\Omega_\mu}(1-\gamma_{\mathbf{K}})^2 L_{\mathbf{K}}(\Omega_\mu+\omega_\nu)L_{\mathbf{K}}(\Omega_\mu)B_2^2(\omega_\nu,\Omega_\mu) \; . \tag{K.17}$$

The value of the block B_2 has been evaluated in Eq. (K.6), then Eq. (K.17) can be written as

$$\mathcal{Q}^{(AL)}\left(\omega_\nu\right) = a^2 g_T^2 \frac{1}{T}\sum_{\mathbf{K}}\sum_{\Omega_\mu}(1-\gamma_{\mathbf{K}})^2 L_{\mathbf{K}}(\Omega_\mu+\omega_\nu)L_{\mathbf{K}}(\Omega_\mu)\Omega_\mu^2 \; , \tag{K.18}$$

where we used the dimensionless tunneling conductance defined in Eq. (5.3).

The sum over Ω_μ can be performed transforming the sum into an integral by means of the following expression, [Eliashberg61, Larkin04]

$$T\sum_{\Omega_\mu} f(\Omega_\mu) = \frac{1}{4\pi i}\oint_{C_0} dz \coth\left(\frac{z}{2T}\right) f(-iz) \; , \tag{K.19}$$

with $z = i\Omega_\mu$; then,

$$T\sum_{\Omega_\mu} L_{\mathbf{K}}(\Omega_\mu+\omega_\nu)L_{\mathbf{K}}(\Omega_\mu)\Omega_\mu^2 = \frac{-1}{4\pi i}\oint_{C_0} dz\, z^2 \coth\left(\frac{z}{2T}\right) L_{\mathbf{K}}(-iz+\omega_\nu)L_{\mathbf{K}}(-iz) \; . \tag{K.20}$$

The function in the integral is not analytical at $\Im\mathrm{m}(z) = 0$ and $\Im\mathrm{m}(z) = -i\omega_\nu$, as shown in Fig. K.1, where $\Im\mathrm{m}(z)$ stands for the imaginary part of z. If the contribution over the circumference goes to zero as the radius $R \to \infty$, then the integral reduces to

$$\begin{aligned}
\oint_{C_0} \;=\; & \int_{-\infty}^{\infty} dz\, z^2 \coth\left(\frac{z}{2T}\right) L^R_{\mathbf{K}}(-iz+\omega_\nu)L^R_{\mathbf{K}}(-iz) \\
+ \; & \int_{\infty}^{-\infty} dz\, z^2 \coth\left(\frac{z}{2T}\right) L^R_{\mathbf{K}}(-iz+\omega_\nu)L^A_{\mathbf{K}}(-iz) \\
+ \; & \int_{-\infty-i\omega_\nu}^{\infty-i\omega_\nu} dz\, z^2 \coth\left(\frac{z}{2T}\right) L^R_{\mathbf{K}}(-iz+\omega_\nu)L^A_{\mathbf{K}}(-iz) \\
+ \; & \int_{+\infty-i\omega_\nu}^{-\infty-i\omega_\nu} dz\, z^2 \coth\left(\frac{z}{2T}\right) L^A_{\mathbf{K}}(-iz+\omega_\nu)L^A_{\mathbf{K}}(-iz) \; ,
\end{aligned} \tag{K.21}$$

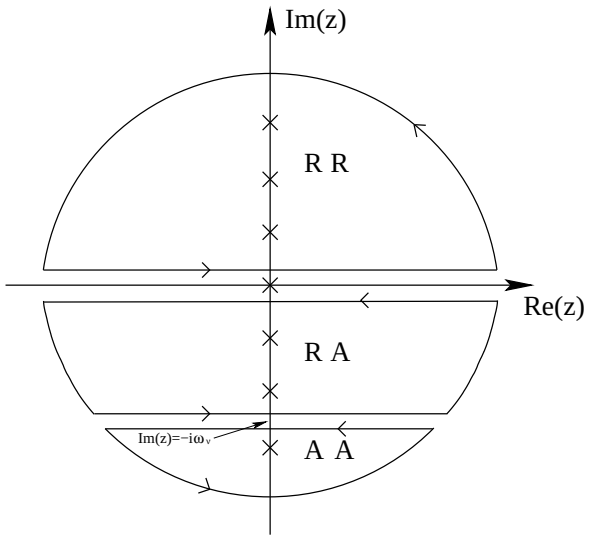

Figure K.1: The sum over Ω_μ in the linear response function can be performed transforming the sum into an integral along the indicated integration contour. The function in the integral is not analytical at $\Im\mathrm{m}(z) = 0$ and $\Im\mathrm{m}(z) = -i\omega_\nu$. Crosses represent the poles of $\coth(z/2T)$, and A and R stand for advanced and retarded, respectively.

where the superscripts A and R stand for advanced and retarded, respectively.

In the third and the fourth integrals of Eq. (K.21), we set $z = z' - i\omega_\nu$. Since $i\omega_\nu$ is the period of the $\coth(z/2T)$, the contour integral reads

$$\begin{aligned}\oint_{C_0} &= \int_{-\infty}^{\infty} dz\, z^2 \coth\left(\frac{z}{2T}\right) L^R_{\mathbf{K}}(-iz+\omega_\nu)[L^R_{\mathbf{K}}(-iz) - L^A_{\mathbf{K}}(-iz)] \\ &+ \int_{-\infty}^{\infty} dz\, (z-i\omega_\nu)^2 \coth\left(\frac{z}{2T}\right) L^A_{\mathbf{K}}(-iz+\omega_\nu)[L^R_{\mathbf{K}}(-iz) - L^A_{\mathbf{K}}(-iz)] \quad \text{(K.22)}\end{aligned}$$

Performing the square in the second integral in the rhs of Eq. (K.22), retaining just the terms proportional to z, and performing analytical continuation $\omega_\nu \to -i\omega$, the sum over Ω_μ can be written as

$$\begin{aligned}T\sum_{\Omega_\mu} L_{\mathbf{K}}(\Omega_\mu+\omega_\nu) L_{\mathbf{K}}(\Omega_\mu)\Omega_\mu^2 = -\frac{1}{2\pi}\Bigg\{ \int_{-\infty}^{\infty} dz \coth\left(\frac{z}{2T}\right) \Im\mathrm{m}(L^R_{\mathbf{K}}(-iz)) \\ \times\Bigg\{ z^2[L^R_{\mathbf{K}}(-iz-i\omega) + L^A_{\mathbf{K}}(-iz+i\omega)] - 2\omega z L^A_{\mathbf{K}}(-iz+i\omega)\Bigg\}\Bigg\}\,. \quad \text{(K.23)}\end{aligned}$$

To evaluate the conductivity, we need the imaginery part of the response function, and then the imaginery part of Eq. (K.23). It can be written as

$$-\frac{1}{4\pi i}\Bigg\{\int_{-\infty}^{\infty} dz \coth\left(\frac{z}{2T}\right)\Im\mathrm{m}(L^R_{\mathbf{K}}(-iz))$$
$$\Bigg\{z^2[L^R_{\mathbf{K}}(-iz-i\omega)+L^A_{\mathbf{K}}(-iz+i\omega)-L^R_{\mathbf{K}}(-iz+i\omega)-L^A_{\mathbf{K}}(-iz-i\omega)]$$
$$-2\omega z[L^A_{\mathbf{K}}(-iz+i\omega)-L^R_{\mathbf{K}}(-iz+i\omega)]\Bigg\}\Bigg\}\,. \tag{K.24}$$

Taking the limit as demanded by linear response theory, Eq. (5.14), and exploiting the definition of derivative, one finds

$$\begin{aligned}\lim_{\omega\to 0}\left[\frac{\Im\mathrm{m}(\mathcal{Q}^{(heat)}_{ret}(\omega))}{\omega T}\right] &= -\frac{1}{i4\pi T}\Bigg\{\int_{-\infty}^{\infty} dz \coth\left(\frac{z}{2T}\right)\Im\mathrm{m}(L^R_{\mathbf{K}}(-iz))\\ &\times \left\{2z^2\left[\frac{\partial}{\partial z}(L^R_{\mathbf{K}}(-iz)-L^A_{\mathbf{K}}(-iz))\right]-4iz\Im\mathrm{m}(L^R_{\mathbf{K}}(-iz))\right\}\Bigg\}\\ &= -\frac{1}{\pi T}\Bigg\{\int_{-\infty}^{\infty} dz\, z^2 \coth\left(\frac{z}{2T}\right)\Im\mathrm{m}(L^R_{\mathbf{K}}(-iz))\frac{\partial}{\partial z}\Im\mathrm{m}(L^R_{\mathbf{K}}(-iz))\\ &- \int_{-\infty}^{\infty} dz\, z \coth\left(\frac{z}{2T}\right)[\Im\mathrm{m}(L^R_{\mathbf{K}}(-iz))]^2\Bigg\}\,,\end{aligned} \tag{K.25}$$

From Eq. (5.50), the expression of the Cooper pair fluctuation propagator is

$$\begin{aligned}L_{\mathbf{K}}(\Omega_\mu) &= -\frac{1}{\nu_F}\frac{1}{\ln\frac{T}{T_c}+\frac{\pi|\Omega_\mu|}{8T_c}+z\frac{g_T\delta}{T_c}(1-\gamma_{\mathbf{K}})}\\ &= -\frac{1}{\nu_F}\frac{1}{m_{\mathbf{K}}+\alpha|\Omega_\mu|}\,,\end{aligned} \tag{K.26}$$

where $m_{\mathbf{K}}\equiv \ln\frac{T}{T_c}+z\frac{g_T\delta}{T_c}(1-\gamma_{\mathbf{K}})$ and $\alpha\equiv\pi/8T_c$. Then,

$$L_{\mathbf{K}}(-iz) = -\frac{1}{\nu_F}\frac{1}{m_{\mathbf{K}}+\alpha|-iz|}\,, \tag{K.27}$$

and

$$\begin{aligned}L^R_{\mathbf{K}}(-iz) &= -\frac{1}{\nu_F}\frac{1}{m_{\mathbf{K}}-iz\alpha}\\ &= -\frac{1}{\nu_F\alpha}\frac{1}{(\delta-iz)}\,,\end{aligned} \tag{K.28}$$

where $\delta = m_{\mathbf{K}}/\alpha$. Then, the imaginery part of $L^R_{\mathbf{K}}(-iz)$ reads

$$\Im\mathrm{m}(L^R_{\mathbf{K}}(-iz)) = -\frac{1}{\nu_F \alpha}\frac{z}{(\delta^2+z^2)} \,. \tag{K.29}$$

The most singular contribution is in the region $z \sim \epsilon \ll T$, where the $\coth(z/2T)$ behaves as $\sim 2T/z$. We just consider the two integrals in the rhs of Eq. (K.25). They can be written by means of previous equations as

$$\int_{-\infty}^{\infty} dz \left[z\,\Im\mathrm{m}(L^R_{\mathbf{K}}(-iz))\frac{\partial}{\partial z}\Im\mathrm{m}(L^R_{\mathbf{K}}(-iz)) - [\Im\mathrm{m}(L^R_{\mathbf{K}}(-iz))]^2 \right] = -\frac{2}{(\nu_F\alpha)^2}\int_{-\infty}^{\infty} dz \frac{z^4}{(\delta^2+z^2)^3} \,, \tag{K.30}$$

where the integral in the rhs of the latter equation can be easily evaluated. Finally, from Eqs. (K.23) and (K.30), the sum over Ω_μ reads

$$T\sum_{\Omega_\mu} L_{\mathbf{K}}(\Omega_\mu+\omega_\nu)L_{\mathbf{K}}(\Omega_\mu)\Omega_\mu^2 = \frac{12T_c}{\nu_F^2 m_{\mathbf{K}}} \,. \tag{K.31}$$

From Eqs. (K.18) and (K.31), the AL correction finally reads

$$\frac{\delta\kappa^{(AL)}}{\kappa_0} = \frac{9}{2\pi}\frac{1}{g_T}\left(\frac{g_T\delta}{T_c}\right)^2 \int_{BZ}(dK)\frac{(1-\gamma_{\mathbf{k}})^2}{\epsilon + z\frac{g_T\delta}{T_c}(1-\gamma_{\mathbf{K}})} \,. \tag{K.32}$$

Bibliography

[Abeles77] B. Abeles, Phis. Rev. B **15**, 2828 (1977).

[Abrikosov75] A.A.Abrikosov, L.P. Gorkov, I.E. Dzyaloshinski *Methods of Quantum Field Theory in Statistical Physics*, (Dover, New York, 1975).

[Abrikosov88] A. A. Abrikosov, *Fundamentals of the Theory of Metals*, (North-Holland, Amsterdam, 1988).

[Altshuler85] B.L. Altshuler and A.G. Aronov, in *Electron-electron interactions in disordered systems*, edited by A.L. Efros and M. Pollak (Elsevier Science Publishers B.V., 1985).

[Akkermans94] E. Akkermans, G. Montambaux, J. L. Pichard, J. Zinn-Justin, *Mesoscopic Quantum Physics, Les Houches 1994-Session LXI* (Elsevier, Amsterdam, 1995).

[Akkermans04] E. Akkermans, G. Montambaux, *Physique mésoscopique des électrons et des photons*, (EDP Sciences/CNRS Édition, 2004).

[Appleyard98] N. J. Appleyard, J. T. Nicholls, M. Y. Simmons, W. R. Tribe, M. Pepper, Phis. Rev. Lett. **81**, 3491 (1998).

[Ashcroft87] N. W. Ashcroft and N. D. Mermin, *Solid State Physics*, (Thomson Learning, 1987).

[Aslamazov68] L. G. Aslamazov, A. I. Larkin, Sov. Solid State **10**, 875 (1968).

[Barber94] R. P. Barber, L. M. Merchant, A. La Porta, R. C. Dynes, Phis. Rev. B **49**, 3409 (1994).

[Beloborodov00] I. S. Beloborodov, K. B. Efetov, A. I. Larkin, Phis. Rev. B **61**, 9145 (2000).

[Beloborodov01] I. S. Beloborodov, K. B. Efetov, A. Altland, F. W. J. Hekking, Phis. Rev. B **63**, 115109 (2001).

[Beloborodov03] I. S. Beloborodov, K. B. Efetov, A. V. Lopatin, V. M. Vinokur, Phys. Rev. Lett. **91**, 246801 (2003).

[Beloborodov05] I. S. Beloborodov, A. V. Lopatin, F. W. J. Hekking, R. Fazio and V. M. Vinokur Europhys. Lett. **69**, 435 (2005).

[Biagini05] C. Biagini, R. Ferone, R. Fazio, F. W. J. Hekking and V. Tognetti, Phys. Rev. B, **72**, 134510 (2005).

[Castellani87] C. Castellani, C. DiCastro, G. Kotliar, P. A. Lee and G. Strinati, Phys. Rev. Lett. **59**, 477 (1987).

[Chester61] G. V. Chester, A. Tellung, Proc. Phys. Soc. London **77**, 1005 (1961).

[Datta97] S. Datta, *Electronic Transport in Mesoscopic Systems*, (Cambridge University Press, 1997).

[DeGennes99] P. G. De Gennes, *Superconductivity of metals and alloys*, (Perseus Books, 1999).

[Deutscher74] G. Deutscher, Y. Imry, L. Gunther, Phis. Rev. B **10**, 4598 (1974).

[DiCastro90] C. Di Castro, R. Raimondi, C. Castellani, A. A. Varlamov, Phys. Rev. B **42**, 10211 (1990).

[Dolcini03] F. Dolcini, H, Grabert, I. Safi, B. Trauzettel, Phys. Rev. Lett. **91**, 266402 (2003).

[Dynes78] R. C. Dynes, J. P. Garno, J. M. Rowell, Phys. Rev. Lett. **40**, 479 (1978).

[Efetov03] K. B. Efetov, A. Tschersich, cond-mat/0302257.

[Eliashberg61] G. M. Eliashberg, Sov. Phys. JETP **14**, 856 (1961).

[Fazio98] R. Fazio, F. W. J. Hekking and D. E. Khmelnitskii, Phys. Rev. Lett. **80**, 5611 (1988).

[Ferone] R. Ferone and F. W. J. Hekking, in preparation.

[Fetter03] A. L. Fetter, J. D. Walecka, *Quantum Theory of Many-Particle Systems*, (Dover, New York, 2003).

[Feynman59] Lecture of R. P. Feynman at the *Annual meeting of the American Physical Society* at the Caltech 1959.

[Gerber97] A. Gerber, A. Milner, G. Deutscher, M. Karpovsky, A. Gladkikh, Phys. Rev. Lett. **78**, 4277 (1997).

[Ginzburg60] V. L. Ginzburg, Sov. Solid State **2**, 61 (1960).

[Gramada97] A. Gramada and M. E. Raikh, Phis. Rev. B **55**, 7673 (1997).

[Haldane81] F. D. M. Haldane, J. Phys. C **14**, 2585 (1981).

[Huang87] K. Huang, *Statistical Mechanics*, (John Wiley & Sons, Inc. 87).

[Imry81] Y. Imry, M. Strongin, Phis. Rev. B **24**, 6353 (1981).

[Imry02] Y. Imry, *Introduction to Mesoscopic Physics* (Oxford University Press, 2002).

[Ioffe60] A. F. Ioffe, A. R. Regel, Prog. Semicond. **4**, 237 (1960).

[Kane96] C. L. Kane and M. P. A. Fisher, Phys. Rev. Lett. **76**, 3192 (1996).

[Krive98] I. V. Krive, Low Temp. Phys. **24**, 498 (1998).

[Kurland00] I. L. Kurland, I. L. Aleiner, B. L. Altshuler, Phis. Rev. B **62**, 14886 (2000).

[Landauer70] R. Landauer, Philosophical Magazine, **21**, (1970), 863-867.

[Langer62] J. S. Langer, Phys. Rev. **128**, 110 (1962).

[Larkin04] A. Larkin, A. Varlamov, *Theory of Fluctuations in Superconductors* (Clarendon Press Oxford) and references therein.

[Levy05] E. Levy, A. Tsukernik, M. Karpovski, A. Palevski, B. Dwir, E. Pelucchi, A. Rudra, E. Kapon, Y. Oreg, cond-mat/0509027.

[Li02] Mei-Rong Li, E. Orignac, cond-mat/0201291.

[Luttinger63] J. M. Luttinger, J. Math. Phys. **4**, 1154 (1963).

[Mahan00] G. D. Mahan, *Many-Particle Physics* (Kluwer Academic/ Plenum Publisher, 2000).

[Maki68] K. Maky, Prog. Theor. Phys. **40**, 193 (1968).

[Maslov95] D. L. Maslov, M. Stone, Phis. Rev. B **52**, R5539 (1995).

[Maslov95b] D. L. Maslov, Phis. Rev. B **52**, R14368 (1995).

[Mattis65] D. C. Mattis and E. H. Lieb, J. Math. Phys. **6**, 304 (1965).

[Meyer04] J. S. Meyer, A. Kamenev, L. I. Glazman, Phys. Rev. B **70**, 45310 (2004).

[Molenkamp92] L. W. Molenkamp, Th. Gravier, H. van Houten, O. J. A. Buijk, M. A. A. Mabesoone, C. T. Foxon, Phis. Rev. Lett. **68**, 3765 (1992).

[Mühlschlegel72] B. Mühlschlegel, D. J. Scalapino, R. Denton, Phys. Rev. B **6**, 1767 (1972).

[Niven05] D. R. Niven and R. A. Smith, Phys. Rev. B **71**, 35106 (2005).

[Niven02] D. R. Niven and R. A. Smith, Phys. Rev. B **66**, 214505 (2002).

[Odom98] T. W. Odom, J. Huang, P. Kim, C. M. Lieber, Nature **391**, 62 (1998).

[Orr86] B. G. Orr, H. M. Jaeger, A. M. Goldman, C. G. Kuper, Phys. Rev. Lett. **56**, 378 (1986).

[Pines89] D. Pines, P. Nozieres, *Theory of Quantum Liquids: Normal Fermi Liquids*, (Addison Wesley Publishing Company, 1989)

[Rickayzen80] G. Rickayzen, *Green's Functions and Condensed Matter* (Academic Press, 1980).

[Safi95] I. Safi, H. J. Schulz, Phys. Rev. B **52**, R17040 (1995).

[Safi97] I. Safi, Ann. Phys. Fr **22**, (1997).

[Shapira83] Y. Shapira and G. Deutscher, Phys. Rev. B **27**, 4463 (1983).

[Schulz95] H. J. Schulz, in *Mesoscopic Quantum Physics, Les Houches 1994-Session LXI*, edited by E. Akkerman, G. Montambaux, J. L. Pichard, J. Zinn-Justin, (Elsevier, Amsterdam, 1995).

[Schwabl92] F. Schwabl, *Quantum Mechanics* (Springer-Verlag, Berlin, 1992).

[Sivan86] U. Sivan and Y. Imry, Phys. Rev. B **33**, 551 (1986).

[Strongin70] M. Strongin, R. S. Thompson, O. F. Kammerer, J. E. Crow, Phys. Rev. B **1**, 1078 (1970).

[Tans97] S. J. Tans, M. H. Devoret, H. Hai, A. Thess, R. E. Smalley, L. J. Geerligs, C. Dekker, Nature **386**, 474 (1997).

[Tarucha95] C. Tarucha, T. Honda, T. Saku, Solid State Commun. **95**, 413 (1995).

[Thompson70] R. S. Thompson, Phys. Rev. B **1**, 327 (1970).

[Tinkham96] M. Tinkham, *Introduction to Superconductivity II ed.* (Dover, 2004).

[Tomonaga50] S. Tomonaga, J. Math. Phys. **5** 544 (1950).

[Ussishkin03] I. Ussishkin, Phys. Rev. B **68**, 24517 (2003).

[Vanwees88] B. J. van Wees, H. Van Houten, C. W. Beenakker, J. G. Williamson, L. P. Kouwenhoven, D. Van der Marel, C. T. Foxon, Phys. Rev. Lett. **60**, 848 (1988).

[Varlamov90] A. A. Varlamov, D. V. Livanov, Sov. Phys. JETP **71**, 325 (1990).

[Varlamov99] A. A. Varlamov, G. Balestrino, E. Milani, D. V. Livanov, Adv. Phys. **48**, No. 6, 655 (1999).

[Voit94] J. Voit, Rep. Prog. Phys. **57**, 977 (1994).

[Vondelft98] J. von Delft and H. Scoeller, cond-mat/9805275.

[Wharam88] D. A. Wharam, T. J. Thornton, R. Newbury, M. Pepper, H. Ahmed, J. E. F. Frost, D. G. Hasko, D. C. Peacock, D. A. Ritchie, G. A. C. Jones, J. Phys C **21**, L209 (1988).

[Wildoer98] J. W. G. Wildoer, L. C. Venema, A. G. Rinzler, R. E. Smalley, C. Dekker, Nature **391**, 59 (1998).

[Yacoby96] A. Yacoby, H. L. Stormer, N. S. Wingreen, L. N. Pfeiffer, K. W. Baldwin, K. W. West, Phys. Rev. Lett. **77**, 4612 (1996).